CHARACTERISATION OF AQUIFERS IN BAUCHI-ALKALERI-KIRFI AREAS, NORTHEASTERN NIGERIA

ABDULLATEEF LAWAL

MATRIC. NO. : 181973

APRIL, 2021

CHARACTERISATION OF AQUIFERS IN BAUCHI-ALKALERI-KIRFI AREAS, NORTHEASTERN NIGERIA

BY

ABDULLATEEF LAWAL
MATRIC. NO. : 181973

B.Sc. Applied Geology (ATBU), M.Sc. Hydrogeology and Engineering Geology (UNIJOS)

A Thesis in the Department of Geology
Submitted to Faculty of Sciences
in partial fulfilment of the requirements for the Degree of

DOCTOR OF PHILOSOPHY

of the

UNIVERSITY OF IBADAN

APRIL, 2021

CERTIFICATION

I hereby certify that this research workwas undertaken by Mr. Lawal Abdullateef (181973)in the Department of Geology, University of Ibadan.

.....

Supervisor

M.N. Tijani.

B.Sc. (Ilorin), M.Sc. (Ibadan), Ph.D. (Muenster)

Professor, Department of Geology,

University of Ibadan, Nigeria

DEDICATION

This work is dedicated to Allah (S.W.T) for his inspiration, guidance and protection; most importantly for his sustenance and blessing through my years of study.

This work is also dedicated Alhaji Abdulganiyu Lawal and Hajiya Nuratu A. Lawal and Hajiya Muniratu Lawal of blessed memory.

ACKNOWLEDGEMENTS

My gratitude goes to Almighty God, the giver of life, the provider of glad tidings and the creator of everything in heaven and on earth, for giving me life, sustenance and the opportunity to come to school. My profound gratitude goes to my supervisor, Professor M.N.Tijani, who despite his very tight schedule still found time to supervise and put me through all the process of this work. May the Almighty bless him and his family and grant him his heart desires.

I will like to acknowledge the Head of Department, Prof. Okunlola for his kindness, fatherly advice and encouragement given to me throughout my stay in the department. May the Almighty provide him and his family a shoulder to lean on in times of need and hardship.My sincere appreciation goes to some special people in the Department of Geology, University of Ibadan, notably Dr. A.S. Olatunji, Dr. I. Oyediran, Prof. Ehiola, Prof. G. O. Adeyemi, Dr. O.C. Adeigbe, Mr. J.A. Aladejana and Dr. O. A Fashea of the Department of Geography. May Allah (S.W.T.) bless them abundantly. Immeasurable gratitude goes to the Head of Department of Applied Geology, Abubakar Tafawa Balewa University, Bauchi, Prof. A.I. Haruna for his unflinching support and understanding and also Prof. N.K. Samaila, Prof.A.S. Maigari and Dr. T.P. Bata, of the same department for their guidance and constructive criticism and all the staff of the geology department of the Abubakar Tafawa Balewa University Bauchi for their support and understanding.

I reserved this paragraph for those people who are close to my heart. This acknowledgement would not have been complete without this paragraph, My parents; Alhaji A.G.Lawal and Hajia Nuratu Lawal, who have been the pillars on which I lean, who provided me with both moral and financial support, who made sure I lacked noting as a son and as a student, who have given me a challenge when I have my children, their kindness and affection cannot be overestimated. May Allah (S.W.T.) in his infinite mercies show them kindness, light and ease in their lives. May He also make them see the joy in us (their children) and live to reap the fruits of their labour. Next, I will like to acknowledge my wife, Hajia Kabirat Abdulrazaq for her understanding and support, and my Sister, Mrs. Madinat Fakorede and her family, who has been of immense assistance to me both financially and morally. May Allah (S.W.T.) grant them all their heart desires and bless

them and their immediate families. My brothers, Saheed Lawal, Abdulazeez Lawal, Abubakar Sadiq Lawal, I thank them all for their support and care throughout my work.
I would also like to acknowledge the management of TETfund and members and staff of the Water Science Laboratory, University of Nebraska, Lincoln, USA, especially Prof. Daniel Snow, Dr. Matheou DAllessio, Christopher Olsen, Dr. Ari, Aaron, Victoria for making my TETfund sponsored benchwork a success.

Finally, this last paragraph is reserved for those whom I have been through thick and thin with my very good friends and cousins, Ayuba Rufai,John Shipurtda, Usman Yero, AbdulMumin,Abdulmajid Isa, Nuru Nabage, Mustapha Aliyu, Fatima Saidu, Umar Sambo Umar, Abdulhakim Lawal, Idris lawal, Abdulkarim Aliyu, Babangida Moh'd, Danlami Abdulkadir and others whom I cannot mention. May God make it easy for them and reward them abundantly.

ABSTRACT

Geological Transition Zones (GTZ) are hydrogeologically problematic, owing to poorly defined basal and lateral contacts between the lithological units that make up the zones. Attempts have been made to delineate the complex lithological contacts in GTZ using geophysical and geological methods. However, the quality, hydrochemical and isotope characteristics of groundwater in GTZ, which are very significant to the sustainable management of the groundwater resources of GTZ, have not received much attention.Therefore, this study focused on characterisation of the aquifers in a typical GTZ in Bauchi-Alkaleri-Kirfi areas, Northeastern Nigeria.

Geological and geophysical studies(aeromagnetic and geoelectric) were carried out for lithological delineation and characterisation of the aquifer systems. Eighty Seven Groundwater samples were collected and in-situ determination pH, conductivity and Total Dissolved Solids (TDS) were undertaken using a digital meter. Hydrochemical and stable isotope analyses were undertaken using atomic absorption spectrometry, ion chromatography and mass spectrometry respectively. Data were analysed using descriptive statistics and standard hydrochemical plots.

The lithological units identified were migmatite/gneiss, granite and charnockite overlain by sandstone units. Three to five geoelectric layers with aquifer thickness of 11-158m were identified in the sandstones units,whilethe Basement Complex areas revealed saprolite thicknesses of 1.3-67.3m (granite), 1.2-44.6m (charnockite)and 2.4-83.8m (migmatite/gneiss).The depth to bedrock is put at 45m below the ground surface in the basement areas and >800m in the sedimentary terrain. The overall groundwater potential map revealed three Groundwater Potential Zones (GPZ) namely: poor (charnockite and granite), moderate (migmatite/gneiss and granite), and good (dominantly sandstone).The TDS and pH values of 95-1,558mg/L and 6.4-7.7 and 15-1,105mg/L and 5.0-8.5,characterised the basement terrain and the sedimentary areas respectively, suggesting a moderately acidic to alkaline low mineralised groundwater. Calcium (2.57-216.20mg/L) is the dominant cation in the basement areas, suggesting silicate weathering/ dissolution, while Na^{+} (1.59-106.30mg/L) dominated the sedimentary zones, indicative of cation exchange reactions. The water quality index revealed 58.5% as potable and 41.05% as unsuitable. The dominant hydrochemical facie in the basement areas was Ca^{2+}-(Mg^{2+})-HCO_3^{-} (54.2%), characteristic of recharge meteoric water. The Na^{+}-(K^{+})-HCO_3^{-}facie (14.1%) characterised the sedimentary zones, indicative of cation exchange reactions. Stable isotopes revealed meteoric source characterised by kinetic evaporation with values of $\delta^{18}O$ =−3.4‰ and $\delta^{2}H$=−19.6‰ for the basement area. However, values of $\delta^{18}O$=−4.1‰, $\delta^{2}H$=−25.7‰ for the sedimentary terrain are indicative of depleted groundwater due to latitude effect and longer residence time.

Saprolites and medium to coarse sandstone units are the aquifer units in the Bauchi-Alkaleri-Kirfi areas. The recharge system of the saprolitic units are more influenced by precipitation as compared to the sandstone aquifers.

Keywords: Water quality index, Aquifer, Thematic maps, Stable isotope, Kinetic evaporation

Word Count: 421

TABLE OF CONTENTS

TITLE PAGE	i
CERTIFICATION	ii
DEDICATION	iii
ACKNOWLEDGMENTS	iv
ABSTRACT	vi
TABLE OF CONTENTS	vii
LIST OF TABLES	x
LIST OF FIGURES	xiii
LIST OF PLATES	xviii
LIST OF APPENDICES	xix
CHAPTER ONE: INTRODUCTION	1
1.1 Background to the Study	1
1.2 Aim and Objectives	8
1.3 Justification	8
1.4 Scope of Study	10
1.6 Overview of Previous Works	11
CHAPTER TWO: LITERATURE REVIEW	21
2.1 Location of Study Area	21
2.2 Topography and Drainage	21
2.3 Climate and Vegetation	23
2.4Review of the Regional Geology of Nigeria	38
2.4.1 Basement Complex Rocks	28
2.4.2 Sedimentary Basins	30
2.5 Regional Geology of the Study Area	30
2.5.1 Basement Complex	30
2.5.1.1 Migmatite Gneiss Complex	31
2.5.1.2 Older Granites	33
2.5.2 Sedimentary Geology	34
2.5.2.1 Stratigraphy of the Northern Benue Trough	35
2.5.2.2 The Kerri-Kerri Formation	37

2.6Review of the Hydrogeology of the Study Area 37
2.6.1 Basement Complex Hydrogeology 39
2.6.2 Hydrogeology of SedimentaryUnits 41

CHAPTER THREE: METHODOLOGY 45
3.1 Desk Study 45
3.1.1Remote Sensing and GIS Study 45
3.1.2Aeromagnetic Data Acquisition 47
3.2 Field Studies 48
3.2.1Geological Mapping 48
3.2.2 Geophysical Field Investigation 48
3.2.3 Groundwater Sampling 53`
3.3 Laboratory Analyses 57
3.3.1 Petrographic Studies 57
3.3.2 Granulometric Analysis 57
3.3.3 Groundwater Analysis 58
3.3.3.1 Alkalinity determination 58
3.3.3.2 Major cations analysis 58
3.3.3.3 Major anions analysis 60
3.3.3.4 Stable Isotopes (^{18}O and ^{2}H) analysis 60
3.4 Quality Control 61
3.5Data Analysis and Evaluation 61
3.5.1 Remote Sensing and GIS Data Analysis 62
3.5.1.1 Preparation of thematic maps 64
3.5.1.2GIS operations 66
3.5.1.3Overall Integration of thematic maps /Delineation of Groundwater potential zones (GWPZ) 67
3.5.2 Hydrochemical Data Evaluation 70
3.5.2.1 Charge balance 70
3.5.2.2 Statistical Analysis 70
3.5.2.3 Drinking water quality index (WQI) and Irrigation Water index 71
3.5.2.4 Hydrochemical Facie Evaluation 74
3.5.3Stable Isotope Data Evaluation 74

CHAPTER FOUR: RESULTS AND DISCUSSION 75
4.1 Thematic Maps 75
4.1.1 Surface thematic maps 75
4.1.2 Subsurface thematic maps 85
4.1.2.1 Lineament density 85
4.1.2.2 Geological characteristics 88
4.1.2.3 Geoelectrical characteristics 93
4.1.2.4Basement weathering profileand hydrostratigraphic units 101
4.1.2.5Aquifer resistivity map 107

4.1.2.6 Aquifer thickness map 109
4.2 Weight Assignment and Normalisation 111
4.3 Overall Integration of Thematic Maps 117
4.4 Delineation of Groundwater Potential Zone Map 117
4.5 Groundwater Potential Map Zone Map Verification 119
4.6 Well Inventory and Groundwater Chemistry 123
4.6.1 Well Inventory 126
4.6.2 Physico-chemial Parameters 128
4.6.3 Cation chemistry (Ca^{2+}, Mg^{2+}, Na^{+}, K^{+}) 135
4.6.4 Anion chemistry (HCO_3^{-}, NO_3^{-}, SO_4^{2-} , Cl^{-}) 139
4.6.5 Lithology Based Hydrochemical Profiles 145
4.6.6 Principal Component Analysis 150
4.6.7 Water Quality Index (WQI) 156
4.6.8 Water Quality for Irrigation Purposes 165
4.6.8.1 Salinity Hazard 165
4.6.8.2 Sodium Absorption Ratio (SAR) or Sodium Hazard 167
4.6.8.3 Residual Sodium carbonate (RSC) 171
4.6.8.4 Soluble sodium percentage (SSP) 173
4.6.8.5 Permeability index (PI) 173
4.6.8.6 Kelly ratio (KR) 175
4.6.8.7 Magnesium hazard (MH) 177
4.6.9 Hydrochemical Facies 182
4.6.9.1 Schoeller diagrams 182
4.6.9.2 Stiff plots 185
4.6.9.3 Piper Trilinear 189
4.7 Mechanisms Controlling the Groundwater Chenistry 193
4.8 Stable Isotope Composition of Groundwater 205
4.8.1 Deuterium excess (D-excess) of Groundwater Samples 211
4.8.2 Origin of Dissolve Ions in Groundwater 214
4.8.3 Latitude (Continental) Effects 216
4.9 Synthesis 218

CHAPTER FIVE: SUMMARY, CONCLUSION AND RECOMENDATIONS 222
5.1Summary 222
5.2 Conclusion 227
5.3 Recommendations 230
5.4 Contributions to Knowledge 230

REFERENCES 231

LIST OF TABLES

Table 1.1. Availability of Global Water Sources 2

Table 3.1. Secondarydata utilized for the study 46

Table 3.2. Distribution of hydrochemical samples based on bedrock setting 55

Table 3.3. (a)Weights assignment and interpretation using Saaty's scale (Saaty 1980, 1992) and
(b) Average Random Consistency index values (Saaty 1980) 68

Table 3.4.Table of pair-wise comparison for themes and weights of thematic maps using analytical hierarchical process (AHP) 69

Table 3.5. WQI Parameters and Weight Assignment Table 72

Table 3.6. Irrigation water quality parameters and mathematical formulars 73

Table 4.1.Graphic mean (grain size) and standard deviation (sorting) of sandstone samples based on the classification by Folk, 1968. 94

Table 4.2. Classification of resistivity for (a) weathered basement and sandstones and (b) basement Complex 98

Table 4.3. Summary of geoelectrical parameters 102

Table 4.4. Assigned and normalised and weightages of the individual classes of surface and hydrological layers 112

Table 4.5.Normalized weights of the classes of hydrogeological thematic layers for Bauchi-Alkaleri-Kirfi area 115

Table 4.6.Well yield record for various bedrocks 121

Table 4.7. Groundwater potential categorization based on the yield of boreholes 121

Table 4.8(a) Results of well inventory 124

Table 4.8(b) Results of physico-chemical parameters 124

Table 4.9 (a)Descriptive Statistics of Well inventory Based on Bedrock Types 125

Table 4.9 (b) Descriptive Statistics of thePhysico-chemical Parameters Based on Bedrock Types 125

Table 4.10. Classes of Hardness in Water 134

Table 4.11. Summary of results of hydrochemistry in Bauchi-Alkaleri-Kirfi area. 137

Table 4.12.Descriptive Statistics of Chemical Parameters Based of Bedrock Types 146

Table 4.13.Correlations between PCA variables and factors 151

Table 4.14.WQI of Water Samples from the Bauchi-Alkaleri-Kirfi area 157

Table 4.15. WQI ratings distribution in the study area 159

Table 4.16.A summary of the descriptive statistics of the irrigation quality parameters of the Bauchi-Alkaleri-Kirfi area 166

Table 4.17 (a) Classification of Salinity Hazard for aquifersinBauchi--Alkaleri-Kirfi area (after Richards, 1954 and Wilcox, 1956), 170

Table 4.17 (b) Classification of Sodium Hazard for Aquifers inBauchi-Alkaleri-Kirfi area (after Richards, 1954 and Wilcox, 1956) 170

Table 4.18. Classification of Residual Sodium Carbonate for Aquifers in Bauchi-Alkaleri-Kirfi area (After Richards, 1954) 172

Table. 4.19. Classification of Soluble Sodium Percentage for Aquifers in Bauchi-Alkaleri-Kirfi area (After USDA, 1954). 174

Table 4.20 (a) Classification of Permeability Index for Aquifers in Bauchi-Alkaleri-Kirfi area (After Doneen, 1966) 176

Table 4.20 (b) Classification of Kelly ratio for Aquifers in Bauchi-Alkaleri-Kirfi Area (After USDA, 1954), 176

Table 4.21. Classification of Magnesium Hazard for Aquifers in Bauchi-Alkaleri-Kirfi area 178

Table 4.22. Hydrochemical facies of the Different Bedrocks in Bauchi-

Alkaleri-Kirfi area. 192

Table 4.23. Stable Isotope Results for Bauchi-Alkaleri-Kirfi area 208

LIST OF FIGURES

Fig. 2.1. Admistrative Map of Bauchi-Alkaleri-Kirfi area 22

Fig. 2.2. Drainage and Topographic Map of Bauchi-Alkaleri- Kirfi Area 24

Fig. 2.3. Mean Monthly Rainfall of Bauchi-Alkaleri-Kirfi area from 2012-2014 25

Fig. 2.4. (a) Mean Monthly Temperature for the Study area (2005-2007) 27

Fig. 2.4. (b) Mean Monthly Relative Humidity for the Study area (2005-2007) 27

Fig. 2.5. Geological Map of Nigeria 29

Fig. 2.6. Generalized Geological Map of Bauchi State Showing the Basement Complex rocks and the Kerri-Kerri Formation 32

Fig. 2.7. Stratigraphic sequences of the Benue and part of Chad Basin Showing the Sedimentary Units in the Study Region 35

Fig. 2.8. Hydrogeological map of Nigeria showing the Study Region. 37

Fig. 2.9. Hydrogeological Map of Bauchi State 39

Fig 2.10. Borehole Logs from the Basement Complex Parts of the study 42

Fig 2.11. Borehole Logs from the central parts of the Kerri Kerri Formation 43

Fig 2.12. Borehole Logs from the northeastern parts of the Kerri Kerri Formation 44

Fig. 3.1. Map showing VES stations 49

Fig. 3.2. Groundwater sample map of Bauchi-Alkaleri-Kirfi area 54

Fig. 3.3. Flowchart for classifying groundwater potential zones using, GIS And Remote sensing approach 63

Fig. 4.1. Elevation map of Bauchi-Alkaleri-Kirfi area 76

Fig. 4.2. Land use/Land cover map Bauchi-Alkaleri-Kirfi area 78

Fig. 4.3. Slope map of Bauchi-Alkaleri-Kirfi area 79

Fig. 4.4. Soil map of Bauchi-Alkaleri-Kirfi area 81

Fig. 4.5. Drainage density map of the area 82

Fig. 4.6. Rainfall distribution map of the area 84

Fig. 4.7(a) Extracted magnetic lineament map 86

Fig. 4.7(b) Lineament trends in Bauchi-Alkaleri-Kirfi area 86

Fig. 4.8. Lineament Density Thematic Map of Bauchi-Alkaleri-Kirfi area 87

Fig. 4.9 Geology map of Bauchi-Alkaleri-Kirfi area. 89

Fig 4.10 (a) Photomicrograph of Migmatite gneiss under transmitted light showing quartz (Q), biotite (B), Hornblende (H), Microcline (M) and plagioclase feldspar (P). 90

Fig 4.10 (b) Photomicrograph of migmatite under transmitted light showing quartz (Q), biotite (B), Microcline (M) and plagioclase feldspar (P). 90

Fig. 11 (a) Photomicrograph of biotite hornblende granite in transmitted light showing quartz (Q), biotite (B), hornblende (H) and plagioclase feldspar (P), Microcline (M) 92

Fig 11 (b) Photomicrograph of charnockite under transmitted light showing quartz (Q), biotite (B), hornblende (H) and plagioclase feldspar (P). 92

Fig 4.12. Representative samples of the geo-electric field curves 95

Fig 4.13(a) Distribution of the various type curves in the different rock units
(b) Relative abundances of the different geo-electric field curves 97

Fig 4.14. Iso-apparent resistivity maps at AB/2 of a. 40 m, b. 60 m, c. 80 m, and d. 120 m 100

Fig. 4.15 (a) Geoelectrical profiles across the basement rocks and Sandstone 105

Fig. 4.15 (b) Geoelectric cross-section C-C', across the sandstone units 105

Fig. 4.16. Thematic Map forAquifer Resistivity 108

Fig. 4.17. Thematic Map for Aquifer Thickness 110

Fig. 4.18. Groundwater Potential Map of Bauchi-Alkaleri-Kirfi area 118

Fig. 4.19.Classification of Boreholeyield for different bedrocks in the Bauchi-Alkaleri-Kirfi area. 122

Fig. 4.20. (a) Bivariate plot of Nitrates vs Well Depth 127

Fig. 4.20. (b) Histogram showing the variation of NO_3 with depth 127
Fig. 4.21. Concentration of physical parameters in the Bauchi-Alkaleri Kirfi area based on bedrock types 130
Fig. 4.22. Bivariate plot of Well Depth vs EC 131
Fig. 4.23. Box and whisker for cations concentration in water samples 138
Fig. 4.24. Bar chart showing the NO_3 sources in wells in Bauchi-Alkaleri-Kirfi area 142
Fig. 4.25. Box and whisker for cations and anion concentration in water samples 144
Fig. 4.26 Concentration of chemical parameters in the Bauchi-Alkaleri-Kirfi area based on bedrock types 147
Fig. 4.27. Distribution of Anions and Cations in (a) Basement Aquifers and (b) Sedimentary Aquifers 149
Fig. 4.28. Active variables plot showing the distribution of the direction of the variousVariables(a).Variables (axes F1 and F2: 78.37 %), (b).Variables (axes F2 andF3: 23.11 %) 153
Fig. 4.29. Scree plot showing the distribution of the samples relative to the various PCA's 155
Fig. 4.30. (a) Distribution of WQI with Well Depth in Bauchi-Alkaleri-Kirfi area 161
Fig. 4.30. (b) Histogram showing the lithology based summary of WQI in the study area. 161
Fig. 4.31. (a) Bivariate of WQI with Well Depth in the study area 163
Fig. 4.32. WQI Map of Bauchi-Alkaleri-Kirfi area. 164
Fig. 4.33. The Wilcox diagram for groundwater samples inBauchi-Alkaleri-Kirfi Area (After Wilcox, 1955) 169
Fig. 4.34Spatial distribution of RSC, Salinity and MH in Bauchi-Alkaleri-Kirfi area 180
Fig. 4.35. Spatial distribution of SSP and Kelly Ratio in Bauchi-Alkaleri-Kirfi Area 181
Fig. 4.36. (a) Schoeller plots for Migmatite aquifers and

(b) Schoeller plots for Biotite hornblende granite aquifers. 183
Fig. 4.37. (a) Schoeller plots for Bauchite aquifers and
(b) Schoeller plots for Kerri Kerri aquifers 184
Fig. 4.38. Hydrochemical Facie Distribution map of Bauchi-Alkaleri-Kirfi area 186
Fig. 4.39. Hydraulic Head Distribution and groundwater flow pattern of Bauchi-Alkaleri-Kirfi area (Contour Interval 10m). 188
Fig.4.40. Combined Piper Trilinear Diagram for Water Samples from Bauchi-Alkaleri-Kirfi area 190
Fig. 4.41. Gibbs Diagram for Groundwater in Bauchi-Alkaleri-Kirfi area for
(a) Cation and
(b) Anions 194
Fig. 4.42. Chadha plot for Groundwater in Bauchi-Alkaleri-Kirfi area;
(a) Bauchite,
(b) Migmatite,
(c) Kerri Kerri
(d) Biotite hornblende granite 196
Fig. 4.43. Combined Chadha plot groundwater in the Bauchi-Alkaleri-Kirfi area 200
Fig. 4.44. Cross plots for (a) Ca^{2+} +Mg^{2+} and HCO_3, (b) Na^{+} and Cl^{-}, (c) Ca^{2+} +Mg^{2+} and total cations 203
Fig. 4.45.(a) Bivariate diagrams for $Mg^{2+}$and Ca^{2+} and
(b) Bivariate diagrams for $HCO_3^{-}$and Ca^{2+} illustrating silicate weathering as the predominant control mechanism. 204
Fig. 4.46Stable isotope ratios in natural water as controlled by chemical processes 206
Fig. 4.47. Plot of Isotopic ratios of samples and Meteoritic Water Line for Groundwater inBauchi-Alkaleri-Kirfi area. 209
Fig. 4.48. Scatter diagram of D-excess vs. $\delta^{18}O$ in Bauchi-Alkaleri-Kirfi area. 213
Fig. 4.49(a). Scatter diagram of Cl vs. δ 18O in Bauchi-Alkaleri-Kirfi area.
(b). Scatter diagram of NO_3 vs $\delta^{18}O$ in Bauchi-Alkaleri-Kirfi area 215
Fig. 4.50. Continental (latitude) Effects on Isotope Composition with Distance from the Coast Inland 217
Fig. 4.51.Cross-sectional Model Highlighting the Process of Evolution of Groundwater in Bauchi-Alkaleri 219

Fig. 4.52. A Flow Chart Highlighting the Process of Hydrochemical Evolution of Groundwater in the Study Area. 227

LIST OF PLATES

Plate 3.1(a) Exposure of granite gneiss,
(b) Boulders of Bauchite
(c) Weathered granite gneiss outcrop
(d) Weathered rock exposure in the Bauchi-Alkaleri-Kirfi area 51

Plate 3.2. (a) Dipping Beds of Kerri-Kerri Sandstone,
(b) Exposures of flat lying Sandstones Beds of the Kerri- Kerri in Kirfi area,
(c) A kaolin mine encountered at the Bauchi-Alkaleri-Kirfi area. 52

Plate 3.3. Field measurement of physico-chemical parameters using portable Multi-parametric meter. 56

Plate 3.4. Measurement of concentration of cations in a sample using the nebulizing hose. 59

Plate 4.1. An unprotected hand dug well in the Bauchi-Alkaleri-Kirfi area 142

LIST OF APPENDICES

APPENDIX I: Field Procedure for Vertical Electrical Sounding (VES) 252

APPENDIX II: Laboratory Procedures for Thin Sectioning and Granulometric Analysis 253

APPENDIX III: Laboratory Protocols for the Determination of Alkalinity of Water Samples 254

APPENDIX IV: Laboratory Protocols for the Determination of Concentration of Cations in Water Using Atomic Absorption Spectrometry 256

APPENDIX V: Laboratory Protocols for the Determination of Concentration of Anions in Water Using Ion Chromatogram 258

APPENDIX VI: Laboratory Protocols for the Determination of Ratios of Stable Isotopes of Oxygen and Deuterium in Water. 260

APPENDIX VII: Mathematical procedure for computation of Saaty's Consistency ratio (C.R) 261

APPENDIX VIII: Mathematical formulation for evaluating Water Quality Index 262

APPENDIX IX: The General Principles of Stable Isotope Studies 263

APPENDIX X: Details of the Aeromagnetic Data Processing 264

APPENDIX XI. Geophysical Type Curves 272

APPENDIX XII. Details of Primary Geoelectrical Parameters 289

APPENDIX XIII. Detailed Results of Hydrochemical Analysis 294

APPENDIX XIV: Result of Stable Isotope Analysis of Water Samples in Bauchi-Alkaleri-Kirfi area 302

CHAPTER ONE
INTRODUCTION

1.1 Background to the Study

The roleof the water in the lives of the entire human populace cannot be overstated, owing to the fact thatpotable supply of this resource has explodedin recent times with the ever increasing population of the world. The United Nations estimate that close to 1.2 billion humans do not have access to potable water supply (DPI, 2006). Consequently, the ultimate survival of the world's population would depend on the availability of clean and affordable water supplies. In order for such water supplies to be sustainable for human, agricultural and industrial needs, a proper management of freshwater resources becomes inevitable. Freshwater is a naturally occurring waterwith electrical conductivity of <1000 mg/l (Heath, 1983) and encompasses groundwater, surface water and glaciers.

The world water statistics revealed that 70% of the earth's globe is covered by water, out of which 97.5% is saline water, with remaining 2.5% representing freshwater sources. Unfortunately, about 70% of the freshwater sources are tied up in frozen ice and glacial areas, while the remaining 30% constitute groundwater and surface water with surface water constituting <1%). 100% of the ice and glacial water are frozen and thus unavailable for human use (UNEP, 1992; WGMS, 1998). However, surface water and groundwater which together constitute over 30% of the earth's freshwater remains the two most accessible sources of freshwater for human, agricultural and industrial utilization. According to Freeze and Cherry, (1979), groundwater constitute a third of world freshwater sources (Table 1.1).Although, rivers covers 231,059,898 km^2 of the earth's surface, the quantity of groundwater storage in aquifers is estimated at 1,000,000 mi^3 compared to 30,000 mi^3 in lakes and 300 mi^3 in world streams (Tijani, 2016).

Table 1.1. Availability the Global Water Sources (modified after Nace, 1971, UNESCO, 1999 and Healy *et al.,* 2007)

Source	Surface Area (10^6 km^2)	Volume (10^6 km^3)	Volume (%)	Availability/Status
Oceans and seas	361	1,370	97	Partly accessible, saline, high cost of treatment
Groundwater	130	8	0.5	Fresh, accessible, good quality and usually less susceptible to contamination
Icecaps & glaciers	17.8	27	2	Fresh, but inaccessible
Lakes & reservoirs	1.55	0.13	<0.01	Fresh, accessible, good quality and usually susceptible to contamination in most cases
Soil moisture	130	0.07	<0.01	Fresh, accessible, good quality and usually susceptible to contamination in most cases
Atmospheric	504	0.01	<0.01	Not accessible
Swamps	<0.1	<0.01	<0.01	Fresh, accessible, good quality and usually susceptible to contamination in most cases
River	<0.1	<0.01	<0.01	Fresh, accessible, good quality and usually susceptible to contamination in most cases
Biospheric water	<0.1	<0.01	<0.01	Not accessible

By implication, the volume of groundwater is 33 times greater than the volume of world fresh water lakes and 3333 times more that the quantity of world streams. Also, in terms of volume, groundwater cover over 90% of the available freshwater resources in the globe (Boswinkel, 2000) and approximately 1.5 billion humans rely on groundwater for their drinking needs (WRI, UNEP, UNDP, World Bank, 1998). The above statistics underscores the fact that groundwater is an invaluable resource, hence the need for sustainable management.These facts clearly underscore the prevailing role of groundwater as a valuable resource to human survival.

However, it is known fact that, adverse climatic condition associated with limited precipitation and drought, high rates of evaporation, unsuitable geological setting, increasing population which has resulted in rapid urbanization and industrialization all have great influence on surface and subsurface water resources (Todd, 1980; Foster *et al.*, 1998).

Therefore, there is no gain saying in the fact that groundwater remains the most valuable water resources that supports human existence, ecosystem diversity and economic growth and development. Owing to its impeccable qualities which include: good natural quality, availability, closeness to point of need, low susceptibility to contamination, low cost development, and resilience to climatic conditions, groundwater is undoubtedly a reliable water source in all geographic and climatic regions and for both third world and developed countries (Todd and Mays, 2005).

In many developing countries like Nigeria with a high rural population, groundwater constitutes a very vital source of drinking water, owing to comparatively low cost of development as compared to surface water. Unfortunately, the increasing mismanagement and overexploitation of water resources to meet the increasing water demands for domestic and industrial use have resulted to water scarcity, ecological degradation and pollution of freshwater resources in developing nations (Tsakiris, 2004). Therefore, proper management and protection of groundwater is correspondingly vital because of its significance to human life and economic activities (Chilton and Sieler, 1996). Especially in developing regions like Africa, which is home to over 800 million people (13 % of

world population) and where water supply problems is endemic (World Wide Fund for Nature, 2002).

Africa has the second largest groundwater storage in the world (5,500,000 km^3) and it is second to Asia with a total groundwater reserve of 7,800,000 km^3 (UNESCO, 1999). However, it is appalling to know that in spite of the abundant groundwater resources in Africa, the continent still remains the second driest in the World and millions of Africans still suffer from water scarcity (World Wide Fund for Nature, 2002). The fundamental issues responsible for the water supply issues in Africa can be summarized as inadequate investment in groundwater exploitation, poor groundwater management and sustainability culture, complex and diverse geology on one hand and poor understanding of the aquifers in this region, on the other hand, which has ultimately, resulted in a huge percentage of abortive borehole in the continent.

Furthermore, the aquifers in the parts of Africa has been described as low productivity aquifers (Wright, 1992), because a large part of the continent is covered by Basement Complex rocks of limited porosity and permeability. The scenario in Nigeria, which is the largest country in West Africa is good example of a country with aforementioned water supply problems. In Nigeria, the distribution and availability of freshwater resources from the northern to the southern parts is mostly driven by climate which is characterised by the equatorial type southwards, tropical at the middle and arid northwards. Annual precipitation ranged between 3000 mm - 4000 mm in the southern parts to about 250 mm to 500 mm around the northern zones, the national mean stands at 1180 mm (JICA Team, 2014).

As reported by FMWR (2011), Nigeria is endowed with 267,000,000,000 m^3 of surface water and 92,000,000,000 m^3 of ground water as compared to 244,000,000,000 m^3 and 142,000,000,000 m^3 reported by the JICA Team (2014) for surface and groundwater respectively. It is so perturbing that with all these large volumes of freshwater resources, 70,000,000 Nigerians lack potable drinking water, with about 50 million living in the rural areas (WSMP Nigeria, 2008). The shortage of safe water is more critical in the rural areas where electricity is usually unavailable or erratic, making the rural dwellers to rely upon

few functional hand pump boreholes and other surface water sources which are mostly susceptible to pollution. Consequently, it is not surprising that about 194,000 deaths involving mostly children of under 5 years of age are recorded annually in Nigeria (WHO AND UNICEF 2008 and UNICEF 2009).

The above scenario is somewhat disturbing, considering the huge amount of investments that have been committed to water supply by the Federal Government, the World Bank and Non-Governmental Organizations like Water aid, UNICEF, over the years, through various intervention schemes. The World Bank has completed several water projects in different parts of Nigeria, from 1985 to 2010 with a total investment of about US$1.4 billion. In addition, agencies like the African Development Bank, Chinese Government and the European Union have variously supported water and sanitation projects in Nigeria with several million Euros. Other external cooperation's like the JICA, UNICEF and USAID have over the years, supported similar programmes in different communities in the Northern parts of Nigeria (UNICEF 2007). In 2011, the Federal Government of Nigeria developed a Water Road Map for the improvement of the nation's water supply between 2011 and 2025.The Road Map which was aimed at providing 75% of Nigerians with potable water by 2015 and 90% by 2025 was funded by special intervention funds. In addition, the government has over the years (2010 to 2016) allocated billions of Naira to the water and sanitation sector, with highest being N112 billion in 2010 (Tijani, 2016).

In spite of all these investments and interventions, the water supply situation in Nigeria still remains bleak, as the Food and Agriculture Organization (FOA) stated during the celebration of World Water Day in 2012, that Nigeria and 47 other countries would experience water scarcity by 2025. Furthermore, the rationale behind the water supply issues in Nigeria can be attributed to corruption and insincerity on the part of the government, who use water projects as a means of gratifying the people that sponsored there election rather than delivering the dividend of democracy to the poor electorates. Based on the above premise, the choice of freshwater supply source in Nigeria, needs to be re-evaluated, considering that 50 out of the 70 million Nigerians without potable drinking water, are rural dwellers, it will be paramount to rely and invest in a freshwater resource that has a relatively widespread occurrence in both rural and urban areas, also, a

source that is sufficiently shallow to permit low cost exploitation, which is commensurate to low level of income in rural communities (Wright, 1992).The water source that exhibits the above attributes is obviously the groundwater resources, which is particularly superior to the surface water resources in terms of reliability, availability and as an economically viable source of potable water (Wright, 1992 and Lapworth *et al*., 2013). While surface water resources in Nigeria have their peculiar problems which include: attendant high cost of impounding, treatment, transmission and maintenance, electricity issues, susceptibility to contamination and limited geographical occurrence amongst others, the groundwater resources are constrained by the complex and diverse geology of Nigeria and erratic distribution of the resources within regolith and underlying bedrocks. Consequently, inadequate pre-drilling investigation of these groundwater resources has resulted to the emergence of high rate of abortive wells (Fashae *et al*., 2014).

Based on a survey conducted by National Water Supply and Sanitation Baseline Survey (NWSSBS), in 2006 and reanalyzed by JICA Project Team, there were about 38,000 boreholes in Nigeria consisting of 12,421 motorized and 25,470 hand pump boreholes, with a nationwide operating ratio of 47% and 57.9% for the motorized and hand pump boreholes respectively. By implication, as at 2006, only 54.3% (20,584) of the boreholes nationwide are in operation, with 46.7% (17,307) boreholes not operational. In 2013, the total number of boreholes in Nigeria has increased to 64,494 and if we assume that the operating ratio remains the same which is highly unlikely, the number of operational boreholes in Nigeria, as at 2013, would be estimated as 50.3% (32,464) leaving us with 49.7% (32,030) non-operational boreholes. The above assertion corroborates with the conclusion of MacDonald *et al*., 2012, who opined that about a third of the boreholes in Africa are not working, but the situation is even worse in Nigeria with close to 50% of the boreholes not functional. In addition, Edet, (1993) attributed the very high failure rate (80%) of boreholes in most rural localities to inadequacies in geological and hydrogeological surveys before the drilling of wells. Based on the above statistics, the alarming ratio of non-operational boreholes in Nigeria demand for improvement in technical capacity in groundwater resource exploration, exploitation and maintenance technology, for proper and long-term utilization of the resources (Tijani, 2016).Therefore, the panacea to the water problems in Nigeria, on one hand is massive and supervised

investment in boreholes, and on the other hand, understanding the geology and hydrogeology of the country.

This study covers the Bauchi-Alkaleri-Kirfi Geological Transition Zones (GTZ) of Bauchi NE-Nigeria. Such GTZ however, have been noted for their unique and problematic nature in terms of groundwater occurrence. The uniqueness of this terrain is attributable to the intricate coexistence of Basement Complex rocks and younger sedimentary rocks, which are normally associated with erratic lateral and basal contacts (Osinowo and Olayinka, 2012; Ariyo and Adeyemi, 2016). Groundwater development in such geological transition zones is challenging, due the erratic nature of the basement topography and uneven aquifer thicknesses which influences the distribution of the resource in such zones. Also, the fact that the Bauchi-Alkaleri-Kirfi transition zone falls within the semi-arid zone where water scarcity occasioned by supply inconsistencies and inadequacies of surface water bodies has necessitated reliance of the populace on groundwater in the peak of dry season. This problem is further escalated by the inadequate knowledge of the different aquifer systems in the area as the primary cause of borehole failures within the research area could not be ascertained. Consequently, over 100 boreholes are non-operational in the study location (BSWB, 2015). In another narrative, over 80% of boreholes drilled in some rural areas become abortive overtime (Edet, 1993). Furthermore, the inadequacies associated with the sanitation, coupled with proliferation of unprotected dug wells in Bauchi-Alkaleri-Kirfi is disturbing owing to the fact that parts of the Bauchi lies within the designated hotspots for cholera in Northeastern Nigeria (Elimian et al., 2018).

Additionally, in the face of the slow burning climate change, it has become paramount toexplore and fully understand the hydrogeologicalcharacteristics of an area, especially in semi-arid regions so as to ascertain the resilience of the groundwater reserves to climate change and for the sustainable management of the resource.

Thus, this study focuses on the characterising aquifers, delineating groundwater potential zones and assessing groundwater quality and recharge characteristics in Bauchi-Alkaleri-Kirfi geological transition zones for effective groundwater management and sustainability.

1.2 Aim and Objectives of the Study

Arising from the introductory background, the main goal of the study is to delineate and characterise aquifers in Bauchi-Alkaleri-Kirfi area, Bauchi, North eastern Nigeria, using combined geospatial, GIS, geophysical, hydrochemical and stable isotopes techniques with a view to fulfilling the following objectives.

The Objectives include:

1. to develop thematic maps for the different of hydrological factors using remote sensing and GIS.
2. to prepare and synthesize the thematic maps of subsurface hydrogeological attributes using geological and geophysical data.
3. to integrate parameters from item 1 and 2 above to delineate the groundwater potential zones using GIS.
4. to determine the spatial distribution of groundwater quality parameters, using hydrochemical analysis.
5. to determine recharge sources/isotopic fingerprints of groundwater using stable isotope techniques.

1.3 Justification

The Rural Water and Sanitation Agency (RUWASSA) Bauchi, recently expressed that only 40% of the populace have access to safe drinking water, while the remaining 60% which is tantamount to over 3 million people across the State do not have access to safe drinking water (People's Daily newspaper, 16 February, 2016). According to Elimian et al., (2018), a total number of 9405 case of cholera with 35 deaths was reported in 2018 in Bauchi state and this was attributed to inadequate or contaminated water sources, poor sanitation facilities amongst others. In the Bauchi-Alkaleri-Kirfi transition zone, there are clear evidences of such sanitation issues ranging from open defecation and agricultural runoffs from farmlands and more disturbing is the abundance of unprotected dug wells which creates a direct pathway for these contaminants to get into the groundwater in the area. As at 1981 the major water supply source to the people of Bauchi area is the Gubi

dam (Abdullahi *et al*., 2014), which serves only 36% of the urban populace, due to inadequate piped water coverage in the state (Usaid-suwasa .org / index. php/projects-and.../38-water-sector-reforms-in-bauchi-state). In recent times, the decay of the reticulations and pipe network in Bauchi area, over time, has further compounded the water problem, leading to the construction of boreholes and dug wells by the non-governmental organizations and the federal government to cushion the effect of inadequatewater scarcity in the state. Consequently, there was an increased dependence of the populace on the available groundwater sources (boreholes and hand dug wells). However, 10-55% of boreholes drilled in Bauchi state are unproductive (with over a 100 abortive boreholes within the study area alone), largely due to poor and improper predrilling investigations or poor understanding of aquifer systems (BSWB, 2015).

In view of the above, there is a need for adequate understanding of the subsurface aquifer medium through detailed hydrogeophysical and hydrogeological mapping. This would assist in the selection of productive sites for construction and development of boreholes thereby forestalling the drilling of abortive wells. Furthermore, groundwater exploration in purely basement and sedimentary terrains are often fairly unambiguous and entails delineation of the overburden, weathered and fractured aquifers in the former or saturated sandy or gravely aquiferous units in the latter, however, geological transition zones are noted to be problematic in groundwater potential and development, due to the erratic and complex nature of the subsurface lithologies (Osinowo and Olayinka, 2012 and Ariyo and Adeyemi, 2016). Such occurrence of complex geological structures coupled with the erratic nature of the basal/lateral contacts in typical basement/sedimentary contact zone implied problematic hydrogeological setting. The Bauchi-Alkaleri-Kirfi areais a typical geological transition zone, where the undefined basal and lateral rock boundaries and associated groundwater problems. Numerous occurrences of borehole failures and dry wells especially in the poorly defined contacts between the basement rocks and the sandstones in the study, can be partly attributed to poor aquifer materials, partially penetrated aquifers or erratic basement topography.

In view of the above, several researches have been conducted to unravel the lithologicalintricacies in different geological terrains in different parts of the country using geophysical and geological methods (Acworth, 1981; Umaru and Schoeneich, 1992;

Shemang, and Jiba, 2005, Osinowo and Olayinka, 2012 and Ariyo and Adeyemi, 2016). However, the quality, hydrochemical and isotope characteristics of groundwater in GTZ, which seem to be extremely consequential for the long-term conservation of the groundwater resources have also not received much attention. This study therefore attempts to delineate and characterise the aquiferous units in the Bauchi-Alkaleri-Kirfi GTZ on the basis of groundwater potential, quality, hydrochemical evolution and recharge source, for sustainable management of the groundwater resource. Such integrated approach will characterise the potential zones for groundwater exploitation (geospatial and geophysical assessment), while the hydrochemical and stable isotope studies will characterise the aquifers in the area in the light of the groundwater chemical character, and residence time with a view to safeguarding human health and understanding the sources of groundwater recharge.

1.4 Scope of the Study

In line with the objectives of this study, a systematic methodological approach was followed which include;

a) Desk work: the desk work entailed preliminary assessment of the research work, through gathering and evaluation of existing literatures and well inventories. Also, other secondary data (remotely sensed and aeromagnetic data) was acquired.
b) Field Study: the field work involved geological mapping, geophysical mapping using vertical electrical sounding and sampling of groundwater hydrochemical and isotope analysis.
c) Laboratory Studies: the laboratory techniques entailed hydrochemical and stable isotope analysis of groundwater samples. In addition, petrographic studies of the basement rocks (to ascertain their mineral composition) and granulometric analysis of the sedimentary units were carried out, for better understanding of the water rock interaction and hydrochemical evolution.
d) Data Evaluation and Statistical Analysis: this entailed the generation of thematic maps in GIS environment, the analysis of aeromagnetic and

resistivity data using relevant software's and hydrochemical/ isotope data analysis using descriptive statistics analysis and hydrochemical plots.

1.5 Overview of Previous Works

Different researchers worldwide have employed various techniques in the characterisation of aquifers and delineation of potential zones for groundwater exploitation. A review of past researches relating to the utilization of remote sensing /GIS, hydrogeophysics, hydrochemistry and stable isotopes techniques in characterising aquifers and delineating groundwater potential zones, covering related researches done outside the shores of the continent and within the country, as well as within the domain the study was undertaken. The researches reviewed for the present study will be grouped into 3 thematic areas on the basis of the research focus and geographical location. The first group would provide an overview on the use of remote sensing, GIS, geophysics (VES), hydrogeological and hydrochemical approaches in the global context and in Nigerian and with emphasis on basement and sedimentary areas. The second group however, would focus on the overview of studies relating to remote sensing, GIS, geophysics (VES), hydrogeological and hydrochemical approaches in Bauchi area. The third aspect would give a summary of applications of stable isotopes in groundwater studies in the global, national and local context.

While some researches have applied remote sensing to analyze several thematic maps, but have assign weight to the thematic layers using personal discretion e.g. Bobba *et al.* (1992); Salama *et al.* (1994); Teewu, (1995) and Dar *et al*. (2010). Other studies have gone a step further to combine RS/GIS with frequency ratio, numerical modelling amongst others and exemplified by the works of Srivastava and Bhattacharya, (2006); Madrucci *et al.* (2008); Murthy and Mamo, (2009); Machiwal *et al*. (2011); Magesh *et al.* (2011); Mukherjee *et al.* (2012); Fashae *et al*. (2014); Mogaji *et al.* (2015) and Arnous, (2016).

Bobba *et al*. (1992) applied remotely sensed data to characterise groundwater regimes in Otter Creek basins in Canada on the basis of the depth to water table in recharge, discharge and transition areas andconcluded that remote sensing is a very useful tool for aquifer delineation. Salama *et al*., 1994, combined aerial photographs and Landsat imagery to decipher the mechanism controlling groundwater discharge and recharge in

Western Australia, utilising thematic maps for structures, geology and geomorphology and concluded that the permeable areas made up of the sand plains were good recharge zones. Lachassagne *et al*. (2001), characterised aquifers in Truyere catchment in central France using MCDA and GIS techniques to map the groundwater potentiality. Madrucci *et al*., 2008, employed multi-criteria decision technique and GIS to prepare groundwater map of part of the Basement Complex terrains of Sao Paulo State, Brazil and concluded that the integrated approach is an efficient technique in mapping groundwater favorability. Dar *et al*. (2010), conducted groundwater prospects evaluation based on hydrogeo-morphological mapping using geospatial methods in Tamil Nadu, India. Magesh *et al.* (2011), delineated groundwater potentiality in Tamil Nadu, through integrated remote sensing/GIS and Multi-influencing factor techniques. Machiwal *et al*. (2011), demarcated four groundwater productivity potential areas in Udiapur district of Rajasthan, western India through remote sensing/GIS and MCDM methods. Mogaji *et al*. (2015) also carried out a groundwater productivity potential mapping in Peninsula Malaysia using a GIS-based prediction model. The results showed the efficacy of the model in reducing the uncertainty related to the predictive potential zones. Shahid and Nath (2002), integrated vertical electrical soundings with remote sensing/GIS to investigate the hydrogeology of sedimentary areas in West Bengal, India. Hadithi *et al*. (2003) integrated VES with remote sensing/GIS to investigate the hydrogeology in the Basement Complex regions of India. A groundwater productivity map was generated through the integration of several relevant thematic layers (i.e. aquifer thickness, depth to water table, overburden thickness, drainage, slope, lineament and hydrogeomorphology) in Arc Info platform. Srivastava and Bhattacharya (2006) conducted a groundwater evaluation in the Basement Complex areas of India using resistivity and remote sensing/GIS approaches. Sub-surface thematic layers for resistivity and aquifer thickness were derived from resistivity surveys and integrated with remotely sensed and other auxiliary data, which accurately captures the methodology for the present study except for the fact that the present study will be undertaken in a geological transition zone with a more complex geology.

In the African context, Teeuw, (1995), employed the remote sensing /GIS approach to characterise borehole sites in parts of Ghana and concluded that the success rate recorded for the remote sensing/GIS approach was 55% compared to the 5% for aerial photographs.

Also, in arid South Sinai in Egypt, Arnous, (2016), studied groundwater potential zones, through geospatial methods. In Nigeria however,suitable zones for groundwater exploitation in Calabar, SE-Nigeria was demarcated by Edet*et al*., 1998, using GIS/geospatial techniques. Remotely sensed data and aerial photographs were used to define surface hydrologic and hydrogeological parameters in parts of Cross River. Fashae *et al*. (2014), deployed an integrated MCDA, GIS and remote sensing techniques to characterise the potentiality of groundwater resource in the southwestern Nigeria. The results, clearly indicated the efficiency of the integrated approaches, as a viable methodology for reliable evaluation of groundwater resources. It is essential to emphasize that there is no record of studies relating to deployment ofGIS and geospatial technique to delineate and characterise aquifers, either in the entire Bauchi area or even the study location, making the present work the first of its kind in the Bauchi-Alkaleri Kirfi zone where there is a challenge of recurring borehole failure and dry wells. Another technique to be considered for the present study is the geophysical technique.

Furthermore, Omran, (2008), applied geospatial/GIS, electrical resistivity and aeromagnetic survey for characterisation of different groundwater potential zones, in Egypt and concluded that integrated approach gives a more reliable groundwater productivity map of an area. The integrated approach adopted by Omran (2008) is similar to that of the present study except for the fact that the present study was conducted in a more diverse geology setting (basement and sedimentary transition zone). Also, the MCDA approach and lineament density thematic was considered for in the present study to improve the reliability of the result. Jha *et al.* (2010) estimated the potentials of groundwater in parts of India using geospatial, multi-criteria decision and geoelectrical technique, using hydrologic and hydrogeological data. Sultan *et al.* (2013), studied the water table in El Qaa Plain, South Sinai, Egypt using integrated optical and radar RS and geophysical data. The drainage networks pattern of the area was digitized from DEM, flow direction of the main channels and the water table maps constructed from interpreted geoelectrical data indicates the hydraulic head decreases from the east and north towards the west. Arising from the above review of integrated remote sensing/GIS and geophysical approach, it would be observed that all the works reviewed are limited to India and North Africa, this is because no literatures has been sighted on similar works in West Africa or

even Nigeria. Hence, making the present study, a good contribution to the existing knowledge gap in Nigeria as a whole and in West Africa.

Other similar studies have combined RS/GIS with hydrochemical data in order to prepare water quality index maps e.g.Yammani, (2007); Balakrishnan *et al*. (2011), Selvan *et al.* (2012), Nur *et al*. (2012), and Hussien *et al*. (2017). Yammani 2007, utilized GIS to delineate groundwater quality zones in Chittoor area, Andhra Pradesh India. Balakrishnan *et al.,* (2011), used groundwater quality data from 76 locations to prepare spatial distribution maps for water quality and a groundwater productivity potential map of the Gulbarga city in India city. Selvan *et al*. (2012) assessed the hydrochemistry and groundwater quality of aquifers of Tamil nadu, India using GIS analysis. In Africa,Hussein *et al*. (2017), integrated remote sensing, geophysics, stable isotopes, field and hydrochemistry to delineate aquifer zones in Wadi Qena Basin, Eastern Desert, Egypt and concluded that the area is characterised by deep seated fractures and the groundwater reflected end members, mixed groups and one evaporated group. The study improved the understanding of the role of structural control and modern recharge in exploration of aquifer potential in arid environments. Hence the interest in using such models in the present research to evaluate the influence of structures and residence time (groundwater) in both sedimentary and basement aquifers in the semi-arid aquifers of Bauchi-Alkaleri-Kirfi transition zone. Nur *et al*. (2012) investigated the relationship between the hydrochemical facies and groundwater flow regimes in Damaturu, Northeastern Nigeria using the hydrochemical and geospatial approach.

Before the advent of the geospatial techniques, the geophysical method, especially the electrical resistivity method, has overtime proved to be reliable in aquifer delineation and characterisation of groundwater potential zones. Many workers have successfully used the DC resistivity, in groundwater studies. Some researchers have used the resistivity method solely or in combination with hydrogeological study.

Velpen (1988) and Zohdy (1989) interpreted of DC soundings in 32 stations, using some automatic interpretation software to show the boundary between aquifers of different geologic terrain in the Netherlands, and concluded that the Quaternary aquifer unit constitute of sand and gravel. Miller *et al*. (2008), integrated static ERT inversions, time-

lapse ERT images with hydrologic data to evaluate seasonal changes in subsurface moisture within an experimental Watershed near Boise, Idaho, U.S.A. In Germany, Kemna *et al.* (2006) and Muller *et al*. (2009) have differently studied the permeability and dispersivity distribution in heterogeneous aquifers through analysis of time lapse direct current resistivity data in Germany. Metalway *et al.* (2012), integrated 1D and 2D resistivity surveys to characterise the aquifers and groundwater productivity potential in the central part of Saudi Arabia. The interpretation of 1D and 2D resistivity data revealed the depth to basement in the area. Chilton and Foster, (1995), conducted a hydrogeological and water supply potential study of Basement Complex rocks in parts of Africa and concluded that basement aquifers in the area are vital sources of water for the rural population, but are often limited by permeability and the occurrence of groundwater in such aquifers is more favourable in humid than arid climates, hence making the present work particularly significant as it is located in a semi-arid terrain. Also, Attawa *et al*. (2014), employed electrical resistivity inversion schemes to characterise groundwater occurrence in part of Egyptand concluded that the integrated approach constitute a reliable technique for aquifer characterisation in the Nile area.

In the Nigerian scenario, Ishola *et al*. (2013) assessed the groundwater productivity potential of the Basement Complex rocks of Ibadan using resistivity sounding. The study was aimed at delineating groundwater potential zones using resistivity soundings. The result revealed a three to four geo-electric layers and the iso-resistivity maps which showed the distribution of the aquifers was useful in mapping promising areas for groundwater exploitation. Salami and Olorunfemi, (2014), evaluated the groundwater potential of the central part of Ogun State, SW Nigeria using thirty VES, combined with hydrogeological data to characterise the aquifer units and subsurface sequence. Olasehinde *et al. (*2015), studied the aquifers around Agaie area in Niger state, using electrical and hydrogeological techniques. The study revealed variation in depth of the aquifers inthe area and the resistivity trends coincides with general lineament trends in the basin and also the direction of flow of groundwater.

In Bauchi area, Ako and Osundu (1986) studied aquifers in Kerri-Kerri Formation in Darazo, using the electrical resistivity method because it was observed that results from

existing borehole data showed the erratic nature of the Paleocene Kerri-Kerri Formation as an aquifer, Ako and Osundu (1986), however, concluded that the areas with the highest traverse resistance (T) corresponded to the zones of high productivity and yield. Furthermore, understanding the subsurface complexity of the Kerri-Kerri Formation vis-a-vis aquifer characteristics becomes consequential and would be better addressed through a multidisciplinary and integrated approach, making this study relevant to the understanding and characterising aquifers.

Furthermore, some notable examples of hydrochemical works relating to hydrogeochemical assessment and water quality are shown by Tijani, (1995); Abimbola, (1999); Olatunji *et al.* (2005); Omotoyinbo and Okafor, (2008) Talabi, (2013); Ravikumar and Somashekar, (2017). Ravikumar and Somashekar, (2017), employed hydrochemical facies studies and multivariate principal component analysis to investigate the quality of groundwater in Varahi river basin, in India. In the Nigerian context, Abimbola *et al*. (1999), conducted a hydrochemical facie assessment of Abeokuta area, SW-Nigeria which revealed the dominance Ca-HCO_3 type groundwater type in the Omotoyinbo and Okafor (2008) investigated the impact of rocks on groundwater chemistry, in SW Nigeria (Ado-Ekiti) and reported that mineral dissolution from bedrocks greatly influences the overall chemistry of the groundwater. Furthermore, Talabi *et al.* (2013), found the surface water in the central zone of Ekiti to be of good drinking quality following a hydrogeochemical study of surface water in the area.

In Bauchi area there is a general paucity of research works relating to remote sensing and GIS. Acworth (1981) noted that while geospatial data, such as Landsat imagery, covering most places, including the Bauchi-Alkaleri-Kirfi transition zoneis available, theanalysed forms of this imagery are generally unavailable, which posed a severe limitation. However, with the development of digital techniques like the GIS which will be employed in this present study, a greater degree of accuracy will be achieved in aquifer characterisation.

The geophysical investigation conducted by Edok–Eter Mandilas Nigeria limited (1976 - 1979), is among the earliest geophysical works done to determine the hydrogeological conditions in specific towns and villages in Bauchi area. The company employed Aerial

photographs, seismic refraction and electrical resistivity methods. Acworth (1981), also assessed the hydrogeology of some basement rocks in Bauchi area using hydrological and electrical methods. The assessment of the groundwater potential in Bauchi area was evaluated through combination of estimated recharge rates in the area and the aquifer storage (estimated). Nur *et al*., 2005, carried out a seismic refraction and vertical electrical sounding tostudy groundwater occurrence inBauchi and environs. The result obtained revealed 3-4 geo-electric layers with the aquifer being the weathered and or fractured basement.

A number of workers have also employed hydrogeological techniques and sometimes in combination with other methods to characterise aquifers: Carter *et al.* (1963), Hazel *et al.* (1963), Schroeder (1974), Umar and Schoeneich (1992). Carter *et al*. (1963) worked on the geology, hydrology and chemical quality of most part of Northern Nigeria. Hazel *et al*. (1963) reviewed the characteristics of regolith aquifer and their dependence on geology and environment with particular emphasis on lithology, weathering pattern and fracturing in Bauchi, Kano and Sokoto States. Schroeder (1974) also discussed the hydrogeological condition in Bauchi and its environment and concluded that the groundwater is stored in the superficial weathered mantle derived from crystalline rock of the basement complex. Umar and Shoeneick (1982), described the hydrogeological properties of the aquifers around Bauchi using field observations and measurement in wells, pumping test, chemical and biological test. Furthermore, Shemang, and Jiba (2005), also studied the groundwater prospects in hard rock aquifers in western part of Bauchi, with a view to delineating areas of high potentials for groundwater. The study which was used to evaluate relationship between rock types and aquifer productivity showed that the granites have high aquifer potential owing to higher yield and higher specific capacity, followed by granite gneiss. The other rocks exemplified by the hornblende biotite granites, biotite granite gneiss, and undifferentiated gneisses, revealed poor groundwater potential. The present study would however, employ an integrated approach which would better tackle the problem. It is important to note that no attempt has been made at using such results to provide a more systematic characterisation of aquifers in the form of aquifer potential maps, groundwater quality maps, and overburden protective capacity maps in the Bauchi-Alkaleri-Kirfi area. Akaha and Promise (2009) also evaluated the hydrogeological properties of the aquifers in

parts of the Kerri-Kerri Formation from boreholes pumping test data in Azare area of Bauchi, N-E Nigeria. The pumping test data revealed poor hydraulic properties of the Kerri-Kerri aquifers and concluded that the available boreholes are inadequate for agricultural and domestic needs of the area. This conclusion is in line with the observation of Ako and Osundu (1986) on the Kerri-Kerri Formation. Hence, creates a need for further studies to ascertain the groundwater potential of the Paleocene Kerri-Kerri aquifers.

Furthermore, some notable examples of hydrochemical works relating to hydrogeochemical assessment and water quality in Bauchi are shown by Dupreeze and Barber, (1965); Dike et al. (2008); Istifanus et al. (2013).Dupreez and Barber (1965) conducted hydrogeochemical investigation of most of the rock formations in northern Nigeria and summarised that the Basement Complex waters are mostly calcium or sodium bicarbonate water type, with high nitrate values. While the samples from the sedimentary zones of Northern and Southern parts of the Benue basin revealed high content of iron especially in the older sedimentary units (Bima and Yolde Formation). Dike *et al. (*2008) conducted a hydrogeochemical study of Railway area in Bauchi metropolis with a view determining the groundwater quality in dug wells and its suitability for consumption. The study reported the groundwater are generally good with few exceptions where Na and Cl is high. Istifanus *et al*. (2013) investigated the physicochemical properties of water in Ganjuwa and Dass areas of Bauchi area to ascertain its suitability for human consumption. However, it is worthy of note that apart from the international work reviewed and some of the works in southwestern parts of the country, which studied the hydrochemical facies characterisation and also evaluate groundwater quality, all other works especially those in the study region dwelt largely on groundwater quality evaluation, rather than the evolution of the groundwater types as determined by their hydrochemical facies. Hence, the need for the present study which fully captures the evolution of the groundwater types, the quality index and also the hydrochemical facies

A few researchers have used stable isotope technique solely or alongside hydrochemistry in groundwater studies in the Nigerian context (Diop and Tijani, (2009); Lapworth *et al.* (2013); Talabi and Tijani, (2013); Faitouri and Sanford, (2015). Faitouri and Stanford, (2015), also conducted stable isotopes analysis of water and ^{14}C activities to estimate

recharge timing and paleo climatic conditions during recharge for three sandstone aquifers in Libya and concluded that the greater activity is likely due to the lowering of the regional potentiometric surface causing younger water to be captured after four decades of well field operation. Furthermore, Lapworth *et al.* (2013) studied resilience of groundwater from shallow aquifers to climate in West Africa using isotope techniques. Stable-isotope results from the study revealed the dominance of meteoric recharge and residence time of 32-65years. Diop and Tijani, (2009), also used hydrochemical and stable isotopes technique to investigate the hydrogeological and hydrochemical profiles of groundwater conditions in the crystalline basement rocks of Eastern Senegal and arrived at the following conclusions: The results demonstrated the use of isotopes together with major ion chemistry as a convenient tool in hydrogeology, as proposed by the present study. In Nigeria, Tijani and Abimbola, (2003), assessed the hydrochemistry and isotopes ratios of saprolitic aquifers at Oke-Ogun area, S.W Nigeria. The surface and subsurface waters in the parts of Sokoto Basin was characterised by Adelana *et al.* (2003), using geochemical and stable isotopes techniques. Talabi and Tijani (2013), also studied the hydrochemistry, water quality and the stable isotope assessments of Basement Complex aquifers in Ekiti State, S.W Nigeria and concluded that the recharge source is meteoric, with limited migration and low water-rock interaction as indicated by the TDS. Isotopic studies undertaken by Edmunds *et al*. (1999), indicates that groundwater from the lower and middle aquifers are 20,000 years or more

However, it is important to note that most of the researches reviewed especially under the remote sensing /GIS technique, were conducted outside the shores of Nigeria, with only few exceptions i.e. Edet *et al.* (1998) and Fashae *et al*. (2014) and a very few others not mentioned in this review, constitute the few notable works of international standard in the country. By implication, studies involving the deployment of geospatial /GIS technique in the groundwater mapping in Nigeria especially in the northern parts of the country are limited, hence the need for present study. In addition, very limited researchers worldwide have integrated remote sensing /GIS with airborne and ground geophysics. Thus, the present work will be the first of its kind in Nigeria and a contribution to knowledge in the world at large. Furthermore, this multidisciplinary approach has rarely been applied in areas with complex and multifaceted geology (Transition zones) as exemplified by the

Bauchi-Alkaleri-Kirfi transition zone and with the recent advancement in remote sensing /GIS technology, a newer version of the ArcGIS software's (10.31 version) and higher resolution input data like the modern aeromagnetic data and Landsat 8 and Aster data will be utilized for the present study. Hence, this research is relevant in understanding the aquifers in Nigeria. In the geophysical aspect, the aeromagnetic technique has rarely been used for groundwater and aquifer studies. The present work has on one hand tried to compare the efficacy of geological structures obtained from remotely sensing (a high definition spot 5) and those from modern aeromagnetic data, with a view to assessing their importance in aquifer characterisation. On the other hand, the present study has integrated modern aeromagnetic studies with the D.C resistivity techniques to delineate groundwater potential zones.

According to Lapworth *et al*. (2013), in recent decades, groundwater isotopes have proved to be valuable tools in determining groundwater recharge and residence time in different parts of the North America, Australia and Europe. However, in the Africa, scanty researches have employed environmental traces groundwater studies. The present work will therefore contribute to the knowledge of stable isotope studies and also breach some of the knowledge gap that exist in Nigeria and Africa at large.

Also worth noting is the fact that previous works in the Bauchi-Alkaleri-Kirfi area are either too regional or too localized and mostly focused on Bauchi metropolis and the northern parts, little or no work has been done in the southeastern zones where the Bauchi-Alkaleri-Kirfi transition zone lies. In terms of the techniques employed, it is necessary to emphasize thatgeospatial, GIS and the stable isotope studies have rarely been applied in thisarea. Also, most of previous works have studied the hydraulic properties of the aquifers from existing pumping test data which are often limited to areas with such data, the geophysical works mainly focused on groundwater prospecting rather that aquifer characterisation, while the hydrogeochemical investigations were centered towards water quality. However, the integration of the above conventional methods (Hydrogeophysics and Hydrochemistry) and remote sensing /GIS and Isotope studies have not received much attention, especially along the lines described in the presentstudy.

CHAPTER TWO

LITERATURE REVIEW

2.1 Location of the Study Area

The Bauchi-Alkaleri-Kirfi lies in the southeastern part of Bauchi State within latitudes and longitude $10^0 00'$N –$10^0 30'$N and $10^0 00'$E –$10^0 30'$E (Fig. 2.1) respectively. The areacovers a total area of 3025km^2 and lies exactly.

The area can be assessed by one major highway roads i.e. the Gombe-Bauchi expressway and several minor roads; Futuk-Alkaleri and Kirfi-Alkaleri roads and Mainamaji-Dindima roads which all link the prominent towns and numerous minor roads and foot paths connecting the villages and farmlands. The Bauchi-Alkaleri-Kirfi area is heterogeneous, with tribes like, Hausa, Fulani, Jarawa, Tangale, Waja, Kirfawa, Sayawa and Tarewa. The major occupations are: farming, trading, cattle rearing and fishery.Major food crops cultivated are rice, millet, maize, sorghum, and other cash crops like beans, groundnut, millet and sugar-cane. Vegetables, pepper, tomatoes and garden egg.

2.2 Topography and Drainage

The region is distinguished by hills that reach an elevation of 706 meters in the northwestern parts and southern regions of the area.The lowlandscorresponds to stream

channels with elevations reaching 275 m. The tributaries of the Gongola River notably the Dindima, Mansuri, Yashi Rivers, which flow through the area, drain the area. The upstream of the Gongola River is located in the Jos Plateau and downstream section is to the Gongola Basin, trending in the northeastern direction until Nafada in Gombe State.

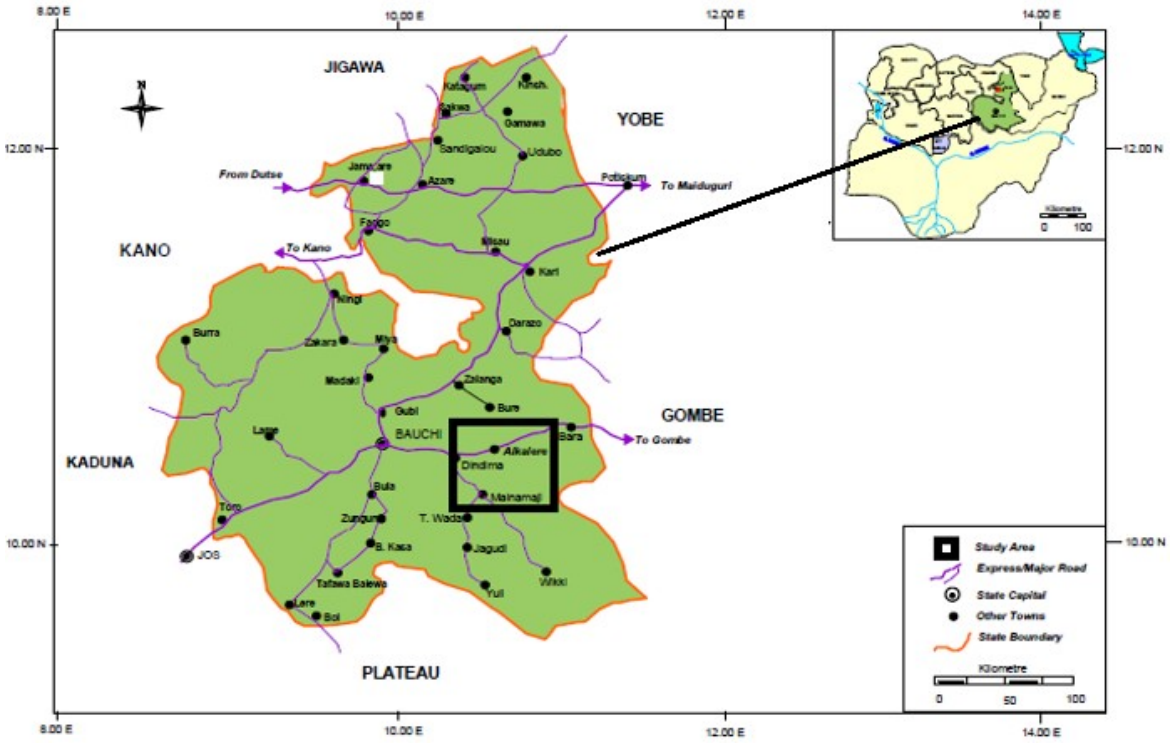

Fig. 2.1. Admistrative Map of Bauchi-Alkaleri-Kirfi area(Modified after Ministry of Land and Survey, Bauchi State 2008).

The Gongola River trend changed southwards and then southeast until it meets the Hawal River in Adamawa State (Ruben 1970). The lower courses of the River Gongola are impounded by two dams: the Dadin Kowa Dam near Gombe, and the Kiri Dam. Following construction of the Kiri dam. A decline in downstream flood peaks occurred from 1,420 to 1,256 cubic m^3/s, while dry season flows increased from 5.7 to 21 m^3/s.

The Gongola River passes through Bauchi State in Tafawa Balewa in the southern part and in Kirfi and Alkaleri in the eastern part of Bauchi, (Fig.2.2). The Bauchi-Alkaleri-Kirfi transition zone is drained by Dindima River, the Mansuri River in the eastern parts, which is a major tributary and the Yashi River in the southwestern corner of the area coupled with other smaller streams which constitute tributaries of the Mansuri and Yashi River, all together forming a dendritic drainage pattern in the area.

2.3 Climate and Vegetation

Two distinct seasons characterise the Bauchi-Alkaleri-Kirfi area. The wet season which runs from April to October and the dry one which runs from the eleventh calendar month of November to March (Fig 2.3). The highest rain in is usually recorded in the month of August (500 mm) and occasionally in July, with the lowest reported in April and October (less than 100 mm). The rainfall begins in the south and are set in motion by the southwesterly prevailing winds,as a result, the northward dryness increased, eventually igniting the desert condition on the northern borders.. The annual average rainfall in the Bauchi-Alkaleri-Kirfi area ranges between 700mm in the north to 1300mm in the south. The monthly variation of relative humidity in the area show similitude with the precipitation pattern (Fig. 2.3). The pattern is unimodal, exhibiting low amounts (20-40%) between January to April. The relative humidity begins to rise in May and attains its maximum (80 percent) in August before descending to about 30 percent in December.

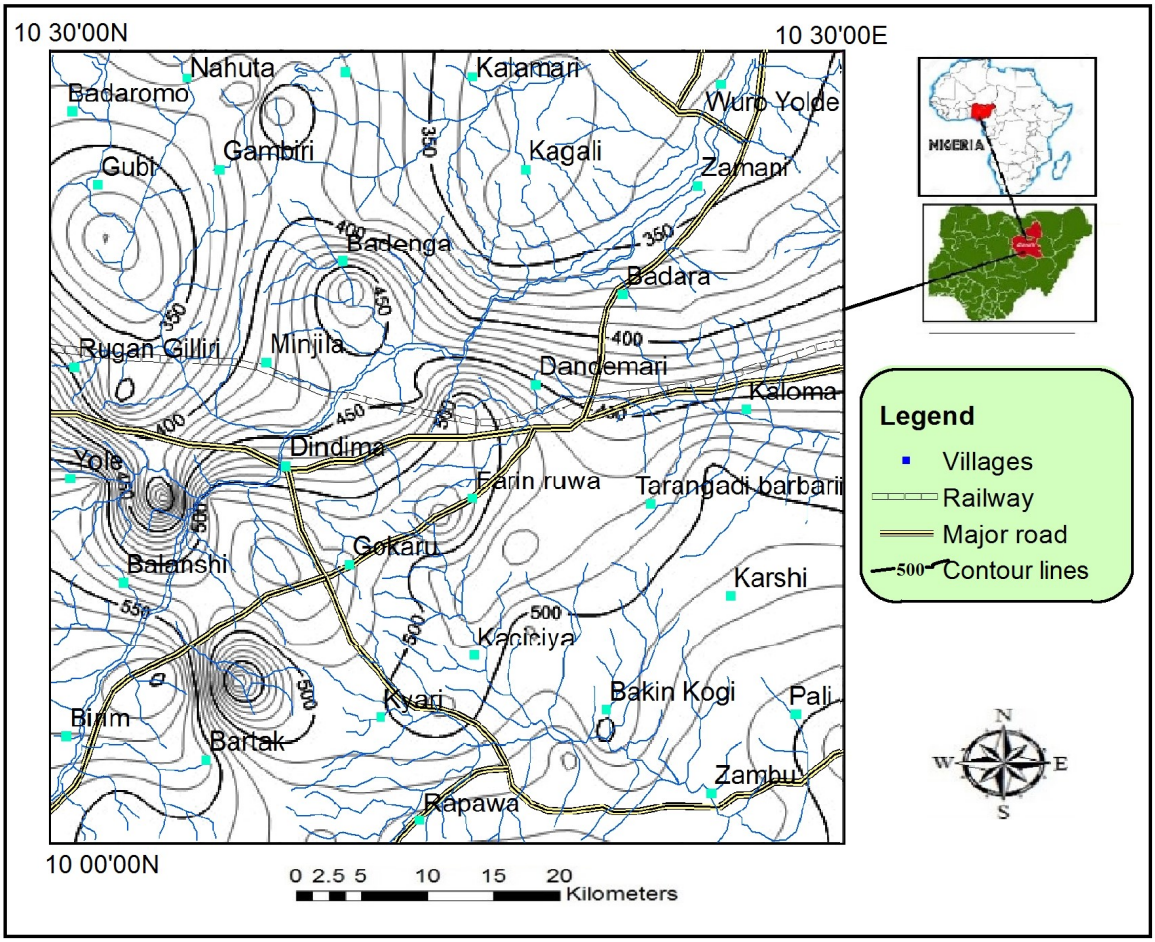

Fig. 2.2. Drainage and Topographic Map of Bauchi-Alkaleri- Kirfi Area

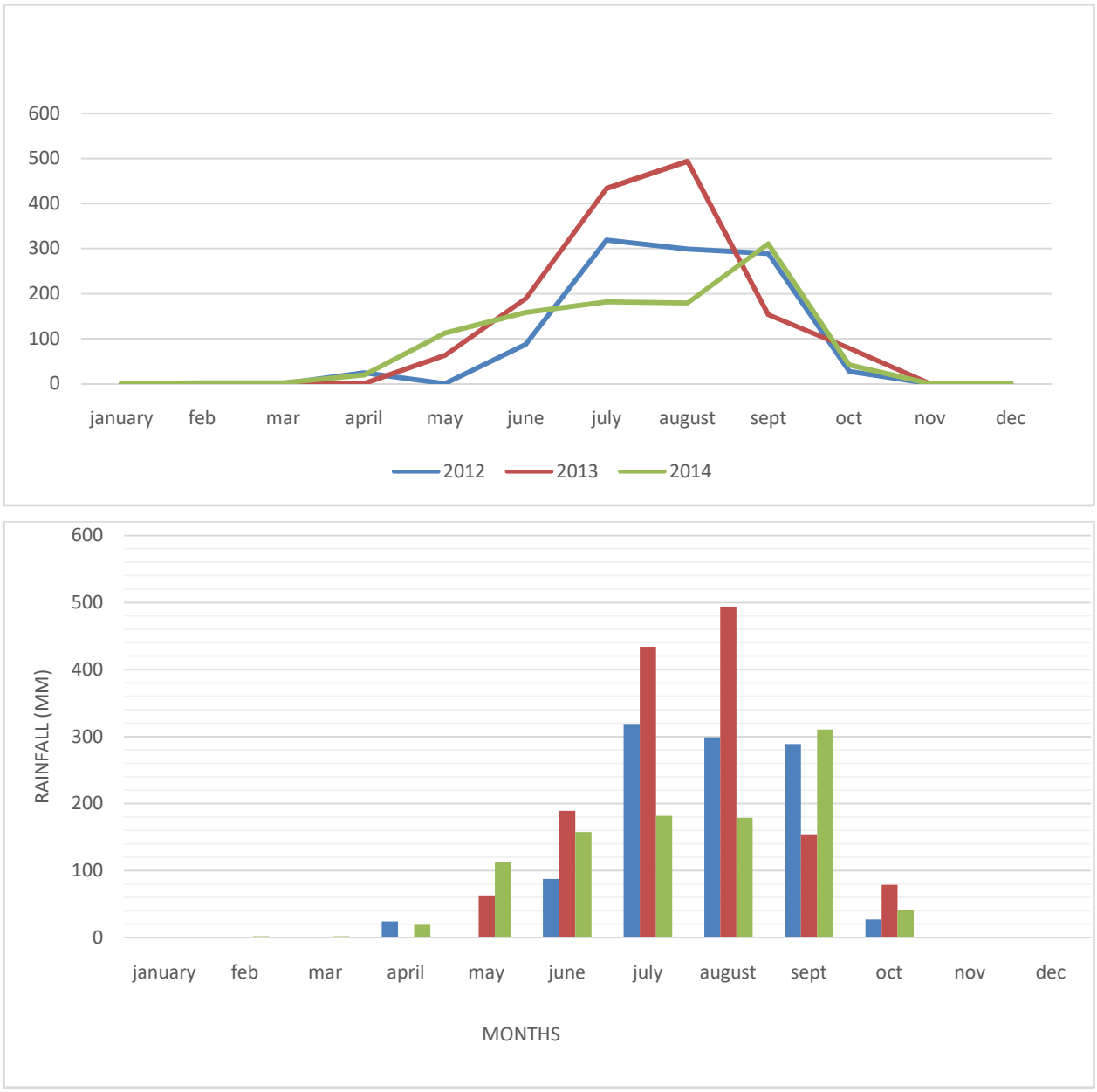

Fig. 2.3. Mean Monthly Rainfall of Bauchi from 2012-2014 (Modified after Buba *et al.*, 2015)

The monthly variation in temperature (Fig. 2.4) in Bauchi area varies between 25^{o}C to >33^{o}C in December and February respectively and the temperature distribution is somewhat uniform when compared to the rainfall and humidity. The dry season may be marked by a rapid drop in temperature to about 11.7^{0}C between December and January (Eludoyin, 2011; Buba *et al.*, 2015).

The vegetation is characteristic of the Sudan Savannah type, with trees and plants widely scattered (Acworth, 1981). The vegetation belt of Sudan Savannah stretches from the Sokoto plains in the west, passing through the northern zones of the central highland. The low yearly rainfall (< 1000 mm) and the extensive dry spells (6-9 months) can only nourish limited trees and relatively shorter grasses. The Sudan Savannah is typified by abundant short grasses and few dwarfed ($\leq$15m). Furthermore, mixed farming practice, especially cattle rearing aspects, is also a major cause of devastation of vegetation.

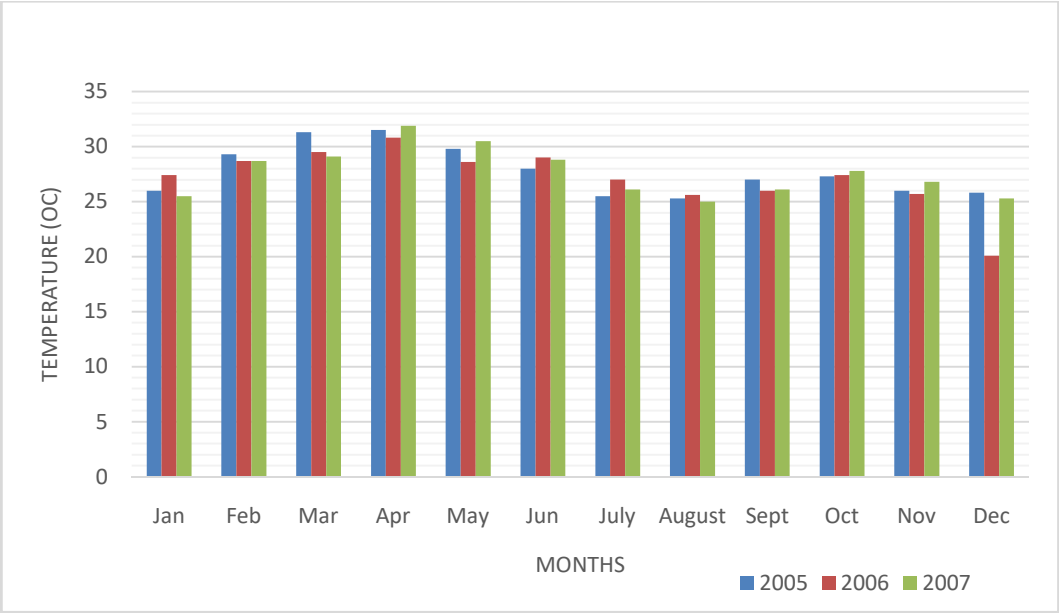

Fig. 2.4. (a) Mean Monthly Temperature for the Study area (2005-2007) (Modified after Buba *et al.*, 2015)

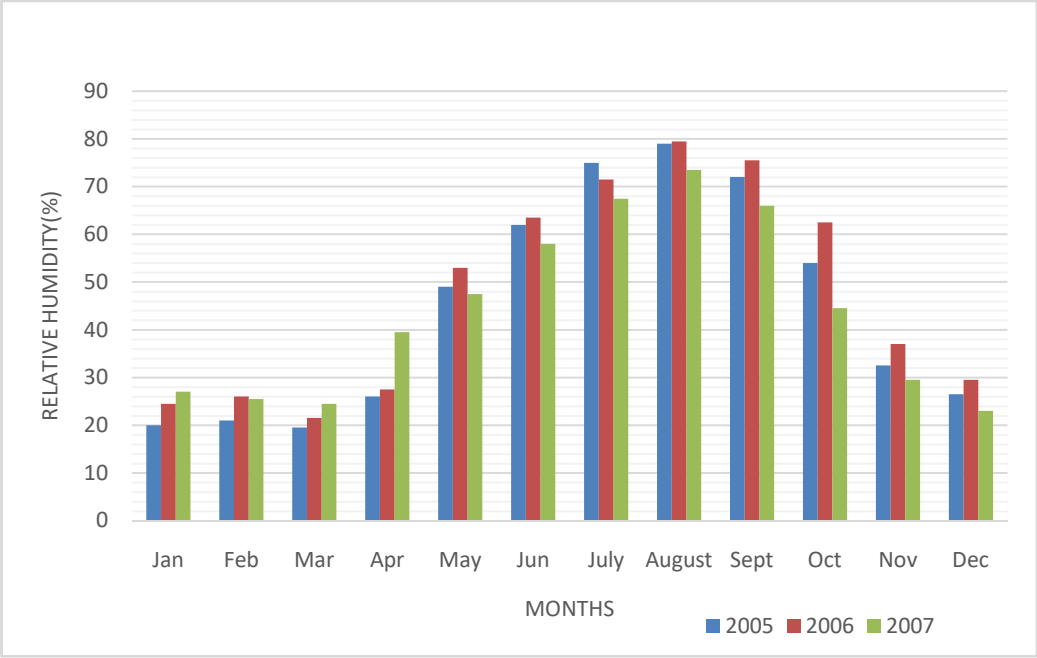

Fig. 2.4. (b) Mean Monthly Relative Humidity for the Study area (2005-2007) (Modified after Buba *et al.*, 2015).

2.4 Review of Regional Geology of Nigeria

Nigeria is geographically situated in the northwestern axis of the Congo Craton and eastern part of the West African Craton (Ajibade and Woakes, 1987). MacDonald *et al.*, 2005 have divided the geology of Nigeria into igneous and metamorphic rocks on one hand and the sedimentary units on the other hand (Fig. 2.5). The igneous /metamorphic rocks were further subdivided chronologically into Tertiary – Recent volcanics, Jurassic Younger granites and the Precambrian Basement Complex rocks. In the same manner the sedimentary rocks were also chronologically subdivided into Quaternary, Tertiary and Cretaceous sediments (MacDonald *et al.*, 2005)

2.4.1 The Basement Complex

The Basement Complex rocks of Nigeria are generally Proterozoic Precambrian in age, and made up of different suite of rocks which include; the Migmatite/Gneiss, Schist and Granites. These basement rocks were deformed during an orogenic episode, 550 million years ago (Burke and Dewey, 1972; Dada, 2006). These rocks constitute more than 50% of the land mass of Nigeria outcropping in virtually all the geographical regions of the country as shown in (Fig. 2.5). The main rock suites that make up the Basement Complex rocks of Nigeria as summarized by Obaje (2009) are itemized as follows:

1. The Precambrian Basement Complex Rocks
    - The Migmatite Gneiss Complex
    - The Schist Belt
    - The Older Granites
2. The Jurassic Younger Granites Suite
3. Tertiary to Recent Volcanics.

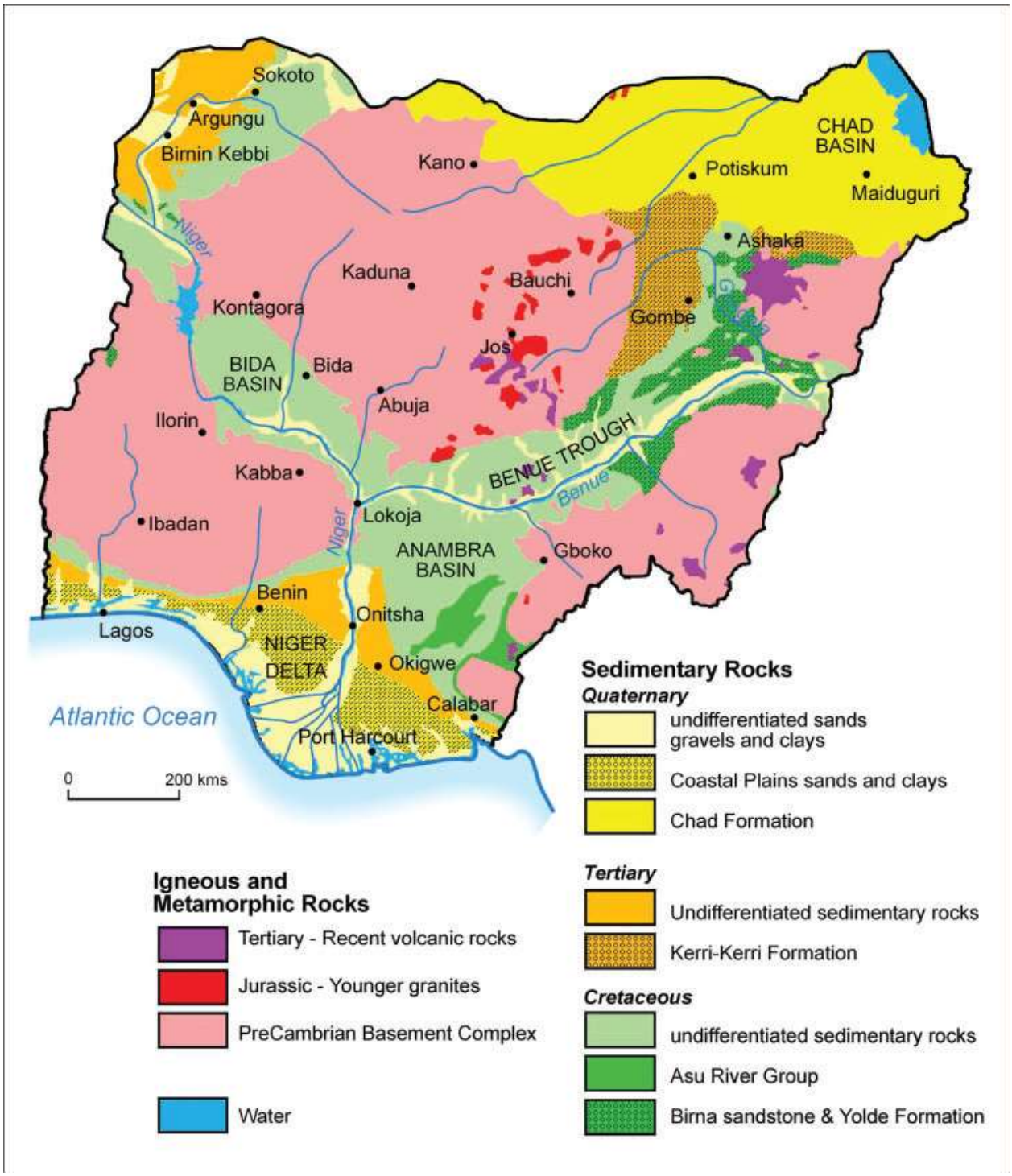

Fig. 2.5 Geological Map of Nigeria(Modified from MacDonald *et al.*, 2005)

2.4.2 The Sedimentary Basins

Overlying the Basement Complex rocks are sediments ranging in age from Quaternary to Cretaceous (Figure 2.5). This sediments are product of sedimentation in in different basins are which unconformably overlies the Precambrian basement rocks. Amongst this basin are the Chad Basin to the northeast, Sokoto basin to the northwest and the Tertiary Niger Delta Basin to the south. The Cretaceous Benue Basin trends in the NE-SW direction and bounded to the north by the Chad Basin and to the south by the Niger Delta. Other basins are the Dahomey Basin, Bida Basin and Anambra Basin. The geographical distribution of the aforementioned sedimentary basins is presented in Fig 2.5 and their detailed geological setting and stratigraphy have been documented elsewhere (Kogbe, 1976; Obaje, 2009; MacDonald *et al.*, 2005).

2.5 Regional Geology of Study Area

The present study is an integral part of northeastern Nigeria and characterised by a diverse geological setting. The region of the present study is underlain by 2 lithological units: the Basement Complex and the Sedimentary basins (Northern Benue Trough and Chad Basin). The succeeding sections will review the local geology of the area on one hand and the hydrogeology on the other hand, with particular emphasis of the aforementioned rock suites.

2.5.1 The Basement Complex Rocks

The study region is mainly underlain by the Precambrian rocks which can be divided into three main groups:

- The Migmatite Gneiss Complex
- The Schist Belt
- The Older Granites

The major geological units in the Bauchi-Alkaleri-Kirfi transition zone are further discussed in the subsequent section below.

2.5.1.1 The Migmatite-Gneiss Complex

The Migmatite – Gneiss Complex is generally considered as the Basement Complex in strict sense and it is believed to have geological ages between Pan-African to Eburnean (Dada, 2006). The Migmatite-gneiss-quartzite Complex covers about 60% of the basement rocks of Nigerian (Rahaman and Ocan, 1978) and are arguably the oldest group of rocks in Nigeria as they have undergone 3 major orogenic episodes ; the earliest event at 2500 M.a; followed by the Eburnean, 2000 ± 200 and finally the Pan-African event, 900 to 450 M.a. The major assemblages of rocks in the Complex comprises migmatite, paragneisses orthogneiss, ultrabasic and basic metamorphosed rocks.

Locally, the distribution of Migmatite – Gneiss Complex rocks in the Bauchi-Alkaleri-Kirfi transition zone is such that the granite gneiss are dominant in the southern zone of Bauchi (Fig 2.6), especially the southwestern areas covering parts of Bauchi, Ganjuwa and Tafawa Balewa Local Government Areas. These gneisses are also exposed in Alkaleri area, southeastern part of the state where it is overlain by the Kerri-Kerri Formation (Ferre and Caby, 2007). As the name implies, the granite gneiss is a product of metamorphism of granites and consequently shows a granitic composition. It is however characterised by a gneissose texture. The mineral assemblage in a typical granite gneiss consist of plagioclase, microcline, quartz and fairly abundant biotite. However**,** the migmatites are associated with medium-and high-grade metamorphic terrains which are heterogeneous microscopically and macroscopicopically.It is made up of at least two petrographically distinct components. One of which is a partial melting product that contains petrogenetically linked rocks separated by the melt from the solid fraction. The partially melted component is typically composed of quartzofeldspathic or feldspathic rocks and mafic rocks.

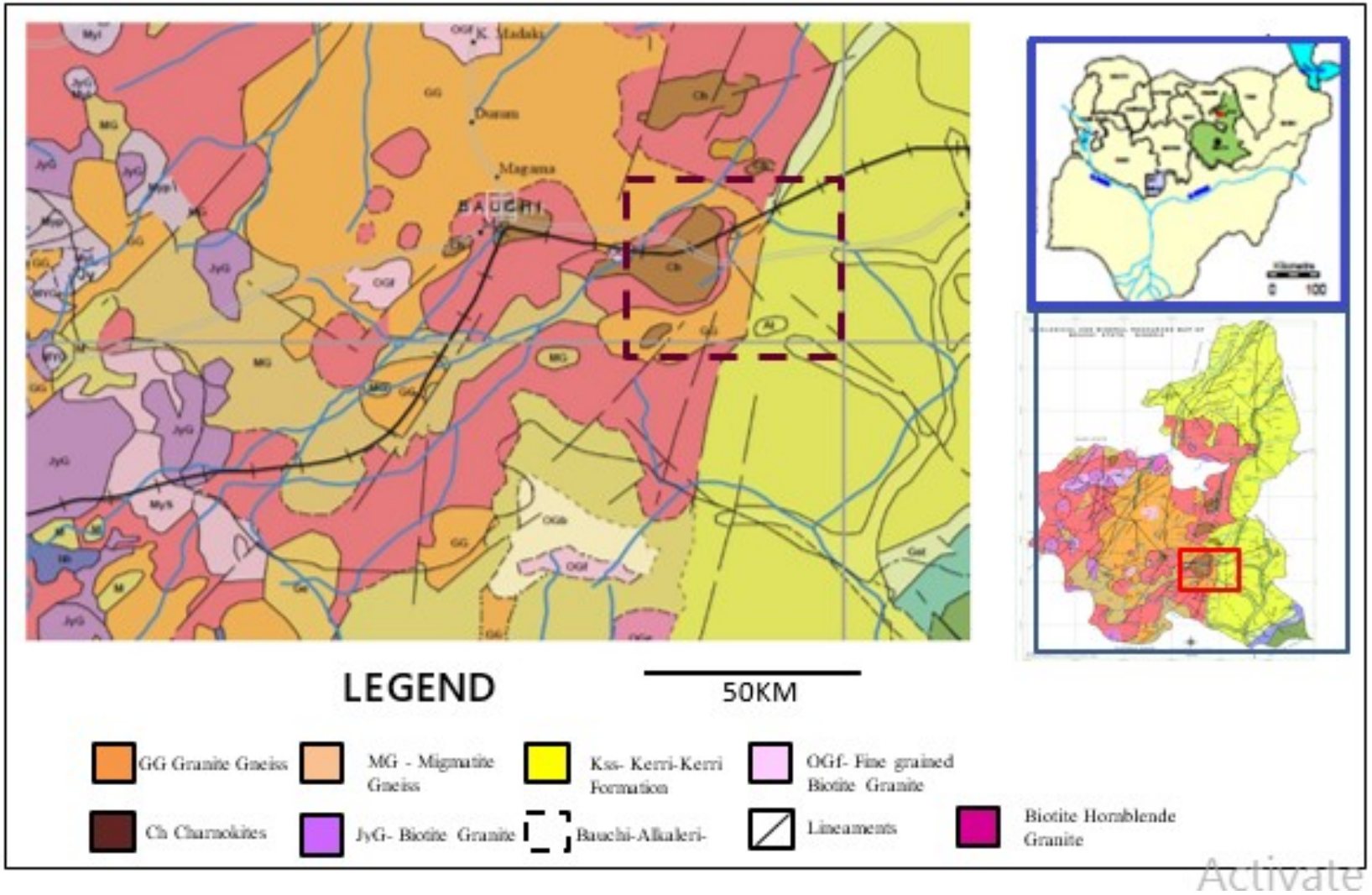

Fig. 2.6. A Generalized Geological Map of Bauchi State Showing the Basement Complex rocks and the Kerri-Kerri Formation(Source: modified after NGSA, 2006)

The partially melted component, however, may simply have modified mineralogy, grain size and microstructure with segregation being total absent (Sawyer and Brown, 2008). Migmatites occur in different forms and the specific forms of migmatite represent different degrees of equilibrium between the hosts and migrating melt during exhumation. Migmatites have been classified into metatexite and diatexite based on the fraction of the melt present in migmatite (First order classification). In these classification, the metatexite have lower melt percentage (a little above 20%), while the diatexite have about 60-80% melt. The second order classification however, divided migmatites into banded orthogneiss, stromatic, schlieren and the nebulitic (Sawyer and Brown, 2008). The second order classification reveals a transition from high-grade banded orthogneiss through stromatic and schlieren migmatite to the almost homogeneous nebulitic migmatite.

All these migmatite forms are found in the southwestern parts in Bauchi area, covering parts of Liman Katagun & Dass and Toro. Exposures of the migmatite occur in the southeastern parts of the state, around Gubi, Tirwun and Alkaleri areas. In the study zone, the migmatites are dominated by the nebulitic forms while pockets of the banded orthogneiss and the stromatic types are exposed in a quarry along the Bauchi-Alkaleri express way.

2.5.1.2 The Older Granites

It is thought that the Older Granites are believed to be post-, syn- and pre-tectonic rocks which intruded both the Schist Belts and the Migmatite-Gneiss-Quartzite Complex. The Older Granites represents magmatic episodes associated with the Pan-African orogeny that is long lasting and varied (750–450 Ma). The rocks are compositionally diverse ranging from diorites and tonalities to genuine granitic rocks. The charnockites are a significant group of rocks emplaced during this period.

The charnokites are mostly high grade intrusions in which anatexis has played significant part (Rahaman, 1981). The Older Granites suite is noteworthy for its general absence of related mineralization although the heat impact may play a part in mineralizing fluids remobilization. In northern Nigeria, the preponderance of Pan-African granites is observed to increase eastward. In the west of Zaria the granites appears as secluded intrusions

(McCurry, 1973), whereas in the region between Rahama and the Mesozoic-Cenozoic cover, remnants of migmatite are embedded into the intrusive granites and other related rocks. The Older Granites show a complex relationship with the Schist Belts and Migmatite-Gneiss Complex into which the granites are generally cross-cutting.

The Biotite granites represents the Older Granite suite which according to Truswell and Cope, (1963) are predominantly porphyritic biotite granite and biotite hornblende gran ites. The granite underlie parts of Birshi, Toro, Burra, Dass, Bauchi and Bayara areas of the state. Some of the granites displayed medium to coarse grained granular textures while others show porphyritic textures. Furthermore, the biotite hornblende granites show faint foliation defined by small streaks of biotite and hornblende alternating with feldspar and quartz. The coexistence of biotite and hornblende in the granites is indicative of the fact that the magma that formed the rocks might be associated with subduction zones.

The charnokites (bauchites) however, are popularly known as the fayalite bearing quartz monzonite (Oyawoye 1972). In Bauchi area (including parts of the Bauchi-Alkaleri-Kirfi area) it is believed that some of the Older Granites rocks defy the Bowen reaction series because the granites contain significant quantities of high temperature minerals like olivine (fayalite) and pyroxene occurring with low temperature ones like quarts, feldspars and micas in the same rock. Oyawoye (1972) was the first to recognize these distinctive quartz-fayalite monzonite called “Bauchite” in Bauchi area. Bauchites are characterised by almost equal amount of Alkali feldspar and Plagioclase and its dominant accessory minerals are biotite and hornblende. Occurrence of bauchite can be found in Bauchi, Yelwa, Gwaskoran, Mangas, Inkil and south of Kangere, in most cases, biotite hornblende granite forms a large part of the complex. McCurry and Wright (1971) recognized the two principal groups of syn-tectonic and late tectonic granite of Older Granites. Bauchites are massive and unfoliated charnockitic rocks and usually outcrops as smooth rounded boulders by spheroidal weathering.

2.5.2 Sedimentary Geology

The sedimentary basin that underlie the region of study is the Benue. The Benue Trough has been geographically divided into three (Obaje, 2009):

1. The Northern (Upper),
2. Central (Middle)
3. Southern (Lower) Benue Basin

The study region is underlain specifically by the rocks of the Northern Benue Trough.

2.5.2.1 Stratigraphy of the Northern Benue Basin

The Northern Benue Basin is the northeastern Y-shaped part of the Benue Trough which divides into an East-West trend Yola Arm and Gongola Arm or Gongola Basin of a North-South trend (Carter *et al*., 1963). A summary of the stratigraphic succession in the Benue Basin is presented in Fig. 2.7. The Pre-Mesozoic rocks which form the basement in the region of the Benue Trough are mainly Migmatites and gneisses.

The lithostratigraphic sequence of the northern Benue Basin are as follows:

1. Bima Sandstone Group
2. Yolde Formation.
3. Pindiga Formation
4. The Gombe Formation
5. Kerri-Kerri Formation

The major sedimentary unit in the Bauchi-Alkaleri-Kirfi transition zone are further discussed in the subsequent section below.

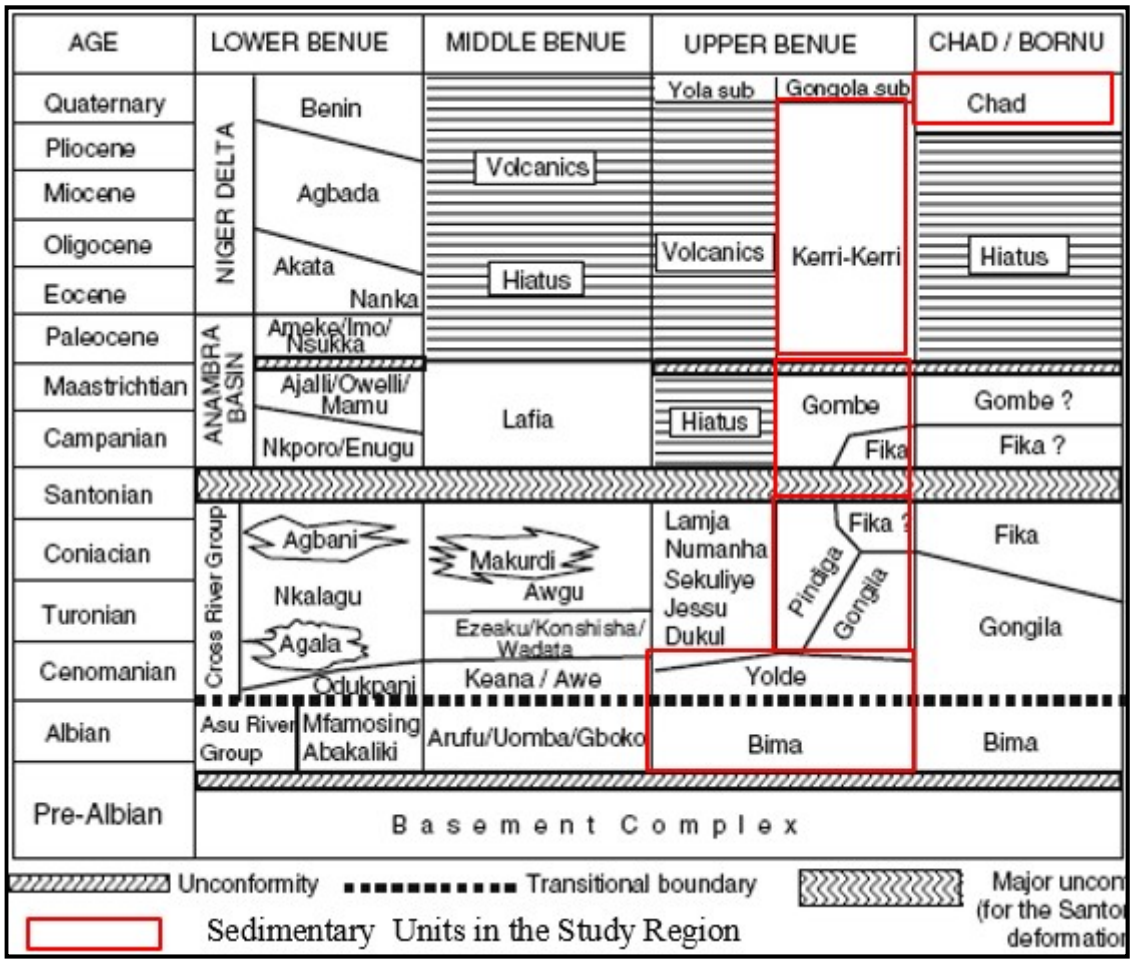

Fig 2.7. Stratigraphic sequences of the Benue and part of Chad Basin Showing the Sedimentary Units in the Study Region(Modified: After Obaje 2000)

2.5.2.2 The Kerri-Kerri Formation

The Kerri-Kerri is defined by fining upward sequences, however coarsening upward sequences have been reported (Dike, 1993).It occupies an area of 30,000 km^2 and found as far north as Chad Basin where it underlies the Chad Formation (Dike, 1993). The depositional environment of this formation has been described by many workers. Carter *et al* (1963) interpreted the Kerri-Kerri Formation to be of a wide range or depositional environments of which lacustrine and deltaic sediments form most of the deposits. Dike (1993) described it as alluvial fluvial deposit while Adegoke *et al.,* 1978, recognized fluviatile, deltaic, marginal lacustrine and transitional environments of deposition for this formation. The Kerri-Kerri Formation have been dated as Paleocene from palynological studies of a borehole sited at Dukku (Adegoke et al., 1978).

2.6 Review of the Hydrogeology of the Study Area

Generally speaking,groundwater distribution in Nigeria is largely determined by the geological make-up. Nigeria has quite a huge groundwater potential that greatly outweighs its surface water resources (Adelana, *et al.,* 2008). Offodile (2002) described the various hydrogeological basins in Nigeria. Generally, aquifer distribution in Nigeria can be divided into 2 along geological lines; basement and sedimentary aquifers.

Groundwater availability in crystalline basement zones is dependent on intensity of decomposition and jointing of the rocks. MacDonald *et al.,* 2012 and Tijani 2016 presented a different view point as regard the hydrogeological setting of Nigerian Basement Complex rocks and the aquifer types (Fig. 2.8). According to said researchers, the Basement Complex rocks cover about 50% of Nigeria and are characterised by very low primary permeability or porosity.

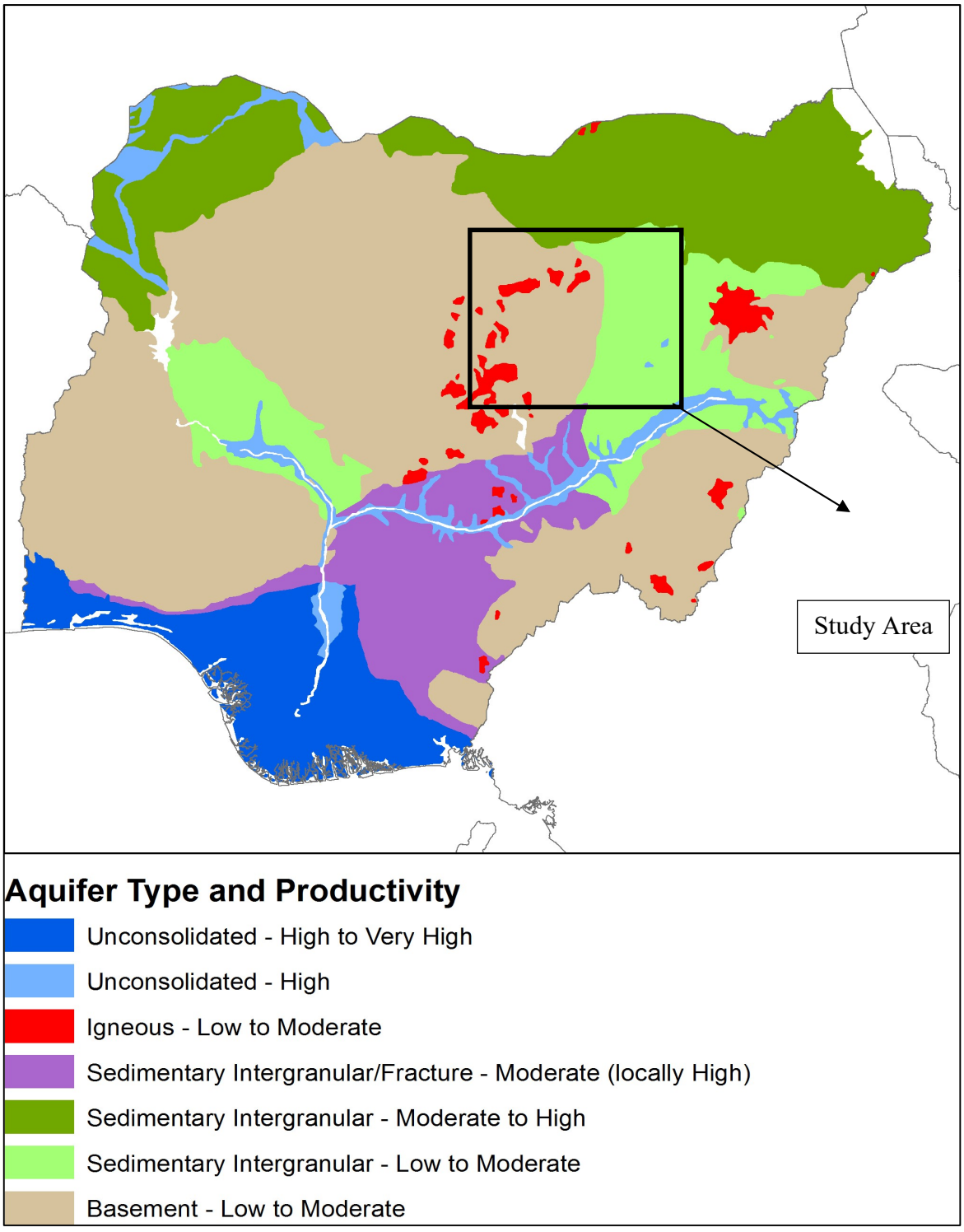

Fig 2.8. Hydrogeological sketch of Nigerian Map showing the Study Region (Modified from Tijani, 2016)

Groundwater occurrences is majorly in the weathered overburden and/or the fractured bedrock. Boreholes yield range from 0.1-1 l/s, but can sometimes reach 10l/s. In addition, these basement rocks are composed mainly of granites.

Bauchi area is drained by several river systems. The major one is the Dindima River which originates from the Jos Plateau, southwest of Bauchi area. It has numerous headwaters and tributaries within the state. Its trends in the NE-SW direction through the southern parts or the state. The western parts of the state are drained by the Bunga River and the Jama'are River systems while to the extreme north of the state is the considerable stretch of the Katagun River system.

The hydrogeology of the study location is broadly divided into two in accordance with the geological setting of the state(Fig. 2.9). The weathered and fractured layers form the aquifers in basement setting while sandstones constitute the aquifers in the sedimentary setting.The maximum groundwater resources in the Basement Complex are to be found in along the main tectonic lines which constitute the preferential flow paths for the groundwater.

2.6.1 Basement Complex Hydrogeology

Locally, groundwater occurrence in the Basement Complex rocks of Bauchi-Alkaleri-Kirfi area is determined by the weathered cover of the Basement Complex which is marked by seasonal fluctuations and the fractured basement rocks or the sap rocks (Shemang and Jiba, 2005). These aquifers are generally of limited capacity, owing to the restricted permeability of the basement rocks. The depth of wells in the basement terrain varies between 13 to 61 m, while the water table and hydraulic head varies between 2 to 4 m and390 to 570m (above sea level), respectively (JICA, 2014). The yields of boreholes however, ranges between 9.6-405.6 m^3/day(Shemang and Jiba, 2005)

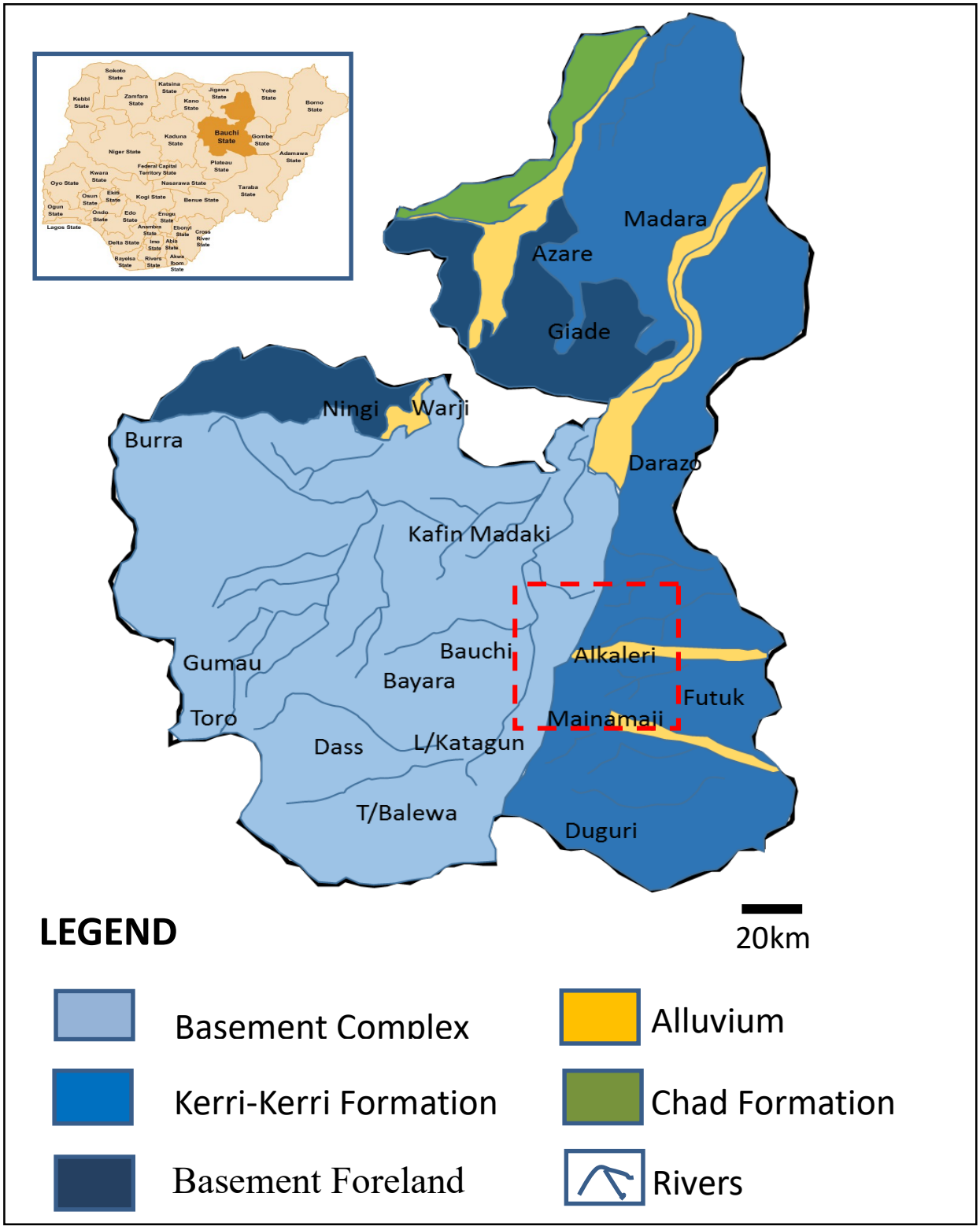

Fig 2.9. Hydrogeological Map of Bauchi area (Modified After: Bauchi State Ministry of lands and Survey 2008).

In summary, regolith, resulting from in-situ weathering of crystalline rocks, are the main water bearing units in the basement settings. The poor and non-uniform hydraulic properties of these aquifers can be attributed to the fact that clay is the main constituent of the parent rock decomposition. Some borehole logs from the Basement Complex zones of Bauchi-Alkaleri-Kirfi area are presented in Fig. 2.10.

2.6.2 Hydrogeology of Sedimentary Units

Hydrogeologically, the Kerr-Kerri Formation can be considered as having higher groundwater potential as compared to the Basement Complex areas of the state, because of their sedimentary nature and hence well-developed primary porosities. Although, the groundwater potential of the Kerri-Kerri Formation itself is somewhat controversial. For instance, out of over 470 boreholes drilled within the Kerri-Kerri Formation by Wardrop Engineering Inc. in 1989, about 90% success was recorded, but workers like Offodile, (1972, Ako and Osundo (1986), Adelana, *et al.,* (2008) and Akaha and Promise (2009), have all described the aquifers of Kerri- Kerri Formation as poor in terms of water bearing capacity . Other researchers, as exemplified by Eduvie, (2006) have mentioned the Kerri-Kerri Formation among the biggest water bearing formations in Nigeria.

The present work will attempt to unravel this controversy using an integrated approach. Based on JICA, 2009, these sandstones of the Kerri-Kerri have depth to the water table of 6 to 68 meters,well depth of 25-165 meters and hydraulic gradient of 250-410 meters respectively (Fig 2.10). Fig. 2.12 and Fig. 2.12 shows that the aquifers in the northeastern parts of the Kerri-Kerri (Shidigawo, Taure, Beni and Zamani areas) are more arenaceous (sandy) in nature.

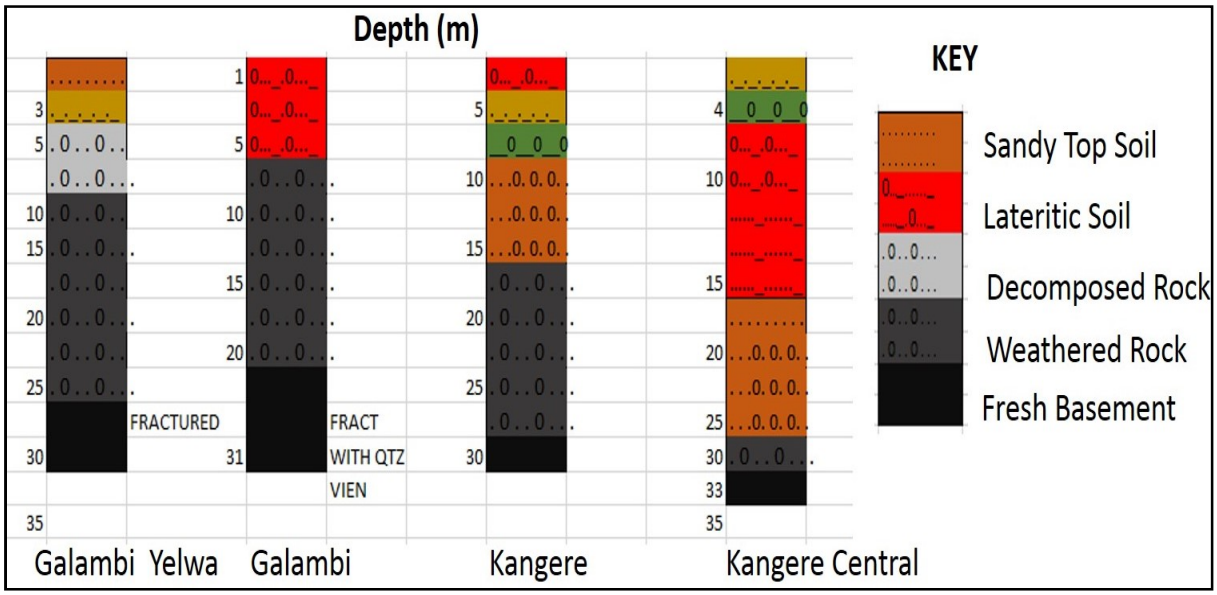

Fig 2.10. Borehole Logs from the Basement Complex Parts of the Bauchi-Alkaleri-Kirfi area (Wardrop Engineering, 1989)

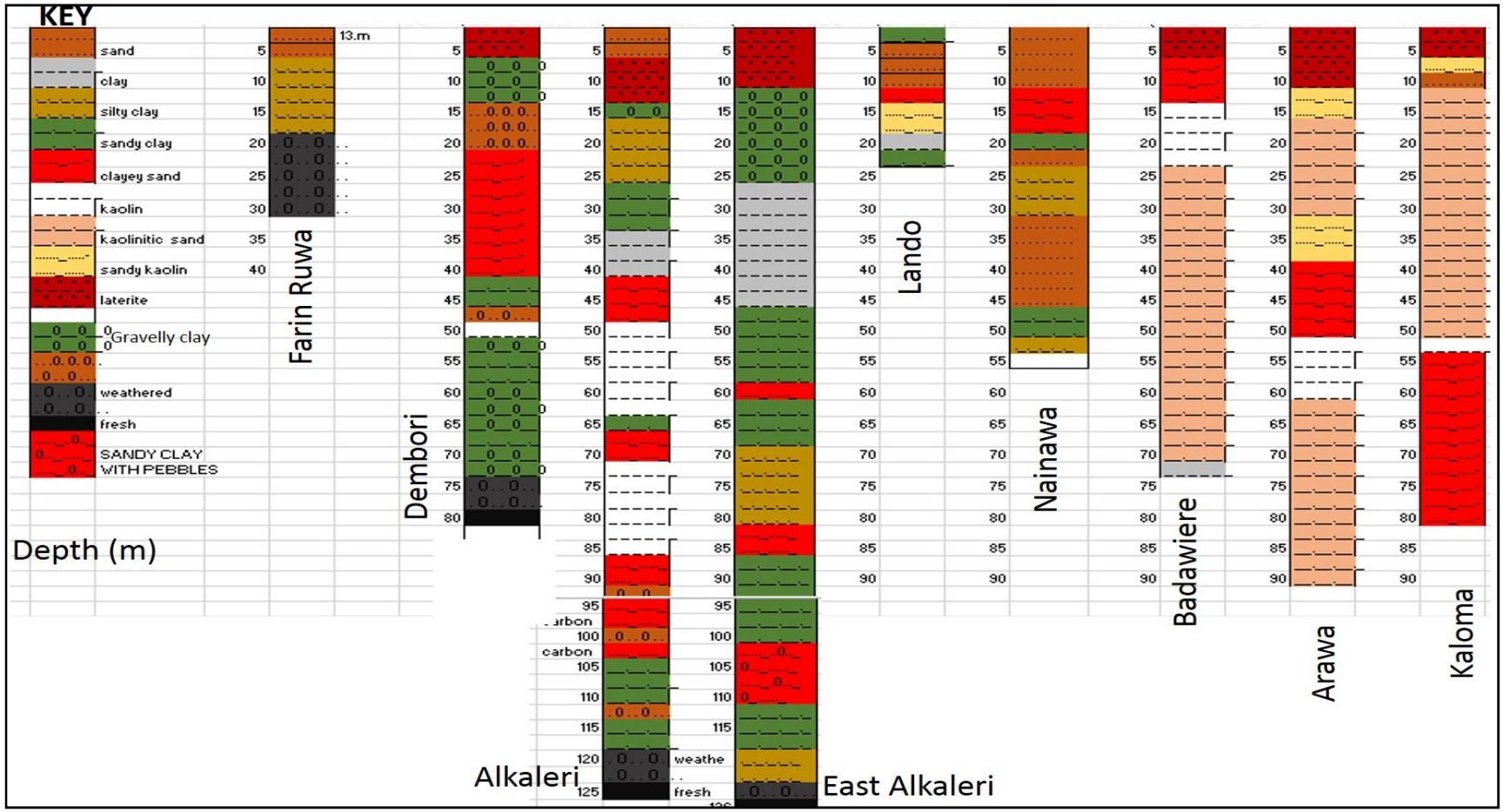

Fig 2.11 Borehole Logs from the Kerri-Kerri Formation (Central Part of the Bauchi-Alkaleri-Kirfi area) (Wardrop Engineering, 1989)

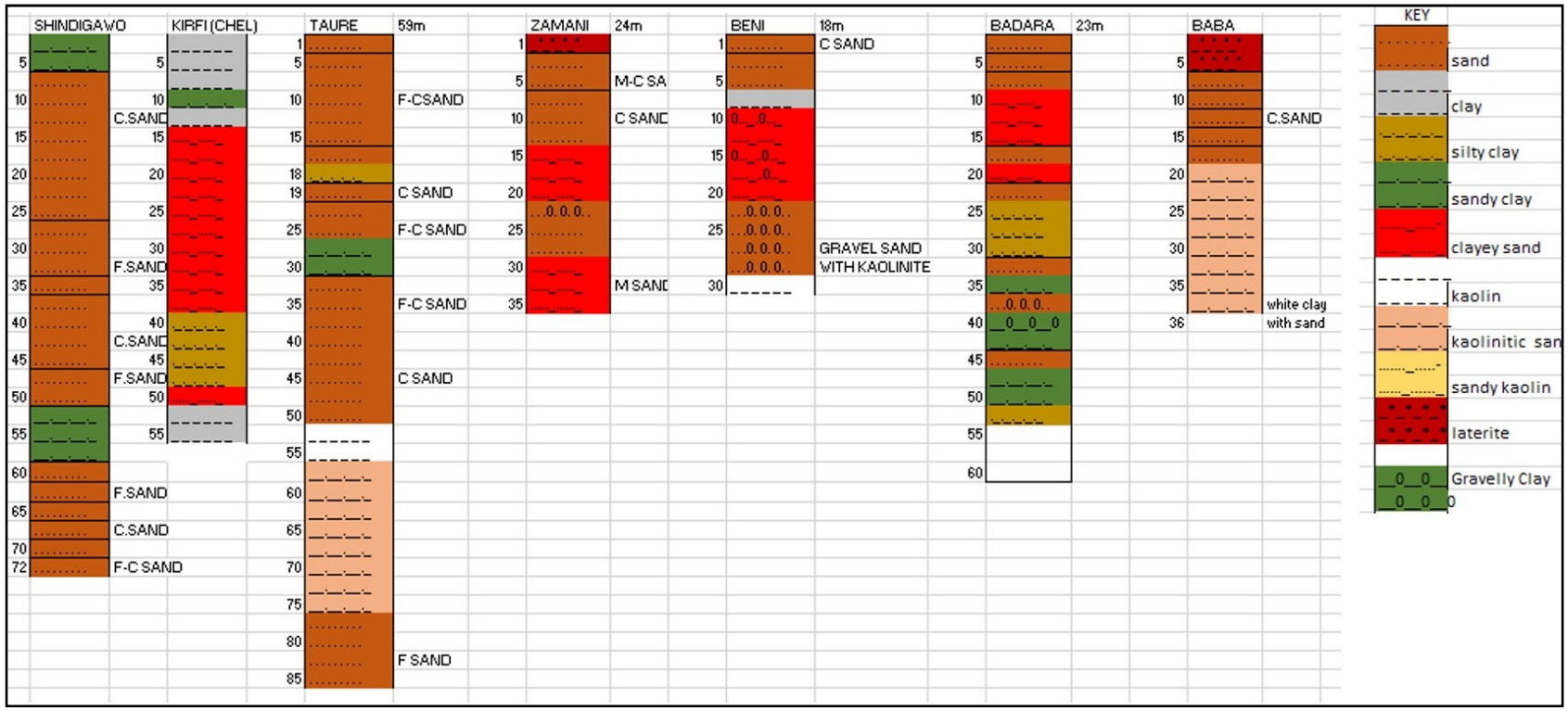

Fig 2.12. Borehole Logs from the Kerri-Kerri Formation (Northeastern Part of the Bauchi-Alkaleri-Kirfi area) (modified from Wardrop Engineering

CHAPTER THREE
MATERIALS AND METHODS

3.1 Desk Study

The desk study entailed gathering and evaluation of existing data. Boreholes inventory were also collected. Information gathered from the Borehole inventories include (depth, static water level and yield). Also, secondary data such as existing maps (geology, soil and rainfall, topographic maps and borehole data, etc.), remotely sensed data (Landsat 8, ASTER, and Spot 5) and aeromagnetic data of the Bauchi-Alkaleri-Kirfi area were all acquired and processed during the desk study stage (Table 3.1.). The analytical aspects of the desk study can be summarised under the remote sensing / GIS component and the aeromagnetic components.

3.1.1 Remote Sensing and GIS Study

As part of the desk study, a spatial database was created for the Bauchi-Alkaleri-Kirfi area, from existing maps (soil, rainfall and topographic maps) and remotely sensed data (Landsat 8, ASTER, and Spot 5), using the GIS tool. The spatial database creation entailed designing and database automation, data gathering for the data base and managing the database.

Designing involved identifying the spatial data required for the analysis, determining the required attributes, setting the Bauchi-Alkaleri-Kirfi area boundary and choosing the required coordinate system. Automating the data which entails digitizing or converting the data from other systems and formats (e.g. hard copies, shape files, tiff) into usable formats as well as verifying the data and correcting errors. During this stage soil, rainfall and topographic maps were scanned and georeferenced to produce digital soil, rainfall and drainage maps of Bauchi-Alkaleri-Kirfi area

Table 3.1 Secondary Data Utilized For the Study

Materials	Contents	Sources
Geological map	Geology	Field Mapping (1:100,000)
Topographic maps	Drainage and Relief	Ministry of Land and Survey, Bauchi Office 1:100,000
Soil map	Soil classification covering the Bauchi-Alkaleri-Kirfi area	Ministry of Land and Survey, Bauchi Office.
Satellite images SRTM DEM (30 m), Spot 5 (5 m), Landsat 8(m) and ASTER (30 m)	Slope map, Elevation map and Land use map.	NCRS Consult, Jos, Plateau State.
Borehole Data	Borehole Depth, Water level, well yield data	Bauchi State Water board and RUWASS, Bauchi, Wadrop Engineering Report
Rainfall Data	Rainfall data	Bauchi State Agricultural Development Board. And ATAP weather stations.
Aeromagnetic Data	Total Magnetic Intensity and lineament Data	NCRS Consult, Jos, Plateau State.

In addition the rainfall map was updated with recent data acquired from meteorological stations in Bauchi and Alkaleri, while the soil map was ground trothed in the course of the geological field mapping. The remotely sensed data which are already in a soft format were also imported to the spatial database in ArcGIS 10.31environment. The land use was generated from a Landsat 8 imagerybya procedure known as image classification while the slope and elevation maps of the study were derived from the ASTER data through interpolations (IDW) using the spatial analyst tool. The Spot 5 was however, employed to generate a lineament map of the area through digitization technique (using the line tool). The final stage involves verifying the coordinate systems of all the maps generated. It is important to note that the completeness and the accuracy of the data in the said stage determines the accuracy of the final results. Arising from the GIS study, a spatial database comprising of seven (7) thematic maps were generated.

3.1.2 Aeromagnetic data acquisition

The aeromagnetic data used represents 1 grid and covers 55 x 55 km^2 (i.e. 3,025km^2). The data was acquired by Fugro Airborne Surveys on behalf of the Nigerian Geological Survey Agency (NGSA)between 2001 – 2009. Magnetic data recording was done at intervals of 0.1 seconds or less than 7m. Sensor mean terrain clearance was 80 meters with a flight line spacing of 500 meters and tie line spacing of 5000 meters. The flight line trend was 1350 and tie line trend was 450. Scintrex CS3 Cesium Vapour magnetometer was used and data acquisition system was FASDAS. King KR405 and King KR405B where the types of radar altimeter used, while the barometric altimeters used were the ENVIRO BARO and DIGIQUARTZ. Flight path tracking was digital using Novatel 3151R and Omnistar RTDGPS for flight path navigation. Real time differential GPS was used for flight path processing and the aircraft types used were: Cessna Caravan (208B ZS-FSA and 208 ZS-MSJ) and Cessna 406 ZS-SSC. The aeromagnetic data was used to evaluate the depth to magnetic basement using a technique known as Euler deconvolution and the distribution of magnetic lineaments in the study was achieved using edge detection analysis. The aeromagnetic data was processed with the Oasis Montag software. Arising from the pre-processing of the aeromagnetic data, detailed analysis of the resulting residual magnetic intensity data followed. The enhancement techniques employed include:

reduction to equator (RTE), upward continuation approach while the horizontal component of tilt derivative was deployed for the extraction of linear structures. The final output map for the lineament was exported from the Oasis montaaj to the Arcmap in CSV format. In order not to digress from the objective of this research which entailed production of subsurface thematic maps, only the result of magnetic lineaments extraction which generated the lineament thematic map was presented in this section. Details of other enhancement techniques are presented in the Appendix X

3.2 Field Studies

The field study commenced with a reconnaissance field work from 15th – 22nd of January 2015, and entailed visiting the field with the aim of confirming some of the information obtained during the desk study and also appraising the Bauchi-Alkaleri-Kirfi area. The reconnaissance survey also entailed well inventory survey of in the area to obtain information such as location, well depth, depth to water table and operational status. The detailed field work is divided into three; the geological mapping, geophysical studies and groundwater sampling.

3.2.1 Geological Mapping

A systematic geological mapping was deployed which involved surface traversal on a 1:100,000 scale, with a view toidentifying the rock types and rock boundariesand verifying and correcting the available maps. Based on the field findings (Plates 3.1 and 3.2), a revised map of the area was created, which will serve as a working map for the subsequent GIS analysis and theme map generation.

3.2.2 Geophysical Investigation.

Geophysical survey was by means of electrical resistivity undertaken within 5km by 5km grid lines proportionally distributed across area. The geoelectrical sounding (VES) approach was used with ABEM-TERRAMETER, SAS 3000 BC and the Schlumberger electrode layout. Four metal electrodes were employed for transmitting and receiving

signals(Appendix I). VES was undertaken at 95 locations using a total current and potential electrodes spread (AB and MN) of 300-500m and 16m

. Twenty one (21) VES points were undertaken on the migmatite/gneiss bedrocks while a total number of 15, 14, and 44 soundings were undertaken in the granites, charnorckites and the sandstones bedrocks respectively (Fig. 3.1).The VES technique uses collinear arrays intended to produce an obvious 1-D vertical apparent resistivity against depth model for a particular point of observation.

For each data point the positive current electrode (A) also known as the source, inject the current into the subsurface, while the negative current electrode or sink (B) retrieves the current. The potential drop is determined by potential electrodes M and N (Revil *et al*., 2012). The VES technique acquires a series of potential differences at larger electrode spacings while maintaining a fixed central point. The induced current passes through progressively deeper layers. At higher electrode spacing the induced current moves through gradually deeper layers in the subsurface. Apparent resistivity values measured by the terrametre or calculated from the measured potential drop, are viewed in terms of overburden thickness, depth to water table, and thicknesses of subsurface geo-electric layers. AB represents the distance in meters between the two current electrodes and designated as 'a', MN is the distance in meters between the potential electrodes and designated as 'b'while R is the resistance read on the tetrameter. With the current electrode increasingly expanding, the potential drop between the potential electrodes becomes lower. Eventually the signal to noise ratio becomes notably infinitesimal which necessitates the need for expansion of the potential electrodes, and a reading is taken without moving the current electrodes. Then the potential electrodes are further spread out and an observation is made with the current electrodes at the same spacing. The survey is continued with the several observations made by increasing the separation of the current electrodes.

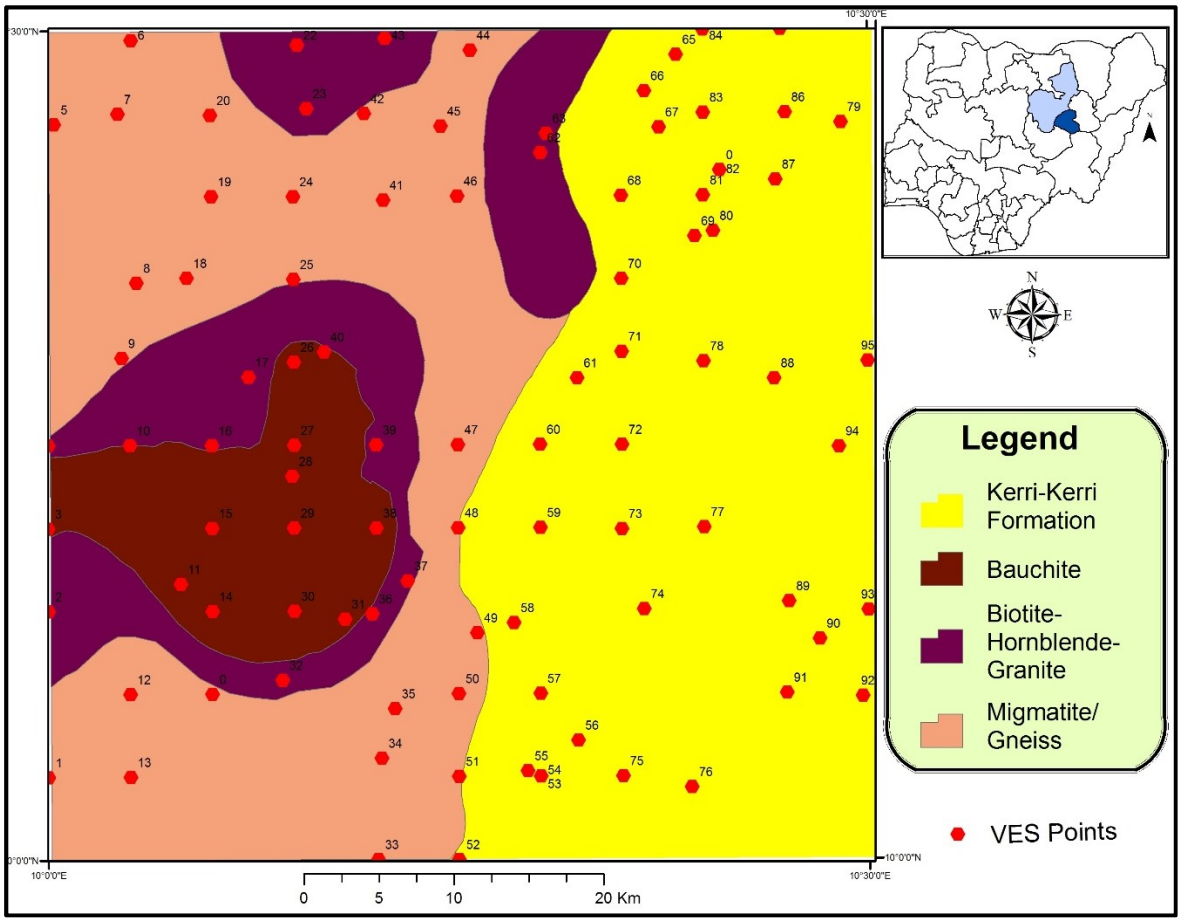

Fig 3.1. Map showing VES stations

.

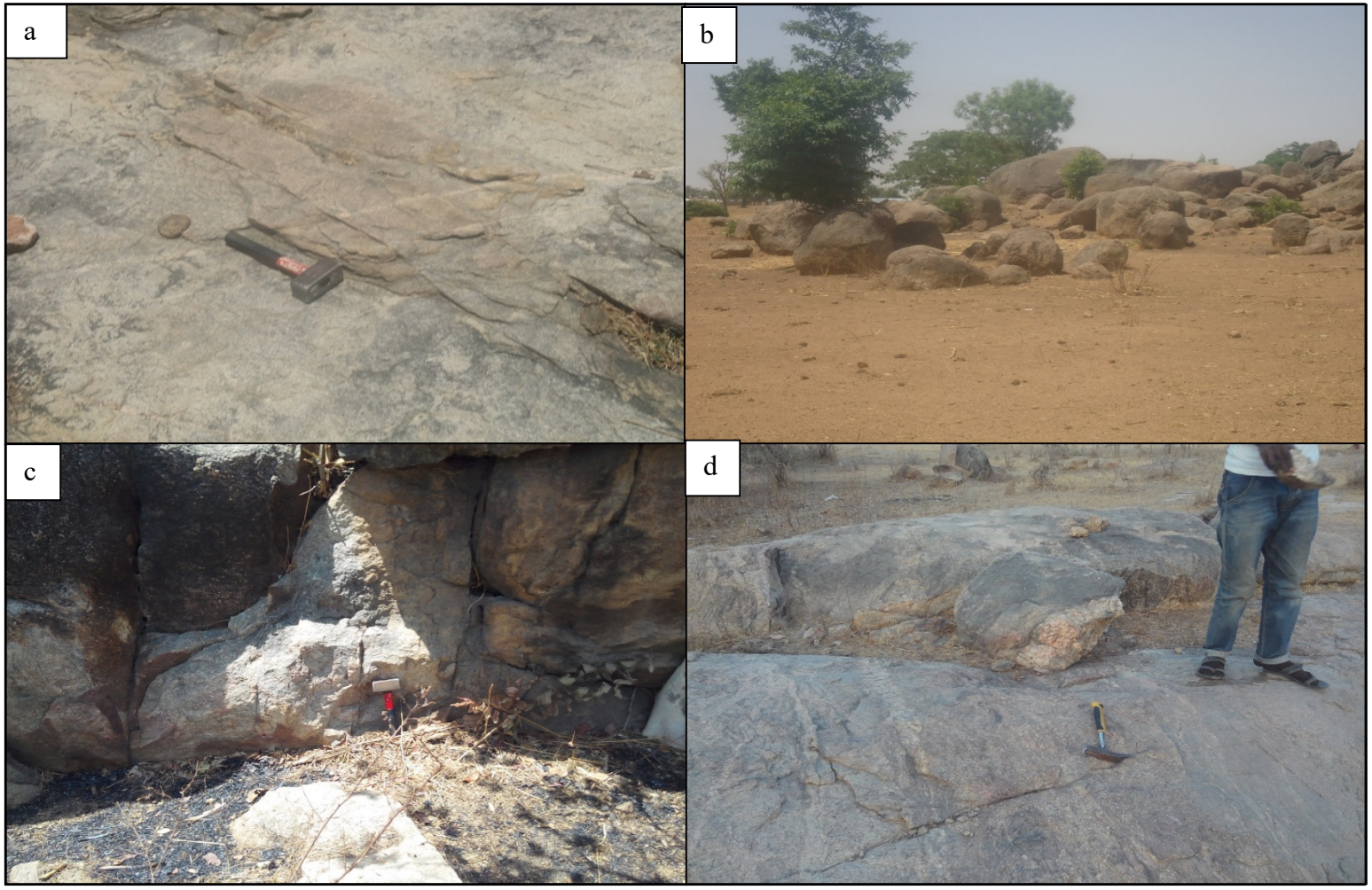

Plate 3.1. (a) Exposure of granite gneiss, b). Boulders of Bauchite in the Bauchi-Alkaleri-Kirfi area, c). Fractures on gneiss outcrop and d). Weathered rock exposure

Plate 3.2. (a) Dipping Beds of Kerri-Kerri Sandstone, b). Exposures of sandstones beds in Kirfi area, c). A kaolin mine encountered at Alkaleri area.

3.2.3 Groundwater Sampling

Eighty seven (87)water samples were obtained in duplicates 100ml bottle polyethylene bottles for major cations and anions analysis for dry season inNovember 2017. Forty five (45) groundwatersamples were earmarked for isotope analysis (Deuterium and Oxygen). The sample location map is presented in Fig. 3.2, while a distribution table showing the groupings of samples based on the bedrocks is highlighted in Table 3.2. On the spot determination of physical parameters (EC, temperature, TDS and pH) was made using potable multi-parametric meter (Plate 3.3).The depth and water level were determinedwith a calibrated water level meter for the dug wells while, for the boreholes the inventories were obtained from borehole owners and drilling companies. The type of well and well protection, major land use and distance from pollution source were also documented.

Subsequent to hydrochemical sampling, the sampling bottles were decontaminated with the sample water and clear pumping/water abstraction was conducted for 10-15 min to get rid of stagnated water in the well or at the region of the pump and to avoid sampling stagnated water. The groundwater sampling was done in accordance with (APHA, 2005). The first set of the samples which were for major cations were preserved by acidification in the field with 3-4 drops of concentrated nitric acid to prevent staking of metals on the wall of the sample container and also form contamination by microorganisms prior to analysis, while the second category of samples which have been earmarked for major anion and stable isotopes studies were collected in separate 100 ml plastic bottles and stored separately at $4^{o}C$ without acidification. Sample preservation and laboratory analysis was done in accordance with APHA, 2005. The field sampling was accompanied by laboratory analysis which has been elucidated in the following section.

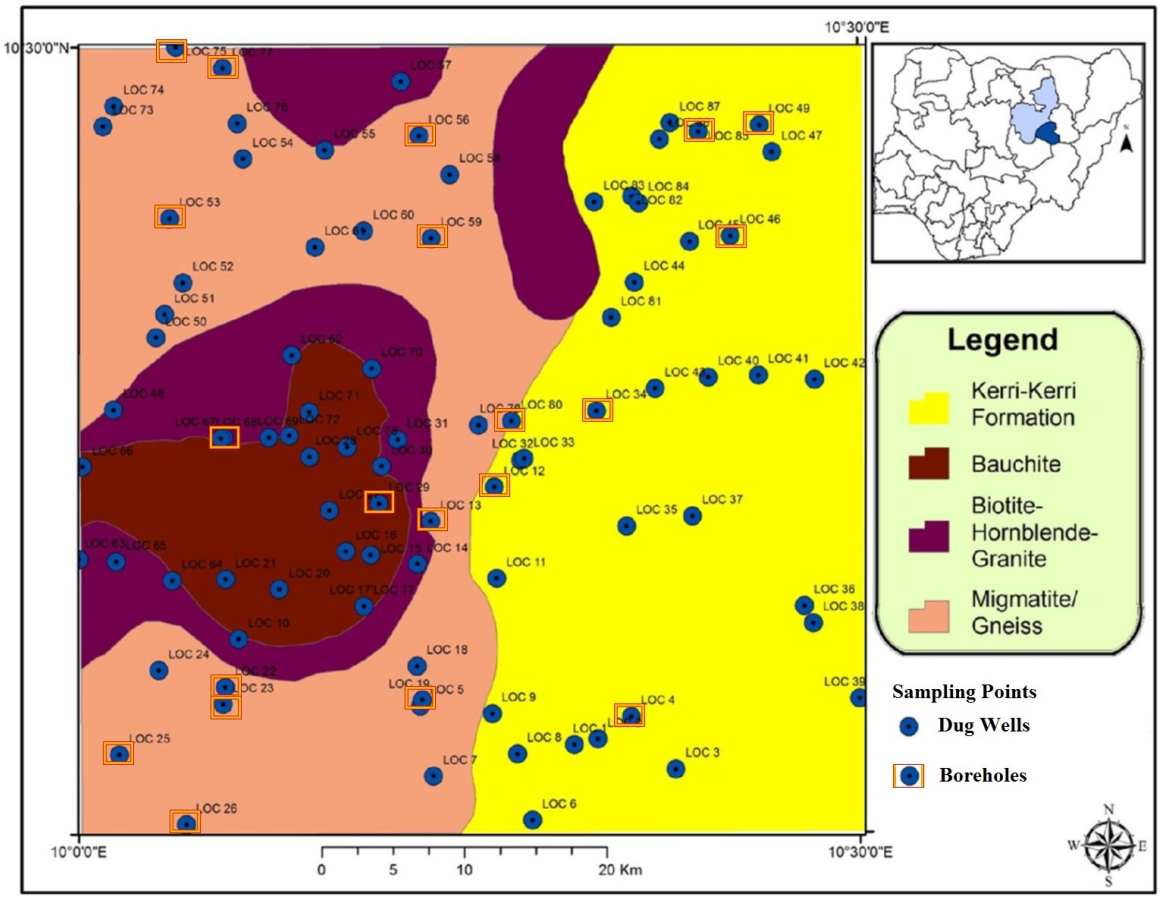

Fig. 3.2. Groundwater sample location map of Bauchi-Alkaleri-Kirfi transition zone

Table 3.2. Distribution of groundwater samples based on bedrock setting

S/n	Bedrock	Major Ions		Isotopes
		Anions	Cations	
1	Migmatite Gneiss	27	27	13
2	Hornblende Granites	12	12	8
3	Charnockite	12	12	7
4	Sandstones	36	36	17
	Total	**87**	**87**	**45**

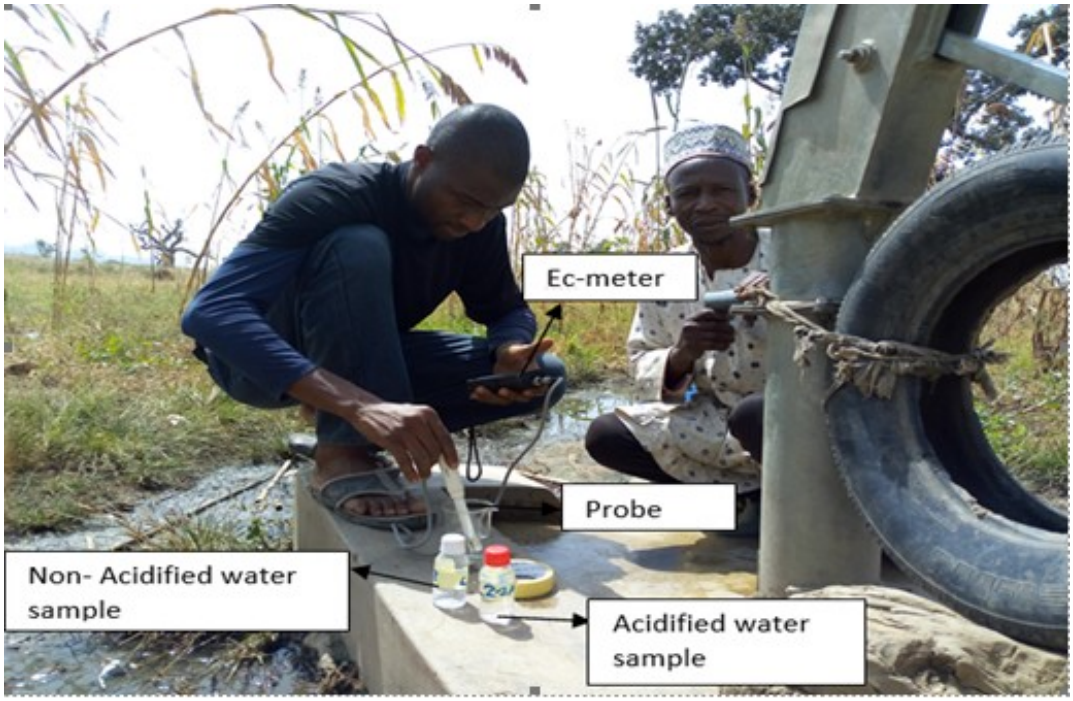

Plate 3.3. Field measurement of physico-chemical parameters using potable multi-parametric meter.

3.3 Laboratory Studies

In the present study the laboratory investigation conducted can be grouped into 4 namely:

i. Petrographic study of rock samples
ii. Granulometric analysis of friable sedimentary rocks
iii. Groundwater analysis
iv. Stable isotope analysis

This section discusses the procedures employed in the laboratory investigation in the order itemized above.

3.3.1 Petrography

A systematic study of samples in hand specimen and thin section was performed. The petrographic analysis was necessary to determine of the mineral composition of the rocks so as to ascertain the rock types that make up the aquifers. Nine (9) representative rock samples consisting of five (5) basement rocks and four (4) sandstone samples were selected for thin sectioning and petrographic studies in the petrology laboratory of the Abubakar Tafawa Balewa University, Bauchi. The detail procedures employed in the preparation of the thin section slides are presented in Appendix II. The result of the petrographic studies was used to produce modal mineral classification tables for all the rock units in the Bauchi-Alkaleri-Kirfi transition zone.

3.3.2 Granulometric Analysis

Granulometric analysis was conducted on thefriable sandstones in the Sieve analysis section of the Geology Department of Abubakar Tafawa Balewa University, Bauchi. A total number of fourteen (14) representative samples were purposively selected. The mesh sizes used from the top to the bottom respectively are: 3.35mm, 2.36mm, 1.18mm, 0.850mm, 0.425mm, 0.300mm, 0.212mm, 0.075mm, and 0.063mm. The corresponding values of weight % and cumulative weight % retained on the respective sieves were computed and tabulated. Using the data so obtained, cumulative frequency curves were plotted, from which, values for sorting and graphic mean (grain size) were duly computed. Details of the methods employed for the granulometric analysis is presented in Appendix II.

3.3.3 Groundwater Analysis

The groundwater samples were subjected to analysis at the Water Science Laboratory, University of Nebraska, Lincoln, USA (WSL, UNL). The laboratory analysis conducted entailed the following:

- Alkalinity ($HCO_3^-$and CaCO3) Test using acid titration method
- Major cations ($Ca^{2+,}$ Mg^{2+},Na^+ and K^+) analysis using the Flame Atomic Absorption Spectrometer (FAAS).
- Major anions (NO_3, SO_4^{2-}, Cl^-) analysis using the Ion Chromatograph
- Stable Isotopes (^{18}O and ^2H) using Isoprime Dual Inlet mass spectrometer

3.3.3.1 Alkalinity determination

The groundwater samples were subjected to acid titration. Alkalinity of water is its capacity to neutralize an acid. Alkalinity determinations was achieved through acid titration which involved the use of a standard acid to titrate the sample to set endpoints, generally pH=4.5 represents total alkalinity while pH=8.3 stands for phenolphthalein alkalinity. The normality of the acid, the amount used in the titration, and the volume of the sample are then used to determine the total alkalinity. The detail procedure involved in the determination of the alkalinity of the water sample is provided in Appendix III.

3.3.3.2 Major cations analysis

Perkin Elmer AA400 Atomic Absorption Spectrometer (AAS) 4.1.1 was deployed in the analysis the major cations. This instrument is suitable for water samples with major cation concentrations between 0.01 and 10.0 milligram/liter. The concentration of the anion in the sample is measured by nebulizing into a flame and specific wavelengths of light are passed through the burning sample while a detector measures the change in the intensity of the specific wavelength (Plate 3.4).

Plate 3.4. Measurement of concentration of cations in a sample using the nebulizing hose.

After comparing the wavelength to a set of calibration standards, the sample's concentration can be calculated. Details of the laboratory procedures for the determination of the concentration of the major cations in water using the atomic absorption spectrometry is provided in Appendix IV. The measured concentrations of the calcium, sodium, magnesium and potassium ions were converted to milligram per liters.

3.3.3.3 Major anions analysis

The Ion Chromatograph (DX-100) System was employed for the analysis of anions. The procedures of analysis was as specified by (ASTM, 1988; Dionex corporation, 1992 and APHA, 2005) and presented in Appendix V. This method describes the sequential determination of fluoride, chloride, nitrite, bromide, nitrate, orthophosphate, and sulfate (F-, Cl-, NO_2-N, Br-, NO_3-N, PO_4-P, and SO_4^{2-}) in water samples by ion chromatography with suppressed conductivity detection. The measured concentration of the Cl-, NO_3^- and SO_4^{2-} was converted to milligram per liters.

3.3.3.4 Stable Isotopes (^{18}O and ^{2}H) analysis

Forty five (45) samples were analyzed for stable isotope ratio (Oxygen and Hydrogen isotopes) using the stable isotope ratio mass spectrometry interfaced with Isoprime Dual Inlet mass spectrometer.Stable isotopes (D and ^{18}O) of water were determined using stable isotope ratio spectrometer. Hydrogen isotopes was measured on a Euro vector EA pyrolyzing furnace packed with chromium set at 1040^0C and interfaced with a Isoprime (GV Instruments, Manchester, UK) continuous flow mass spectrometer. The isotope ratio of the groundwater samples denoted as (δ) were expressed relative to a standard SMOW times 1000. Hence, values of δ are reported in parts per thousand (denoted as ‰ or permil) and δ values were calculated using:

$$\delta \text{ (in ‰)} = (R_{SAMPLE} / R_{SMOW} - 1) \times 1000 \qquad (3.3)$$

Where R_{SAMPLE} and R_{SMOW} represents either the ratios of $^{18}O/^{16}O$ or the $^{2}H/^{1}H$ of the sample and the standard (V-SMOW) respectively.

The Deuterium and Oxygen 18 concentrations of the groundwater samples was plotted into the global meteoric water equation (GMWL; $\delta^2H=8\ \delta^{18}O +10$; Craig 1961) to obtain the GMWL reference line and to characterise the isotopic fingerprints of the groundwater in the area. The detail procedure involved in the analysis of stable isotopes is provided in Appendix VI.

3.4. Quality Control

To ensure high accuracy in the course of the laboratory analysessome precautions were taken. This include the use of some standard reagents to ascertain the performance and accuracy of the equipment at certain intervals. Laboratory reagent blanks (LRB), lab fortified blanks (LFB), lab fortified matrix (LFM), and laboratory duplicate samples (LD1 and LD2) were always included in laboratory analysis to monitor performance of different methodologies.

3.5 Data Analysis and Evaluation

Arising from the detailed field and laboratory investigation, data evaluation and analysis ensued using various softwares. In order to effectively analyse and evaluate the remotely sensed, auxiliary and field data, the following computer packages were utilized: Microsoft Excel, Surfer 12, IX1D software, Arc GIS version 10.1 and Oasis Montaaj software, Aqua Chem and Origin 8 Pro. The first stage of data evaluation involved creation of an automated database for the surface (hydrological) parameters derived from secondary data using the ArcGIS 10.31software. This was followed by generation of the subsurface (hydrogeological) parameters which includes; magnetic lineament map, lithology map, aquifer resistivity map and aquifer thickness map. The Oasis Montaaj Software was employed in the analysis of the Total Magnetic Intensity (TMI) data in order to obtain magnetic lineament map of the area.The lithology map was generated through systematic geological mapping while the themes for thickness and resistivity (aquifer) were obtained from the analysis of 87 vertical electrical sounding across the different geological formations in the area. The interpretation of the resistivity data was executedwith IX1D software to obtain the layer resistivity and thickness. The geo-electric parameters were analyzed qualitatively and quantitatively to delineate the various aquifer units in the area.

Subsequently 10 thematic maps were created from the surface and subsurface parameters using the ArcGIS software. Details of the procedures are provided in the subsequent subsections. Individual weights which depends on the influence of the parameters were assigned to all the 10 thematic maps produced based on the perceived contribution of these maps to groundwater potential and consistency ratio of the weight assigned was evaluated using the AHP multi-criteria decision analysis tool.The weight assignment was followed by rasterization of the maps, reclassification of the thematic maps followed using the reclassify feature of the ArcGIS and integration of thematic maps using the overly analysis to producethe groundwater potential map. The map was subsequently validated using existing borehole data.

The hydrochemical data was analysed using descriptive statistics, bivariate plots, multivariate principal component analysis, hydrochemical plots (piper, ternary, Gibbs, Chadha etc.).Water quality index and irrigation quality indices were also evaluated. The Deuterium and Oxygen 18 concentrations of the groundwater samples was interpreted using the global meteoric water plot and different cross plots.

3.5.1 Remote Sensing /GIS Data Analysis

Using the GIS tool (Arc GIS version 10.3.1), the remotely sensed data (Landsat and ASTER image), other auxiliary data (soil, rainfall and drainage) which constitute the surface and hydrological themes were integrated with 4 subsurface maps derived from geological mapping and geophysical studies in order to develop an overall groundwater potential map of the Bauchi-Alkaleri-Kirfi transition zone. The procedures employed for GIS data analysis and the input data used to produce the thematic maps which are in tandem Lawal et al., 2021 are summarized in a flowchart (Fig 3.3).

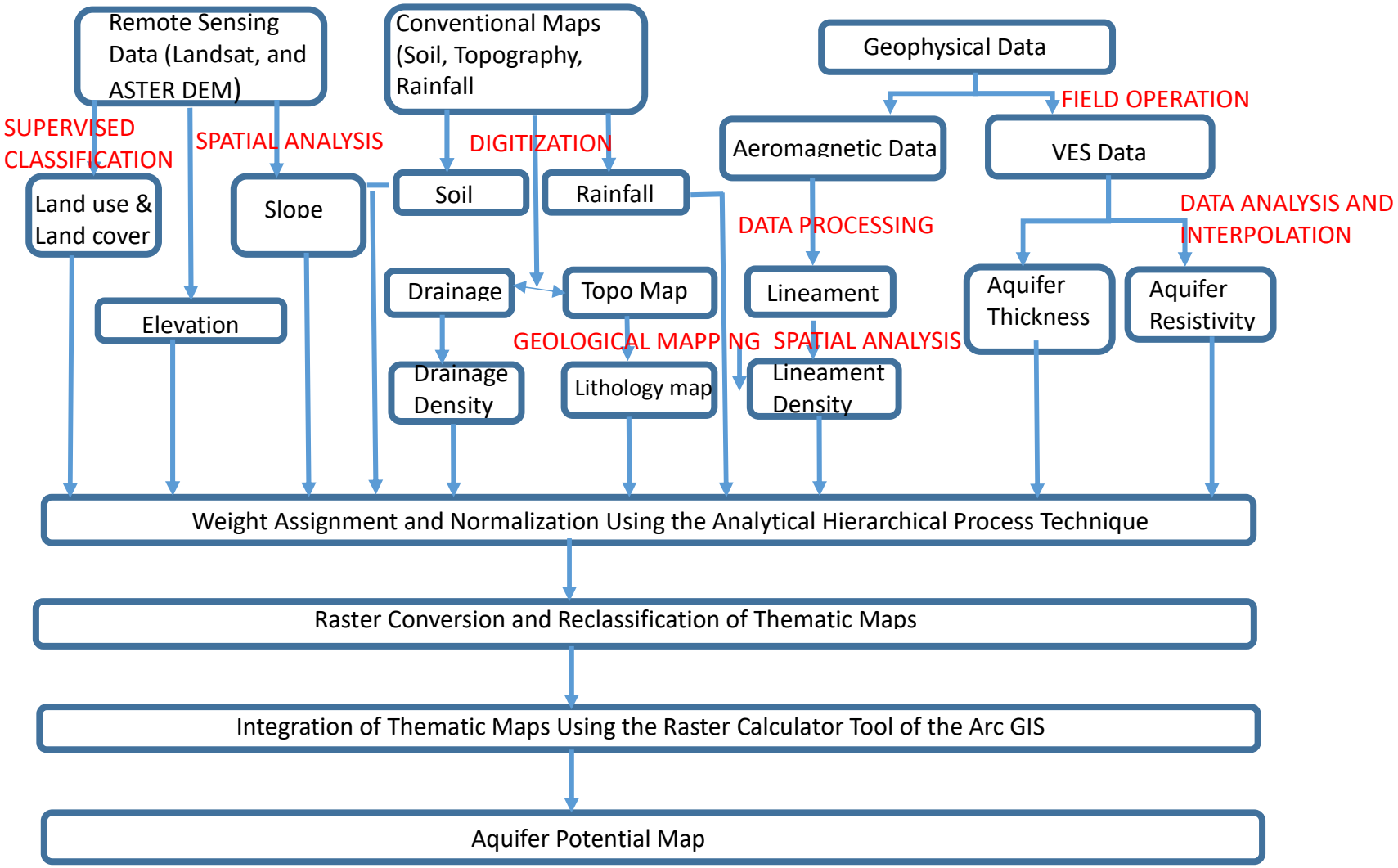

Fig. 3.3. Flowchart for classifying groundwater potential zones using, GIS and remote sensing and geophysical approach in the Bauchi-Alkaleri-Kirfi area

3.5.1.1 Preparation of Thematic maps

Using the aforementioned input maps the thematic layers for surface and subsurface parameters were produced as elucidated in the following section.

a) Elevation map

The elevation map was created using the elevation function of the ArcGIS software's spatial analyst tool using data from an ASTER satellite 30 m resolution.

b) Land use/Land cover map

The land use/land cover map for the present study was generated by image supervised image classification of the Landsat 7 image of the area (30m resolution) using the false color composite (FCC). The supervised classification uses the spectral signatures obtained from training samples to classify an image. For the present study the land use/land cover map was divided into 5 classes namely: forest, water body,built areas shrub lands and bare land.

c) Slope map

In addition, the slope map was created from an ASTER DEM using the slope feature in the ARCMAP environment.The slope has a significant impact on rainfall infiltration. A steeply sloping location has limited infiltration/recharge and consequently low groundwater prospects. Conversely, gentle slope regions are usually associated with high infiltration of rainwater which would translate to good groundwater potential.

d) Soil map

The area's soil map was obtained from the Bauchi State Agricultural Development Programme Office in Bauchi and preprocessed using ArcGIS 10.3.1 software to create a soil thematic map.The soil map was classified into 3 groups: sandy, clay loam and loam soil. Soil is the product of weathering of rocks. The nature of the soil in a particular area determines the amount of infiltration.

e) Drainage map

The drainage of the area was digitised from the topographical map of the Bauchi-Alkaleri-Kirfi transition zone and updated with ASTER (DEM). The drainage map of a location givesa clueof the hydraulic conductivity of the bedrocks as well as an overall picture of the area's groundwater potential. (Fashae et al., 2014).

f) Rainfall map

In preparing the rainfall map, 10-years rainfall information (2005–2014) for the area was used to update a digitized existing rainfall distribution map of the area produced in the eighties by National Airspace Space Agency (NASA) USA. The rainfall distribution was delineated into three zones; 850 mm, 1000mm, and 1100 mm. In order to compliment the surface thematic maps, four (4) subsurface thematic layers which were derived from geological mapping (lithology thematic map), aeromagnetic (lineament map) and resistivity data (aquifer resistivity and thickness map) were produced.

g) Lithology map

As outlined in the flow chart (Fig. 3.3), anexisting geological map and field mapping were used to generate an up-to-datelithological map. An existing geology of the Bauchi-Alkaleri-Kirfi transition zone was updated by field geological mapping. The resulting geology map was preprocessed, georeferenced and digitized to produce the thematic layer for lithology and an updated geology map of the area.

g) Magnetic lineament map

The magnetic lineament of the Bauchi-Alkaleri-Kirfi transition zone was produced from an aeromagnetic data covering the research area. Linear structures were delineated with the aid of thegrid analysis tool in Oasis Montaj Geosoft environment.The extracted lineaments were exported to the ArcGIS software platform in csv format where the map was digitized and interpolated to produce a lineament density map.

h) Aquifer resistivity map

In addition to the two subsurface maps produced an aquifer resistivity was also generated.The geophysical field data obtained from the qualitative analysis were subjected to computer iteration to derive the true resistivities and thicknesses of the subsurface layers (primary geo-electrical parameters). The interpreted resistivity data and the coordinates of all the VES points was entered into a Microsoft EXCEL worksheet, saved in 2003xls format, and exported to the ArcGIS software. The data was then used to create a spatial resistivity map of the Bauchi-Alkaleri-Kirfi area using the inverse distance weighted (IDW) approach.IDW has the advantage that it is easy to define and therefore easy to understand the results. In comparism with kriging, IDW has simpler operation and fewer steps(Setianto and Triandini, 2013).

i) Aquifer thickness map

The interpreted aquifer thicknesses was tabulated alongside the geographic coordinates of all the VES points in a Microsoft EXCEL worksheet, saved in 2003xls format, and exported to the ArcGIS software using the Add XY data feature of the ArcMap. The data was then interpolated using IDW method to produce an aquifer thickness thematic layer.

3.5.1.2 GIS operations

Following the generation of the thematic layers, weights were assigned and normalized, maps were rasterized, and reclassified accordingly.The normalization process is the conventional way of reducing the bias related to weight assignment to the themes and their sub classes. The consistency of the resulting normalized weights of the themes and those of their sub classes were checked as suggested by Saaty (1986, 1992). A consistency ratio of less than 0.1 was adjudged to be good. Through the AHP technique, representative weights ranging from 1 to 9 based on Saaty's proposed assignment scale was assigned to the themes (Table 3.3a and b), indicating the proportionate influence of the respective layers to groundwater potential.Table.3.4 shows the pair-wise comparison of the surface and subsurface themes.Details of the mathematical procedures is however, presented in Appendix VII. Following the weight assignment process, the maps in vector format (e.g. lithology, soil and rainfall) were converted to raster format for easy reclassification and

homogenization of the thematic maps. Themaps were categorized into: very good, good, moderate and poor and ranked 5, 4,3,2,1 respectively. Appropriate values were assigned to the distinct classes. The categorization and class assignment were based on the groundwater potential. This process is called reclassification and it was actualized by using the re-class tool under the arc tool box of the ArcGIS 10.3.1.

3.5.1.3 Delineation of groundwater potential zones (GWPZ)

The Groundwater Potential Index (GWPI) arising from the integration of the thematic layers is given by:

$$GWPI = EwEr + SLwSLr + SwSr + DDwDDr + RFwRFr + LUwLUr\ LwLr + LDwLDr + RSwRSr + ATwATr \quad 3.6$$

where E is elevation, SL represents slope, S represents soil, DD represents drainage density, RF represents rainfall, LC represents land use and cover, RS is resistivity, L represents lithology, LD represents lineament density, AT represents aquifer zone thickness w is the standardized theme weight and r is the standardized individual class weight. The resulting groundwater potential Index (GWPI) is a quantity with no physical dimension that helps to delineate areas of prospective groundwater potential. The reclassification of the GWPZ map into suitable classes was achieved the using the reclass tool in the GIS environment.

The verification of the GWPZ map was actualized with pumping test results from existing borehole records of the area. The well yields were compared to the aquifer potential zone map to ascertain the efficacy of the procedure and the reliability of groundwater productivity map so produced.

Table 3.3 (a). Weight assignment scale of Saaty and its interpretation (Saaty 1980)

Less important				Equally Important	More important			
Extremely	Very strongly	Strongly	Moderately	Equally	Moderately	Strongly	Very strongly	Extremely
1/9	1/7	1/5	1/3	1	3	5	7	9

2, 4, 6 and 8 are intermediate values that denotes comprise

Table 3.3 (b)Average Random Consistency index values (Saaty 1980)

Order of Matrix	Randomized Index
3	0.90
4	1.12
5	1.24
6	1.32
7	1.41
8	1.45
9	1.51

Table 3.4. Pair-wise comparison matrices table of the different themes and weights using the Saaty's (AHP) technique

	THEMES										RANKS			
1	LITHOLOGY	1	3	3	5	5	5	7	7	7	9			
2	AQUIFER THICKNESS	0.3333	1	1	3	3	3	5	5	5	8			
3	RAINFALL	0.3333	1	1	3	3	3	5	5	5	7			
4	AQUIFER RESISTIVITY	0.2	0.3333	0.3333	1	1	1	3	3	3	6			
5	SLOPE	0.2	0.3333	0.3333	1	1	1	3	3	3	5			
6	ELEVATION	0.2	0.3333	0.3333	1	1	1	3	3	3	5			
7	LANDCOVER	0.1429	0.2	0.2	0.3333	0.3333	0.3333	1	1	1	4			
8	SOIL	0.1429	0.2	0.2	0.3333	0.3333	0.3333	1	1	1	4			
9	LINEAMENT DENSITY	0.1429	0.2	0.2	0.3333	0.3333	0.3333	1	1	1	4			
10	DRAINAGE DENSITY	0.1111	0.1111	0.1429	0.1667	0.2	0.2	0.25	0.25	0.25	1			
	SUM	2.8063	6.7111	6.7429	15.1667	15.2	15.2	29.25	29.25	29.25	53			
	STANDARDISED MATRIX											TOTAL	WEIGHT	%
1	LITHOLOGY	0.3563	0.4470	0.4449	0.3297	0.3289	0.3289	0.2393	0.2393	0.2393	0.1698	3.1236	0.3124	31
2	AQUIFER THICKNESS	0.1188	0.1490	0.1483	0.1978	0.1974	0.1974	0.1709	0.1709	0.1709	0.1509	1.6724	0.1672	17
3	RAINFALL	0.1188	0.1490	0.1483	0.1978	0.1974	0.1974	0.1709	0.1709	0.1709	0.1321	1.6535	0.1654	17
4	AQUIFER RESISTIVITY	0.0713	0.0497	0.0494	0.0659	0.0658	0.0658	0.1026	0.1026	0.1026	0.1132	0.7888	0.0789	8
5	SLOPE	0.0713	0.0497	0.0494	0.0659	0.0658	0.0658	0.1026	0.1026	0.1026	0.0943	0.7699	0.0770	8
6	ELEVATION	0.0713	0.0497	0.0494	0.0659	0.0658	0.0658	0.1026	0.1026	0.1026	0.0943	0.7699	0.0770	8
7	LANDCOVER	0.0509	0.0298	0.0297	0.0220	0.0219	0.0219	0.0342	0.0342	0.0342	0.0755	0.3542	0.0354	4
8	SOIL	0.0509	0.0298	0.0297	0.0220	0.0219	0.0219	0.0342	0.0342	0.0342	0.0755	0.3542	0.0354	4
9	LINEAMENT D	0.0509	0.0298	0.0297	0.0220	0.0219	0.0219	0.0342	0.0342	0.0342	0.0755	0.3542	0.0354	4
10	DRAINAGE D	0.0396	0.0166	0.0212	0.0110	0.0132	0.0132	0.0085	0.0085	0.0085	0.0189	0.1591	0.0159	2
	SUM	1	1	1	1	1	1	1	1	1	1	10	1	100

CONSISTENCY RATIO = 0.044 (C.R <0.1)

3.5.2 Hydrochemical Data Evaluation

Statistical techniques were deployed to extract relevant information from the area's hydrochemical results. Water and irrigation quality indices were also examined using standard and established protocols. The hydrochemical data evaluation is described in the following subsections.

3.5.2.1 Charge balance

The overall charge balance which is estimated by summing the electrical charges in elemental analysis can be used as a measure of accuracy of the analysis. This is based on the fact that water is neutral, hence, the sum of positive charges equals the sum of negative charges in solution (Electroneutrality). Therefore, the result of the groundwater analysis were checked for accuracy using the electroneutrality equation given below.

$$\sum \text{Cations} - \sum \text{Anions} / \sum \text{Cations} + \sum \text{Anions X } 100$$

3.5.2.2 Statistical analysis

Descriptive statistics were used to summarize the hydrochemical data. Also, some plots including the box and whisker and bivariate plots were employed to compare the relative proportions of the chemical species in the samples and to provide information on the processes that control groundwater chemistry respectively. The influence of dissolution of rocks and human related activities on water quality was evaluated using thewater quality index(WQI). Evaluation of theWQI entailed the assignment of weight the physico-chemical parameters based on the relative impact of the parameters on the general quality of water (Table 3.5).

Principal component analysis (PCA) was utillised as quantitative method to decrease the dimensionality of the hydrochemical data by evaluating the association between the variables of the samples and as a measure of correlation between the groundwater constituents.

3.5.2.3 Drinking water quality index (WQI) and irrigation index evaluation

WQI is a dependable and effective technique for evaluating, interpreting and reporting of water quality information (Asadi *et al*., 2007). In line with Vasanthavigar *et al.,* 2010, suitable ranks were allocated to the physical and chemical parameters (Table 3.5)whereas the relative weight Wi for every component was calculated using the equation provided by Krishna et al., 2015. Detailed account of the mathematical procedures for evaluating the WQI is presented in Appendix VIII.

A number of indices have been suggested to infer the viability of water for irrigation purpose. The indicators of irrigation quality were assessed using the following parameters: salinity hazard, residual sodium carbonate, soluble sodium percentage, sodium absorption ratio, residual sodium bicarbonate, permeability index, Kelly ratio, and magnesium hazard. The mathematical formulars of the irrigation quality indices are presented in Table 3.6.

As can be seen from Table 3.6, salinity hazard is a measure of the electrical conductivity. A high amount of dissolved salts in water can affect the uptake of water by the roots of the plant, leading to stunted growth in plants (Selvan *et al.,* 2012). SAR isa measure of the ratio of monovalent sodium to divalent calcium and magnesium in water, which affects the accessibility of water to the plant and the structure of the soil as it renders the soil impervious and compact (Wilcox, 1955). However, residual sodium carbonate (RSC) as outlined by Eaton, 1950 and Richards, 1954 relates the amount of bicarbonates and carbonates ion to the alkali earth metals. The soluble sodium percentage (SSP) also known as % Na is a measure of the dissolved sodium content of the water and an indication of Na hazard in water. While Kelley's ratio (KR) defines the balance between Na^{+}, $Mg^{2+}$and Ca^{2+} in water. Kelly Ratios> 1 connotesa high level of sodium ion in water, magnesium hazard (MH) which is synonymous to magnesium adsorption ratio (MAR) represents the ration of magnesium ion to the alkali earth metals expressed as a percentage.

Table 3.5. WQI Parameters and Weight Assignment Table

S/no.	Parameters	Weight(wi)	Relative Weight (Wi)
1	Electrical Conductivity	5	0.16
2	Total Dissolved Solids	5	0.16
3	HCO_3	3	0.09
4	Cl	3	0.09
5	NO_3	5	0.16
6	SO_4	4	0.13
7	Ca	2	0.06
8	K	2	0.06
9	Mg	1	0.03
10	Na	2	0.06
	Total	32	1

Table 3.6 Irrigation water quality parameters and mathematical formulars

S/n	Parameters	Formulars	Sources
1	Salinity	Measure of Electrical Cond.	Selvan *et al.,* 2012
2	Sodium absorption ratio (SAR)	$SAR = \frac{Na^+}{\sqrt{\frac{(Ca^{2+} + Mg^{2+}}{2}}}$	Wilcox, 1955, Richards (1954)
3	Residual sodium carbonate (RSC)	$(HCO_3^- + CO_3) - (Ca^{2+} + Mg^{2+})$	Eaton, 1950 Richards, 1954
4	Soluble sodium percentage (SSP)	$\frac{(Na^+ + Ca^{2+})}{(Ca^{2+}\ Mg^{2+} + Na^+ + K^+)} \times 100$	Wilcox 1955 Richards, 1954
5	Permeability index (PI)	$= \frac{Na^+ + \sqrt{HCO_3^-}}{Na^+ + Mg^{2+} + Ca^{2+}} X100$	Doneen, 1964
6	Kelly ratio (KR)	$(Na^+ + Ca^{2+}) / Mg^{2+}$	Kelly (1963)
7	Magnesium hazard (MH)	$(Mg^{2+} / Ca^{2+}\ Mg^{2+}) \times 100$	Raghunath, 1987

`Units in Meq/l

3.5.2.4 Hydrochemical facie evaluation

Hydrochemical facies and the mechanism governing the hydrochemistry of the undergroundwater in the research area were evaluated with Piper trilinear, Stiff, Schoeller, Gibbs and Chanda's plot using the Aquachem version 2014.2 and Origin pro 8 softwares.

3.5.3 Stable Isotope Data Evaluation

The stable isotope ratios of the ^{2}H and ^{18}O in rainfall is a linear correlation controlled by thermo-dynamical processes at phase transformations. When the isotopic compositions of rainfall from different part of the globe are plotted against each other on $\delta^{18}O$ versus δD plots, a linear band of data is obtained which that can be defined by equation 3.18 (Craig, 1961):

$$\delta D = 8\ \delta^{18}O + 10 \qquad (3.18)$$

For the purpose of this study the Oxygen-18 and Deuterium ratios of the groundwater samples was inputted into the global meteoric water plot generated from the equation GMWL; $\delta^{2}H=8\ \delta^{18}O +10$; (Craig 1961).

A correlation between the depletion of the deuterium and oxygen-18 in the groundwater samples was established; the locus line of such samples in δD was defined by equation (3.18). The slope value is 8 due to the fact that the value given by equilibrium Rayleigh condensation of precipitation at a humidity of 100% is close to the value 8. The value of 8 is also approximately equal to the equilibrium fractionation ratios for Deuterium and O

isotopes at 25-30^{o}C. The intercept value of 10 shown in equation 3.18 (Craig line) is a very significant parameter in the interpretation of stable isotope data and it is termed the deuterium excess (or d-excess) value for this equation. Details of the principles of stable isotope is presented in Appendix IX.

CHAPTER FOUR

RESULTS AND DISCUSSION

4.1 Thematic Maps

In line with the main objective of this research a total number of 10 thematic maps were created in the ArcGIS software platform. Six (6) of these maps comprising of elevation, slope, soil drainage density rainfall and land use constitute the surface maps. However, the second group of maps which consist of lineament density,aquifer thickness,aquifer resistivity and lithologymake up the subsurface thematic maps of the area.

4.1.1 Surface thematic maps

The thematic maps are representing the surface processes are presented in Fig. 4.1-4.6.

I. Elevation

The altitude of a geographic area calculated from a given (i.e. sea level) reference point is defined as elevation. The elevation of the area is depicted on a thematic map in Fig. 4.1. The elevation of the area ranged from 275-706 m, as shown on the thematic map.

The sedimentary terrain are generally characterised by low-moderate relief areas, which will inherently favor more groundwater recharge, whereas the topographically high-moderate relief sections in the basement setting will normally constitute higher run-off locations which are detrimental to groundwater recharge.

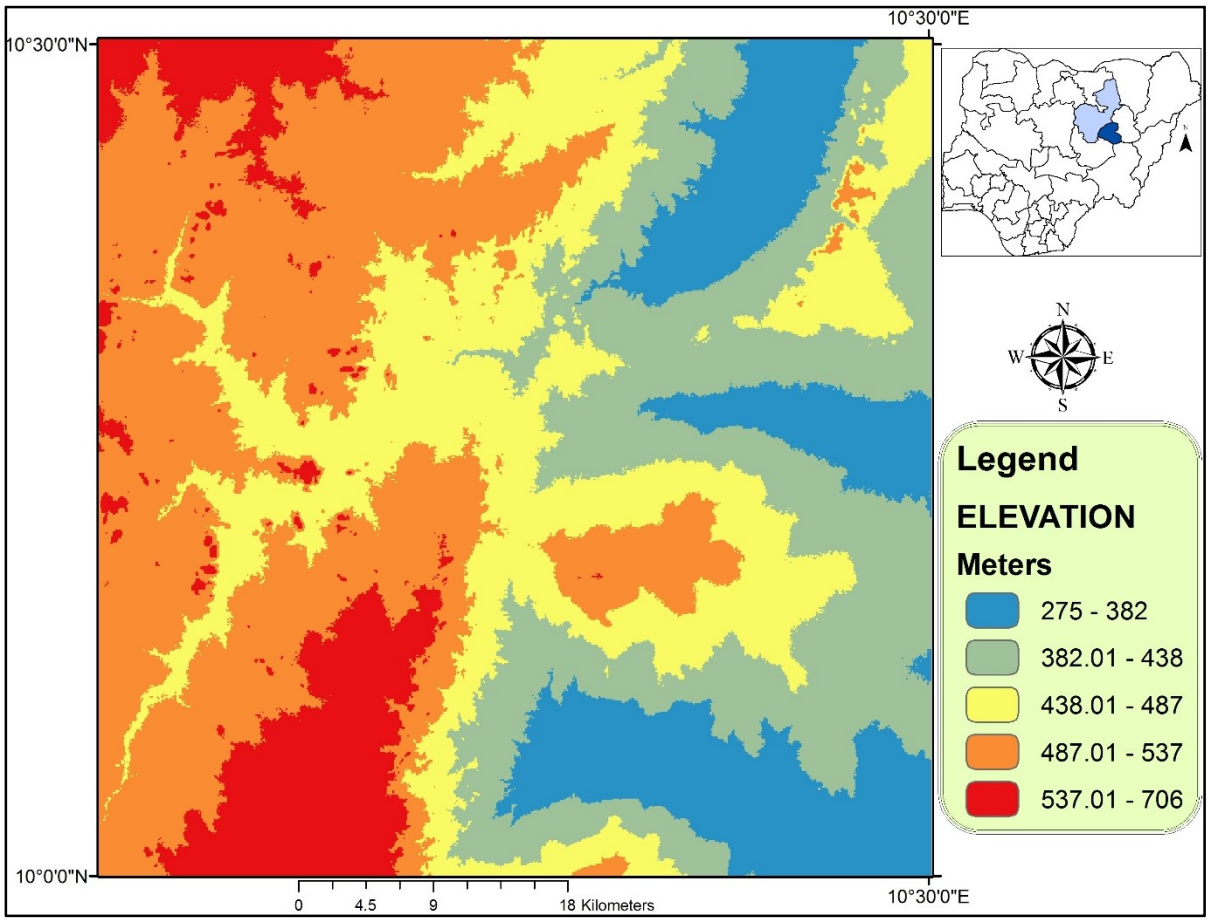

Fig. 4.1. Elevation map of Bauchi-Alkaleri-Kirfi transition zone

II. Land use/ cover (LULC)

The LULC of a given location has an impact on groundwater infiltration since it gives crucial information on the degree of groundwater use and demand (Narendra et al., 2013). Five major LULCcategories were delineated. This includebare land (48%), scrubland (31%), forest (17%), water body (3%), and built areas (1%) (Fig. 4.2). In the different terrains, water bodies that are regarded to be good sources of groundwater recharge are almost evenly distributed.However, vegetation regions and scrubland predominate in sedimentary terrain, which have the ability to slow runoff and increase the percolation of groundwater (Lawal et al., 2021). Built-up areas and exposed rock surfaces are generally devoid of flora, making meteoric recharging challenging.

III. Slope

The slope of a region influences surface water circulation and ultimate infiltration into the aquifer. (Fashae *et al*., 2014). The slope in the area, as illustrated in Fig. 4.3, varies from 5% to >20%, indicating the heterogeneity of run-off water and groundwater replenishment., which corresponds to variation in aquifer potential within the area's varied geological settings. In terms of groundwater recharge, zones with a gentle slope (0-5 percent), which are moreprevalent in sedimentary basin, were found to be more promising than areas with steep inclines (15->20 percent) which characterise the hard rock terrain.Steep slopesgenerally exhibit limited infiltration/recharge and consequently low groundwater prospects.Gently sloping lands, however, are associated with significant rainwater infiltration.

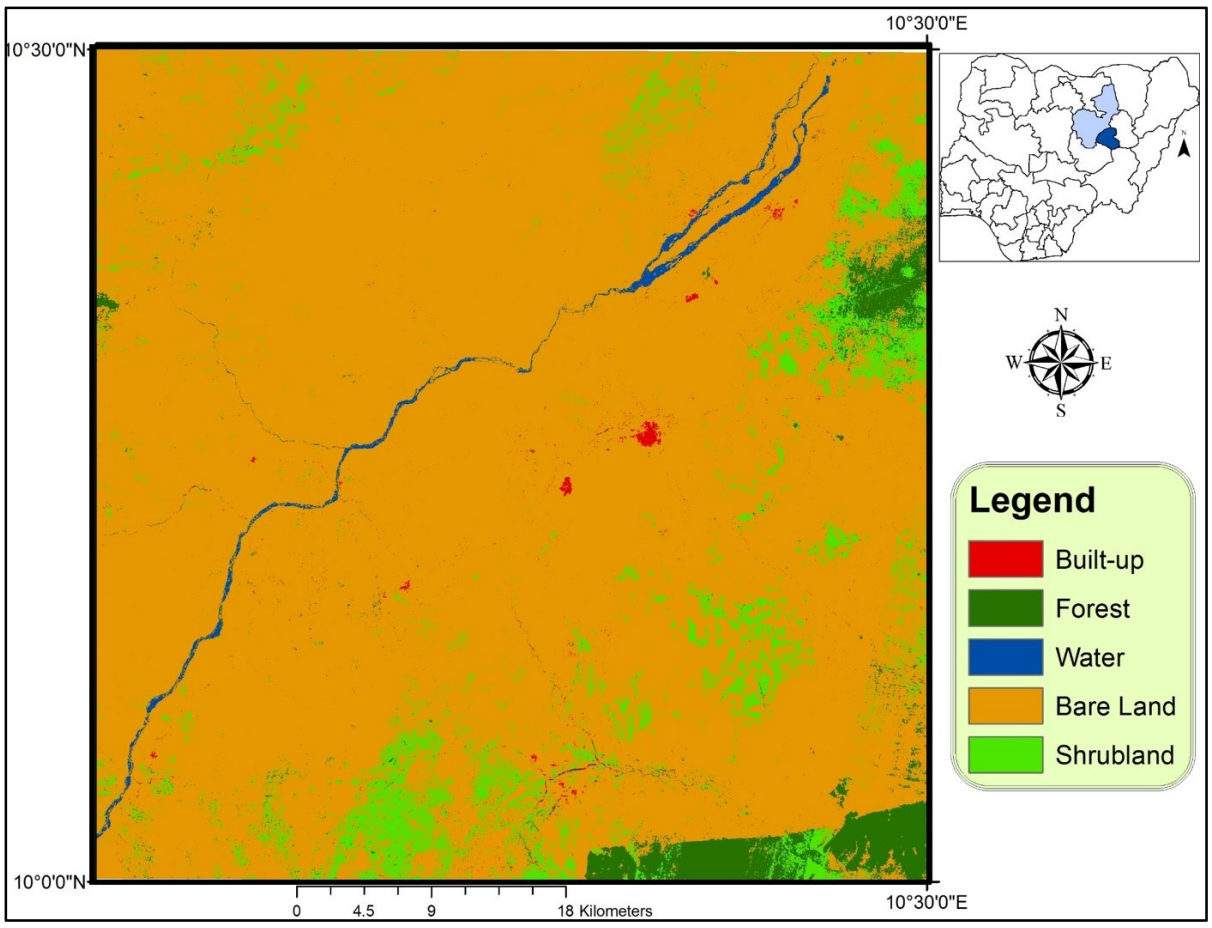

Fig. 4.2. Land use/land cover map of Bauchi-Alkaleri-Kirfi transition zone

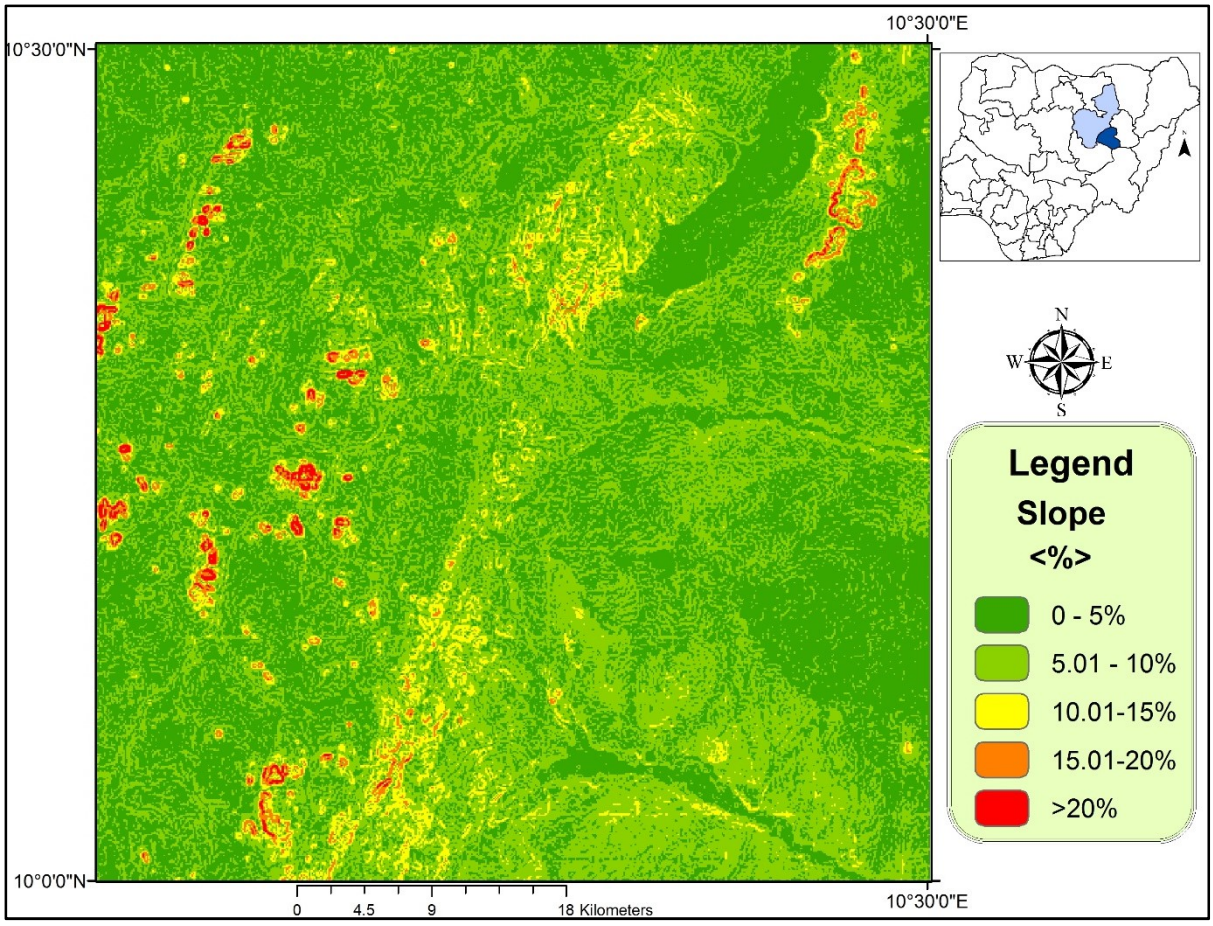

Fig. 4.3. Slope map of Bauchi-Alkaleri-Kirfi area

IV. Soil

The nature of the soil in a particular area determines the amount of infiltration and hence groundwater recharge in the area. Porous and permeable sands produce excellent platforms for groundwater replenishment, impervious materials like clays and mudstones increases runoff rather than infiltration (Narendra *et al*., 2013). As indicated by the soil thematic map of area (Fig. 4.4), 3 soil divisions were identified: sandy clays, sandy loam and alluvium covering 1200.2 km^2 (39.2%), 1704.7 km^2 (55.7%) and 155.8 km^2 (5.09 %) of the total Bauchi-Alkaleri-Kirfi area, respectively. The sandy loam soil type is predominantly occurs in the sedimentary settings, suggestive of higher rates of groundwater infiltration while the sandy clay soils occupy most parts of the basement terrain implying less permeable soil covers which would retard groundwater recharge.

The infiltration capacity of soils is very vital to groundwater accumulation as it determines the quantity and rate of aquifer recharge in an area. The infiltration rate of soils is controlled by the sorting and grain size distribution of the soil. Sands and sandy soils are generally have higher infiltration capacity (more permeable) than clay soils and as a result areas with sandy soils will be favorable for recharge of groundwater.

V. Drainage Density

The importance of drainage density in surface-runoff processes cannot be overstated.Drainage density and groundwater infiltration have an inverse relationship, making it a useful metric for determining groundwater potential.The map showing the drainage densityshown in Fig. 4.5 revealed a drainage network with low-moderately density (0.34 km/km^2) to highly dense (<1.72 km/km^2). However, low density zones account for 78.05 percent of the total area, whereas high drainage density zones account for 3.49 percent.

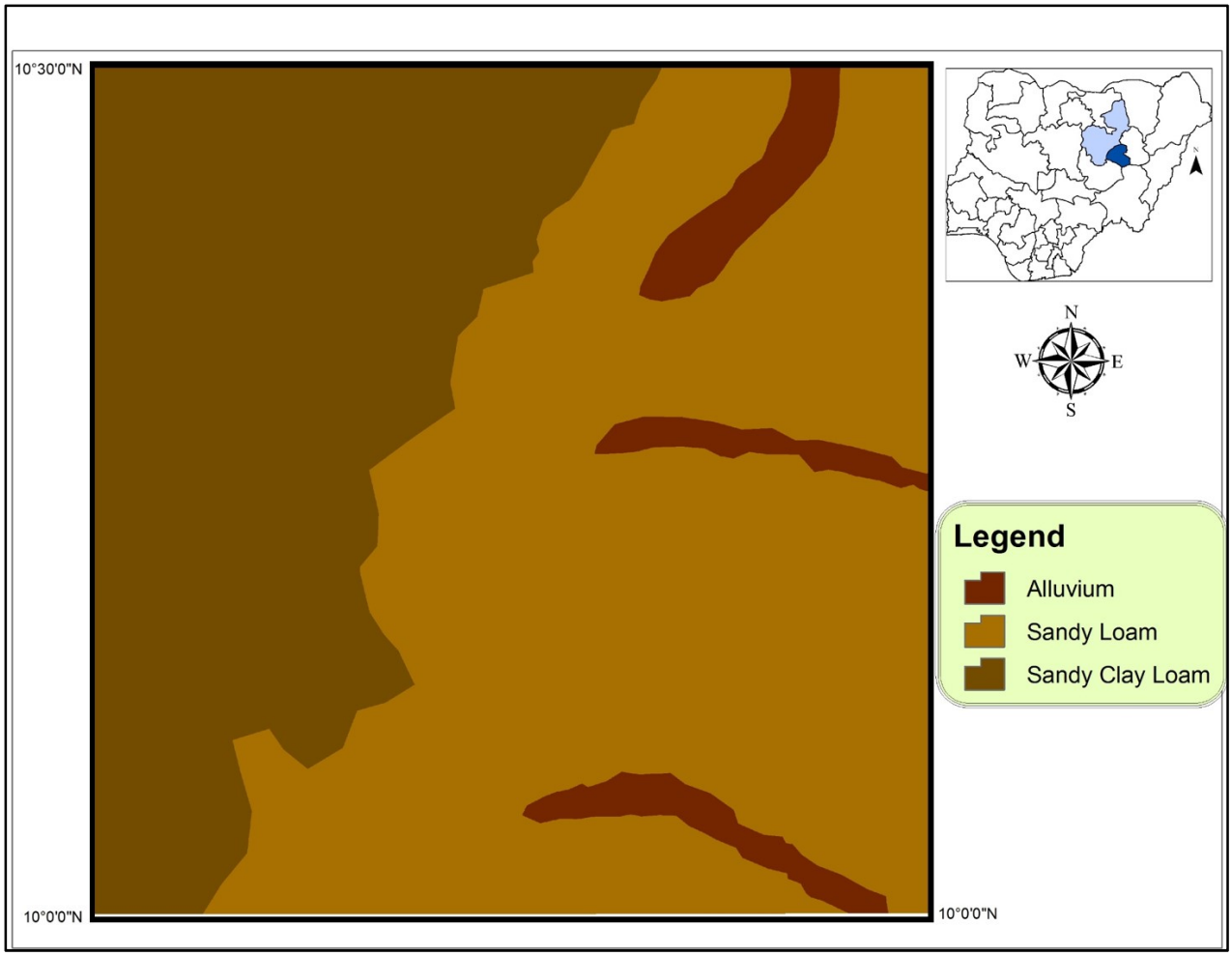

Fig. 4.4. Soil map of Bauchi-Alkaleri-Kirfi Area

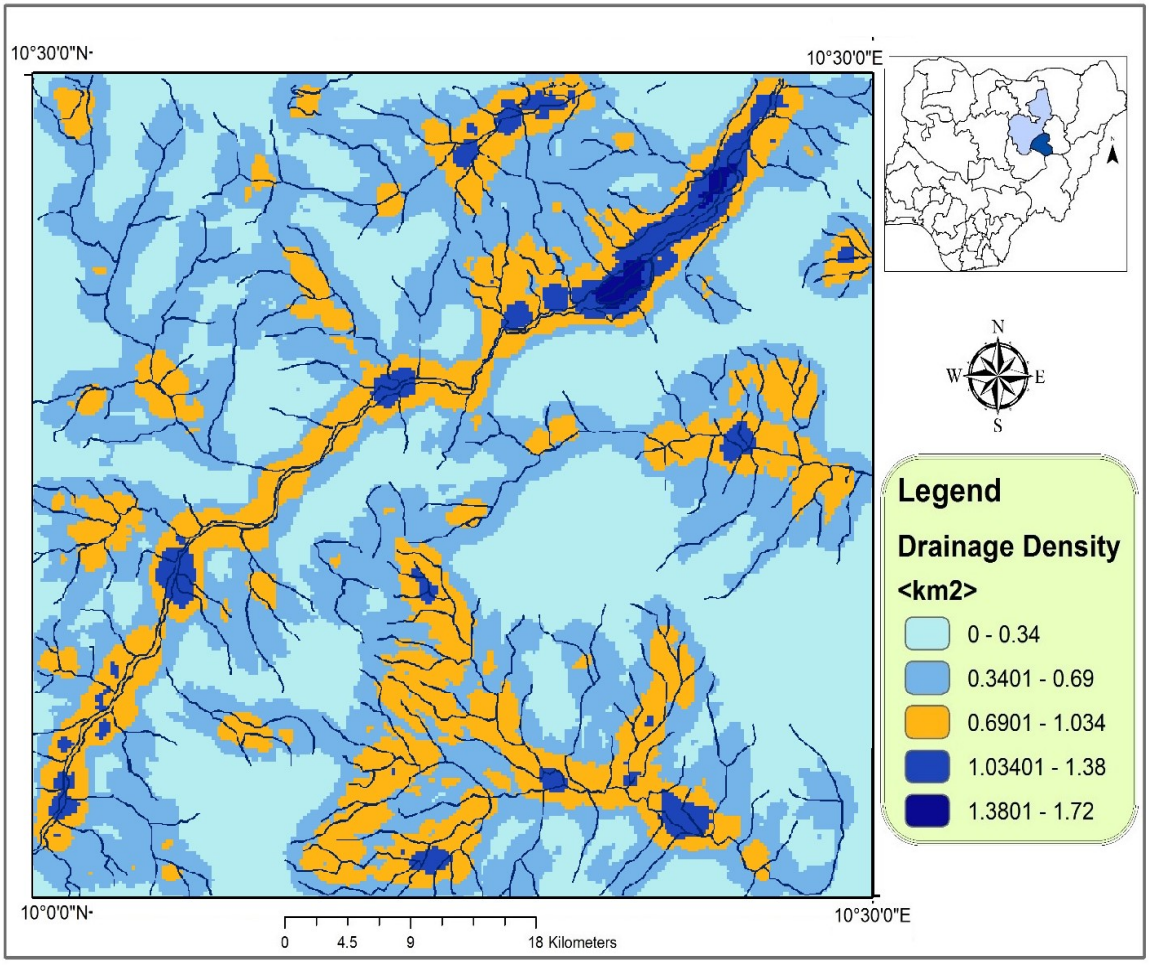

Fig. 4.5. Drainage density map of Bauchi-Alkaleri-Kirfi Area

Generally, the Bauchi-Alkaleri-Kirfi transition zone can be said to have low to moderate drainage density which implies high to moderate infiltration capacity for over 78 % of the area. The area with very high drainage density is usually characterised by a concentration of drainage channels, which translates to greater amount of runoff with little or no recharge while the lower the density of the drainage, the lesser the concentration of the run-off and the higher the possibility of groundwater recharge and hence a potential groundwater zone (Mukherjee, 2007).

The drainage density can also be viewed as a measure of permeability because in areas with low drainage density, surface water has more time to infiltrate as opposed the high areas. Dense drainage network is usually characterised by a concentration of drainage channels, which translates to greater amount of runoff with little or no recharge while the lower the density of the drainage, the lesser the concentration of the surface flow and the greater the possibility of water percolation (Mukherjee, 2007).

VI. Rainfall

Rainfall regulates the quantity of infiltration and runoff. The primary source of groundwater recharge in the area is believed to be precipitation. According to Tijani, (1994) and Mc Donald *et al.,* (2012), effective rainfall is one of the critical elements determining the amount of groundwater in a region. Sometimes, rain generates runoff along primary streams in the area which usually flows to less elevated regions. The distribution of rainfall in the area varies between 850 to 1,100 mm (Fig. 4.6). By implication, the generally mountainous Basement Complex zones receives more precipitation compared to sedimentary areas which are mostly flat lying. Consequently, significant quantity of precipitation flows down through open spaces and fractures in rocks to the subsurface aquifers in the area.

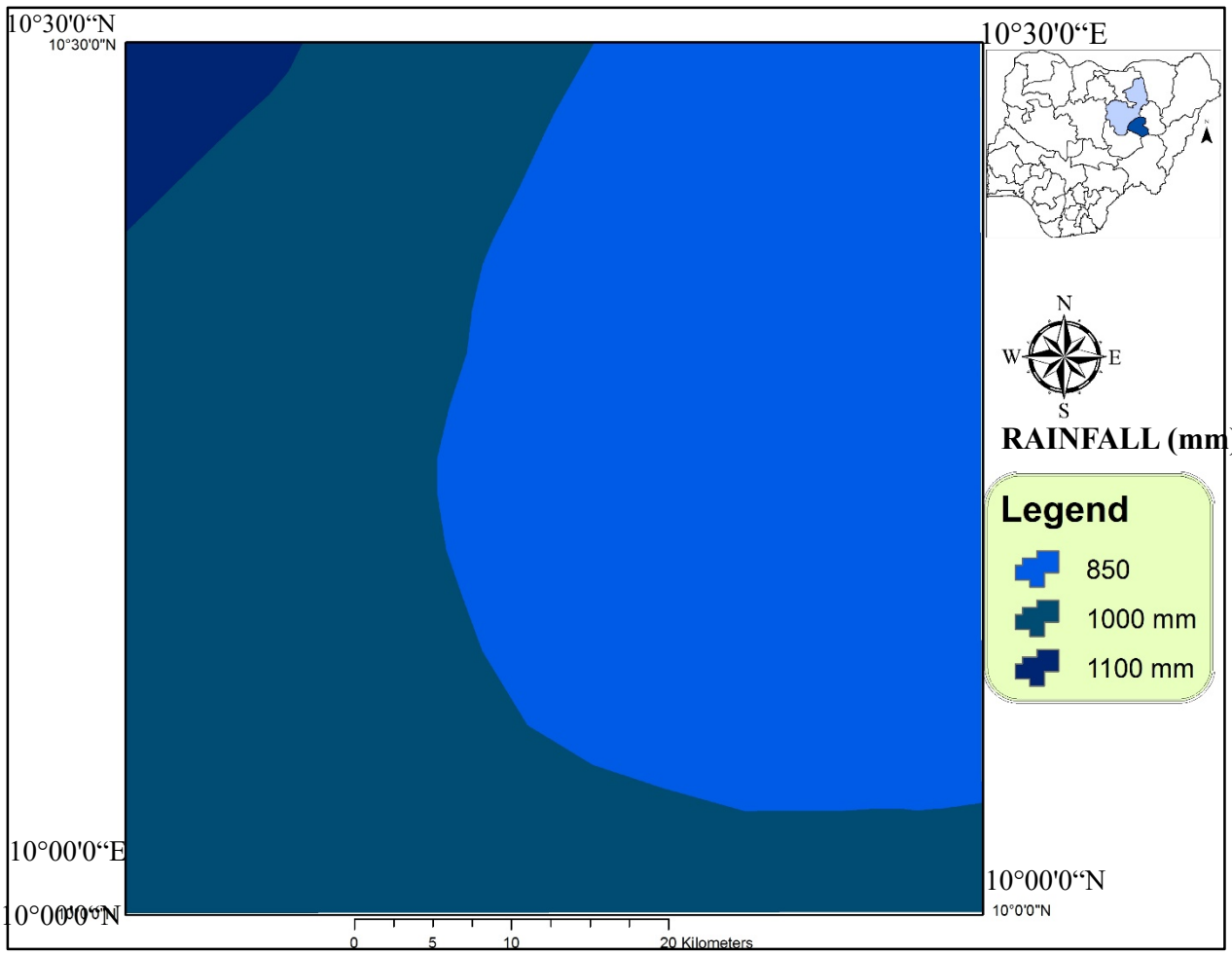

Fig. 4.6 Rainfall Distribution map of Bauchi-Alkaleri-Kirfi Area

By and large, high rainfall imply the possibility of higher groundwater recharge and hence, higher groundwater prospects. Conversely, areas characterised by low rainfall would be associated with poor groundwater replenishment and prospects.

4.1.2 Subsurface thematic Maps

In order to compliment this surface maps, another set of thematic maps of subsurface parameters were generated from aeromagnetic data (lineaments), geological mapping (lithology) and geophysical investigation (aquifer resistivity and thickness) respectively.

4.1.2.1 Lineament density

Linear structures within the Bauchi-Alkaleri-Kirfi transition zone is presented in Fig. 4.7a and the rose diagram showing the structural trends in Fig. 4.7b. Lineament patterns are NW-SE,NE-SW, and ENE-WSW, with minor N-S and E-W trend. The major trends observed corresponds to those of the Pan-African event (Ajakaiye *et al.,* 1986), while the minor ones have been linked to the tectonism of Jurassic and end-Cretaceous (Dike, 1993). Most of the post Kerr-Kerri faults and joints runs parallel to the Pan African, Jurassic and end-Cretaceous trends, which suggests the reactivation of older structures during the early Tertiary extensional tectonism (Benkhelil, 1989). All these structural trends conforms with those reported by earlier researches on the Kerri-Kerri Formation and adjoining Basement Complex exemplified by Cater *et al*., 1963; Adegoke *et al*., 1986; Benkhelil, 1989; Dike, (1993). According to most of the aforementioned authors the Kerri-Kerri formation occupies a slightly asymmetric elongate basin bounded to the west (part of the study) by closely spaced normal faults which trend between North and East and this is also in tandem with the results of the present study (Fig.4.7a and 4.7b). Furthermore, according to Dobrin and Savit (1988), linear trends in the magnetic contours are mostly in cormformity with regional geology (e.g., extensive faults and dykes) making them significant in mapping structural trends. In the Bauchi-Alkaleri-Kirfi transition zone, the lineament density rangesfrom less than 0.17 to 0.88 km/km^2 (Fig. 4.8).

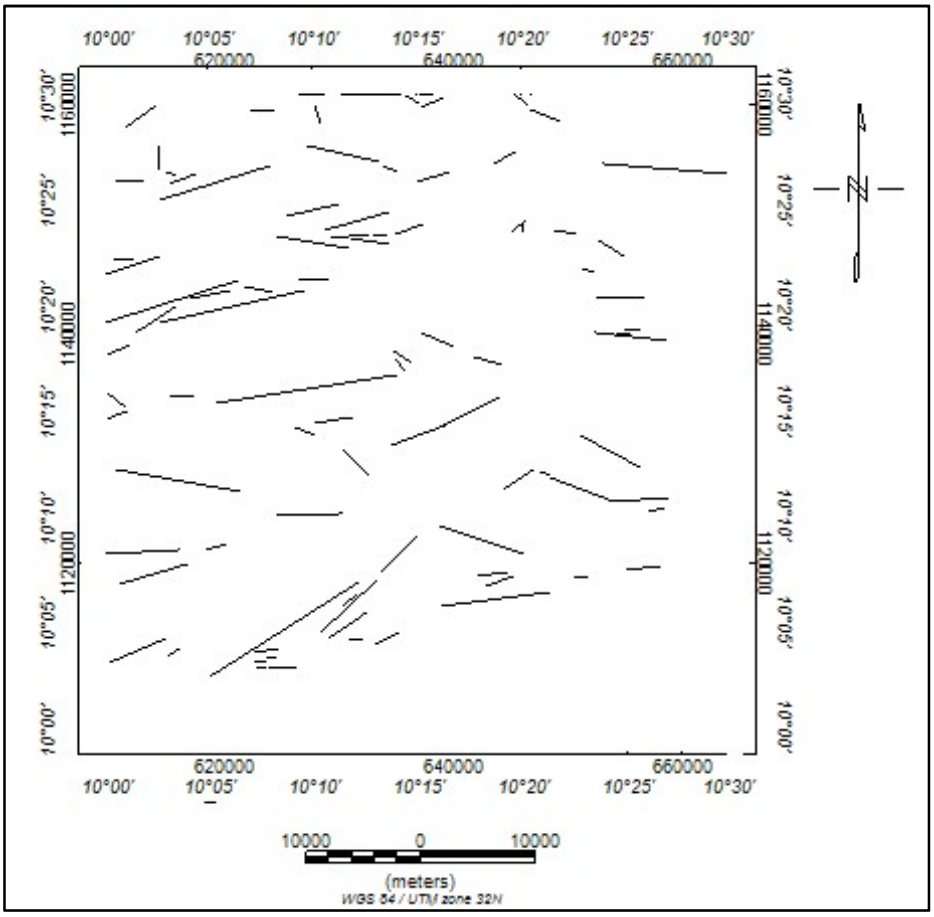

Fig. 4.7(a) Extracted magnetic lineament map

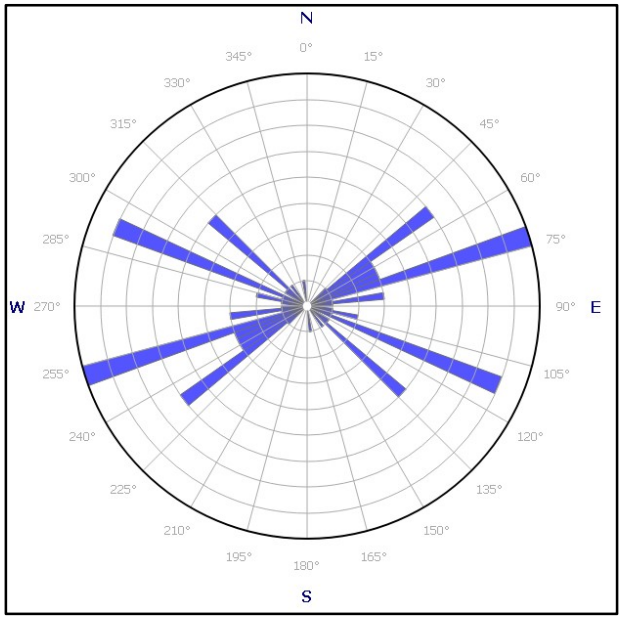

Fig. 4.7(b) Rose Diagram showing lineament trends in the study area

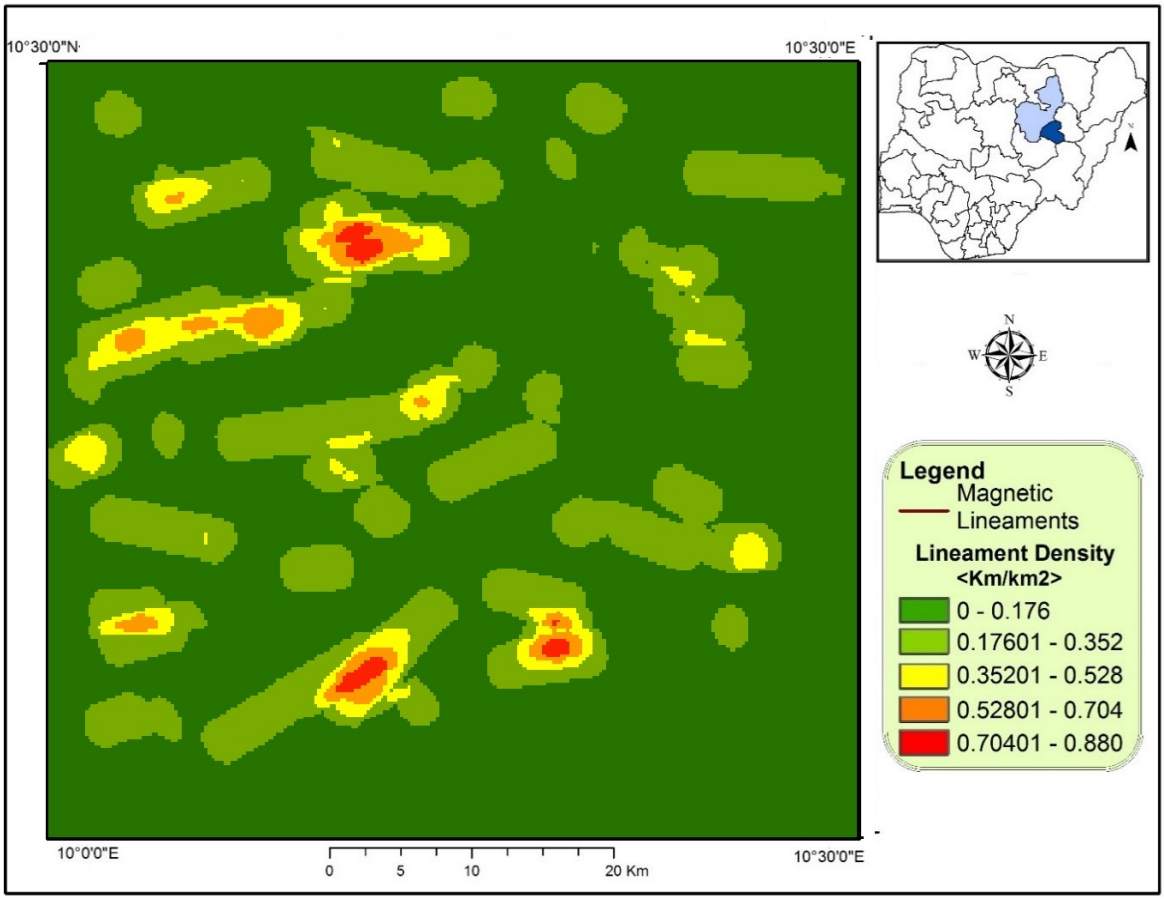

Fig. 4.8 Lineament trends in Bauchi-Alkaleri-Kirfi Area

As shown in Fig. 4.8,the densities of the lineaments in the crystalline basement rocks generally supersedes those of the sedimentary terrain, which is attributable to their tectonic history. The migmatite and gneiss revealed lineament densities of 0.35–0.88 km/km^2 while the bauchites and the Biotite hornblende granites indicated 0.17–0.52 km/km^2. Nonetheless, enclaves of medium to high lineament domains exist around the southeastern and northeastern regions underlain by the Tertiary sediments, the sandstones generally exhibited a low density of lineaments.

4.1.2.2 Geological characteristics

The geological mapping combined with petrographic and granulometric studies revealed four major rock types in the area: (i) Migmatite gneiss, (ii) Biotite hornblende granites, (iii) Bauchite and (iv) Sandstone, with minor variations in the form of granite gneiss, biotite gneiss and biotite granites and quartzites. The updated geology map (Fig. 4.9) revealed the hitherto concealed lineaments in the area, which mostly trend in the NE-SW direction. Bedding planes in Kerri- Kerri formation showed high dips (about 60^0) up north and low dips (about 12^0) southward and exfoliation planes in the basement part show dips of 20^0-30^0. All dipping in the southeastern direction. The revised geological map from which the lithology theme was derived is presented in Fig. 4.9 and the field occurrence of the rocks encountered is presented in the following chapter while detailed account of the petrographic and granulometric analysis is provided in Fig 4.10 to Fig 4.12 and Appendix XI.

(a) The Migmatite/Gneiss

The migmatite underlieabout 919 km^2 of the area (Fig 4.9),withexposures in the southwestern, northwest and central and portions of the area.The gneisses are metamorphic rocks having a distinct alternation of felsic and mafic colored bands. Under the thin section the granite gneiss comprises of quartz (33%), microcline (22%), plagioclase (17%), biotite (19%), hornblende (5%) and opaque minerals.

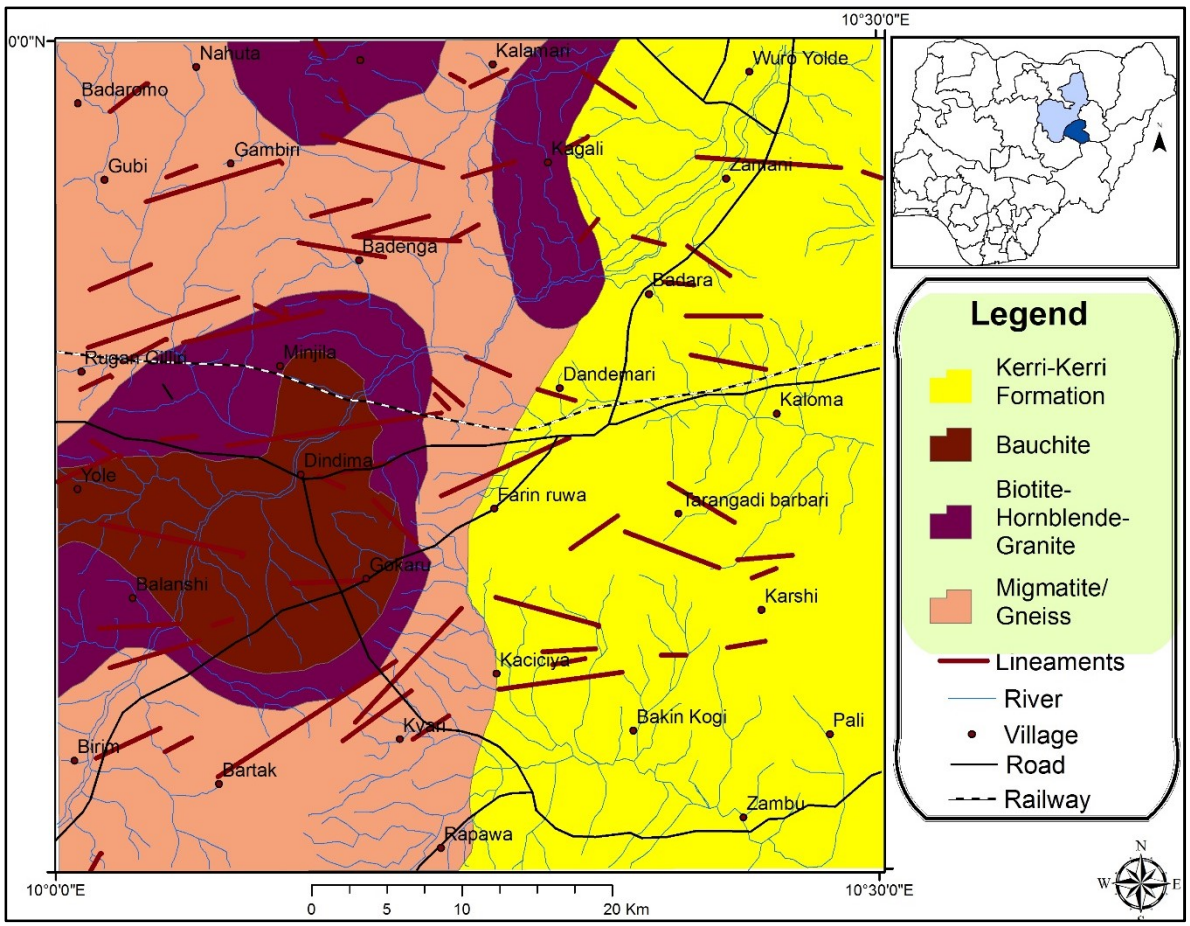

Fig. 4.9. Geology map of the Bauchi-Alkaleri-Kirfi transition zone

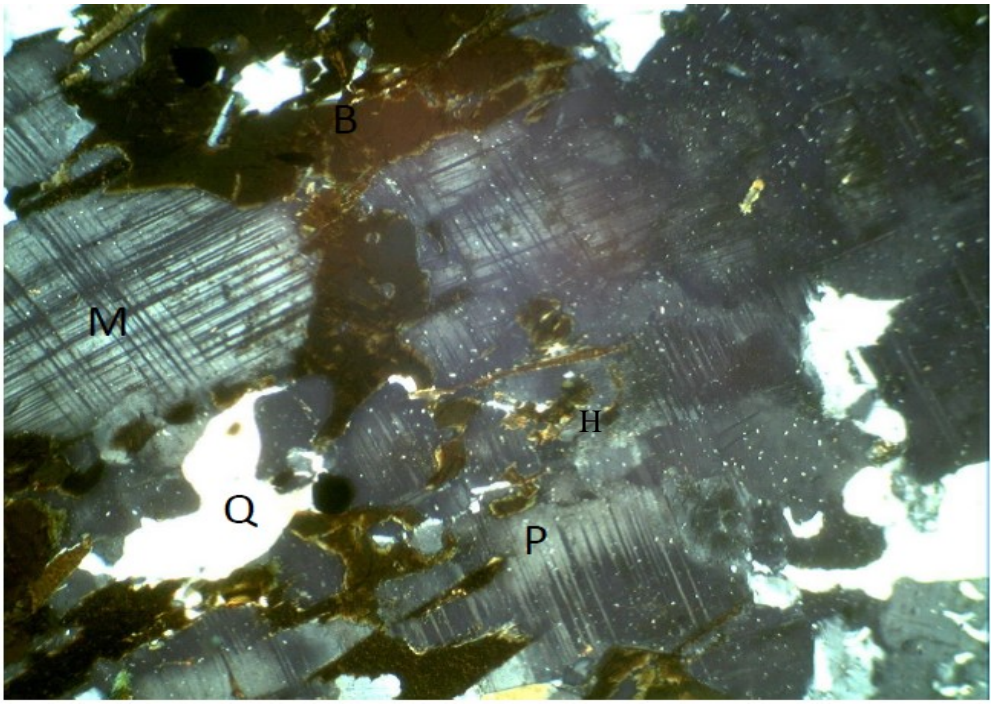

Fig.4.10 (a). Photomicrograph of Migmatite gneiss under transmitted light showing quartz (Q), biotite (B), Hornblende (H), Microcline (M) and plagioclase feldspar (P).

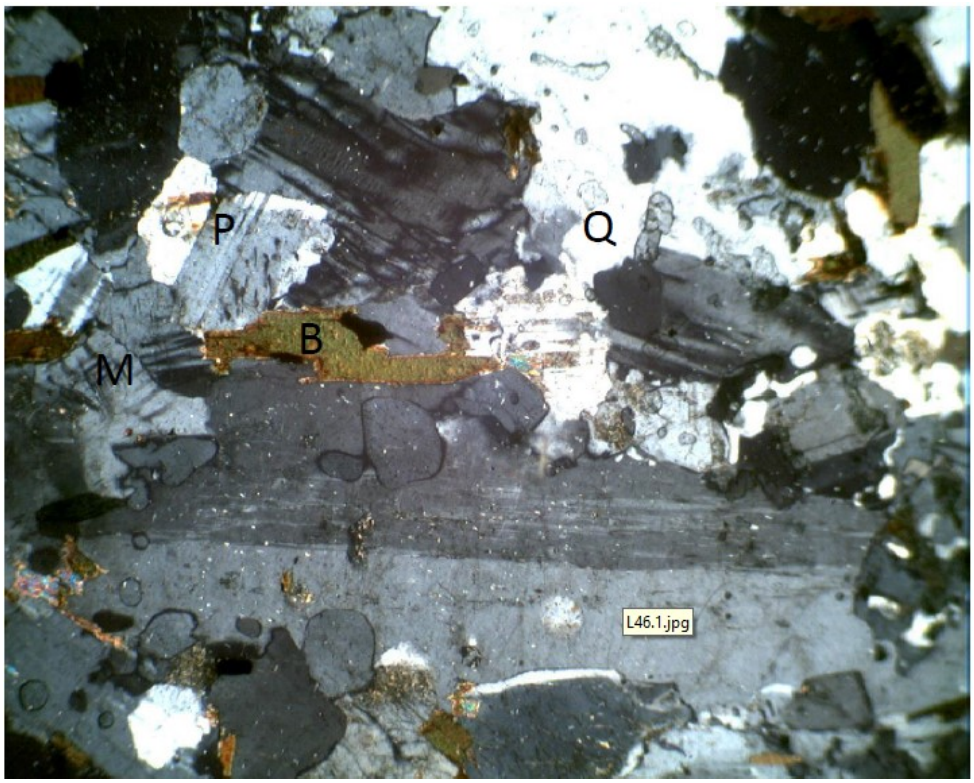

Fig.4.10 (b). Photomicrograph of migmatite under transmitted light showing quartz (Q), biotite (B), Microcline (M) and plagioclase feldspar (P).

The gneisses observed are represented by mostly regular gneiss with pockets of banded orthogenesis. The outcrops shows a high degree of weathering and jointing and in some places appear as boulders. Individual bands in some of the gneiss varies between 1-10 mm in thickness, an indication of partial melting or the introduction of new material. The migmatite gneiss indicated a modal composition of quartz (48%), microcline (21%), plagioclase (12%), biotite (12%) muscovite (7%) and opaque minerals (Fig. 4.10 b).

(b) The Biotite-hornblende granite

These granites cover approximately 15.25 percent of the research area and are exposed as low, medium, and high level outcrops in the northern, western, and southwestern parts of the studied area.The granitic rocks are thought to have intruded into the migmatite gneiss, resulting in batholiths that are usually elevated and massive in size. In hand specimen, the biotite-hornblende granites are coarse to very coarse grained equigranular igneous rock and are sometimes porphyritic in texture. The modal composition of the rock from the petrography revealed quartz (16%), microcline (10%), plagioclase (24%), biotite (36%) muscovite (16%) and opaque minerals (Fig 4.11a).

(c) The Charnockite (Bauchite)

The bauchitescover approximately 12 percent of the area. Oyawoye, (1972) discovered these distinctive quartz-fayalite monzonite and named the rocks “Bauchite” in 1962 in Bauchi area. Charnockites are fine - medium grained, granitic rocks with a greenish black color (Dada, 1989).Outcrops of charnockitesare conspicuous in the southwestern part of the research area, along Bauchi-Gombe road, where they occur predominantly in the form of boulders, with indications of onion skin weathering. The petrography of the charnockites showed that the rocks are composed of quartz (30%), microcline (10%), plagioclase (21%), biotite (22%), hornblende (8%) fayalite (7%) and opaque minerals (3%) (Fig. 4.11b).

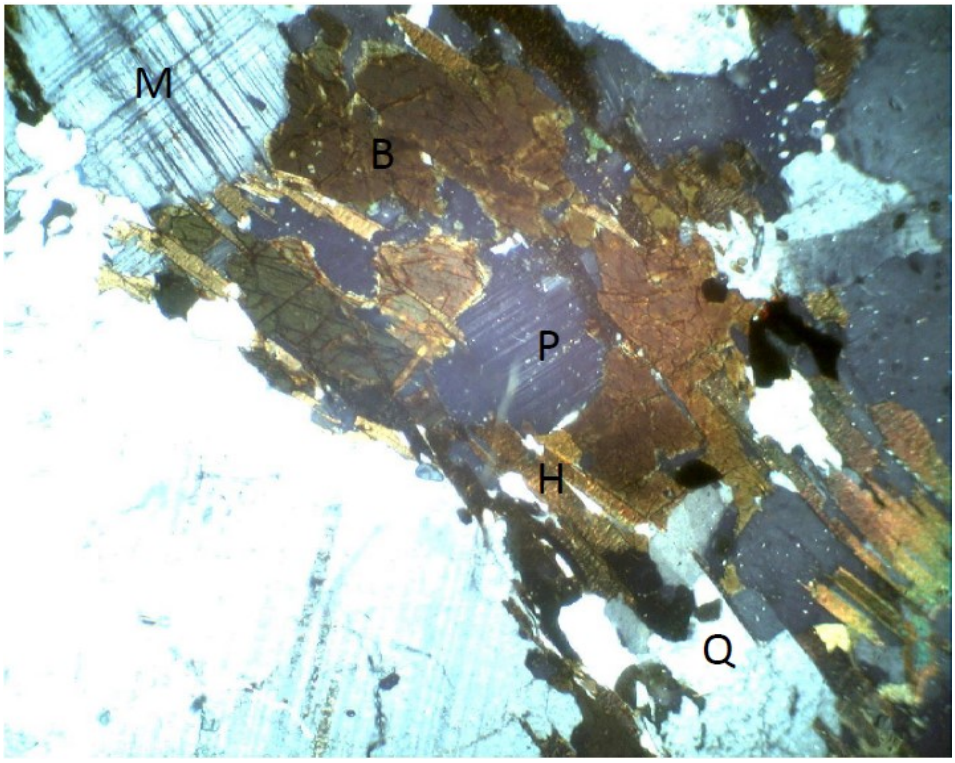

Fig. 4.11 (a). Photomicrograph of biotite hornblende granite in transmitted light showing quartz (Q), biotite (B), hornblende (H) and plagioclase feldspar (P), Microcline (M)

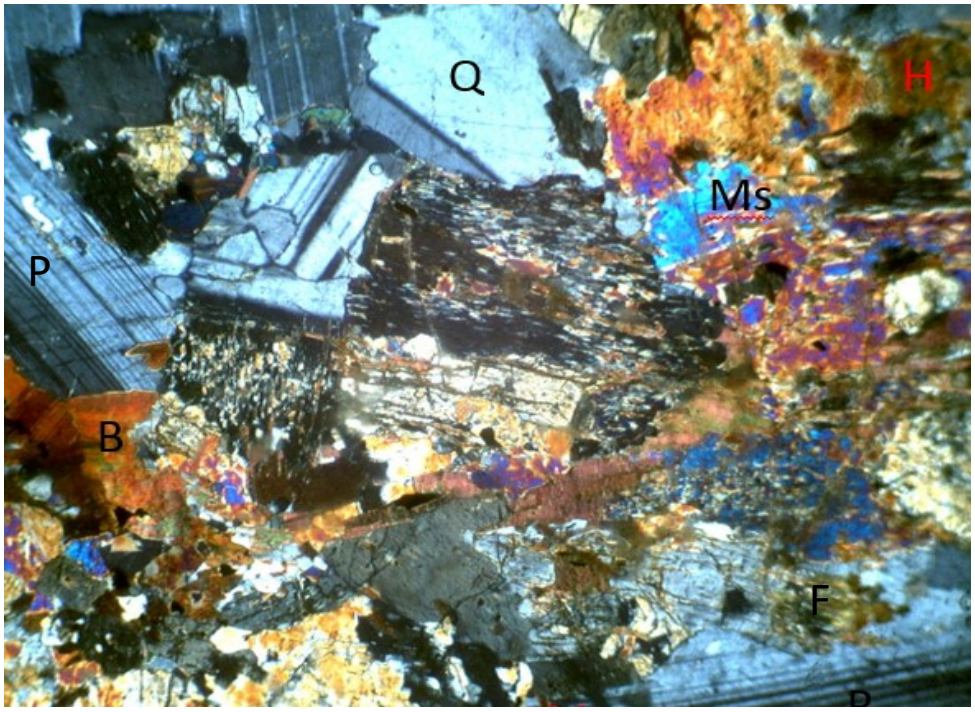

Fig. 4.11 (b) Photomicrograph of charnockite under transmitted light showing quartz (Q), biotite (B), hornblende (H) and plagioclase feldspar (P).

(d) Sandstone

The sandstones coversabout 42.5 percent of the total area.Thesesandstones which are medium to coarse grained and associated with clays and siltstones underlie the northeastern and the southeastern parts of the area. In the course of the field mapping, two of the three litho-facies were identified and mapped are consistent with that of Adegoke, (1986) and Dike, (1993). These include: ferroginised sandstone facies and the kaolinitic sandstone facies. The ferroginised sandstone facie was observed in the northeastern part of the area, around Gwaram and Badara areas. These sandstones are usually dark brown in color and highly indurated and occur mostly as fragmented rocks.

Petrographic studies show that the sandstones samples are generally medium to coarse grained and arkosic in nature, with modal classification as quartz (48%), Feldspar (11%) and rock fragment (41) in sample L60 and a composition of quartz (57%), feldspar (11%) and rock fragment (31%) in sample L80. Granulometric analysis show that the graphic mean of the samples ranged from 0.06 to 1.36Ø, which indicates that the sandstones are medium (1.36Ø) and coarse grained (0.06Ø) in nature based on Folk, (1968) while, the sorting of the sample grains ranged from 0.93 to 2.23 Ø, which reflects moderately sorted (0.7 to 1.0Ø) to a very poorly sorted sands (2 to 4Ø) (Table 4.1).

4.1.2.3 Geoelectrical characteristics

The results of the VES comprising the sounding curves, subsurface geo-electric layers and corresponding thickness and other details of the resistivity data analysis are presented in Appendices XII and XIII.The following sections providedetails of the VES curves and a summary of the geo-electrical characteristics utilized in the generation of the aquifer resistivity and thickness thematic map.Three (3) tofive(5) geo-electric layers where identifiedwithin the research area (Fig 4.12). The curves are K, H and A curve types (3-layers),KQ, AH, HK, KH, HA and AK (4-layers) as well as AAA, QHA, AKH, HAK, and HAA (5-layers). The distribution of the various type curves in the different rock units and the relative abundances of the different curve types in the Bauchi-Alkaleri-Kirfi area are shown in Fig. 4.13 (a) and 4.13(b).

Table 4.1. Graphic mean (grain size) and standard deviation (sorting) of sandstone samples based on the classification by Folk, 1968.

S/NO.	SAMPLE	GRAPHIC MEAN	SORTING
1	L55	0.06	2.16
		Coarse Sand	Poorly Sorted
2	L58	1.36	1.5
		Medium Sand	Poorly Sorted
3	L60	1.3	1.44
		Medium Sand	Poorly Sorted
4	L67	1.15	1.68
		Medium Sand	Poorly Sorted
5	L70	0.68	2.23
		Coarse Sand	very poorly sorted
6	L71	0.43	1.46
		Coarse Sand	Poorly Sorted
7	L74	0.06	2.16
		Coarse Sand	very poorly sorted
8	L76	1.06	1.11
		Medium Sand	Poorly Sorted
9	L79	1.07	1.4
		Medium Sand	Poorly Sorted
10	L80	0.41	0.93
		Coarse Sand	moderately sorted
11	L87	0.86	0.93
		Coarse Sand	moderately sorted
12	L88	0.76	1.06
		Coarse Sand	Poorly Sorted
13	L92	1.03	1.5
		Medium Sand	Poorly Sorted
14	L94	1.1	1.32
		Medium Sand	Poorly Sorted

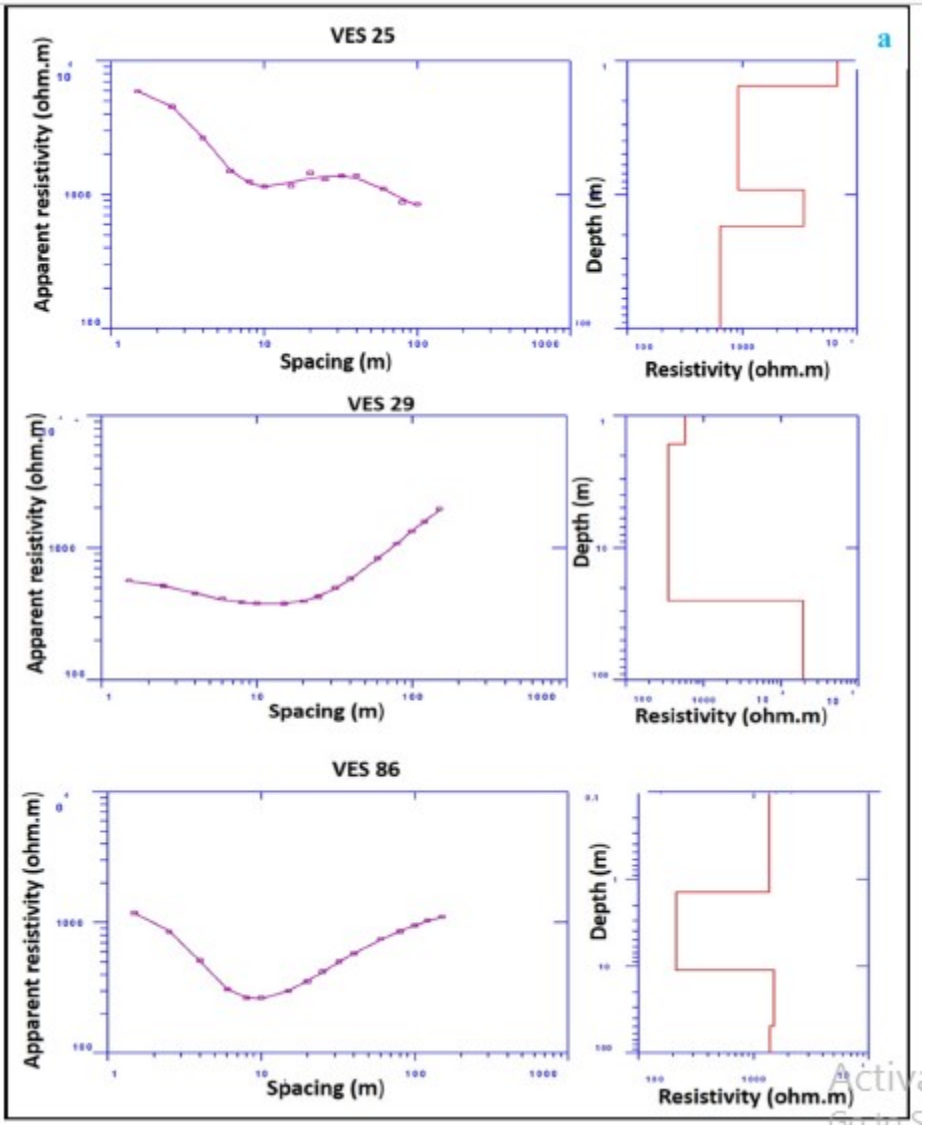

Fig. 4.12. Representative samples of the geo-electric field curves.

The HA curve which is the predominant curve type has resistivity relationship of $\varrho_1 > \varrho_2 < \varrho_3 < \varrho_4$ and it is unequally distributed across all the lithological units in the area. The H-type curve ranks second in terms of dominance as it constitutes 18.09% of the total curves and it is known to be characterized by a relatively conductive intermediate layer.

Table 4.2 shows the classification of resistivityof weathered basement and sedimentary aquifers based on groundwater potentials. Aquifers in the basement setting are generally the product of decomposition and intense weathering of the underlyingparent rocks. This aquifers would constitute poor groundwater bearing units when they argillaceous (resistivity < 50 Ωm), owing to low transmissivity. However, compacted clays and lateritic clayscould have considerably higher apparent resistivity (> 400 Ωm). Furthermore, weathered basement rocks with resistivity of51-150 Ωm are suggestive of clayey sand ofmedium groundwater bearing capacity. Saprolites which are sandy and gravelly however,would have good prospects for groundwater (Akanbi, 2018).

Conversely, the aquifers within the sedimentary terrainwere groupedas follows; apparent resistivity of between 1-100 Ωm (clay rockswith poorprospect), 20-150 Ωm (clayey sands of moderate prospects), 100-1000 Ωm (sandstones indicative of good groundwater bearing capacity). Resistivity between 1000-5000 Ωm (gravelly or more compacted sandstones with reducedpermeability due to increased burial depth). The classification of the groundwater prospects of the slightly weathered bedrock is such that; resistivity range of 400 and 750 Ωm depicts slightly weathered basement (moderate prospects). While resistivity > 750 Ωm to 5000 Ωm have poor potential for groundwater (Table 4.2). To obtain a clearer picture of the lateral vertical variations of apparent resistivity in the subsurface, iso- resistivity maps were constructed for AB/2 = 40, 60, 80, and 120m (Fig. 4.14 a-d) respectively.

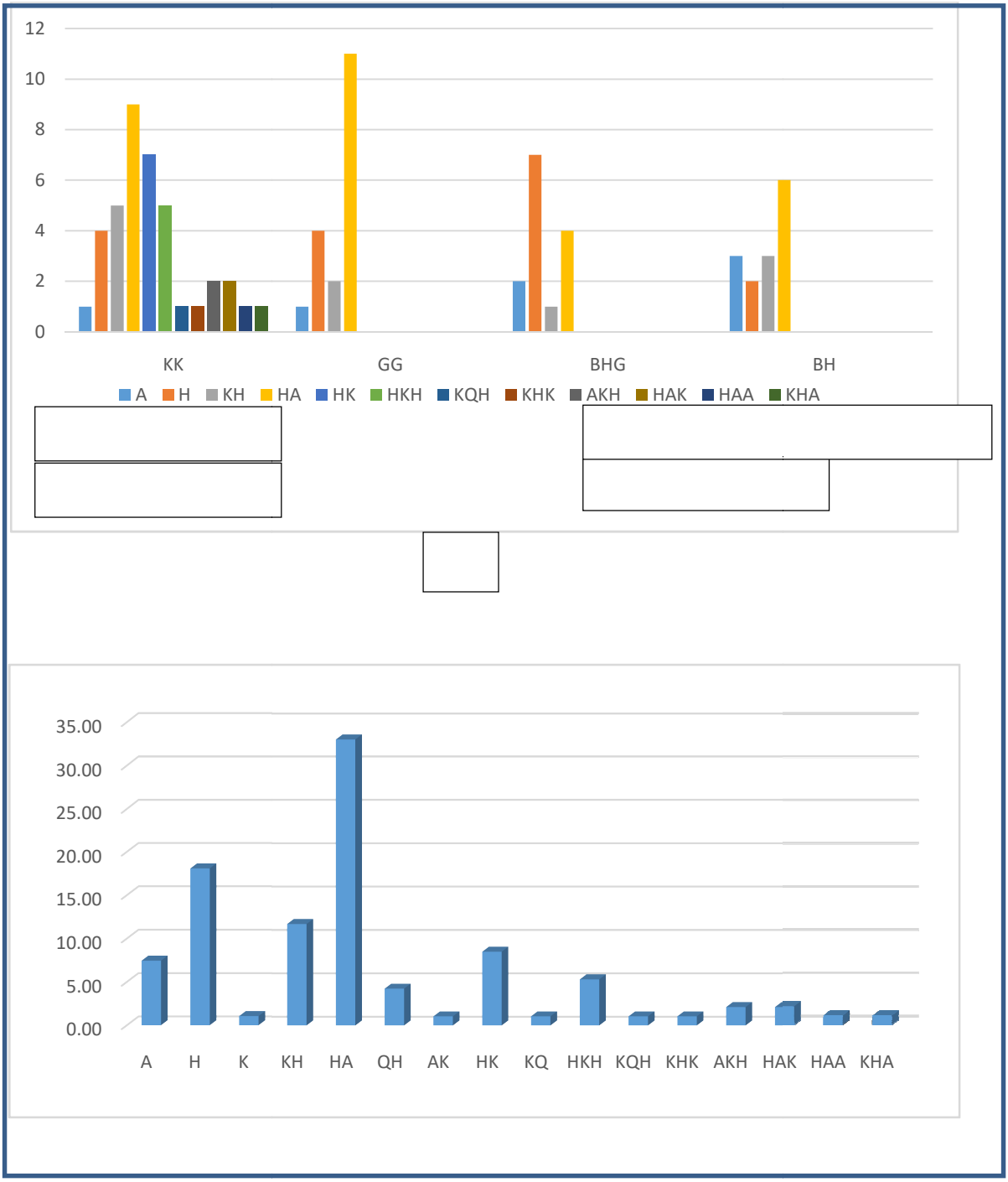

Fig. 4.13. (a) Distribution of the various type curves in the different rock units
(b) Relative abundances of the different geo-electric field curves

Table 4.2. Classification of resistivity for (a) weathered basement and sandstones and (b) Basement complex with respect to lithological character and groundwater potentials (adopted from Olayinka *et al*, 1997 ; Akanbi, 2018; Lawal *et al*., 2020)

(a)

	Basement Complex setting			Sedimentary rocks setting		
S/n	**Resistivity (Ωm)**	**Description**	**Groundwater potential**	**Resistivity (Ωm)**	**Rock description**	**Groundwater potential**
1	0 – 50	Clayey	Poor	1-100	Clays	Poor
	> 400	Compacted clay and Laterites	Poor	20-150	Clayey sands	Moderate
2	51 – 150	Clayey sand	Moderate	100-1000	Sandstones	Good
3	151 – 400	Sandy and gravelly material	Good	1000-5000	Gravelly sandstones and conglomerates	Moderate

(b)

Bedrock setting			
S/n	**Resistivity (Ωm)**	**Description of bedrock**	**Groundwater prospect**
1	> 400 – 750	Moderately weathered/fractured	Good
2	> 750 - < 5000	Slightly weathered to fresh	Poor
3	> 5000	Fresh bedrock	Poor

The spatial distribution of areas of equal resistivity in the Basement Complex zones at AB/2 = 40,revealed preponderance of sandy/gravely saprolitic units (151- 400 Ωm) and the clayey sand units (50-150 Ωm).With increasing depth(AB/2= 60-120), a decreasing amounts ofdecomposition (weathering) was discerniblebecause the amount of decomposed saprolitic units decreased significantly, while the percentage of slightly weathered bedrock increased. Additionally, the increasing amountof high resistivity zones is noticeable in thesouthwestern and northwestern parts (Fig 4.14 d). In the sandstones however,at AB/2 of 40 m, the dominant apparent resistivity recordedwas between 150-1000 Ωm (sandstones) with parts of the northeastern zone of the areashowing more resistive zones (resistivity > 1000 Ωm). With increasing depth of AB/2 (60, 80 and 120 m), the aforementioned resistive areas increased throughout the sandstone terrain. This scenario suggestan increasing level of compaction in the sediments as vertical pressure increases due to increasing depth of burial, leading to decreasing porosity and permeability of the sandstones.

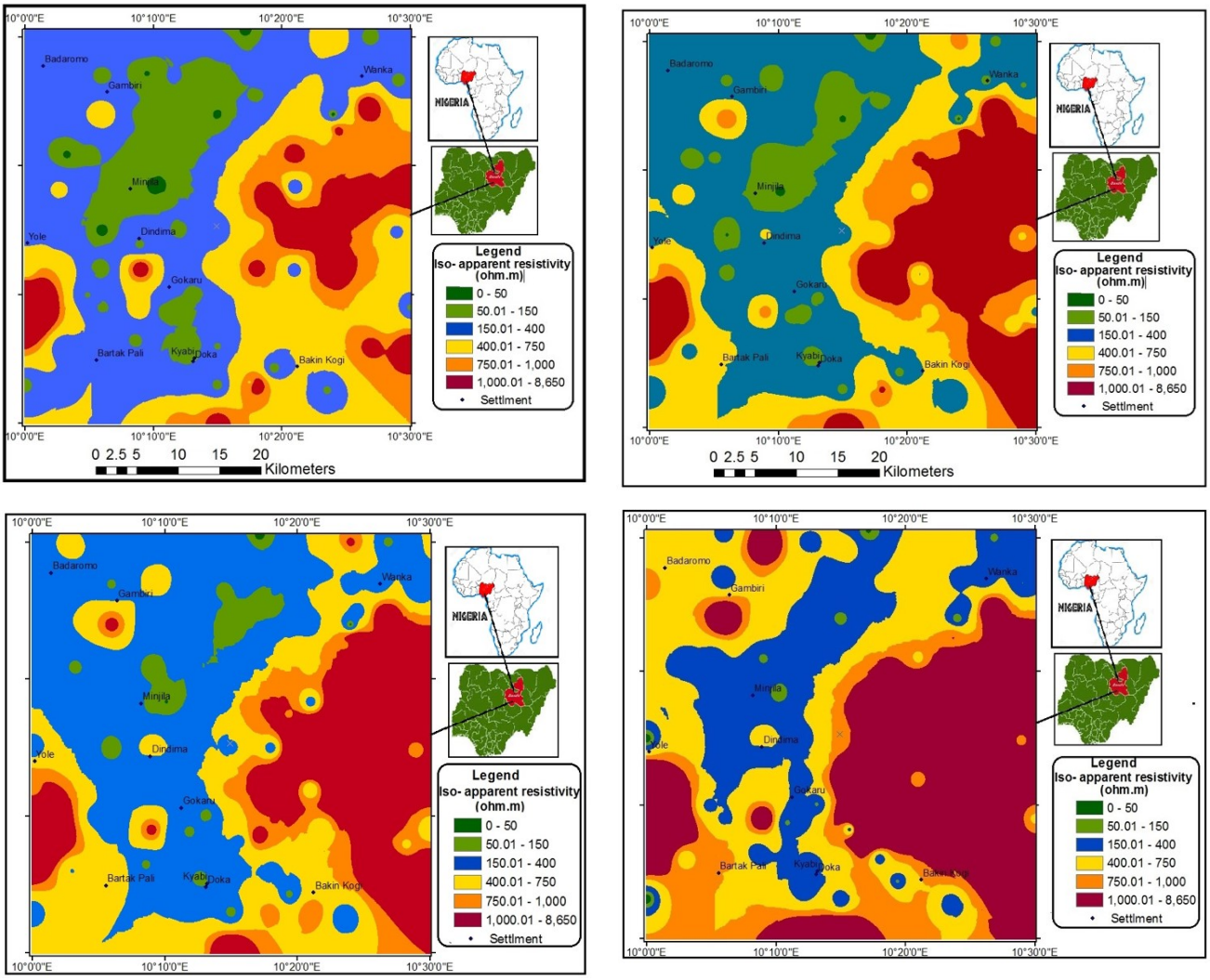

Fig. 4.14. Iso-resistivity maps of the study area at half current electrode separation (a) 40 meters, (b) 60 meters, (c) 80 meters, and (d) 120 meters

The high values of apparent resistivity values observed in southwestern parts of the study area are attributable to occurrence of shallow basement rocks.

4.1.2.4 Basement weathering profile and Hydrostratigraphic units

The geoelectrical cross-section B-B' indicated that the basement setting of the area consists of 3-4 layers (Fig. 4.15 a); top soil, the weathered basement and the fractured and/or unaltered bedrock rock. The model resistivity values of top soils range from 16 - 6508 Ωm, 5-581 Ωm, and 6-906 Ωm for migmatite, granite, and bauchite zones, respectively (Table 4.3). The huge disparity observed in the conductivity of the surface layeris a reflection of differing chemical content, temperature and amount of moisture in the soils. Top soil with a range of resistivity between 50-100 Ωm are indicative of argillaceousmaterials which are predominant in the older granites, due to the occurrence of high temperature minerals (fayalite, enstatite and feldspars) which easily decomposes to form clays. However, soilswith resistivitybetween 100-150Ω are suggestive of clayey sand and sandy clay saprolitic units (Omosuyi et al. 2008; Oladapo et al. 2004). This top soil typecoversa large part of the basement settings.In the migmatite zone, some of the top soils exhibited resistivity values greater than 1000 ohm-m,an indication of a hard pan (lateritic). The thickness of the top layers for the different bedrocks averages 1.52 m (migmatite), 1.48 m (granite) and 1.30 m (bauchite).

Table 4.3. Summary of primary geo-electric parameters

(a)

Lithology: Migmatite Gneiss **Number of VES points**: 21

s/n	Lithology	Resistivity (Ωm)	Thickness (m)	Overburden (m)
1	Top Soil	16.6-6508.3 (980.9)	0.2-3.7	
2	Highly weathered	5.1-1911.9 (292.7)	0.4-14.9	4.9-99.2
3	Weathered	11.1-1528.3 (275.9)	2.4-83.8	
4	Bedrock	30.05-80734 (19001.7)	Infinity	

(b)

Lithology: Biotite Hornblende Granite **Number of VES points**: 15

s/n	Lithology	Resistivity (Ωm)	Thickness (m)	Overburden (m)
1	Top Soil	5.1-6623.7 (616.4)	0.2-6.1	
2	Highly weathered	1-338.2 (67.6)	0.3-10.5	21-78.8
3	Weathered	1.2-2371.4 (275.9)	1.3-69.5	
4	Bedrock	459.6-69087.1	Infinity	

		(26296.7)		

(c)

Lithology: Bauchite **Number of VES points**: 14

s/n	Lithology	Resistivity (Ωm)	Thickness (m)	Overburden (m)
1	Top Soil	6.2-906.6 (212.6)	0.2-3.1	1.7-49.3
2	Highly weathered	9.3-223.1 (71.3)	1.1-12	
3	Weathered	18.9-1487.8 (298.9)	1.2-44.6	
4	Bedrock	143.3-88295 (12902.9)	Infinity	

(d)

Lithology: Kerri-Kerri Formation **Number of VES points**: 44

s/n	Lithology	Resistivity (Ωm)	Thickness (m)
1	Top Soil	16.5-6688.9 (1485.2)	0.4-4.6
2	Layer 2	12.2-4388.9 (613.5)	0.5-33.5
3	Layer 3	13.7-7842.2 (1558.1)	2.4-77.4
4	Layer 4	9.6-1895.1 (416.4)	2-138.5
5	Layer 5	39.8-99662.1 (18123.1)	Infinity

The average thickness of the highly decomposed layers are; 3.77m, 3.96 and 4.17 in biotite hornblende granite, bauchite and migmatite gneiss settings respectively. Conversely, the weathered layer thickness averages 17.84m in the bauchite zone, 25.6m and 29.7 min the granite and migmatite areas respectively (Table. 4.3). It noteworthy that close to 80% of the highly weatheredunitsoverlying the basement are argillaceous in nature with the granites showingabout 85 percent.Generally, zones with appreciable overburden and low percentage of argillaceous materialswould exhibitgood prospects for groundwater, particularly in hard rock settings (Okhue and Olorunfemi 1991). Additionally, areas wherethe thickness of the aquifer is > 25 m and low percentage of clay are expected to have good potential for groundwater (Abiola et al., 2009). Based on the above premise the gneiss terrain with mean thickness of 29.7 m would have the best aquifers considering their percentage of clayey aquifers (33%). The granites and charnockites were ranked the second on third respectively.

The resistivity values for themigmatite bedrocks ranged between 30 -80724 Ωm while the granites and charnockite revealed values between 459 - 69087 Ωm and 143 -88295 Ωm respectively.Resistivityof< 750 Ωmin basement bedrocks suggests fracturing and hence, good for groundwater storage (Olayinka et al., 1997). Six of such points (fractured bedrock)were identified in the migmatite bedrock (VEs 6, 9, 24, 34, 41, and 49), and within the charnockite zone (VES 11, 28, 31, 37, 38, and 39).

By and large, the weathered layers comprising the highly weathered layer and the weathered and fractured basement rocks constitute the key aquiferous units in the hard rock setting. The details of geophysical curves are presented in Appendix XI while the primary geoelectrical parameters are shown in Appendix XII.

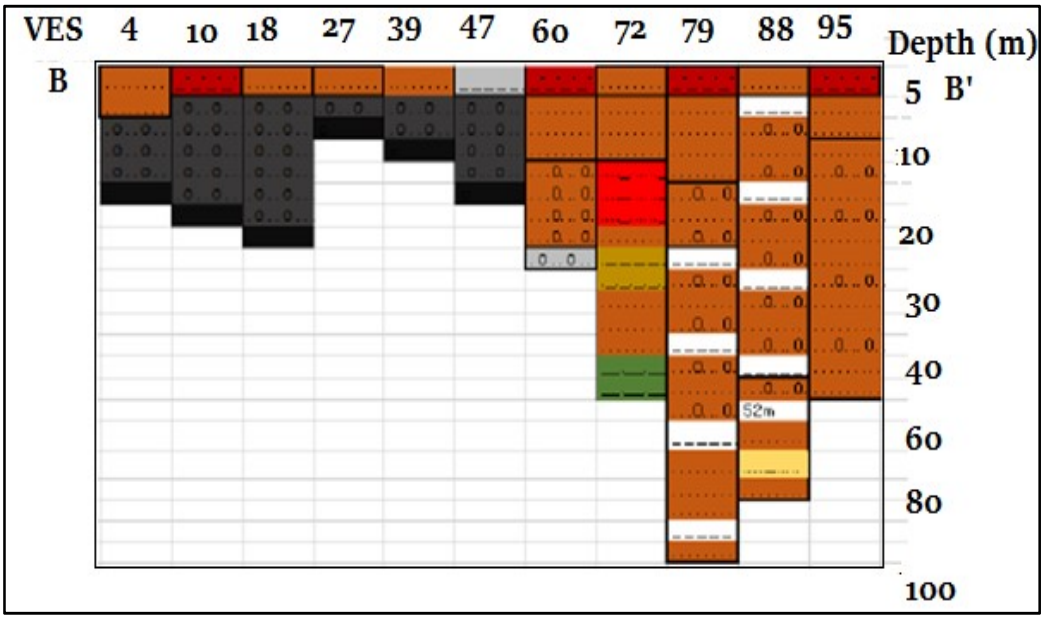

Fig 4.15 (a) Geoelectrical cross-section B-B' running from east-west of the study area

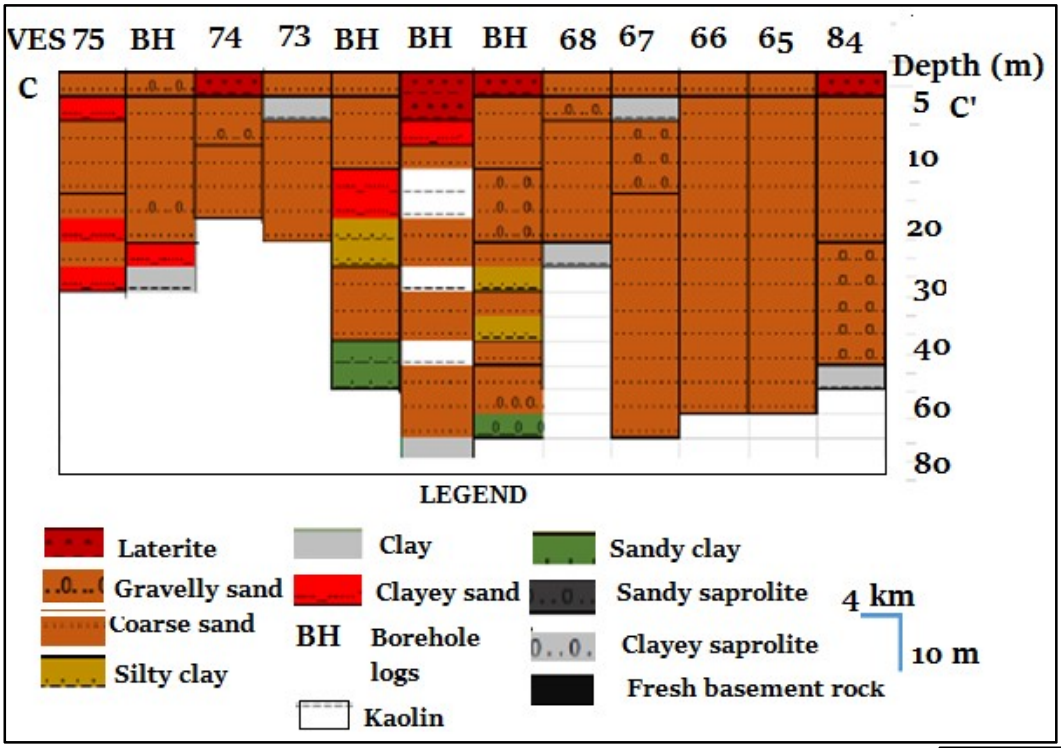

Fig. 4.15 (b) Geoelectrical cross-section C-C', across the sandstone units

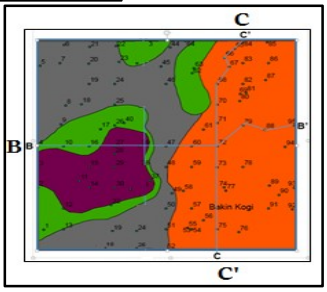

The interpretation of the VES stations from the sandstones indicated 3-5 geoelectrical layers.The first layerexhibited a meanresistivity of 238.1 Ωm (16.5-723.4 Ωm)suggestive of clays and clayey sand. Anomalous resistivity values of > 3501Ωm in some parts of the sandstones top soil are reflective of sandy and ferroginised capping. The first layerin the sandstone terrain are dominantly sandy and lateritic withsmall percentage of argillaceous material. These soils were formed from chemical decompositionof crystallinerocks and the parts of the sandstones in the area.

The second layer consist of sandstones of medium to coarse grained (partially saturated)with claysand sands in places. This layer revealed an average resistivity of 352.3Ωm (range from of 12.2-1663.3 Ωm). The layer is generally thicker(25-30m) in parts of the basin (northern and southern parts) where they appear to be saturated as suggested by the water level depth (19-25 m). However, in other parts of the basin (the central), the second layer revealed a thickness range of 5 to 10m (water level of 23-24 m), hence unsaturated.

The third hydrostratigraphic layer consists of fine-coarse grained sandstone interbedded with clayey sand(116 Ωm to 155 Ωm) and clays. The layer exhibits resistivity of 60.0 Ωm to 1493.2 Ωm with thickness of less than 5 m (central portion) and 60 m in the southern fringes. Overall, the thickness of this layer varies substantially towards and away from the transition zone, and it is generally thinner southwards than it is in the center and northern regions.

The fourth hydrostratigraphic unit represents the Kerri-Kerri Formation's basal part, with resistivity values ranging between 9.6 m to 464 m, suggestive of clay beds, sands and clayey sand (Table 4.3). The layer thickness varies between 2 - 61 m and averages 29.2 m. Within this layer, however, the occurrence of gravelly materials in the sandstone layer couldincrease the resistivity values considerably as observed in location 94. The clays in the fourth layer (often containing conglomerates) are mostly observed near the transition zone, suggesting possible non-conformity zones with the basement rocks.

In the sandstone setting, the resistivity of last layer varies from 39.8 to 99662 Ωm, suggestive ofextremelyweathered bedrock (clayey), sandstones, to unaltered bedrocks.

Also worth noting is the fact that the bedrock resistivity of 38% of the sedimentary area particularly around the GTZ and the eastern margins is> 5,000 Ωm, suggesting shallow basement rocks, which will influence the groundwater prospects in such areas considerably.

4.2.1.5 Aquifer resistivity map

On the aquifer resistivity map (Fig. 4.16), the resistivity of the aquifers were depicted, and suitable ranks were assigned on the basis of the prospectivity of the aquifer materials.The saprolitic aquifer materials were categorized into 4 different classes: 0-50Ωm, 51-150 Ωm, 151-400 Ωm and 400 - 750 Ωm.Sedimentary aquifers were however,divided into 5 groups: 0-100Ωm, 100-300 Ωm, 300-1000 Ωm and 1000-3000 Ωm and >3000 Ωm. The ranking was aided by comparison of resistivity data to litho-logs of existing boreholes in the Bauchi-Alkaleri-Kirfi area and existing literatures (Olayinka et al., 1997; Lawal et al, 2020).According to Fig. 4.16, the dominant resistivity rating in the basement terrain is 151-400 Ωm (35%) i.e. sandy to gravely saprolitic units, seconded by clayey sand saprolitic units (51-150 Ωm), partially weathered basement rocks (400 - >750Ωm), and clay units (0-50Ωm) (Table 4.2). In contrast, the resistivity range of 1000-3000 Ωmpredominates the sedimentary area, followed by > 3000 Ωm, 300-1000 Ωm and 0-100 Ωm. As a result, the sedimentary regions have a modest groundwater prospects.However, an overall assessment of the Bauchi-Alkaleri-Kirfi transition zone based on aquifer resistivity found that the basement areas have a significant percentage(45 percent) of good prospects for groundwater than the sedimentary regions, which had a modest aquifer prospects. Although, the spatial extent and thicknesses of weathered regolith (saprolites) are limited as they are determined by the mineralogy of the rocks and the extent of weathering in the area as reported by Wright. (1992) and Eduvie, (2006).

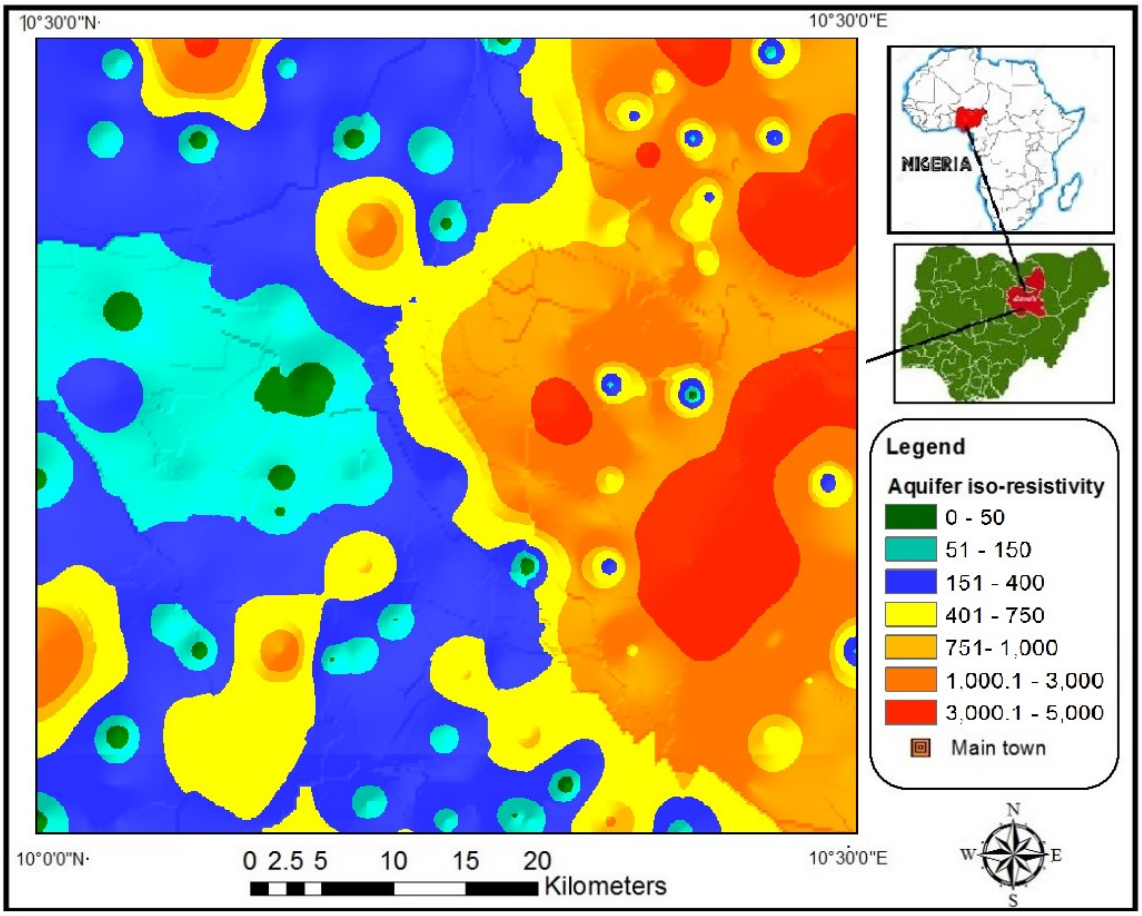

Fig. 4.16. Aquifer resistivity map of Bauchi-Alkaleri-Kirfi area

4.1.2.6 Aquifer thickness map

The theme mapfor aquifer height revealed 6 subdivisions;: 0-5m, 5-10 m, 15-25m and 25-35m, 35-50m and >50m. According to Fig. 4.17, aquifer thicknesses of 35-50 m and >50 m predominate in the sedimentary areas, while thicknesses of 0-5 m, 5-10 m, 15-25 m, and 25-35 m cover an appreciable section of the crystalline basement region.Even though,sections of the hard rock terrain, particularly in the south and northwest, have thick weathered regolith (35-50 m).As shown by the aquifer thickness map, the 0-5m range covers 0.5% of the area, 5-10 m (13.76%), 15-25m (19.5%), 25-35m (18.3%) and 35-50 m (28.05%). In line with Oladapo and Akintorinwa, 2007, aquifer units which are low in clay and have appreciable thickness > 25 m and resistivity values >100 Ω-m are considered to have high prospects, while aquifer thickness of 10 to 25 m suggests moderate groundwater prospects. However, zones where the thickness is< 10 m constitute zones of low groundwater prospect. Based on this classification scheme, over 60% of the Bauchi-Alkaleri-Kirfi GTZ, particularly the granular aquifersrevealed high groundwater prospects, while a little above 30% displayed modest to low prospects (a good percentage of the basement terrain).The southwestern boundary and pockets of the northwestern parts of the Bauchi-Alkaleri-Kirfi area will have the minimum groundwater prospects, owing to low-moderate aquifer thicknesses.Overall,based on aquifer thickness, the sedimentary regions will have a greater proportion of groundwater as compared to the basement sections. In order to characterise the potentials of these aquifers more accurately, the integration of the geophysical data with remotely sensed data using overlay analysis in GIS environment was undertaken as elucidated in the next section.

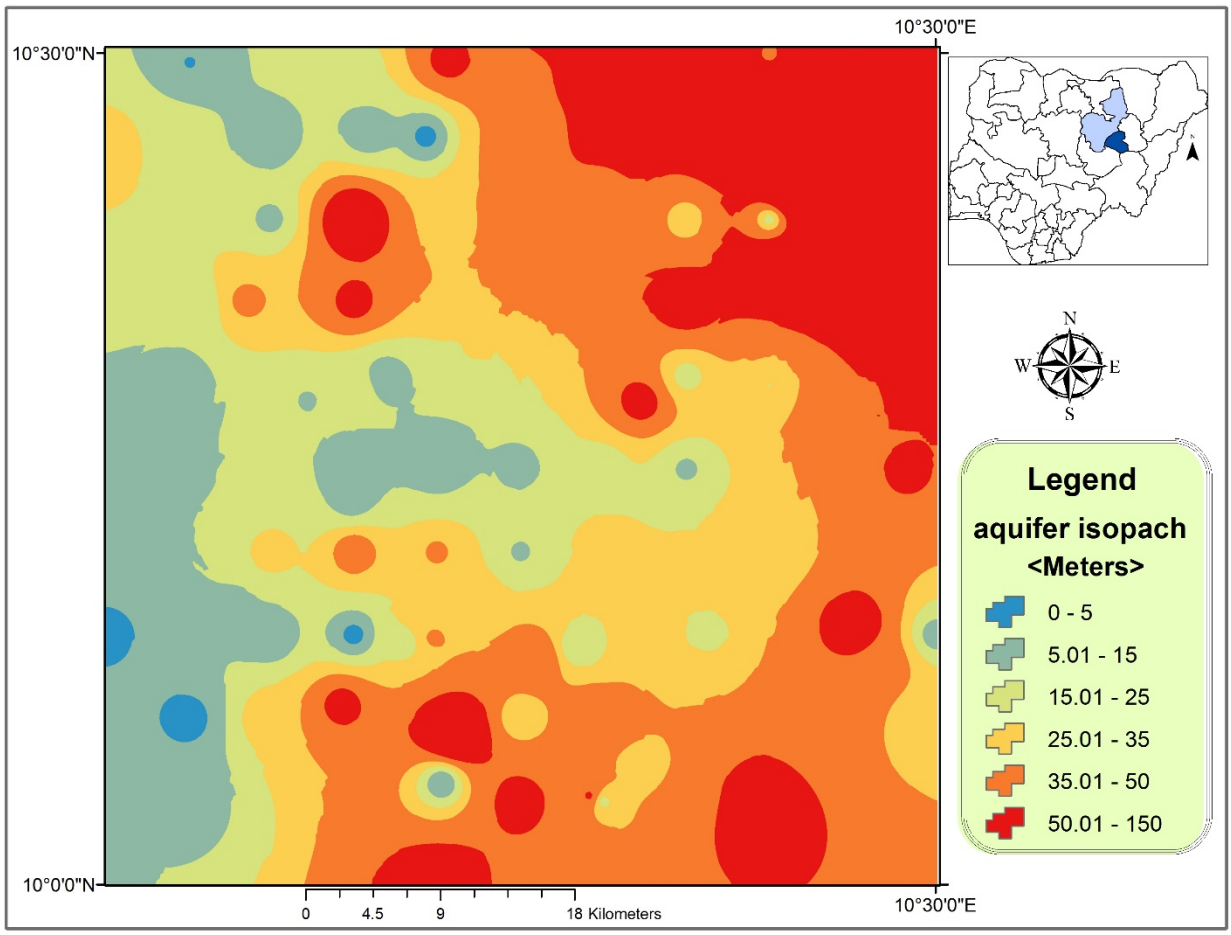

Fig. 4.17. Aquifer thickness map of Bauchi-Alkaleri-Kirfi transition zone

4.2. Weight Assignment and Normalistion

The assigned and normalised weightages of the surface and subsurface thematic layer in the Bauchi-Alkaleri-Kirfi transition zone is presented in Table 4.4 and Table 4.5 respectively. As can be seen in Table 4.4, altitudes in the area ranged from 275-706m and were classified into 5 categories with rankings ranging from 1 to 5. The highest rating (5)was assigned to the minimum altitude areas (275-382m) and lowest ratings was assigned to elevated regions (576-706m). Naturally, areas with minimal elevation favour the recharge of aquifers, howevermediumand highaltitude areas supports runoff hence, ranked low (Lawal et al. 2021)

According to Table 4.4, the 5 key land use /cover classes (LULC) delineatedare bare land, scrubland,forest, water body, and built up areas, with relative percentages of 48, 31, 17, 3, and 1% respectively.In terms of ratings of LULC map, the water bodies were ranked high as they constitute excellent recharge areas,scrubland and vegetation zoneswere rank next to water bodies due to the fact that this zones have the capacity to slow runoff and facilitate meteoric rechargeNarendra *et al.*, 2013; Fashae *et al.*, 2014. The least ratings were allocated tobuilt-up regions and bare land owing to the general absence of vegetation.

The slope of the Bauchi-Alkaleri-Kirfi region (Table 4.4) was categorized into five different classes. The slope map revealed that over 70 % of the research area are gently sloping (0-5%) and such zones are generally favorable for groundwater recharge, hence,rated 5. Comparatively, zones with slope percentages of 15% to > 20% are suggestive of steep to very steep zones. These zoneswould have poor prospects for groundwater storage because of the generally high runoff in such zones (Lawal et al. 2021). The steep zones were rated 2 and 1 respectively. The implication lies in the fact that is that gently sloping regions are favorable for precipitation recharge while for the steeper areas, the reverse is the case.

SURFACE THEME	CLASSES	WEIGHT	NORMALISED WEIGHT	RANK	AREA(km^2)	PERCENT
RAINFALL	0-850	2	0.2	0.165353	1494.2	48.85
	850-1000	3	0.3		1481.7	48.44
	1000-1100	5	0.5		84	2.75

Table 4.4. Assigned and normalised and weightages of the individual classes of surface and hydrological layers in the Bauchi-Alkaleri-Kirfi area

SLOPE	0 to 5	5	0.5	0.076992	2256.2	73.73
	5 to 10	4	0.4		634.5	20.73
	10 to 15	3	0.3		84.1	2.75
	15 t0 20	1	0.1		30.2	0.99
	>20	**1**	0.1		55.2	1.80
LANDUSE	Built	1	0.09	0.035424	30.6	1.00
	forest	2	0.18		520.2	17.00
	water body	4	0.36		91.8	3.00
	bare land	1	0.09		1468.9	48.00
	Shrub land	3	0.27		948.7	31.00
SOIL	Alluvium	2	0.29	0.035424	155.8	5.09
	sandy loam	4	0.57		1704.7	55.71
	Sandy clay	1	0.14		1200.2	39.22
		7				
ELEVATION	275-382	5	0.33	0.076992	427.1	13.95
	382-438	4	0.27		667.8	21.82
	438-487	3	0.20		714.0	23.33
	487-537	2	0.13		967.4	31.61
	537-706	1	0.07		284.0	9.28
DRAINAGE DENSITY	0 to 0.3	5	0.33	0.015915	1153.0	37.68
	0.3-0.6	4	0.27		1235.6	40.37
	0.6-1.0	3	0.20		565.1	18.46
	1.0-1.3	2	0.13		97.3	3.18
	1.3-1.7	1	0.07		9.4	0.31

As shown in Table 4.4, three main soil units were distinguished in the area: sandy clay soils, sandy loam soils and alluvium covering 1200.2 km^2 (39.2%), 1704.7 km^2 (55.7%) and 155.8 km^2 (5.09 %) of the total Bauchi-Alkaleri-Kirfi area, respectively. Based on the above premise, higher ranking was given to soils high proportion of sand; thus sandy loam was ranked highest (4), followed by Alluvium (2) and sandy clay units with

assigned rank of 1 indicating lower groundwater potentials as suggested by Fashae *et al*., 2014.

The density of the drainage in Bauchi-Alkaleri-Kirfi region (Table 4.4), varied from 0.34 km/km^2 to >1.72 km/km^2, suggestive of modest –low densities to high densities.According to Lawal et al., 2021, low drainage networks densityreflects increased meteoric recharge which will maximize the groundwater prospects accordingly. However,for highnetworks density zones the reverse is the case as runoff would be more.Maximum ranks (4 and 5) was allocated to the zones ofminimal density which approximately covers 2388.6 km^2. The high density zones (1.03-1.37 and 1.37-1.72 km/km^2) covering approximately 106.7 km^{2}of the research areagot ranks of between 1 and 2 while zones of medium density were ranked 3.

The rainfall distribution in the area (Table 4.4) was categorized into high moderate and low. The highest rainfall area (1100mm) is in the far northwestern corner of Bauchi-Alkaleri-Kirfi area underlain by migmatite and accounts for about 2.75% (84 km^2) of the area. However, the moderate rainfall zones (1000 mm) which represents 48.4% (1481.2 km^2) and dominates the basement settings while low rainfall zones (850mm) constituting 48.8% (1494.7 km^2) predominate the sedimentary zones. The classes are assigned weight factors of 5, 3, and 2 from the highestto the lowest respectively.

As revealed by Table 4.5, which summarizes the normalized weights for the subsurface thematic maps, the density of the lineaments in the Bauchi-Alkaleri-Kirfi transition zone varies between < 0.176 km/km^2 to 0.88 km/km^2.These spatial distribution of these linear structures is reflective of the tectonic evolution of the bedrocks underlying the research zone., The migmatite/gneiss which represent the oldest bedrocks in this region revealed values between 0.35–0.88 km/km^2 and were ranked accordingly (4 and 5). Zones were lineaments are sparse - medium in density were given ranks of 3 (e.g. granite/bauchitebedrocks). The Kerri-Kerri sandstones which are the youngest rocks in the region were however, characterised by low density of lineaments (0.0–0.17 km/km^2) and ranked1.

The different bedrock units were ranked between 1 and 5 based on their prospects for groundwater (Table 4.5). The maximum rank (5) was given to the sandstone units, while ranks of 3 was assigned to the migmatite /gneiss. Biotite granite and bauchitegot the same rank (2). The general idea lies in the fact that crystalline rocks exhibit poor transmissivity while the sandstones because of their granular nature tend to have better permeability and porosity which is very key to groundwater recharge (Eduvie, 2006). Within the basement setting,the older rock units (migmatite/gneiss) got higher ratings than the bauchites and Biotite granitesowing to the higher lineament densities in the former.

With respect to aquifer resistivity the research area was categorized into 2partsbased on the underlying bedrocks; crystalline bedrock and sedimentary groups and these division was prompted by the idea of the variations that existbetween the resistivity of granular sedimentary rocks and the hard rocks.

Table 4.5. Normalized weights of the classes of hydrogeological thematic layers for Bauchi-Alkaleri-Kirfi area

SUB-SURFACE	CLASSES	WEIGHT	NORMALISED	RANK	AREA	PERCENT

THEME			WT		(km^2)	
GEOLOGY	Bauchite	2	0.16667	0.3124	372	12.17
	Biotite granite	2	0.16667		466	15.25
	Migmatite/ Gneiss	3	0.25		919	30.07
	Keri-Kerri	5	0.41667		1299.0	42.51
AQUIFER THICKNESS	0-5	1	0.04762	0.1672	17.2	0.56
	5-15	2	0.09524		420.4	13.76
	15-25	3	0.14286		595.6	19.50
	25-35	4	0.19048		590.6	19.334
	35-50	5	0.24		857.0	28.05
	>50	6	0.29		574.2	18.80
AQUIFER RESISTIVITY	0-50	1	0.11	0.0789	131.1	4.29
Basement	51-150	5	0.56		1074.2	35.15
	151-400	4	0.33		465.9	15.2
	401- >750	1	0.00		86.2	2.82
Sedimentary	0-100	1	0.07		0.91	0.03
	100-300	4	0.29		14.6	0.48
	300-1000	5	0.36		256.7	8.40
	1000-3000	3	0.21		761.1	24.91
	>3000	1	0.07		265.2	8.68
LINEAMENT DENSITY	0-0.176	1	0.07	0.0354	1499.3	49.08
	0.116-0.352	2	0.13		1098.3	35.95
	0.352-0.528	3	0.20		296.2	9.70
	0.528-0.704	4	0.27		138.7	4.54
	0.704-0.880	5	0.33		22.5	0.74

As can be seen in Table 4.5, the crystalline rock aquifers got the following ranks: ρ=0-50Ωm (1), ρ=51-150Ωm (5), ρ= 151-400 Ωm (4) and ρ= 400 - >750 Ωm (1). In the

granular (sedimentary) aquifer units however; ρ= 0-100Ωm (1), ρ=100 - 300 Ωm (4) ρ=300-1000 Ωm (5) ρ=1000-3000 Ωm (3) and ρ >3000 Ωm (1).

This ranking was deduced from analogues made from Table 4.2 and the following related resistivity studies; Wright, 1992; Olayinka *et al.*, (1997), Oladapo and Lawal *et al*., 2020). However, the overall assessment of the Bauchi-Alkaleri-Kirfi area on the basis of aquifer resistivity revealed that the basement areas general shows good groundwater prospects, although the spatial extent and thicknesses of the weathered regolith (saprolites) are known to be limited as they are determined by the mineralogy of the rocks and the extent of weathering as reported Wright. 1992 and Eduvie, 2006. Conversely, the aquifer units in the sedimentary settings which revealed moderate aquifer rating have a comparative advantage owing to their primary porosities coupled with their extensive lateral and vertical extent which is controlled by sedimentary processes rather than weathering of rocks (Eduvie, 2006). The aquifer thickness in the Bauchi-Alkaleri-Kirfi region varied from 5 to >50 m and revealed 6 classes: 0-5m, 5-10 m, 15-25 m, 25-35m, 35-50 m and >50m, with weights of 1,2,3,4,5 and 6 correspondingly (Table 4.2). It is noteworthy that while the thicker aquifers generally occupy the Kerri-Kerri sedimentary basin 35-50 m and >50m) the crystalline rock terrain are predominantly covered by aquifer thicknesses of while 5-10 m and 15-25m, suggesting low-moderate prospects.

According to Oladapo and Akintorinwa, (2007), aquifers where the overburden materials are low in clay and have appreciable thickness > 25 m and resistivity values >100 Ω-m are considered to have high groundwater prospects, while overburden thickness of within 10 to 25 m are zones of moderate groundwater prospects. Zones where the thickness are less than 10 m constitute low groundwater potential zones. Consequently, over 65 percent of the research region particularly the granular sandstone aquifers will have good prospects for groundwater while approximately 33 percent consisting dominantly of the crystalline rocks are characterised by low- medium prospects.

In a summary, the charnockite and biotite hornblende granites saprolitic units would generally exhibit moderate-low groundwater prospects whereas the sandstone settings

will generally have a greater prospects owing to the comparatively thicker aquifers in these zones.

4.3 Overall Integration of thematic maps

The integration of the layers was accomplished through overlay analysis using the ArcGIS version 10.1 software. The integration of the thematic maps yielded a groundwater potential zone map (GWPZ), which was further reclassified to delineate the various groundwater potential zones in the Bauchi-Alkaleri-Kirfi transition zone into three classes (good, poor and moderate) which are elucidated in the following section.

4.4 Delineation of Groundwater Potential Zones

Following the integration of the 10 thematic maps, a prospective groundwater index map was generated (Fig. 4.18). The GWPZ map of the Bauchi-Alkaleri-Kirfi transition zone was demarcated three distinctive zones, namely: poor zones, covering 645.1km^2 (21.12%), moderate zones, occupying 1134.1km^2 (34.12%) and good zones constituting 1275.8 km^2 (41.8km^2) of the Bauchi-Alkaleri-Kirfi area. The GWPZ map (Fig. 4.18) revealed that the good zones occupy the eastern half of the Bauchi-Alkaleri-Kirfi region, underlain by the granular aquifer (sandstones). This is attributable to a good mix of favorable surface, and subsurface parameters.

According to the statistics, 34.12 percent of the area exhibited moderate groundwater potential zones, which characterize a large section of the basement areas. The central and some fraction of southwestern parts of the Kerri-Kerri Formation also displayed moderate GWP. As evidenced by a large portion of the area's southwestern flanks, which are dominated by bauchite and partly biotite hornblende granites, around 21.12 percent of the overall research territory falls within the poor or low prospective zone.Additionally, pockets of poor GWPZ can be seen along the contact zones.

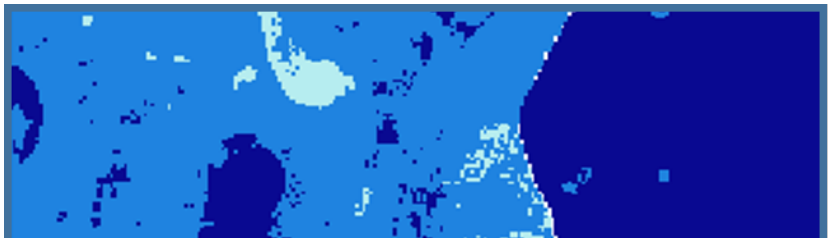

Fig. 4.18. Groundwater Potential Zone Map of Bauchi-Alkaleri-Kirfi transition zone

According to Fashae et al. (2014), the current study's low - to - medium aquifer prospectivity in basement locations reflects the limited aquifer output known to be linked with fissure type aquifers in most basement settings. Furthermore, lineaments play a less

role in the Kerri-Kerri areas than in the basement portions of the research, confirming the prevalence of secondary porosities in Basement Complex rocks.

The comprehensive GWPZ evaluation of the Bauchi-Alkaleri-Kirfi shows that areas largely covered by bauchite and hornblende granite, as demonstrated by the southwestern flanks, which are characterised by moderate rainfall, indicated poor to marginal groundwater prospect, due to the prevalence of rock outcrops, medium - to - high gradient percentages, and often limited saprolite thickness. Conversely, areas covered by gneiss, and partly hornblende granites, exhibitmoderate groundwater prospectivity which is occasioned bypreponderance of high to moderate lineament densities and overburden thickness whereas areas underlain by sandstones exhibit high-medium prospectivity, owing to their primary porosities, appreciable aquifer thickness, permeable soils, and gentle slopes that creates an enabling environment for rainfall recharge.

4.5 Groundwater Potential Zones (GWPZ) Map Verification

The verification of the GWPZ map was undertaken using boreholeyield data for over 120 existing boreholes (Table 4.6 and 4.7). Generally, the borehole depth ranges from 13 to 61m and 18-55m across the migmatite/gneiss and granite bedrocks in the area which reflects the erratic nature of the aquifers the basement terrain, while the sandstones (Kerri Kerri Fm.) revealed depth ranges of 25-165m depicting deeper sedimentary aquifer systems. The static water level which determines the water column in the wells ranges as follows; 2-24m (Migmatite and gneiss), 2.2-21.8(Granite) and 5.9-68.1 (Sandstones). The well yields ranged from 9.6 to 331.2 m^3/day (mean value of 68.4 m^3/ day) in the migmatite/gneiss bedrock, while varying from 11.5 to 405.6 m^3/day (mean value of 77.6 m3/day) in the granites compared with 31.7 to 830 m^3/day (mean value of 400 m^3/day) in Kerri-Kerri sandstones. The pumping test data was acquired from the JICA basic report on the water supply project in Bauchi and Katsina (2009) and Wadrobe Engineering report (1989). Borehole yields >100m^3/day was ranked as high, 50m^3/day as low yield whilemoderate yield was set at 50 to 100m^3/day (Fig. 4.19). From the figure, low and moderate yields predominate the basement terrain. According to the pumping test data analysis, 83 percent of the boreholes in the sandstone region had a high yield, as

compared to the granites (22.5 percent) and the migmatite/gneiss (25.6 percent).Conversely, the migmatite/gneiss and granites had 57.5 percent and 58.1 percent of poor yield wells, respectively, while the sandstones indicated 11 percent.The GIS-based groundwater potential map is supported by the high proportion of low and moderately yielding boreholesin the basement settings. Furthermore, the dominance of the high-yielding boreholesin thesandstone units also corroborate the high-to-medium-prospectsindicated by the GIS-based GWPZ map.

In a summary, the overall evaluation of the GWPZ map showed that the topographically complex basement areas with associated high percentage of slope, owing to the predominance of rock outcrops, in the northwestern and southwestern sections of the area are dominated by low-medium groundwater potential. Although, the migmatite/gneiss showed a slightly higher percentage of high yield wells (25.6%) as compared to 22.5% in the granites and this is attributable to dominance of lineament and apparently higher degree of weathering.

Conversely, the sandstones occupy relatively flatter zones with more permeable soils, and low slope percentages, hence constitute areas of high groundwater potential. While the occurrence of permeable overlying soils in the sedimentary terrain could be favorable for aquifer recharge on one hand, it could also become a disadvantage when the aquifer protective capacity of these aquifers is put into consideration.

Table 4.6 Well yield record for various bedrocks (modified after JICA, 2009)(modified after JICA, 2009)

Rocks	Migmatite/Gneiss (N=43)			Granites (N= 40)			Sandstone Kerri-Kerri Fm. (N=42)		
Parameters	BH Depth (m)	D.W.L (m)	Yield m^3/Day	BH Depth (m)	D.W.L (m)	Yield m^3/Day	BH Depth (m)	D.W.L (m)	Yield m^3/Day
Minimum	13	2.0	9.6	18	2.2	11.5	25	5.9	31.7
Maximum	61	24	331.2	55	21.8	405.6	165	68.1	830.4
Mean	30.3	9.8	68.4	30.4	10.4	77.6	63	31.1	400
Median	29	8.4	36	30	9.6	43.2	54.5	26	522
Std. Dev.	10	4.9	74.5	8.8	5.5	95.6	32.7	19.9	238

Charnockite =No data

Table 4.7 Groundwater potential categorization based on the yield of boreholes

Yield	<50 (Low)		50-100 (Moderate)		>100 (High)	
	No. of boreholes	%	No. of boreholes	%	No. of boreholes	%
Granites	23	57.5	8	20	9	22.5
Migmatite/gneiss	25	58.1	7.0	16.3	11.0	25.6
Sandstone	5	11.9	3.0	7.1	35.0	83.3

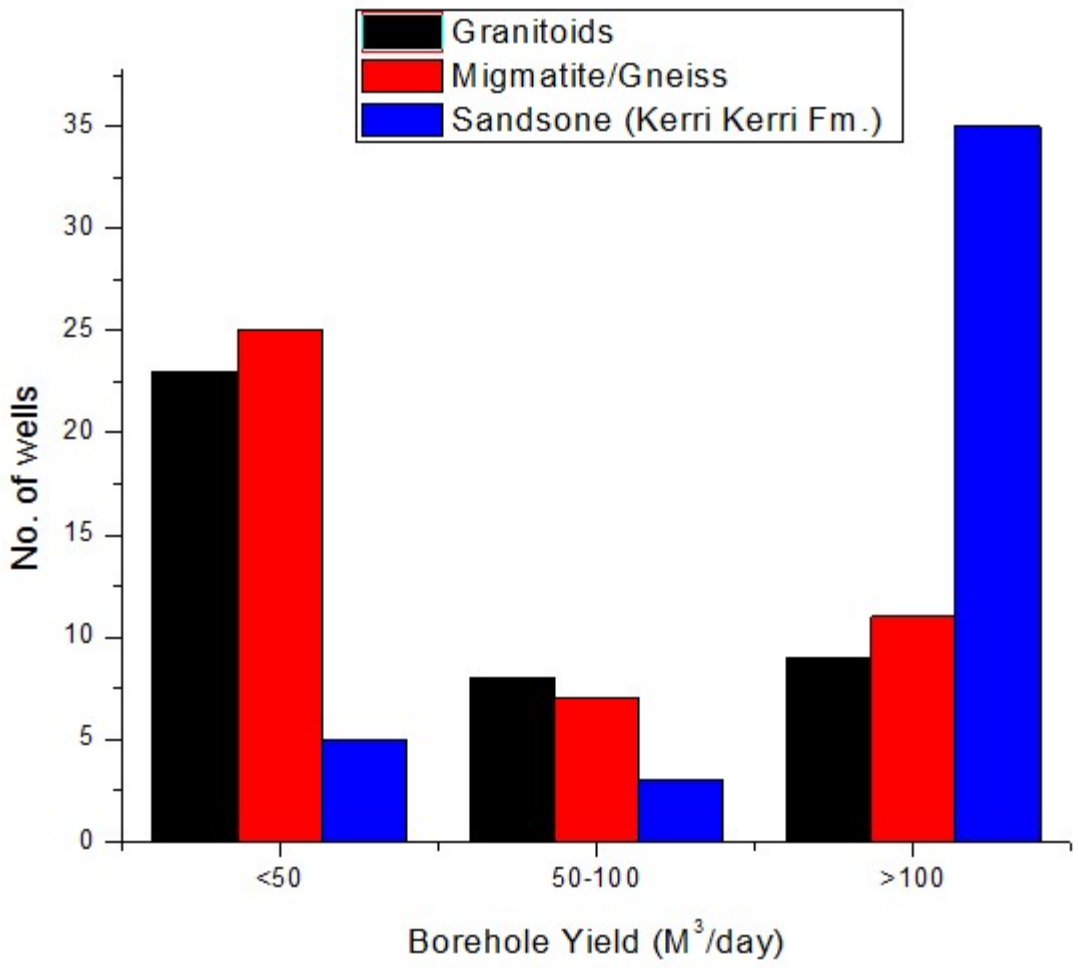

Fig. 4.19. Borehole yield classification based on the different bedrocks in the Bauchi-Alkaleri-Kirfi transition zone.

4.6 Well inventory and Groundwater Chemistry

The analysis of well inventory and chemistry of groundwater samples from the Bauchi-Alkaleri-Kirfi transition zone are presented under the sections; well inventory, physico-chemical parameters and cations and anions. The descriptive statistics of well inventory and physico-chemical compositions of the studied groundwater samples, vis-a-vis the World Health Organization (WHO, 2011) and Nigerian Standard for Drinking Water Quality (NSDWQ, 2007) are shown in Table 4.8 while Table 4.9 provides a summary of the physico-chemical parameters based on the different bedrock types in the area. The detailed hydrochemical results are presented in Appendix XIII.

Table 4.8 (a). Result of Well inventory

Parameters	Units	Mean	Min.	Max.	Standard Dev.
Elevation	m	459.95	308.00	572.00	79.74
Depth	m	24.68	3.00	114.00	20.76
DWT	m	15.11	1.20	100.00	18.59
SWL	m	444.70	292.0	561.4	75.98
W.C	m	9.87	0.50	12.61	9.40

DWT- depth to water table, SWT-static water level, water column

Table 4.8 (b). Result of Physico-chemical Parameters

Parameters	Units	WHO (2011)	NSDWQ (2007)	Mean	Min.	Max.	Stand-ard Dev.
Temp	^{o}C	n/a	n/a	26.42	21.40	31.70	2.26
pH	n/a	6.5-8.5	6.5-8.5	6.70	5.00	8.50	0.75
EC	µS/cm	1500.00	1000.00	519.77	10.00	2040.00	416.63
TDS	mg/L	500.00	500.00	368.60	15.0	1558.00	302.13

EC-electrical conductivity, TDS-total dissolved solids

Table 4.9 (a) Descriptive Statistics of Well inventory of Boreholes across the Different Bedrock Types.

Parameters	Migmatite/gneiss Aquifers N=27			Biotite Hornblende Granite Aquifers N=12			Bauchite Aquifers N=12			Sandstone (Kerri Fm.) N=36		
	Mean	**Min**	**Max**	**Mean**	**Min**	**Max**	**Mean**	**Min**	**Max**	**Mean**	**Min**	**Max**
Elevation (m)	508.11	417.00	572.00	496.08	401.00	534.00	503.58	469.00	545.00	397.25	308.00	518.00
Depth (m)	17.80	3.00	45.00	16.64	7.50	53.00	10.08	4.20	20.00	37.39	8.00	114.00
DWT (m)	6.62	1.20	12.50	5.01	3.00	8.50	5.05	2.40	10.30	28.20	6.00	100.00
S.W.L (m)	501.49	411.4	561.4	490.01	396.9	529.80	498.53	462.50	542.60	369.05	292	489
W.C (m)	12.61	1.80	37.00	10.57	1.30	35.00	5.03	1.50	15.00	9.18	0.50	34.00

DWT- depth to water table, SWT-static water level, water column

Table 4.9 (b) Descriptive Statistics of Physico-chemical Parameters of Boreholes across the Different Bedrock Types.

Parameters	Migmatite gneiss			Biotite Hornblende Granite			Charnockite			Sandstone		
Temp (^{o}C)	26.85	22.50	29.50	25.78	21.50	29.10	25.97	22.40	28.90	26.46	21.40	31.70
pH	7.16	6.40	7.70	7.09	6.80	7.50	7.18	6.40	7.70	6.05	5.00	8.50
EC(µS/cm)	666.67	120.00	1290.00	897.50	230.00	2040.00	542.50	190.00	1580.00	276.11	10.00	1520.00
TDS (mg/L)	481.07	95.00	945.00	660.92	169.00	1558.00	394.67	154.00	1154.00	205.06	15.00	1105.00
TH	227.67	11.73	547.87	311.89	44.66	747.91	135.59	23.94	386.65	54.33	0.17	417.99

EC- electrical conductivity, TDS-total dissolved solid, TH- total hardness

4.6.1 Well inventory

Well inventory studies revealed that elevations of the wells in this study ranged between 572m (basement terrain) to 308m (sandstone) with an average of 459.95m. The static water level which governs the general direction of groundwater flow in the area ranged between 292.0m in the sandstones to 561.4m in the basement terrains and averages 444.7 m, implying that groundwater flow is mainly from the basement terrain in the western parts to the sandstones which occupy the eastern zones of the area. The water column in the study region ranged between 0.5 to 12.6m and averages 9.87m while and well depths ranged between 3.0 to 53m (basement setting) and 8-114m in the sedimentary terrain. The average static water levels of 501.49, 490.01 and 498.53m in the migmatite, Biotite hornblende granite and Bauchite bedrocks respectively, while the well depths averages 17.80, 16.64 and 10.8m in the same order.

Conversely, average static water levels in the sandstone aquifers is 396.05m while well depths ranged between 8 and 114m. The above statistics suggests that the basement settings are characterized by weathered overburden materials whose spatial extent and thicknesses are limited as they are determined by the mineralogy of the rocks and the extent of weathering in the area as reported Wright (1992) and Eduvie (2006). The sandstone aquifers however, are characterised by larger spatial extent, and thicknesses in addition to well-developed primary porosity (Eduvie, 2006). The implication is that the shallower weathered regolith's (with < 20m depth) consisting dominantly of the aquifers in the basement terrain, are more susceptible to local anthropogenic contamination considering their relatively shallow nature, especially when well head are not adequately protected from unhygienic human activities and runoff water. Consequently, the shallow and unprotected well are prone to contamination from anthropogenic sources. Given the above, nitrate concentrations greater than 50 are clear indications of shallow groundwater contamination (WHO, 2011; Tijani, 2016). As shown in Fig. 4.20, the variability of nitrates was found to be greatest in wells with depth range of 0-20m. This susceptibility was found to reduce in wells with depths between 20-40m consisting largely of the sandstone aquifers and wells greater than 40m which are mainly from the Kerri Kerri only showed very few cases of contamination.

(a)

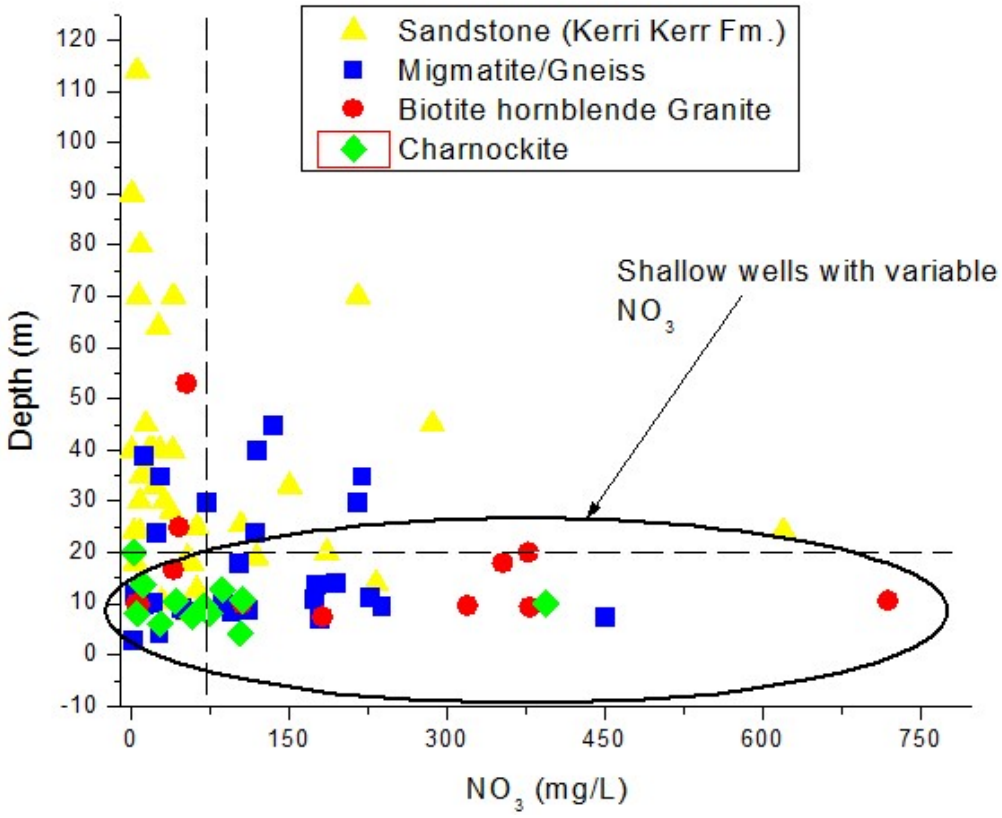

(b)

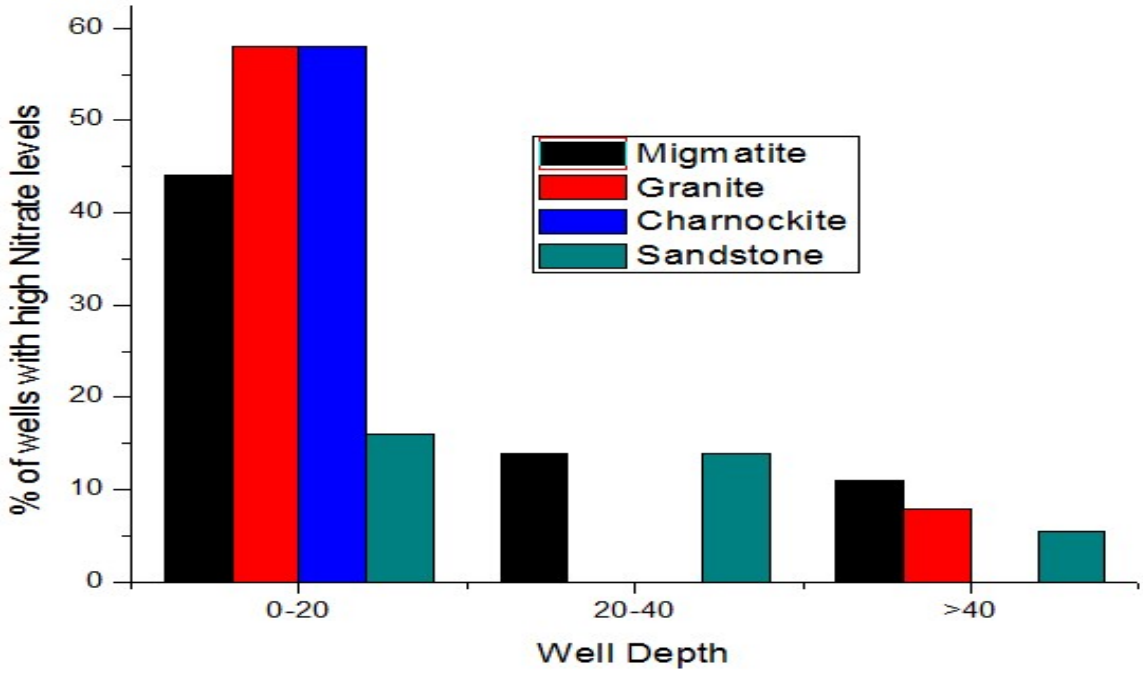

Fig. 4.20 (a) Bivariate plot of Nitrates vs. Well Depth, (b) Histogram Showing the variation of NO_3 with depth

4.6.2 Physico-chemical Parameters

The hydrogen ion concentration (pH) in the Bauchi-Alkaleri-Kirfi transition zone varies between 6.4 to 7.7 (Table 4.9), in the weathered basement aquifer and 5.0 to 8.5 (average = 6.0) in the sandstone aquifers, indicating a moderately acidic to slightly alkaline groundwater system. The range and the mean values of pH values for the different aquifer settings are 6.4-7.7 (7.16) for migmatite, 6.8-7.5 (7.09) in the granite, 6.4-7.7 (7.18) in the charnockite and 5.0-8.5 (6.05). While the pH values for the aquifers are normal (Hem, 1985), some of the sandstone aquifer samples revealed relatively low pH values (<6.5) and might have resulted from the oxidation of organic carbon in parts of the sedimentary basin, which produces CO_2, thereby lowering the pH of the aquifers (Kehew, 2001). Furthermore, considering that the variability of bicarbonate species in groundwater is controlled by pH, the generally low amounts observed in the sedimentary setting (5.0 to 8.5) could suggest lower level of bicarbonates in the groundwater as compared to the basement settings. For this reason, 20 % of the samples from the sandstone aquifers showed pH values (5-6.4) which are slightly above the NSDQW standard (6.5–8.5) (NSDQW, 2007).

The EC and TDS values ranged from 10-1520 µS/cm (mean value 276.11 µS/cm) and 15-1105 mg//l (205.6 mg//l). However in the basement setting the EC and TDS range from 120-2040 µS/cm (mean value 706.06 µS/cm) and 95-1558 mg/l (512.43 mg//l). EC and TDS in the migmatite bedrock ranged between 120 to 1290µS/cm (average of 666µS/cm) and 95-945mg/l (average of 481mg/L) respectively. In the granite settings EC and TDS ranged between 230 to 2040 µS/cm (ave. 897µS/cm) and 169-1558mg/l (average of 660mg/l) in the granite aquifers correspondingly. Similarly, in the charnorckite bedrock, EC and TDS ranged between 190 to 1580µS/cm (averages 542µS/cm) and 154-1154 mg/l (average of 394 mg/l) respectively. However in the sandstones the EC varies from 10 to 1520µS/cm (averages 276µS/cm) while TDS ranged between 15-1105 mg/l and averages 205 mg/l. This statistics clearly indicates generally low mineralized groundwater with the sedimentary settings having more limited migratory history. Electrical conductivity (EC) is the degree to which the dissolved

species in groundwater conduct current. Higher values of electrical conductivity reflects high concentration of dissolved salts in the groundwater.

However, based on the NSDQW standard 5 out of 12 groundwater samples from the Biotite hornblende granite aquifers, exceeded the permissible limits of 1000 µS/cm. As revealed by Fig. 4.21, the Biotite hornblende granites exhibited the highest value of EC and TDS which could be linked with the dissolution of unstable minerals which are more susceptible to weathering than feldspar and quartz (Jackson, 1970). It is noteworthy that most of locations with high EC values corresponds to samples collected from dug wells sited at the vicinity of waste drainages and dumpsites in the villages or wells sited close to latrines in residences, suggesting that the sources of contamination are likely anthropogenic. The TDS limit desirable for drinking water based on NSDQW, 2007 and WHO, 2011 is 500 mg/L and 28% of the groundwater samples in the research location displayed TDS values exceeding the aforementioned standards with a greater percentage of the high TDS water belonging to the basement rocks owing to their high composition of soluble and unstable silicate minerals as compared with the sandstone aquifers which are rich in less soluble minerals like quartz and feldspars. It is also noteworthy that the TDS values of Kerri-Kerri samples are the lowest with 44% of the samples having TDS values of <100 mg/l. Davies and Dewiest, (1996) opined that TDS of 500-1000mg/l is good for consumption purposes, up to 3000 mg/l is suitable for agricultural purposes while> 3000 mg/l is not good for the duo. The variation of EC and TDS with well depth in the study area is presented in Fig 4.22. The trend displayed by EC and TDS values in the water samples validates the linear correlation that exist between the duos (Al-Shaibani, 2008).

$$\text{TDS (mg/l)} = 0.78\text{EC (µS/cm)}$$

When the variation of EC and TDS was considered with depth it was observed that the parameters were both higher in the shallow aquifers especially those at the depths of 0-20m and this covers both aquifer types (Fig. 4.22). A significant decrease was however, observed at the depth of 20-40m, dominated by the sandstone aquifers while all wells > 40m showed the lowest EC and TDS values and lie in mostly within the sandstone setting thus, indicating that the variability of dissolved solids with depth.

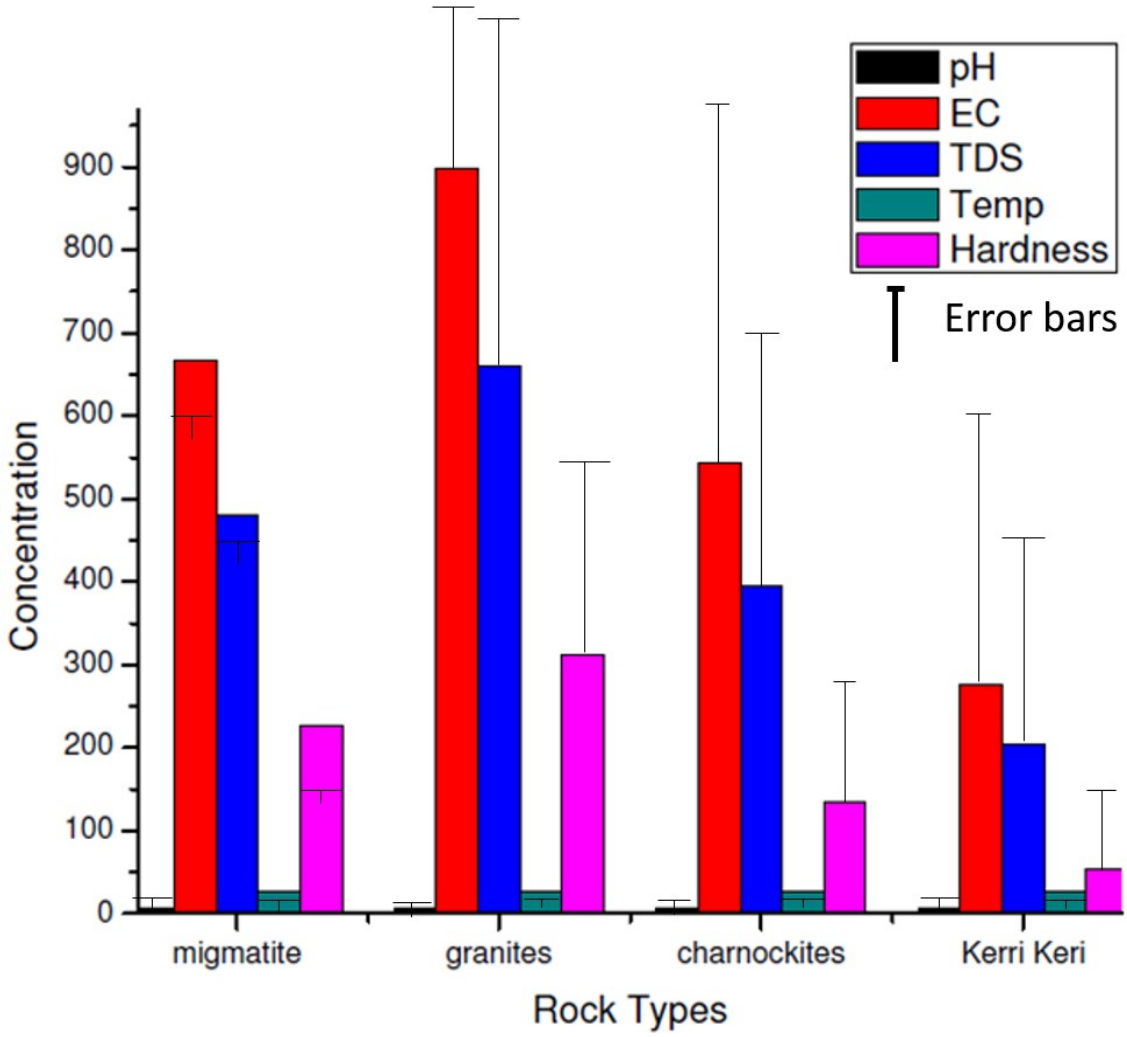

Fig. 4.21. Concentration of physical parameters in the Bauchi-Alkaleri-Kirfi transition zone based on rock types

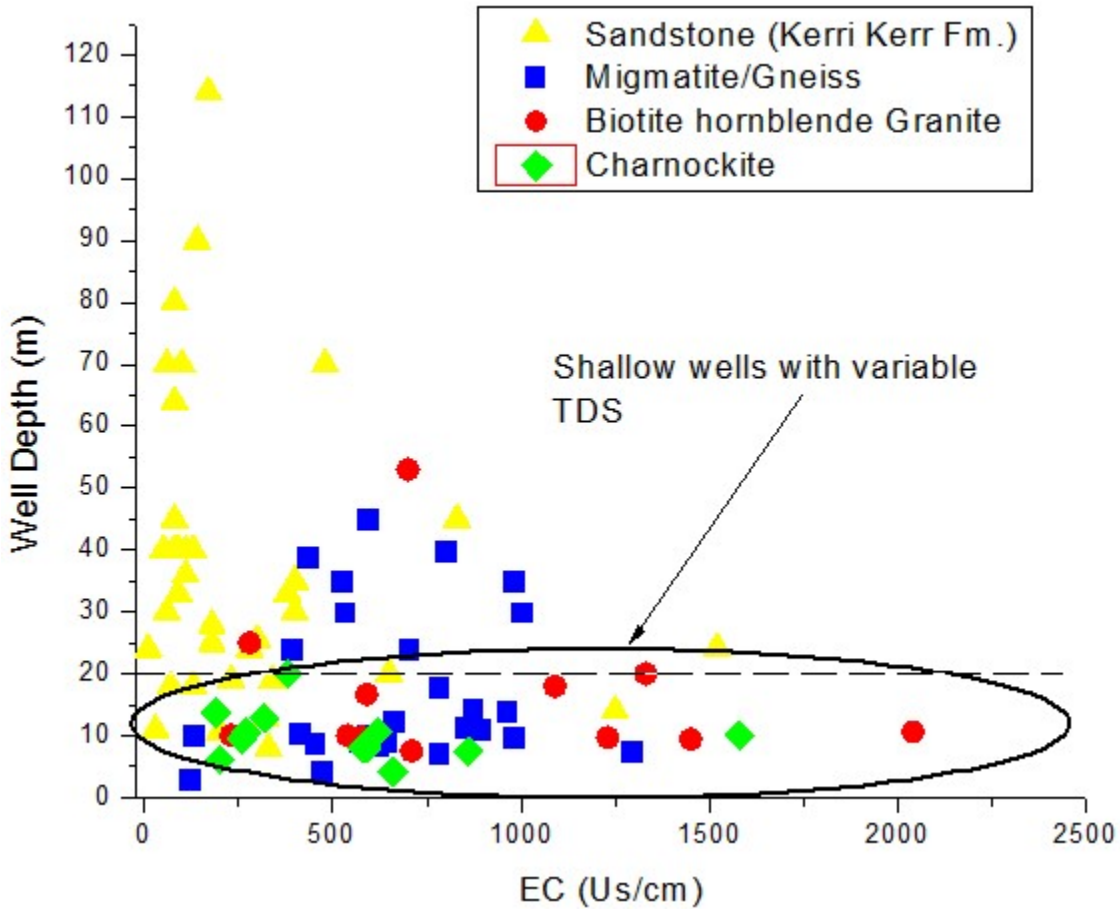

Fig. 4.22. Bivariate plot of Well Depth vs. EC

area. In terms of decreasing EC and TDS the aquifers in the research area can be arranged as follows: Biotite hornblende granite > Migmatite > Bauchite > Kerri-Kerri, which can also be attributed to inadequate well head protection and the poor sanitation around close vicinity of the wells. Given that the EC and TDS values that exceeded the permissible limits (1000 µS/cm and 500 mg/l correspondingly) were often located in wells at the vicinity of waste drainages and dumpsites in the villages or wells sited close to latrines in residences, pointing to a possibly contribution from anthropogenic sources. Based on the above premise it is evident that well depth, well head protection, anthropogenic and geogenic processes has profound effect on the groundwater quality in the Bauchi-Alkaleri-Kirfi transition zone.

The temperature of the sampled groundwater ranged between 21.5 and 29.5^{o}C with an average of 26^{o}C (Basement) and 21.4 and 31.4^{o}C (26 ^{o}C average) in the sedimentary area (Table 4.9). Temperatures range between 22.5 to 29.5^{o}C (averages 26.8 ^{o}C) in the migmatite bedrocks, 21.5 to 29.1^{o}C (averages 25.7)in the granite aquifers, 22.4 to 28.9 ^{o}C (averages 25.9 ^{o}C) in the charnockite setting and 21.4 to 31.7^{o}C (averages 26.7 ^{o}C) in the sedimentary aquifers, which is a general reflection of the surface temperature and time of sampling. Samples collected in the morning hours showed lower temperatures than those collected when the sun was overhead. Also, the average groundwater temperature in the area is similar to the prevailing local air temperature (26°C) and varies very little between the aquifer types.

The total hardness varies between 0.2 and 747.87 mg/l and averages 154.85 mg/l. The values of total hardness of the groundwater in the area (Table 4.10) revealed that the Biotite hornblende granite settings have the highest average values of 311.8mg/l (very hard), followed by the migmatite, the Bauchite and the sandstone aquifers with mean values of 227.6 (hard), 135.9 (moderately hard) and 54.3 (soft) respectively. The total hardness of water can be said to be related to its EC and TDS because these are all controlled by dissolved ions in the water especially the alkaline earths (Calcium and Magnesium) as outlined by Sawyer et al., (2003), in the following expression.

$$\text{Total Hardness } (CaCO_3) = (Ca^{2+} + Mg^{2+}) \text{ (meq/l) } x50$$

Total hardness (TH) is mainly due to the presence of specific metals in water, particularly magnesium and calcium. Evidences has linked water hardness to heart and kidney diseases (Schroeder, 1960; Jain, 1998), especially if the hardness is in the region of 150–300 mg/l or greater.

Total hardness is consequential parameter for water utillised for domestic purpose because it reduces the effectiveness of soaps and affects the taste of the water in an unpleasant manner. The acceptable limits in domestic use as specified by WHO, 2011 and NSDQW, 2007 is 100 mg/l and 150 mg/l respectively. Consequently, 55% of the samples in the area comprising largely of those from the Kerri-Kerri (89%) and the Bauchite terrain (58%) displayed hardness values below 150 mg/l (NSDQW, 2007) while 45% of the samples dominated by those from the migmatite and Biotite hornblende granite zone (75% each) showed hardness values beyond permissible limits of >150 mg/l. Based on Sawyer and Mc Carty, 1967 classification (Table 4.10), 43.7% (38 samples) of the total samples fall within the soft water class with 74% (28 samples) of the soft groundwater samples falling in the Kerri-Kerri zone, followed by Biotite hornblende granite with 16% (6 samples) and migmatite and Bauchite bedrocks displayed the least percentage of soft water, 5% (2 samples) each. The hard and very hard water constitute 17.2% and 27.6% respectively.

However the migmatite and the Biotite hornblende granite samples revealed higher percentages of hard and very hard (58% hard water and 47% very hard water type) and the Biotite hornblende granites which showed 17% (hard) and 33% (very hard) in the hard and very hard water as a greater percent of the both where observed on the migmatite samples (58% hard water and 47% very hard water type) and the Biotite hornblende granites which showed 17% (hard) and 33% (very hard).The sandstones and Bauchite bedrocks reveal relatively lower amounts of hard and very hard water with having 12% (3 samples) falling under the hard category and 6% (1 sample) and 13% (3 samples) under the very hard water type respectively. From the above discourse, it can be summarized that the migmatite bedrocks showed the lowest well depth while sandstones displayed the highest, however based on the EC, TDS and total hardness values the basement bedrocks exhibited comparatively higher values (EC ave. 512.43 mg/l;

hardness of 311 mg/l) which is attributable to the weathering and dissolution of silicate minerals in the terrain.

Table 4.10. Classes of Hardness in Water (Sawyer and Mc Carty, 1967)

Hardness (as $CaCO_3$) mg/l	**Water Class**	**Samples based on bedrock**				**Total**	**% of samples**
		KK	**MG**	**BH**	**BHG**		
0-75	Soft	28	2	6	2	38	43.7
75-150	Moderately Hard	4	4	1	1	10	11.5
150-300	Hard	3	14	3	4	24	27.6
>300	Very hard	1	7	2	5	15	17.2

KK=Kerri-Kerri,
MG=Migmatite/gneiss
BH= Bauchite
BHG= Biotite
Hornblende Granite

Although, the TDS were within the permissible limits on the average but are generally lower within the Kerri-Kerri samples (TDS of 205 mg/l) which is an indication of low dissolved constituents with limited history of migration (Talabi and Tijani, 2013).

The migmatite gneiss and Biotite hornblende granite bedrocks however, displayed relatively higher TDS values (481 and 666 mg/l) owing to the dissolution of silicate minerals. Conversely, the soft water species are predominant in the Kerri-Kerri formation as compared with the basement settings and this can also be attributed to the fact that the Kerri-Kerri Formation are majorly sandstones, which are rich in silica and generally low in feldspars and other calcium and magnesium rich minerals. The above assertion is in tandem with the generally low dissolved species recorded by the groundwater from the Kerri-Kerri. Conversely, the hard and very hard water types are prevalent in the migmatite and Biotite hornblende granite area which is due to dissolution of silicate minerals from rocks (Ali and Ali, 2018).

4.6.3 Cation Chemistry (Ca^{2+}, Mg^{2+}, Na^{+}, K^{+})

The results of the cation chemistry is presented in Table 4.11 and the detailed results in Appendix XIII. The charge balance of the samples are generally <10 %, although some samples revealed charge balance of >10, which can either be attributed to their low ionic strength (sandstone aquifers) or due to errors associated with alkalinity measurements (Fritz, 1994). The concentration of the alkali earth metals ranged from 0.2-216.2 mg/l Ca^{2+}(ave. 38.2 mg/l) and 0.1 – 57. 7 mg/l Mg^{2+} (ave. 14.4 mg/l) (Table 4.11). Calcium and magnesium generally exist in an equilibrium state most groundwater systems and constitute the major cause of hardness in water. However, calcium is the dominant cation in most of the samples analysed and this abundance is attributable to the fact that calcium is one of the commonest cation in groundwater. Also, calcium is abundant in most rocks owing to it high solubility in water. (Ali and Ali, 2018). Furthermore, occurrence of Ca^{2+} in water depends on the weathering and dissolution of calcium carbonates or silicate

minerals in Basement Complex rocks which characterise the area as revealed by studies conducted by Fisher and Mullican, (1997) and Ali and Ali, (2018). The calcium concentration in almost all the samples (82%) fall within desirable limit for drinking purposes based on WHO, 2011 and NSDQW, 2007. As can be seen from the results of the cations concentration (Table 4.11), magnesium (Mg^{2+}) is generally less abundant than calcium in groundwater owing to the fact that it less soluble and magnesium-rich minerals naturally dissolve slowly as compared to those of calcium which are have high dissolution and are more abundant in the crust as compared with magnesium. While Mg^{2+} is very essential for the smooth running of cells in the body, it influences taste to the water in an unpleasant way, if its concentration in drinking water exceed the permissible limit which is 50 mg/l (WHO, 2011 and NSDQW, 2007). The Mg^{2+} content in the studied samples averages 14.42 mg/l, which implies that the samples are within desirable limits based on the already established standards. On the basis of magnesium content, 92% of the samples fall in desirable limit for drinking purposes based on WHO, 2011 and NSDQW, 2007.

Among alkali metals, sodium and potassium are common cations dissolved in underground water. As presented in Table 4.11, the concentration of Na^{+} ions ranged from 1.59 to 130 mg/L, and averages 27.64, which way below the NSDQW, 2007 and WHO, 2011 standard of 200 mg/L in all the samples analysed. However, the potassium concentration ranged between 0.2 to 134.9 mg/L with average of 9.23 mg/l. The WHO standard permissible limit for potassium is 12 mg/l (WHO, 2011) and in research area, 15 of the analysed groundwater revealed potassium levels greater than permissible limit. While sodium ions are commonly derived from halite dissolution, weathering of silicates and agricultural activities, potassium ions are released by conversion of feldspars to clay minerals (Fisher and Mullican, 1997; Ali and Ali, 2018). This assertion is in tandem with the scenario in the Bauchi-Alkaleri-Kirfi transition zone in that aside from being a farming community, the area is dominated by crystalline rocks which are rich in feldspars and other silicate minerals like biotite and hornblende which are known to be unstable and susceptible to weathering. Based on the above premise the order of abundance of major cations in the groundwater from the study area is such that $Ca^{2+} > Na^{+} > Mg^{2+} > K^{+}$

and their concentrations (in mg/l) averages 42.69, 30.88, 16.11 and 10.3, respectively (Fig. 4.23).

Parameters	Units	WHO (2011)	NSDWQ,(2007)	Mean	Min.	Max.	Standard Dev.

Table 4.11. Summary of results of groundwater hydrochemistry in the study area

Ca	mg/L	75.00	75.00	38.21	0.21	216.20	41.70
Mg	mg/L	50	50	14.42	0.12	57.70	15.32
Na	mg/L	200.00	-	27.64	1.59	130.50	27.87
K	mg/L	12.00	-	9.23	0.19	134.90	21.68
HCO_3	mg/L	500.00	-	125.40	4.18	385.93	103.84
CI	mg/L	250	100	33.56	0.43	317.54	50.23
SO_4	mg/L	250.00	100.00	12.60	0.00	116.49	19.17
NO_3	mg/L	45.00	50.00	106.23	0.00	718.85	136.34

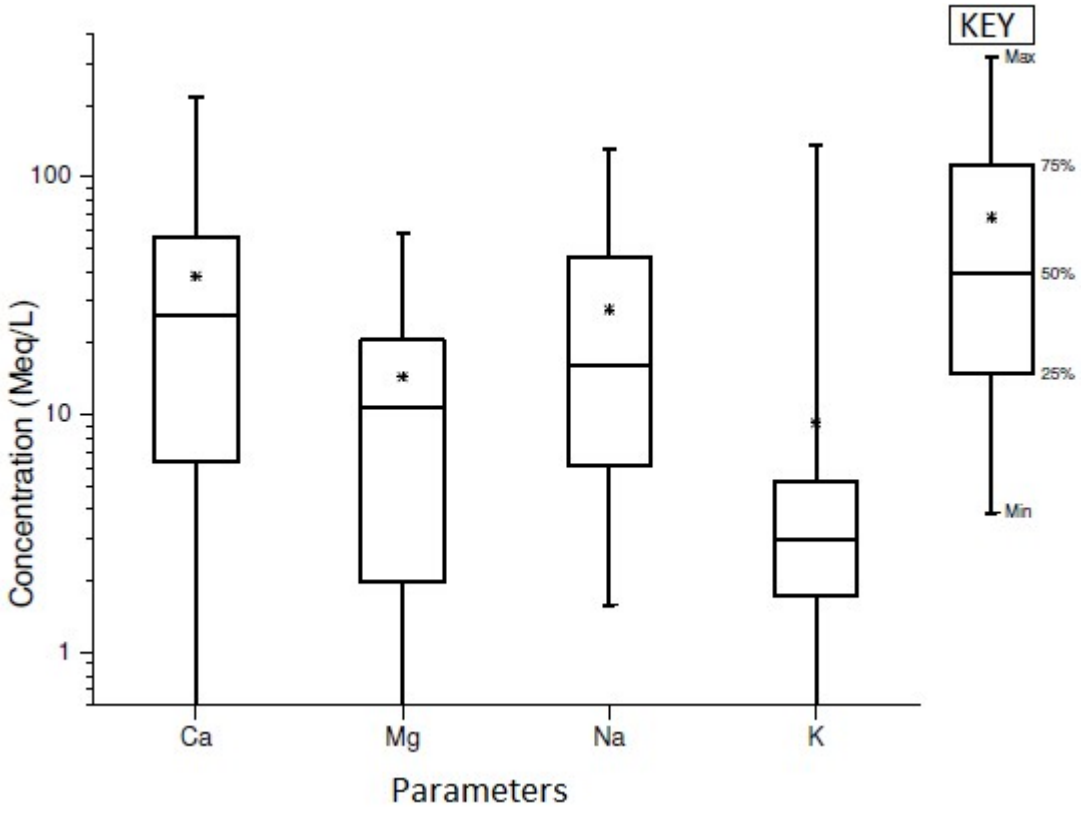

Fig. 4.23. Box and whisker plot showing the concentration of the cations in groundwater

4.6.4 Anion Chemistry (HCO_3^-, NO_3^-, SO_4^{2-}, Cl^-)

Groundwater alkalinity is a measure of its neutralization potential (Kumar *et al*., 2006), which is basically determined by the bicarbonate (HCO_3^-). Considering that bicarbonate (HCO_3^-) is the predominant anion in the studied samples, more than half over 50% of the samples are bicarbonate waters. The carbonate and bicarbonate concentration in groundwater originate from dissolution of carbonic acid or during carbonate weathering as shown in the equations 4.1 & 4.2. (Kumar *et al*. 2009).

$$CaCO_3 + CO_2 + H_2O \rightarrow Ca^{2+} + 2HCO_3^- \quad (4.1)$$

$$CO_2 + H_2O \rightarrow H^+ + HCO_3^- \quad (4.2)$$

Bicarbonate control water absorption in humans and neutralises the acidity of proteins and other dietary components (Kessler and Hesse, 2000). The concentration of HCO_3^-, ranged between 4.18 mg/l to 385.9mg/l in the area and averages 125.4 mg/l. The alkalinity of all the groundwater tested were within the desirable limit of 500 mg/l (WHO, 2011). The pH range in the study (5 and 8.5), further confirms the preponderance of bicarbonates specie in the research area, owing to the fact that the pH controls the variability of the different carbonates species in groundwater.

As presented in Table 4.11, the chloride concentration in the area showed variation from 0.43 mg/l in the basement terrain to 317.9 mg/l in the sandstones. The permissible limit

for Cl^- (mg/l) in groundwater is 250 and 100 mg/l according to WHO, 2011 NSDQW, 2007 respectively. Only 8% (7 locations: 14, 15, 33, 55, 64, 66 and 84) of the groundwater samples displayed chloride values exceeding the NSDQW standard and they are reflective of either evaporate deposits or anthropogenic sources. In the Bauchi-Alkaleri-Kirfi transition zone, high concentration of chloride were in most cases, associated with samples collected from wells at the vicinity of waste drainages and dumpsites in the villages or wells sited in residences and this scenario is in tandem with the general assertion that chlorides are also indicative of contamination (Alhajjar *et al*., 1990).

As shown in Table 4.11, sulphate is the least anion in the samples analysed which ranged between bdl to 116.5 mg/l and averages 12.60 mg/l. Observed sulphate concentrations is within the permissible limits of both WHO, 2011 and NSDQW, 2007 which stipulates 250 mg/l and 100 mg/l correspondingly. Soluble sulphates are introduced into groundwater and other natural water sources through dissolution of evaporite minerals and, anthropogenic sources (Ali and Ali, 2018). Sulphates are known to cause dehydration, catharsis, and gastritis in human beings when it occurs beyond the permissible WHO threshold of 250 mg/l (Ali and Ali, 2018). On the basis of the preceding premise, the sequence of quantity of anions in the samples isHCO_3^-> Cl^- > SO_4^{2-}, and contribute an average of 45.08, 12.06, and 4.53%, respectively. Only a few locations (0-8%) indicated concentration of HCO_3, Cl, and SO_4, above their respective threshold values (NSDQW 2007; WHO 2011). However more than 50% of the studied samples revealed nitrate levels exceeding the permissible limits of 50 mg/l.

Nitrates are generally abundant in the groundwater in the research area. Nitrogen is the most abundant element in the atmosphere, it is usually deposited from the atmosphere and then mineralized into ammonium by soil bacteria (Selvam *et al*., 2012). Nitrates are also sourced from anthropogenic sources which include human and animal sewage, fertilizers from farms and etc. High amounts of NO_3 in drinking water is hazardous as it causes gastric cancer and affects blood circulation (CPCB, 2008). Nitrate (NO_3) concentration the sampled wells ranges from bdl to 718.8 mg/l and averages 106.63 mg/l. Fifty three percent (53%) of the water samples were above the WHO, (2011) threshold of

45 mg/l and NSDQW, (2007) standard of 50 mg/l. In the research area, field observation revealed that the nitrates contamination in wells are related to inputs from domestic waste/sewage, open defecation and ponding of waste water in the well vicinity (< 5m), as well as agro-pastoral activities of the farming communities in the area. (Fig. 4.24 and Plate 4.1).

As presented in Fig. 4.24, the predominant source of nitrate contamination in the area is attributable to the agro-pastoral activities, which is responsible for 60% of the nitrate contamination in the migmatite/gneiss aquifers and 40%, 30% and 15% in the granite, charnockite and the sandstone aquifers respectively. However, the household related nitrate contamination are predominant in the granite and charnockite setting with 25% each for both rock types and 5% and 15% for the migmatite/gneiss and sandstones correspondingly. Based on the above premise, the major source of nitrate contamination in the Bauchi-Alkaleri-Kirfi transition zone can be attributed the agro-pastoral activities relating to application of fertilizers and animal waste.

However, the basement complex aquifers are the most affected by nitrates from agro-pastoral activities and this is in tandem with the result of the study by Hallouche *et al*., 2017. The household contamination with respect to nitrate, which is dominant in the granite and charnockite setting suggest that most of the affected wells are sited close to latrines in residences or at the vicinity of waste drainages and dumpsites in the villages. It is noteworthy that the sedimentary aquifers are the least influenced by NO_3 contamination owing to their depths and well head which are well protected from infiltration of contaminants from unhygienic human activities around the well. From the above statistics, the comparative order of abundance of the anions is $HCO_3^- > NO_3^- > Cl^- > SO_4^{2-}$, and contribute an average of 45.08, 38.32, 12.06, and 4.53%, respectively. Only a few locations (0-8%) indicated concentration of HCO_3, Cl, and SO_4, above their respective threshold (NSDQW 2007; WHO 2011). Furthermore, more than 50% of the studied samples revealed nitrate levels exceeding the permissible limits of 50 mg/l. As shown in Fig. 4.25, the dominant cation in the Bauchi-Alkaleri-Kirfi area is Ca^{2+} which is suggestive of weathering of rock forming minerals that make up the basement rocks. Also, the prevalence of HCO_3^- anion in the groundwater samples from the Basement

Complex setting suggests CO_2-charged infiltrating recharge rainwater. Groundwater with HCO_3 as the most abundant anions are believed to have derived their solutes from CO2-charged meteoric recharge coupled with silicate weathering and dissolution (Fisher and Mullican 1997).

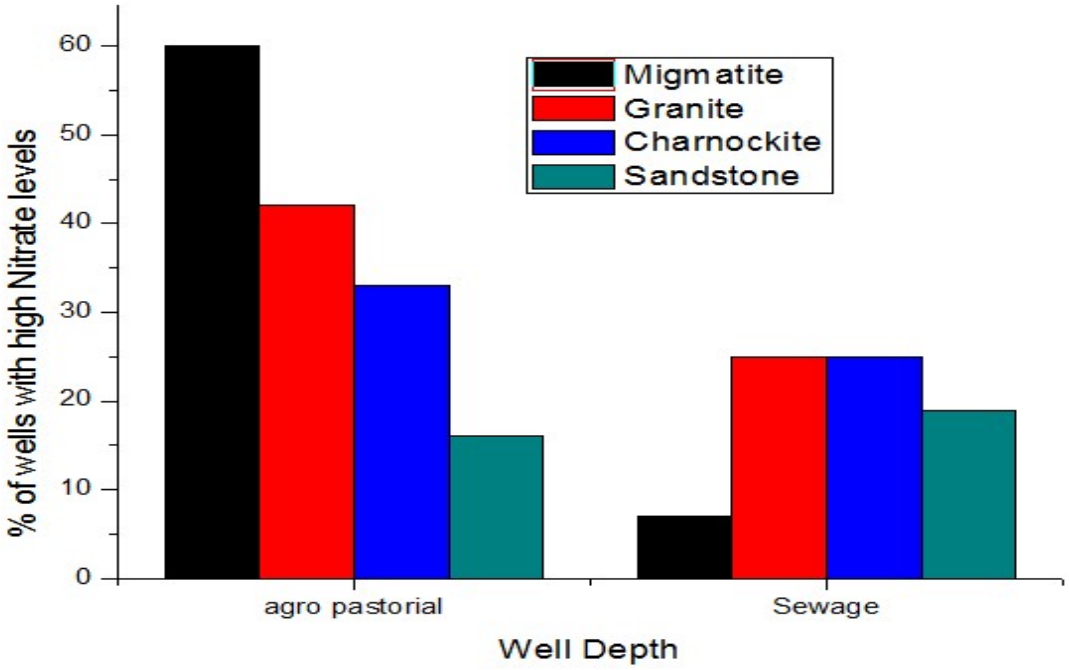

Fig. 4.24. Bar Chart showing the proportion of the wells and the various NO_3 sources in Bauchi-Alkaleri-Kirfi area

Plate 4.1. An unprotected hand dug well in the Bauchi-Alkaleri-Kirfi area.

A significant number of research have shown that the main variables that lead to increased nitrate emissions into surface and groundwater systems are anthropogenic activities involving Nitrogen Compounds like organic and mineral fertilizers and septic systems (Rao, 2006). Water recharging from the ground surface via direct infiltration and flow from neighboring mountainous regions coupled with waste from dumpsites, human sewage and agro-pastoral activities account for the nitrate content of the groundwater in the saturated aquifer (Akiti, 1986; Gibrilla *et al.,* 2010, Hallouche *et al.,* 2017)

Having considered the general outlook of the physico-chemical parameters of groundwater samples in the study, it is paramount explore the variation or similitude of these parameters within the different lithological units in the Bauchi-Alkaleri-Kirfi transition zone as highlighted in the subsequent section.

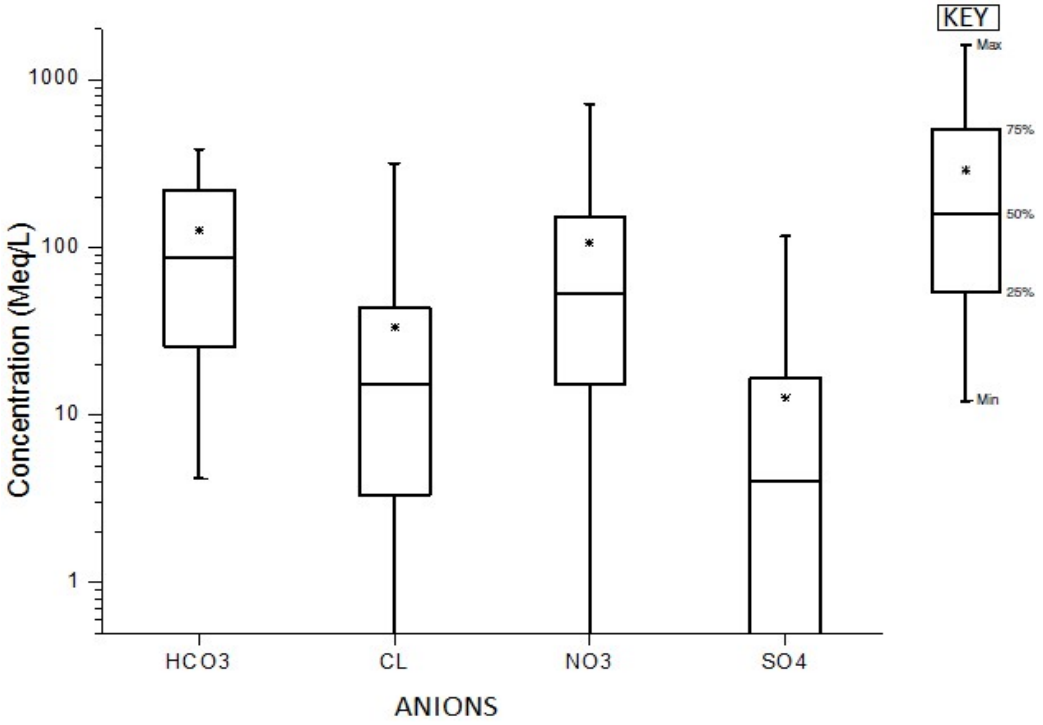
KEY
Max
75%
50%
25%
Min
1000
100
10
1
Concentration (Meq/L)
HCO3
CL
NO3
SO4
ANIONS

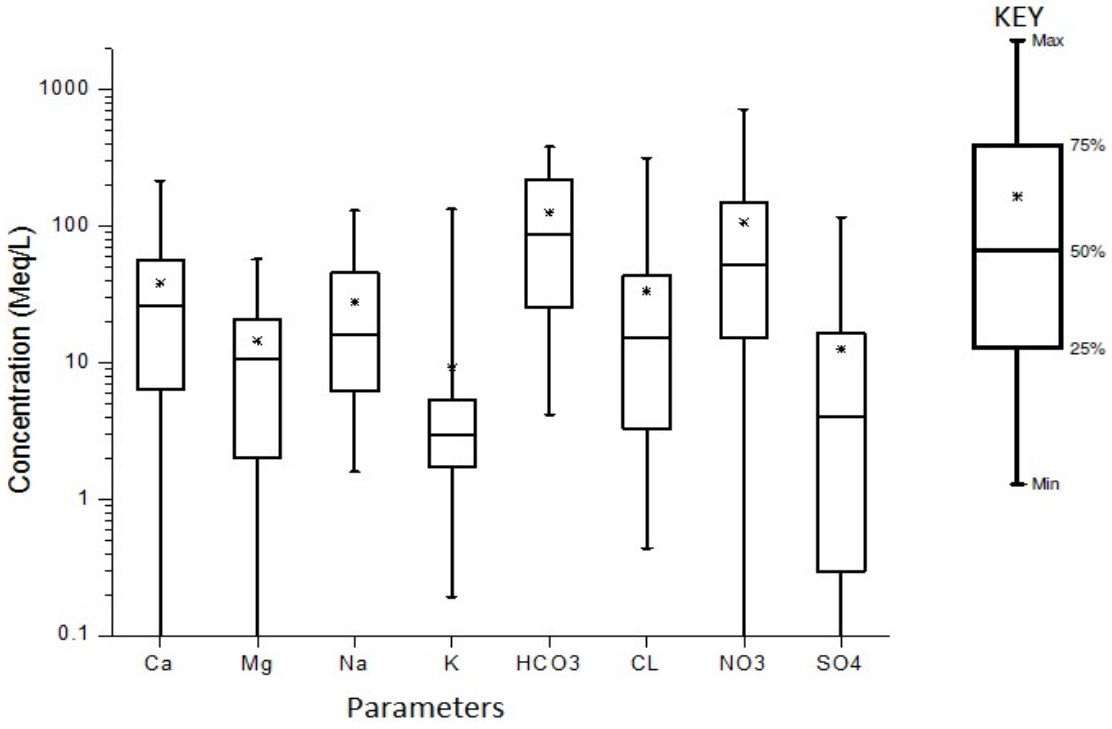
KEY
Max
75%
50%
25%
Min
1000
100
10
1
0.1
Concentration (Meq/L)
Ca
Mg
Na
K
HCO3
CL
NO3
SO4
Parameters

Fig. 4.25 (a). Box and whisker plot showing the concentration of the anions in groundwater

(b). Box and whisker plot showing the concentration of the cations and anions in groundwater.

4.6.5 Lithology Based Hydrochemical Profile

The statistical summary of the analysed chemical parameters within the various bedrocks are presented in Table 4.12 and Fig. 4.26. The average concentration of calcium (Ca^{2+}) in the basement setting (Table 4.10) is highest in the biotite hornblende granite zone with a value 81.16 mg/l, followed by the migmatite with 53.61 mg/l and the Bauchite with the least concentration of 39.10mg/l. The concentration is comparatively lower in the sedimentary terrain where it averages 13.57mg/l. However, Mg^{2+} displayed an average concentration of 26.49 mg/l, 22.75 mg/l, 9.19 mg/l and 5.88 mg/l in the biotite hornblende granite, migmatite, Bauchite and the Kerri aquifers respectively. The low quantities of the alkali earth metals in groundwater from the sandstone aquifers are attributable to the low amounts of unstable silicate minerals in the sandstones compared to the basements terrain (Fisher and Mullican 1997).

As shown in Table 4.12, Na^{+} averages 43.22mg/l (migmatite bedrocks), 36.24 mg/l (biotite hornblende granites), and 26.24 mg/l (Bauchite) and 13.57 mg/l in the sandstone aquifers and this also corroborates the general decrease in TDS from the Basement Complex areas to the sedimentary zones. Potassium (K^{+}) which is generally less abundant that sodium in nature averages 3.74 mg/l, 8.17 mg/l, 15.72 mg/l and 11.5 mg/l in migmatite, biotite hornblende granite, bauchite and sandstone aquifers respectively, suggestive of the fact that the bauchites and sandstones (arkosic in nature) have substantial amounts of orthoclase feldspar. The K^{+} in the orthoclase may replace divalent calcium from the calcic plagioclase, thereby releasing K^{+} in water through cation exchange reactions (Morales et al. 2015). The overall assessment of the cations in this study revealed that there is a general depletion of alkali earth metals (Ca^{2+} and Mg^{2+}) and an overall enrichment of the alkalis (Na^{+} and K^{+}) as you move from the basement aquifers to the sedimentary aquifers suggestive of possible cation exchange reaction (Eqn 4). As shown by the equation a monovalent K^{+} may replace divalent cations from

feldspars, as exemplified by the reaction of an orthoclase (Na, K) $AlSi_3O_8$) to produce anorthite ($CaAl_2Si_2O_8$) as shown in Eq. (4.5), releasing Na^+ and K^+

$$2(Na, K)\,AlSi_3O_8(s) + Ca^{2+} \longrightarrow CaAl_2Si_2O_8(s) + (Na^+; K^+) + 4SiO_2 \quad (4.)$$

Orthoclase anorthite monovalent ions silica

Table 4.12. Descriptive Statistics of Chemical Parameters Based of Bedrock Types

Parameters	Migmatite			Biotite Hornblende Granite			Bauchite			Sandstone		
	Mean	**Min**	**Max**	**Mean**	**Min**	**Max**	**Mean**	**Min**	**Max**	**Mean**	**Min**	**Max**
Ca	53.61	2.57	128.55	81.16	12.40	216.20	39.10	6.30	123.55	12.05	0.04(BDL)	97.65
Mg	22.75	1.29	57.70	26.49	3.32	57.60	9.19	0.44	33.05	5.88	0.02(BDL)	42.25
Na	43.22	2.47	100.85	36.24	5.96	75.20	26.24	5.90	130.50	13.57	1.59	106.30
K	3.74	0.84	26.95	8.17	1.30	57.00	15.72	1.03	132.55	11.55	0.19	134.90
HCO_3	206.71	25.69	341.12	197.15	66.31	385.93	121.13	34.05	276.60	41.94	4.18	246.73
Cl	33.95	1.93	120.78	79.81	3.27	317.54	35.54	3.29	140.27	17.19	0.43	179.14
SO_4	18.20	0.33	68.77	30.12	1.30	116.49	9.29	0.00(BDL)	34.19	3.67	0.00(BDL)	70.37
NO_3	115.07	0.00(BDL)	449.46	215.00	4.26	718.85	81.40	2.08	393.75	71.63	0.00(BDL)	619.62

BDL-Below Detection Limit

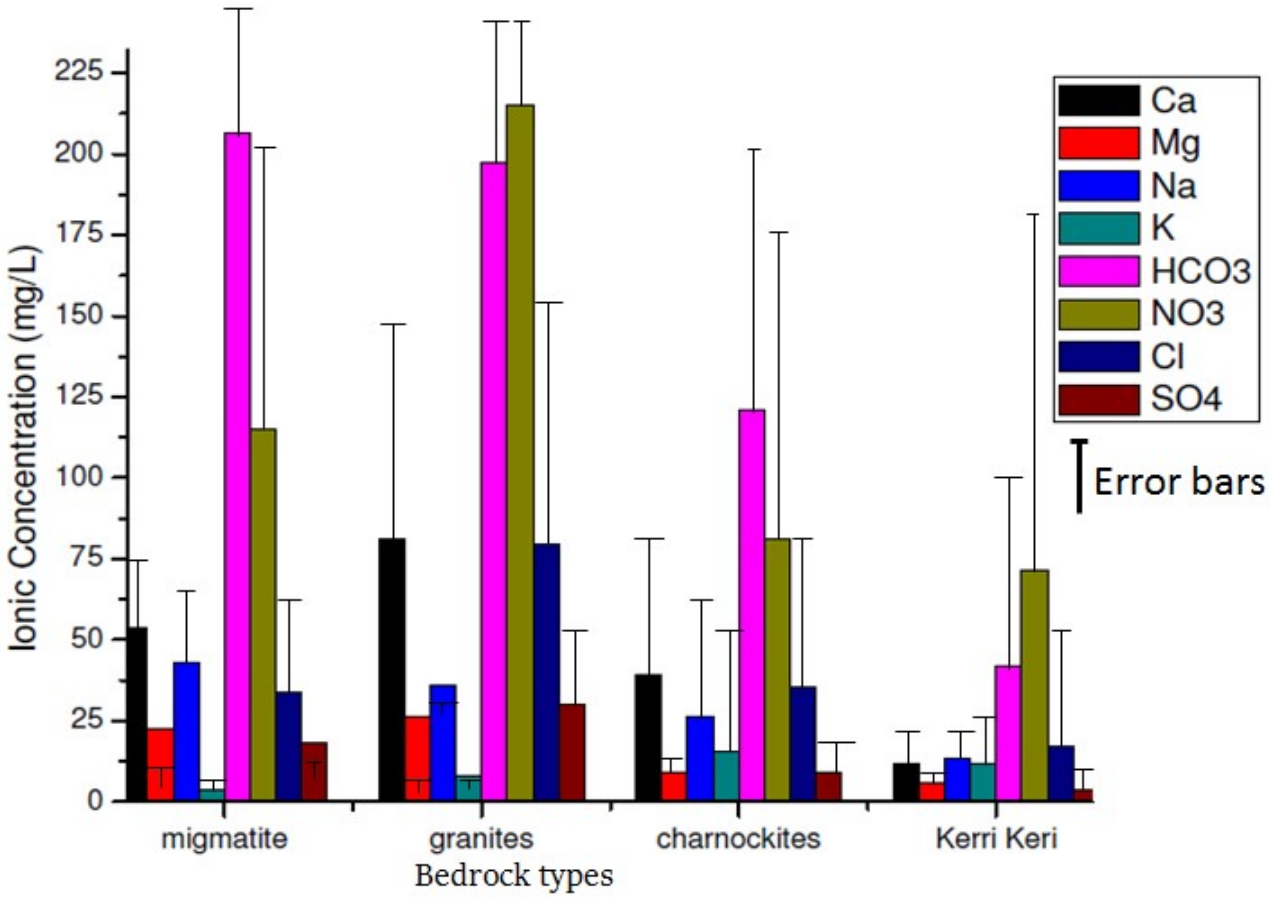

Fig. 4.26. Concentration of chemical parameters in the Bauchi-Alkaleri-Kirfi transition zone based on rock types

The comparative abundance of the cations in the basement setting is such that Ca^{2+}> Na^{+}> Mg^{2+}> K^{+} in the groundwater from migmatite and biotite hornblende setting while in the bauchite the order is Ca^{2+}> Na^{+}> K^{+} > Mg^{2+}. In a typical basement setting, the amount of alkaline earths metals in the groundwater are expected to considerably surpass the alkali metals which is the scenario in basement terrain in the research area and this in tandem with studies by Mapoma *et al*. (2014). In the sandstone aquifers however, a different trend was observed; Na^{+}> Ca^{2+}> K^{+} > Mg^{2+} which reveals enrichment of the alkalis and depletion of the alkali earth metals suggestive of cation exchange reaction.

As revealed by Table 4.12, HCO_3^{-} is the most prevalent anion in the area with the migmatite showing the highest mean concentration of 206.71mg/l, followed by the biotite hornblende aquifers which averages 197.15 mg/l and the bauchite aquifers revealed a concentration of 121.13 mg/l. The concentration of bicarbonates in the sandstones averages 41.94 mg/l. Nitrates averages 71.63 mg/l in the sandstone aquifers and 215 mg/l, 115.07 mg/l and 81.40 mg /l in migmatite, biotite hornblende and bauchite aquifers respectively. Groundwater with HCO_3 as the most abundant anions displayed by the basement aquifers in the Bauchi-Alkaleri-Kirfi area are believed to have derived their solutes from silicate weathering which is consistent with work of Fisher and Mullican, 1997 in Texas, USA, while relatively high NO_3 content indicates point source pollution primarily related to agro-pastoral activities in the area which is also in agreement with the work of Hallouche *et al*., (2017) who characterized the water chemistry in a similar geological setting in NW Algeria.

The concentration of the strong acids (Cl^{-} and SO_4^{2-}) is dominant in the basement settings as compared to the sedimentary terrain (Fig. 4.27). The concentration of Cl^{-} ranged between 79.81 mg/l in the biotite hornblende granite to 17.19 mg/l in the sandstone aquifers, with the migmatite and bauchite averaging 33.95 mg/l and 35.54 mg/l respectively. It is important to note that the SO_4^{2-} also showed the same increasing order as the Cl^{-} with respect to the different bedrocks.

(a)

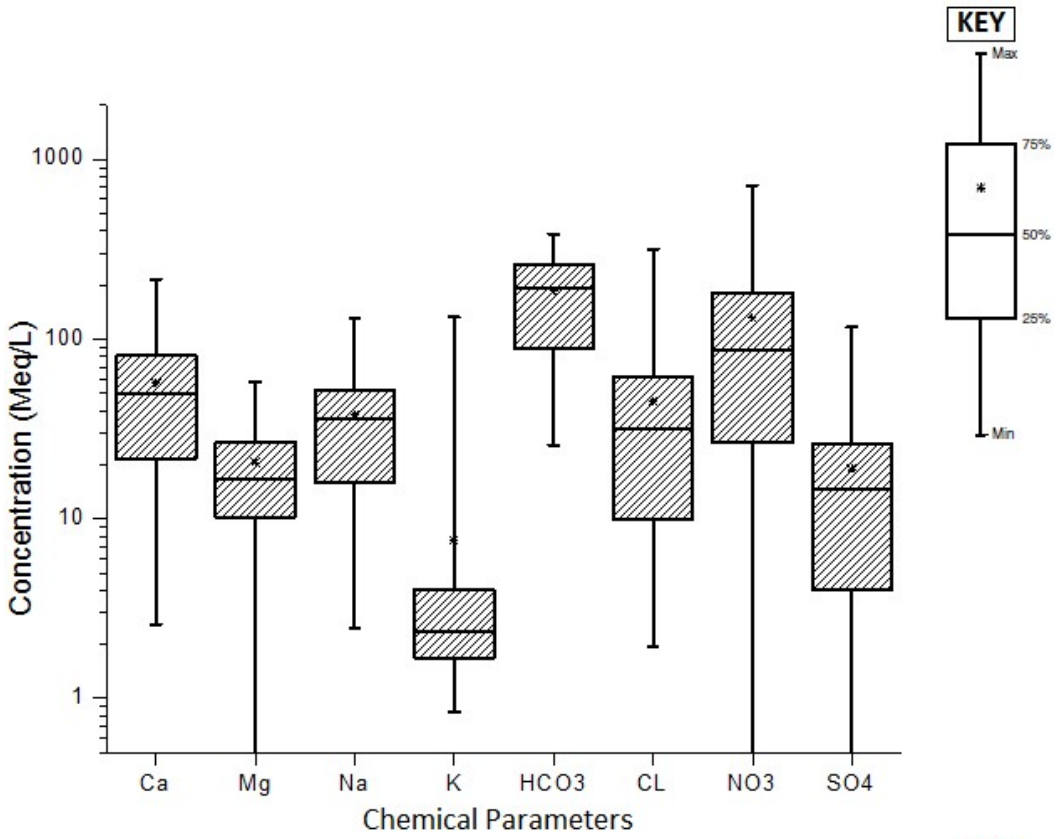

(b)

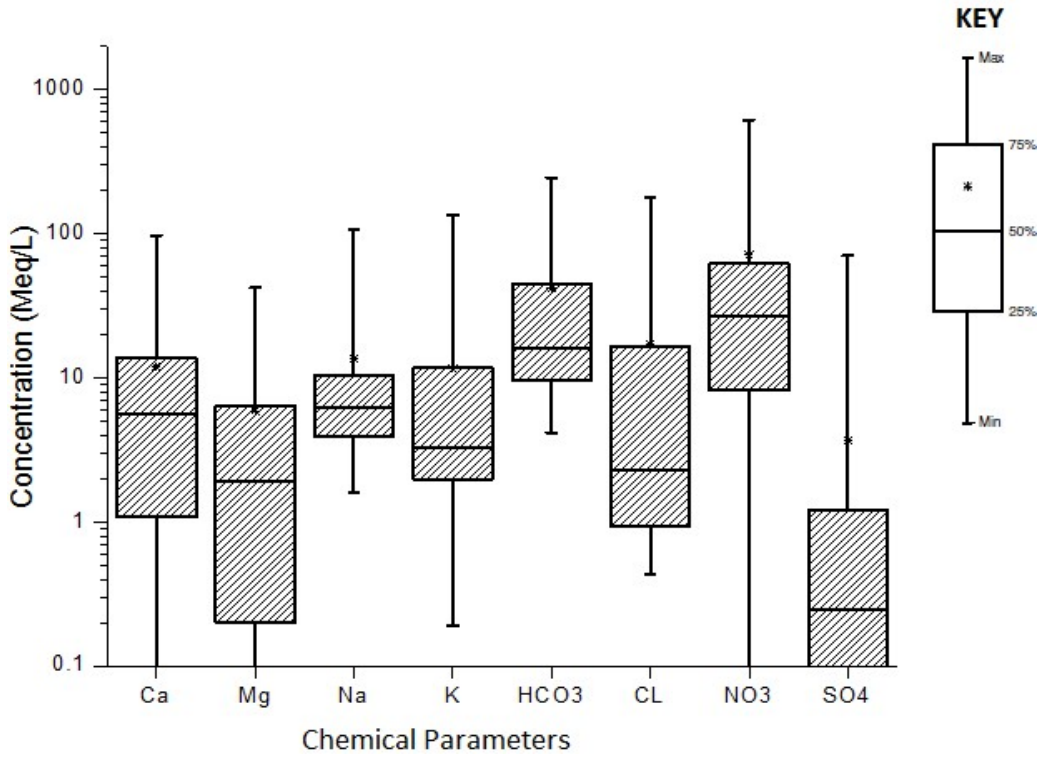

Fig. 4.27. Distribution of Anions and Cations in (a) Basement Aquifers and (b) Sedimentary Aquifers

The biotite hornblende granite revealed an average SO_4^{2-} concentration of 30.12 mg/l while migmatite, bauchite and the sandstones averaged 18.2 mg/l, 9.29 mg/l and 3.67 mg/l respectively. The order of abundance of major anions in the wells is $HCO_3^- > Cl^- > SO_4^{2-}$. The hydrochemical profile of the Bauchi-Alkaleri-Kirfi transition zone has revealed that the dominant cation and anion in the basement setting are calcium and bicarbonate respectively and this is attributable to CO_2-charged meteoric recharge in basement rocks as suggested by Lloyd and Heathcoat, 1885. Although, the possibility of having calcite and dolomite dissolution in the Bauchi-Alkaleri-Kirfi area is very low owing to the generally low range of pH in the area (pH between 5-8.5) and coupled with the fact that the average TDS is are generally < 600 as confirmed by Zhang *et al*., 2007. The sedimentary aquifers on the other hand revealed Na^+ and bicarbonates as the dominant ions indicating possible case of CO_2-charged meteoric water and ion exchanged water. Furthermore, the influence of anthropogenic factors in this study is suggested by the general abundance of nitrates in the groundwater in the area. Based on the above discourse, the groundwater in the Bauchi-Alkaleri-Kirfi area can be said to influenced by both natural/geogenic factors possibly precipitation and silicate weathering (as reflected by the dominance of HCO_3^-) and anthropogenic factors as suggested by the high content of nitrates in some of the groundwater.

4.6.6 Principal Component Analysis (PCA)

Due to the willingness to enhance data for better evaluation and understanding, the use of PCA in hydrochemical research has increased overtime (Helena *et al*., 2000). PCA is a measure of how each variable is associated with one another (Covariance matrix), the directions in which our data are dispersed (Eigen vectors) and the relative importance of these different directions (Eigen values), thereby making it possible for us to eliminate the unimportant Eigen values. The principal component analysis for the present study, yielded 3 significant principal components (factor loadings) based on Eigen value ≥ 1 and their high cumulative variance of 87.0% as shown in Table 4.13. The first factor accounts for 63.8% of the total variance and it is characterised by very high loadings of EC, TDS,Cl^-,NO_3^-,SO_4^{2-}, Ca^{2+}, Mg^{2+},HCO_3^- and Na^+.

Table 4.13. Correlations between PCA variables and factors

	F1	F2	F3
EC	**0.984**	-0.098	0.017
TDS	**0.949**	0.024	-0.154
pH	0.447	**0.688**	0.394
HCO_3	**0.669**	**0.627**	0.220
CL	**0.874**	-0.333	-0.094
NO_3	**0.861**	-0.386	-0.227
SO_4	**0.835**	0.009	0.032
Ca	**0.947**	0.049	-0.165
K	0.328	-0.639	**0.628**
Mg	**0.885**	0.173	-0.168
Na	**0.711**	-0.153	***0.456***
T.H	**0.969**	0.085	-0.173

Values in bold correspond strong (>0.6) and positive factor loadings while italised values represent moderate loadings

Low loadings of pH and K^+ were also indicated in the PC1. It is represented by the elements defining the mineralization, groundwater quality and the observed hydrochemical facies.

Component 1 reveals that EC and TDS values are contributed by the major groundwater cations and anions, possibly through silicate weathering or carbonate dissolution, while the strong loadings of Cl^-, NO_3^-, SO_4^{2-} suggest a possible of influence agricultural fertilizers and human and animal sewage confirming presence of significant anthropogenic activities in the Bauchi-Alkaleri-Kirfi area. Component 2 accounting for 15.4% of the total variance revealed strong positive loading of pH and HCO3- which signifies that the presence of different carbonate specie in water is controlled by the pH variability. The third factor accounting for 8.6% of the total variance revealed strong positive loadings of K+ attributable to release of potassium ions as a result of conversion of feldspars to clay minerals in agreement with the studies by Fisher and Mullican, 1997 and Ali and Ali, 2018. As can be observed from the loadings plot of the three principal components presented in Fig. 4.28, the loadings plot for PC1 and PC2 shows the distribution of all the physico-chemical parameters in the upper right and lower right quadrants of the PCA score plot of the analyzed water samples (Fig. 4.28a), while PC2 and PC3 (Fig. 4.28b) revealed pH, HCO_3, K^+ and Na^+ as the most active variables in the upper quadrants. In the correlative circle the vector lengths (lines joining the variables) represents the contribution of the variables to the samples in the investigated PCA dimension (Ravikumar and Somasheka, 2017).

The horizontal axis (E-W trend) is the first PCA dimension and represents 63.8% of the initial information, while the vertical axis is the second PCA dimension representing 15.4% of the data while the red vectors represents the investigated variables. The angular relationship between these variables or lines is significant as it indicates the correlation between the variables. Narrow angles signifies the strength and reciprocal association between variables, by implication proximity between two lines or variables is an indication of positive correlation according to Qu and Kelderman, 2001. In the present study, the parameters (EC, TDS, Cl^-, NO_3^-, SO_4^{2-}, Ca^{2+}, Mg^{2+} and Total Hardness) in the loadings plot reflects their significant mutual positive correlation. Variables at right

angles as exemplified by K^+ and HCO_3^- are unrelated, while those variables that form an obtuse angle have negative relations (K^+ and pH).

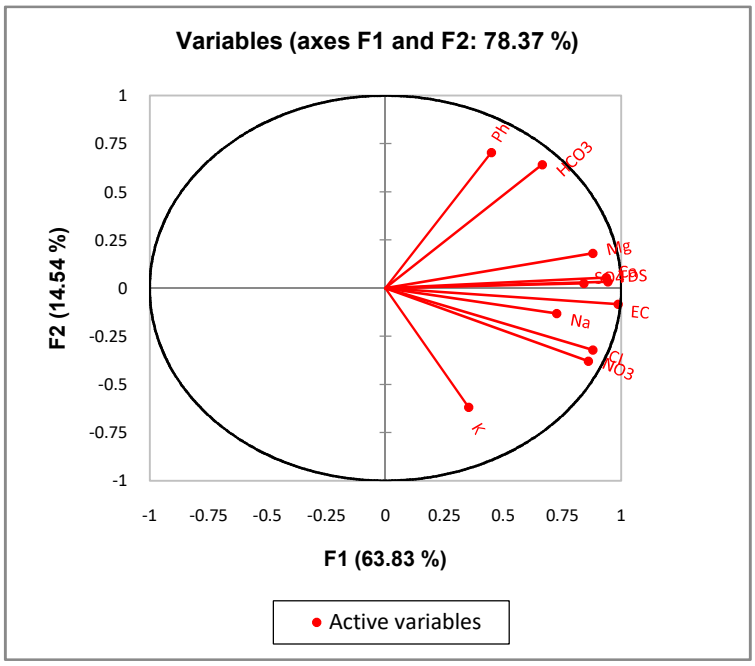

(a)

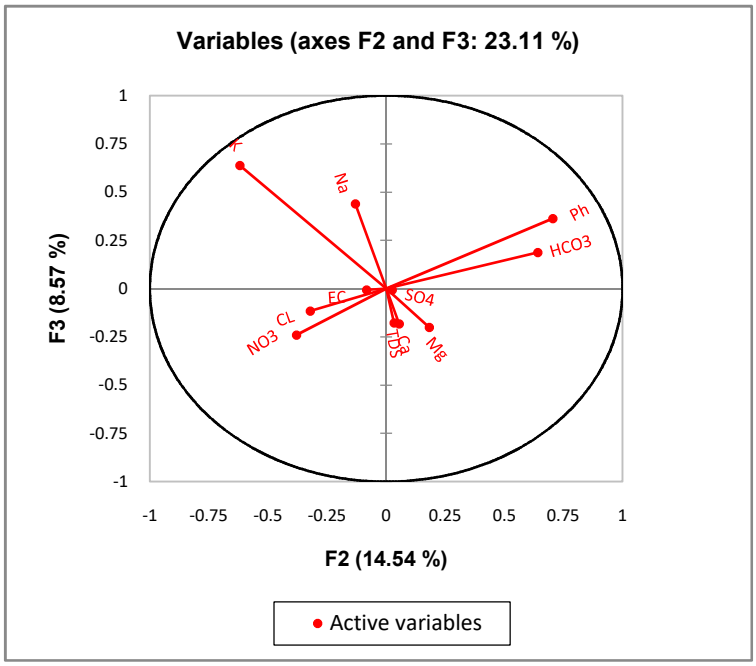

(b)

Fig. 4.28. Active variables plot showing the distribution of the direction of the various variables **(**a).Variables (axes F1 and F2: 78.37 %), (b).Variables (axes F2 and F3: 23.11 %)

The PCA score plots (Fig. 4.29) portray how the characteristics of the groundwater are related to the variables (the physico-chemical parameters) and also revealed the spatial distribution of the samples relative to the variables. Based on 4.41, it would be observed that the samples are disproportionately distributed in all the four quadrants. The variables associated with PC1 dimension in upper quadrants are Mg^{2+}, TDS, T.H, SO_4^{2-} , Ca^{2+}, and T.H, while pH, HCO_3^- are in the PC2 dimension. Consequently, the samples in the first quadrant (upper right) would be more concentrated with the aforementioned parameters, while the samples on the 4th quadrant (upper left) would show low doses of Mg^{2+}, SO_4^{2-} and Ca^{2+}, TDS, and T.H. Samples in 2nd quadrant (lower right), which is related to EC, Na^+,Cl^-,NO3$^-$ and K^- would have high concentration of EC, Na^+,Cl^-,NO_3^- and K^- but the 3rd quadrant would have lesser amounts of the same parameters.

Based on the above premise, the samples in the right quadrants are highly mineralized and belong largely to the migmatite, biotite hornblende granite and bauchite aquifers (92%), owing to their high amounts of unstable silicate minerals as compared to the sedimentary areas. Conversely, the left quadrants which constitute (72%) of sedimentary aquifers are generally poorly mineralized. However, it is important to note that while some pockets of the basement aquifers fall under the poorly mineralized water (locations 7,18,23,24,27,29,68,73, 75 and76), some fractions of the sandstone aquifers especially those that fall at the transitional zones (locations 6, 33 and 84) displayed high level of mineralization suggesting possible influence from the basement rocks.

The overall interpretation of the PCA analysis suggests that the physico-chemical parameters controlling the mineralization of the basement aquifers in the Bauchi-Alkaleri-Kirfi area are Mg^{2+}, TDS, T.H, SO_4^{2-} Ca^{2+}, pH, and HCO_3^- and this reflects mineral dissolution (mostly silicate weathering). In contrasts, the sandstone aquifers are defined partly by EC, Na^+, Cl^-, NO_3^- and K, which is an indication of possible cation exchange and some influence of anthropogenic factors.

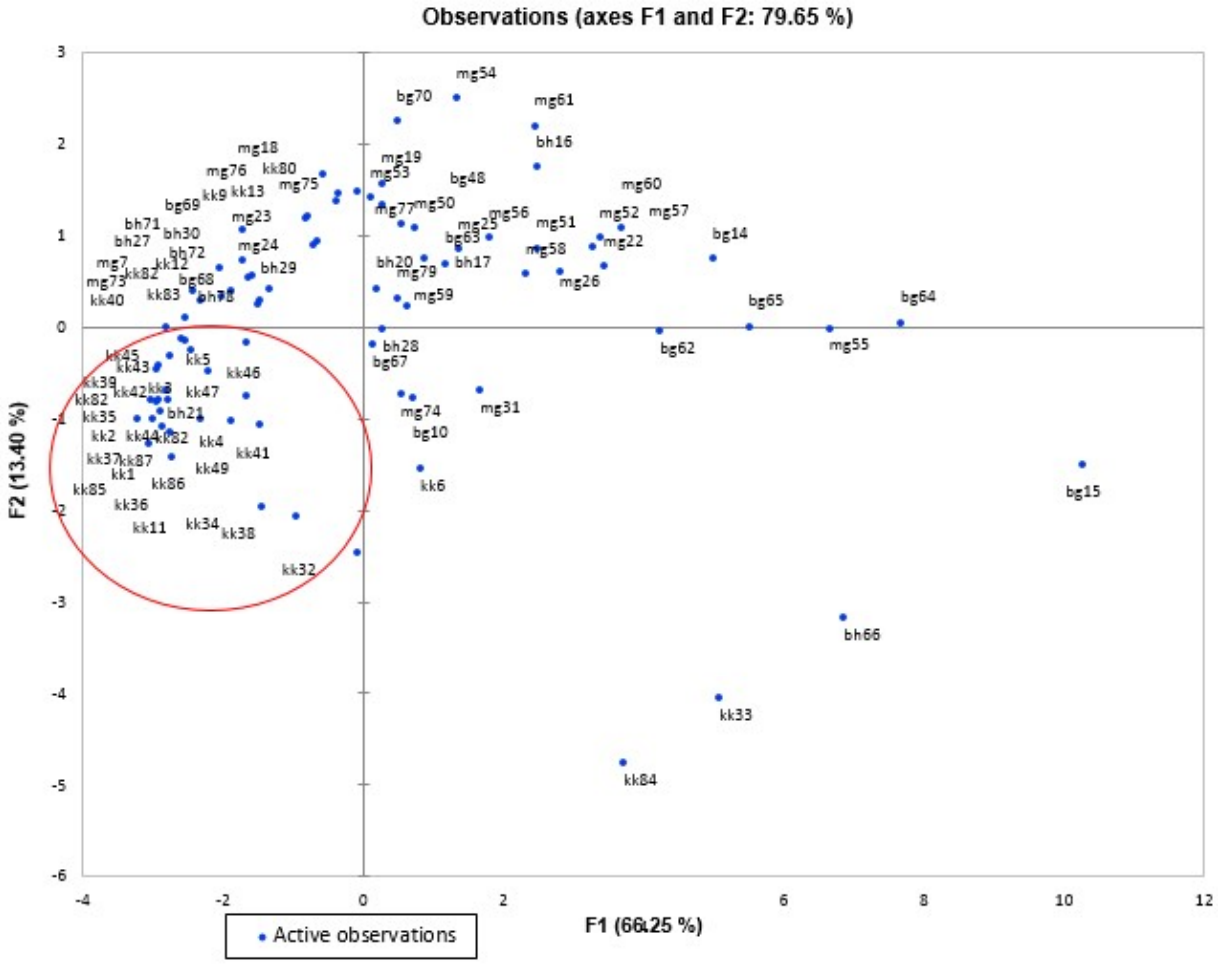

Fig. 4.29. Scree plot showing the distribution of the samples relative to the various PCA's

In conclusion, the assessment of the PCA resulted in three principal components of which, PC1, PC2 and PC3 accounted for 63.8% and 15.4% & 8.57 % of total variance, respectively, and are mainly the determining factors of the hydrochemistry of the groundwater in the research location. It also revealed the likely mechanism controlling the hydrochemistry of the aquifers is silicate weathering by CO_2 charged precipitation. The influence of the dissolved species in groundwater in determining the water quality for various utility purposes like human consumption and agricultural purposes would be considered in the following sections.

4.6.7 Drinking Water Quality Index (WQI)

The quality of water defines water's physical, chemical and biological qualities in terms for a specific purpose. Water quality can also be perceived as a property that determines whether water is contaminated or polluted. The primary basis for water quality characterisation is to ascertain that the water is physically, chemically and biologically suitable for the intended use i.e. for drinking, domestic, agricultural and also safe for human contact and for health of the ecosystem. In the present study however, the drinking water quality index of groundwater was computed based on ten physico-chemical parameters and there WHO drinking water standards using an equation developed by Krishna *et al*., 2015. The results of the calculated drinking water quality indices for different bedrocks are presented in Table 4.14. The WQI of groundwater from the sandstone setting ranged between 2-114 with an average of 24.1 while in the basement setting the WQI ranges between 8 and 115 and averages 58.25. However, four (4) groundwater samples from the sedimentary setting and 6 groundwater samples from the basement bedrocks revealed anomalously high WQI values of between 140-370 and 182-374 respectively, attributable to contamination from nitrates, chlorides and sulphates arising from human sewage (as suggested by the prevalence of open defecation in the study area), salts from fertilizers' and other pesticide utilized by farmers and leachates from dumpsites in these areas. In line with WQI ratings developed by Mapoma *et al*., 2017 (Table 4.15), the sedimentary bedrocks generally have very good drinking WQI (i.e. < 25) as compared to the Basement Complex bedrocks which generally revealed poor WQI (i.e. 55-70).

Table 4.14. WQI of Water Samples from the Bauchi-Alkaleri-Kirfi area

S/No	Locality	WQI	Quality
KK1	Maccido	27	Good
KK2	Sangar	8	very good
KK3	Shafan Banu	29	Good
KK4	Bakin Kogi	67	Poor
KK5	Rapawa	142	Unsuitable
KK6	Alkaleri Town	74	Unsuitable
KK7	Kufa	10	very good
KK8	Tumuru	6	very good
KK9	Tarangadi Fulani	14	very good
KK10	Sabon gari	99	Poor
KK11	Mararaban Pali	5	very good
KK12	Arawa (Mainari)	6	very good
KK13	Kaloma	19	very good
KK14	Jagalwa	6	very good
KK15	Badawere	20	very good
KK16	Badara	37	Good
KK17	Bedoji	13	very good
KK18	Zamani	14	very good
KK19	Taure	13	very good
KK20	Wanka	10	very good
KK21	Kafin Maigari	17	very good
KK22	Guyaba (Upstream)	7	very good
KK23	Doka	40	Moderate
KK24	Kungibar	51	Moderate
KK25	Unguwar wake	21	very good
KK26	Farin Ruwa	18	very good
KK27	Minza	28	Good
KK28	Woso	22	very good
KK29	Guyaba (Downstream)	195	Unsuitable
KK30	Kucha	13	very good
KK31	Tumburwo	2	very good
KK32	Gumnalwo	14	very good
KK33	Gar	43	Good
KK34	Gwaram Mosq	114	Unsuitable
KK35	Gwaram Town	307	Unsuitable
KK36	Sabuwar Gwaram	29	Good
MG1	Kyawun Gani	8	very good
MG2	Kenda	32	Good

MG3	Kyabi	52	Moderate

MG4	Lariyel	133	Unsuitable
MG5	Jama (Bartak Pali)	32	Good
MG6	Yola Doka	41	Moderate
MG7	Yuguda	81	unsuitable
MG8	Zan Filani	130	unsuitable
MG9	Shafan Fulani	117	unsuitable
MG10	Gilliri	67	Poor
MG11	Alkama	115	unsuitable
MG12	Beru	115	unsuitable
MG13	Jinkiri	41	moderate
MG14	Gambiri	43	moderate
MG15	Habli	239	unsuitable
MG16	Takalafiya	87	unsuitable
MG17	Garwali	120	unsuitable
MG18	Mangawa	123	unsuitable
MG19	Jalia	78	unsuitable
MG20	Rugan Badembo	138	unsuitable
MG21	Gulawa	81	unsuitable
MG22	Katallen Badaromo	10	very good
MG23	Badaromo Town	77	unsuitable
MG24	Dargome	30	Good
MG25	Kanawa	37	Good
MG26	Nahuta	55	Moderate
MG27	Shafan Dambo	65	Poor
BG1	Kaciciya	124	Unsuitable
BG2	Buda	188	Unsuitable
BG3	Gokaru	374	Unsuitable
BG4	Bagali	50	Moderate
BG5	Minjila	182	unsuitable
BG6	Bidolo	62	Poor
BG7	Balanshi	228	unsuitable
BG8	Minjin	205	unsuitable
BG9	Birshi Central Mosque	68	Poor
BG10	Birshi Village	31	Good
BG11	Yardin Birshi	15	very good
BG12	Siri	39	Good
BH1	Rugan Kela	78	unsuitable
BH2	Guma	83	unsuitable
BH3	Shafa	71	unsuitable
BH4	Pau	51	moderate
BH5	Dadin Kowa	16	very good
BH6	Dindima	61	Poor
BH7	Kwagal Pri School	20	very good
BH8	Kujamba	22	very good
BH9	Yole	289	unsuitable
BH10	Barnawa	37	Good
BH11	Kwanan Dutse	29	Good
BH12	Turiya	26	Good

Table 4.15 WQI ratings distribution in the study (After: Mapoma *et al.,* 2017)

Water Quality	Range	% of samples
Very Good	WQI < 25	31.03%
Good	25 >WQI < 40	17.24%
Moderate	40 >WQI < 55	10.34%
Poor	55 > WQI < 70	8.05%
Unsuitable	WQI > 70	33.33%

The evaluation of groundwater quality is usually based on physico-chemical parameters which includes temperature, pH, and total dissolved solid (TDS), alkalinity and electrical conductivity (EC). It is on this basis that WQI weightings for TDS and EC were rated

higher (4&5 respectively). Groundwater with very high amounts of EC (>1500mS/cm) and TDS (>500mg/l) as exemplified by parts of the basement groundwaters are likely constitute poor to unsuitable WQI. The values of TDS are comparatively higher (TDS of 512.43 mg/) in the shallow wells which dominate the Basement Complex zones and thus partly responsible for the generally poor drinking water quality conditions observed in the basement setting.

Conversely, in the sedimentary zones, the wells are naturally deeper with low TDS (206 mg/l), hence better WQI ratings. The second step in groundwater quality assessment is the evaluation of the chemical species in water (Anions and Cations) which has been captured by the WQI analysis. Nitrates, sulphates and chlorides were given higher ratings because this anions have higher impact on drinking water quality (Sahu and Sikdar 2008; Mapoma *et al*., 2017). While nitrates are mostly from anthropogenic sources, sulphates and chlorides are derived from both geogenic and anthropogenic processes. Generally, groundwaters with higher amounts of the aforementioned anions as typified by parts of Basement Complex groundwaters, are mostly categorized as poor to unsuitable (55> WQI < 70). Having considered the water quality in the sedimentary and Basement Complex zones of the Bauchi-Alkaleri-Kirfi area, an analysis of WQI based on different bedrock settings is presented in the next paragraph.

The percentages of poor and unsuitable waters in this study as captured in Fig 4.30, is 19.4% in the sandstone setting as compared to 66.7% in the biotite hornblende granite setting, 59.3% in the migmatite setting and 41.7% in the bauchite setting as revealed by their high WQI values (WQI = 55 - >70). Conversely, 27 out of 36 samples from the sandstone aquifers fall under the good and very good (25 > WQI < 40), as compared to 6 out of 12 samples in the bauchite setting and 3 out of 12 in the biotite hornblende granite setting. However in the migmatite bedrocks only 6 out of 27 samples were within good to very good category (Fig. 4.30).

(a)

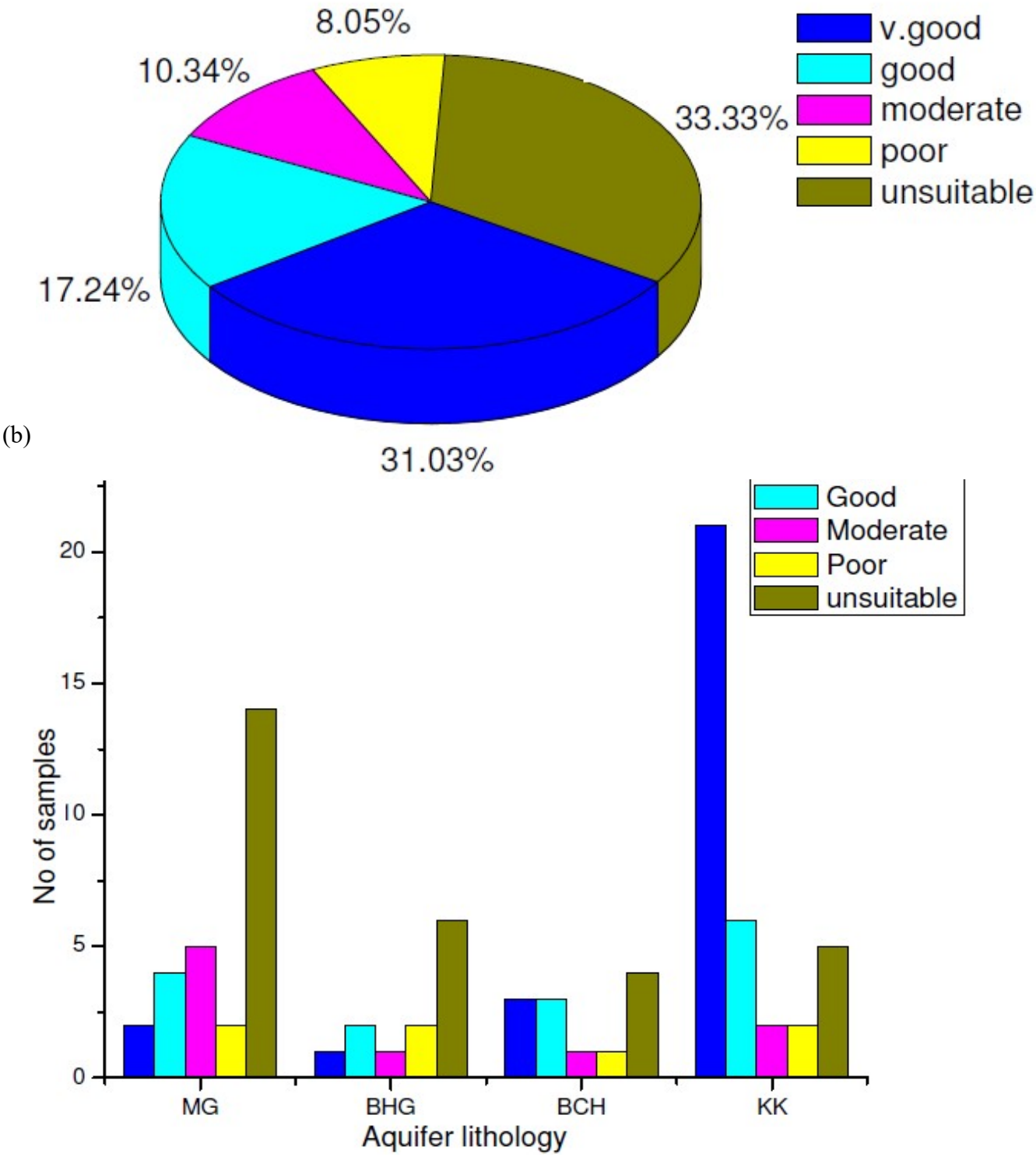

Fig. 4.30. (a) Distribution of Drinking WQI in the Bauchi-Alkaleri-Kirfi area, (b) Histogram showing the lithology based summary of WQI.

The quality of groundwater in the area as revealed by the WQI could also have been affected by the depth of the wells as well as inadequate well protection and sanitation in the vicinity of the wells as can be seen from Fig. 4.31. As shown in the figure the wells in Kerri- Kerri settings with depths of between 15-114m generally revealed good and very

good (25 >WQI < 40) ratings while the basement settings which are dominated by shallow wells with depths between 3-20m are characterized by predominantly poor WQI (55 >WQI >70). The above scenario can be attributed to contamination of the shallow basement wells by nitrates derived from human sewage, chlorides and sulphates, from fertilizers and other dissolved chemicals form open dumpsites. This contaminants easily find their way into shallow dug wells (characteristic of the basement setting) where well heads are predominantly uncovered and unprotected. As can be observed from the plot (Fig. 4.31) a some samples (13 in number) from the biotite hornblende granite and migmatite settings revealed exceptionally unsuitable WQI (>100), which can be attributed to the positioning of the wells close to latrines, dumpsites and farmlands where the effects of fertilizers and open defecation are particularly high. By and large, the influence of anthropogenic factors on the groundwater have shown to decline with increasing well depth owing to the fact that the longer times required for the dissolved nitrates to travel from the surface to the well, allows for attenuation or denitrification of the nitrates before the contaminate the wells. By implication deeper wells which are mostly the sedimentary wells are less susceptible to surface contamination than the shallower wells which dominate the basement areas (Fig. 4.31). However, there are some exceptions where unsuitable water type occur in the very deep wells (KK5, KK6, KK29 and KK35). This is attributable to evaporite dissolution in the deeper parts of the sedimentary rocks possibly from the lacustrine units of the sandstone aquifers, inadequate well head protection from unhygienic human activities and poor sanitary condition around the wells. From the spatial distribution map of the WQI of the research area, presented in Fig. 4.32, it is evident that the sandstone aquifers have the best drinking WQI, followed by the bauchite, migmatite and biotite hornblende granite settings respectively. In conclusion, the WQI result indicated that 33.3% of the entire samples are unsuitable for drinking (WQI > 70), while 31% belongs to the very good category (WQI < 25). 17.1% are classified as good (WQI >25< 40) and 10.3% and 8.1% fall under moderate (WQI > 40< 55) and poor water quality (WQI > 55< 70) respectively.

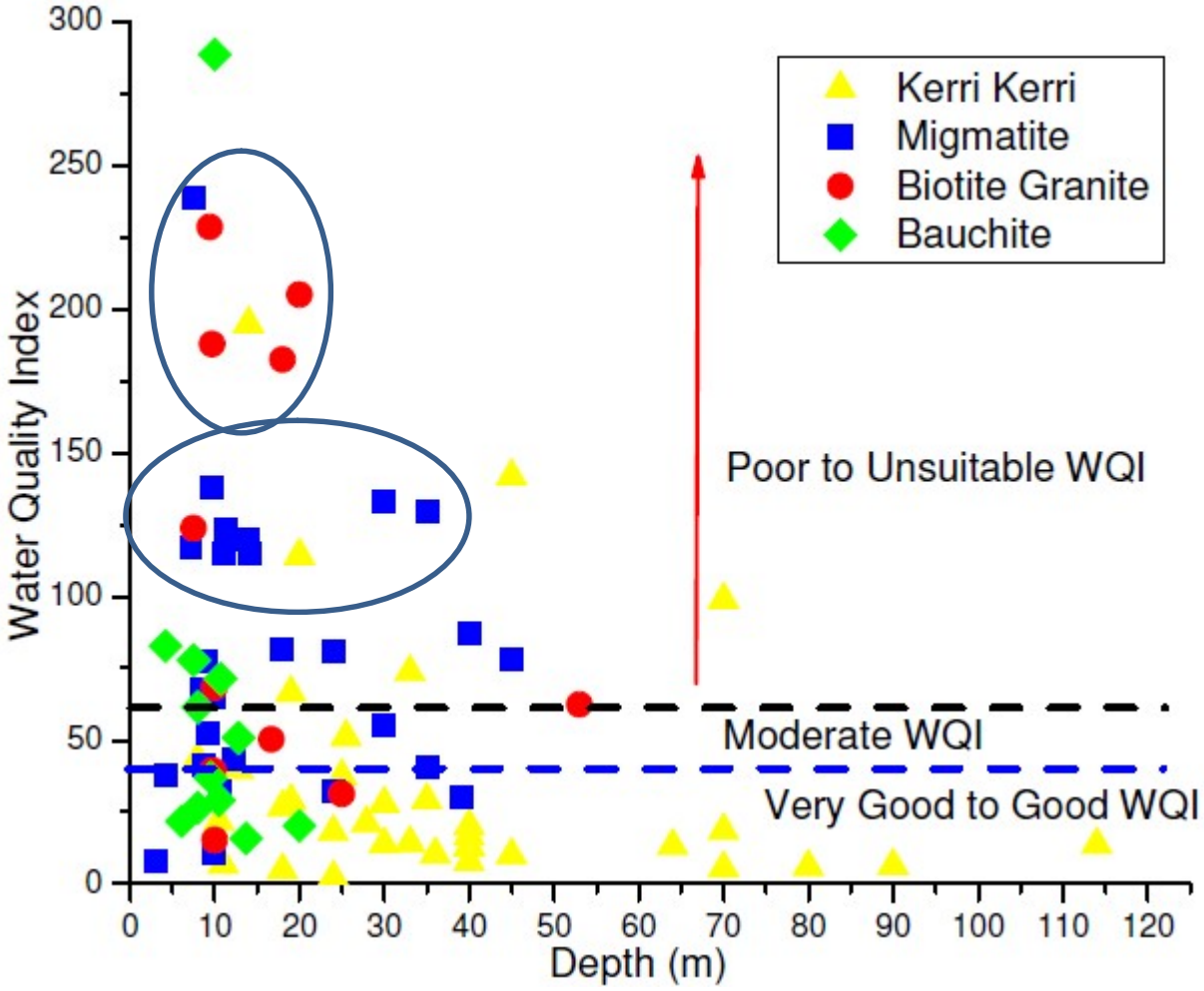

Fig. 4.31. Bivariate of WQI with Well Depth in the Bauchi-Alkaleri-Kirfi area

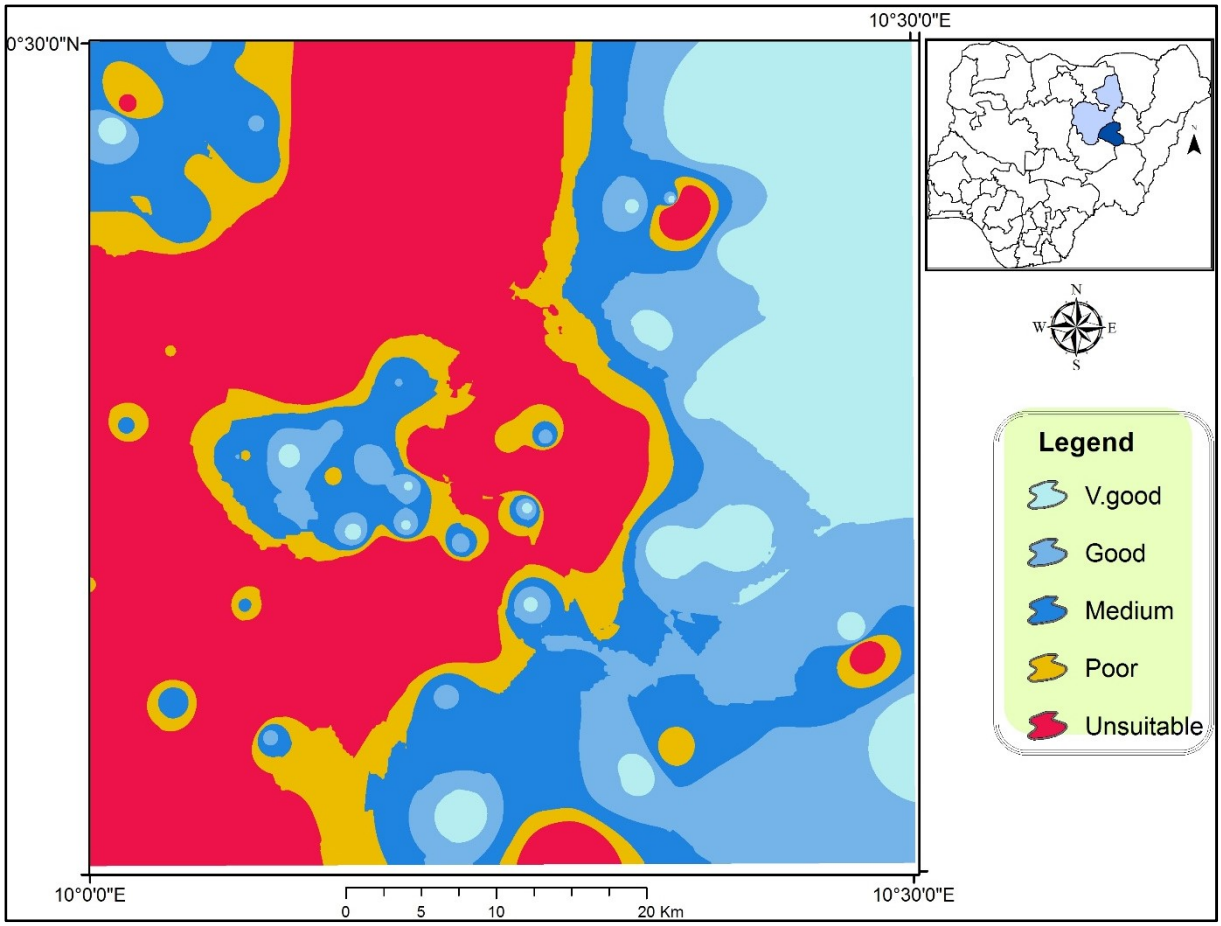

Fig. 4.32. Spatial Distribution Map of WQI in the Bauchi-Alkaleri-Kirfi area.

In addition, the WQI appears to be largely controlled by anthropogenic factors relating to human sewage and agro-pastoral activities. Consequently, the groundwater from the sedimentary settings are adjudged to be of best quality on the basis of the drinking WQI as compared to the basement bedrocks which are mostly of lower quality. This conclusion is in agreement with the works of Sahu and Sikdar 2008 and Mapoma *et al*., 2017, who studied the hydrochemistry and quality of groundwater in similar aquifer settings in India and Malawi respectively. The irrigation indices of the groundwater samples from the aquifers under study are elucidated in the next section.

4.6.8 Water Quality for Irrigation Purposes.

The quality of water utilized for irrigation/agricultural purposes is consequential as it has a detrimental effect on the overall crop yield and soil productivity (Ali and Ali, 2018). The efficacy of water for irrigation is mainly governed by the TDS (salinity) and the ratio Na to Ca and Mg in the water (Alagbe, 2006). The importance of water quality in agricultural purposes cannot be underestimated as the use of low quality water can create undesirable effects such as infiltration /permeability problems, toxicity, salinity and others (Ayers and Westcot, 1985). In this study, the indicators of irrigation quality were assessed using the following parameters: salinity hazard, sodium absorption ratio (SAR), residual sodium carbonate (RSC), soluble sodium percentage (SSP), permeability index (PI), Kelly ratio (KR) and magnesium hazard (MH). A summary of the irrigation quality parameters of the study area is presented in Table 4.16 and discussed in the following section.

4.6.8.1 Salinity hazard

The most crucial water quality parameter as far as crop performance is concerned is the water salinity hazard which is a measure of the electrical conductivity (EC) of the water. Physiological drought is the main impact of elevated concentration of salts in water on plants (Ali and Ali, 2018). In the Bauchi-Alkaleri-Kirfi area, salinity values ranged from 10 to 2040 µs/cm and averages 519.8 µs/cm. Richards (1954) classified EC of < 250 µs/cm as good and EC > 750 µs/cm as poor for agricultural purposes.

Table 4.16. A summary of the descriptive statistics of the irrigation quality parameters of the Bauchi-Alkaleri-Kirfi area

Indices	Mean	S.D	Minimum	Median	Maximum
Salinity	519.77	416.63	10.00	430	2040.00
SAR	1.19	1.09	0.09	0.96	8.55
RSC	-1.04	2.38	-11.73	-0.02	2.97
SSP	37.49	22.09	3.93	35.06	99.06
PI	75.01	81.28	8.62	48.78	473.95
KR	2.46	11.61	0.04	0.54	104.96
MH	39.97	13.99	3.61	41.60	69.06

.

Wilcox, 1955, further classified the salinity values into low (C1) when EC is ≤ 250 µs/cm, medium (C2) with EC is between 250-750 µs/cm, high (C3) with EC is between 750-2250 µs/cm and very high (C4) when EC is > 2250 µs/cm. Based on the aforementioned salinity classification (Richards, 1954 and Wilcox, 1955) 28 groundwater samples (36.4%) fall within excellent or low salinity hazard category (C1), 38 samples equivalent to 49.4 % fall under the good or medium salinity hazard (C2), while 21 samples (27.3%) are in the high fair to medium or high categories (C3). No samples was recorded under the C4 category. While the good samples are the best for irrigation use, samples withmoderate salinity may be utillised if there is a modest level of leaching. However, high salinity groundwaters are restricted to well drain soils. According to Tijani, 1994, EC values > 3000 µs/cm may cause growth retardation in crops while EC values < 700 µs/cm would cause limited or no harm to most crops. Furthermore, the EC of water affects transpiration in plants because the greater the EC, the lesser the quantity of beneficial water available to plants. Also, high levels of EC (i.e. 750 - >2250 µs/cm) in irrigation water reduce the osmotic activity in the roots of plant thereby impacting the salt absorption capacity of the plants (Ali and Ali, 2018). Based on the above premise the sedimentary aquifers dominates the excellent to good (i.e. low-medium) category with 91.7%, followed by the bauchite aquifers with 83.3% as compared to 59.3 and 58.3 in migmatite and biotite hornblende granites respectively. The variation in salinity hazard within the different bedrock setting is attributable to weathering of rocks/ dissolution of silicate minerals and anthropogenic activities prevailing in the different regions.

4.6.8.2 Sodium absorption ratio (SAR) or Sodium hazard

High sodium concentration in irrigation water impacts soil's physical characteristics. High SAR is known to reduce soil permeability (Tijani, 1994). This index which is synonymous to sodium hazard measures the amount of sodium in the water relative to calcium and magnesium ions (Alagbe, 2006). As revealed in Table 4.16, the values of SAR in this study ranged from 0.09 to 8.55 with an average value of 1.19.

As can be seen from the Wilcox diagram (Fig. 4.33) the Kerri-Kerri groundwaters mostly fell within C1S1 (low salinity with low sodium) and C2S1 (medium salinity with low sodium) which means that some of the samples (C1S1 type) can be used on all kinds of soils for irrigation, however, samples of medium salinity hazard (C2S1) may be used where minimal leaching occurs and where proper drainage exist. Conversely, the migmatite and biotite hornblende granite bedrocks in the basement zones occupied the fields C2S1 (medium salinity, low sodium) and C3S1 (high salinity, low sodium) of the plot, implying that the groundwater can only be utilized for irrigation purpose where minimal leaching occurs and where proper drainage exist, considering that groundwater of elevated salinity cannot be applied to soil with limited drainage. This assertion is in agreement with the studies by Gnanachandrasamy *et al.,* 2014 and Ali and Ali, 2018. The bauchite bedrocks however, mostly plotted within the C2S1 (medium salinity, low sodium), suggesting that these irrigation waters can be applied if there is mild leaching. Sodium weakens the soil mechanical characteristics, decreasing the interconnectivity of the pore spaces within the soil and reduced water infiltration (Richards 1954; Srinivasamoorthy *et al*., 2009).

By and large, with respect to salinity and sodium hazard, most of the Kerri groundwater revealed predominantly C1S1 (low salinity with low sodium) and C2S1 (medium salinity with low sodium) while the bauchite settings mostly C2S1 (medium salinity with low sodium) and may be applied to soils with moderate leaching. The migmatite and biotite hornblende bedrocks however, revealed medium (C2S1) to high (C3S1) salinity water which can only be utilized for irrigation purposes on well drained soils with moderate leaching potential.

Based on the summary of the salinity and sodium hazard presented in Table 4.17a and 4.17b respectively, the salinity hazards are generally higher in the basement setting (salinity of >500 mg/l) owing to higher degree of mineralization as compared to the sedimentary groundwater with generally lower salinity hazards (< 500) which further confirms the short history of the groundwater migration in the Kerri-Kerri bedrocks. The sodium hazard in this study however, fall within the acceptable limits of 0-10 (low).

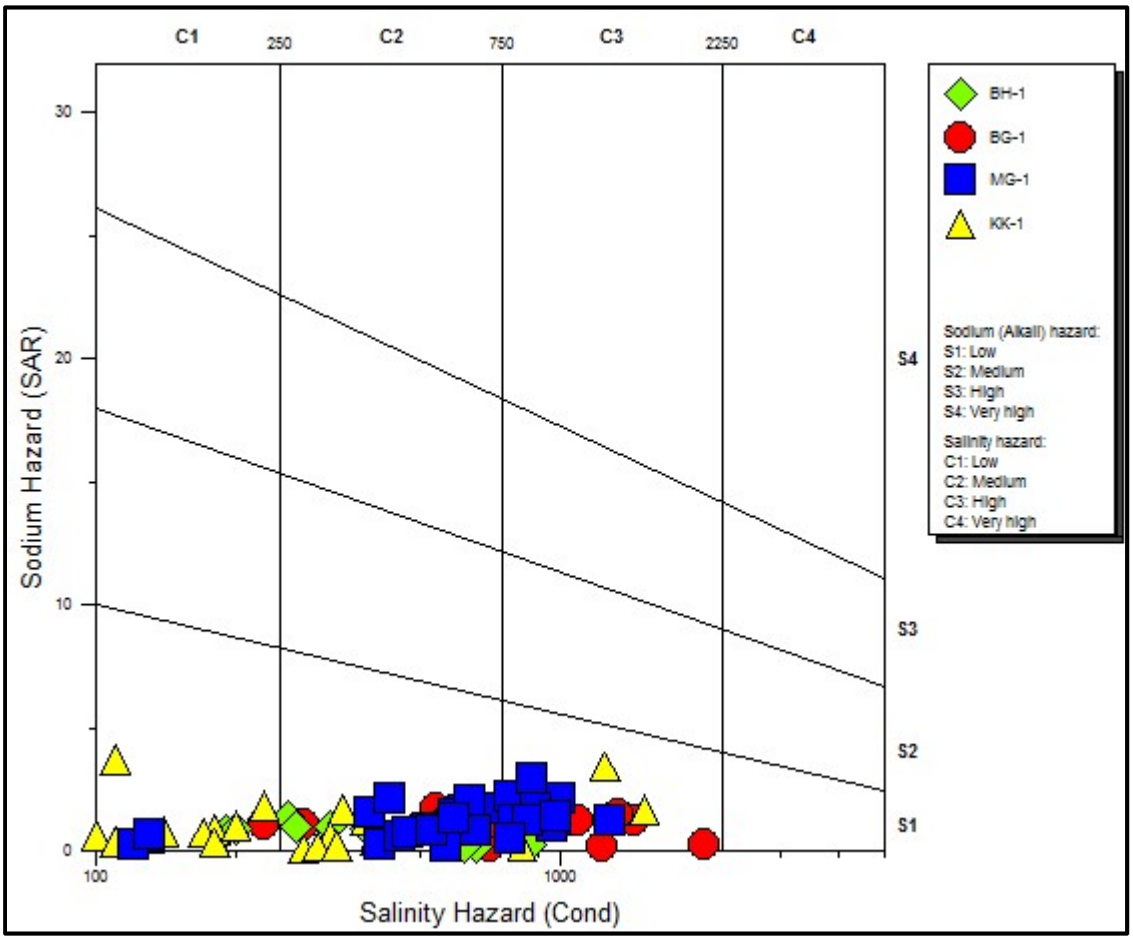

Fig. 4.33. The Wilcox diagram for groundwater samples in the Bauchi-Alkaleri-Kirfi area (After Wilcox, 1955)

Table 4.17 (a) Classification of Salinity Hazard for Aquifers in the Bauchi-Alkaleri-Kirfi area (after Richards, 1954 and Wilcox, 1956), (b) Classification of Sodium Hazard for Aquifers in the Bauchi-Alkaleri-Kirfi area (after Richards, 1954 and Wilcox, 1956)

(a)

	low (C1)	**Medium (C2)**	**High (C3)**	**Very High (C4)**
Rock type	Samples	samples	samples	Samples
Migmatite	2	14	11	0
Biotite hornblende	1	6	5	0
Bauchite	2	8	2	0
Sandstone	23	10	3	0
Total	28	38	21	0
Percentage	36.4	49.4	27.3	0.0

(b)

	Excellent (S1)	**Good (S2)**	**Fair/ Moderate (S3)**	**Poor/ Bad (S4)**
Rock type	Samples	samples	samples	Samples
Migmatite	27(100%)	0	0	0
Biotite hornblende	12(100%)	0	0	0
Bauchite	12(100%)	0	0	0
Sandstone	36(100%)	0	0	0
Total	87	0	0	0
Percentage	100	0	0	0.0

4.6.8.3 Residual sodium carbonate (RSC)

A significant parameter in assessing the suitability of irrigation waters is residual sodium carbonate (RSC). High amounts of carbonate and bicarbonate in water, particularly when their level in groundwater exceeds that of calcium and magnesium, reduce irrigation quality and it is also detrimental to plants (Eaton 1950; Richards 1954). As revealed in Table 4.18, the values of RSC in this study ranged from -11.7 to 2.97 meq/l with an average value of -1.04 meq/l.

In line with Richards, 1964, RSC < 1.25 meq/l, is regarded secure for agricultural purposes, RSC values between 1.25 and 2.5 meq /Lare marginal, while RSC values greater than 2.5 meq / L indicates unfit water. Based on the above classification scheme of groundwater according to the RSC values, 94.3% of the water samples in the studied samples are safe category, 5.7% of the samples are marginal and none is unsuitable for agricultural purposes. It would be observed that the RSC values within the good category for the aquifers under study are 92.6%, 83.3%, 100% and 97.2% for the migmatite, biotite hornblende granite, bauchite and the sandstone aquifers respectively (Table 4.18). The generally low amounts of RSC (<1.25 mg/l) observed in this study can be ascribed to the absence of carbonates in the studied groundwater as revealed the pH levels in 5-8.5 which is mostly conducive for bicarbonates dissolution. High RSC in water leads to high pH, which leads to loss of soil fertility due to the precipitation/ deposition of sodium carbonate in the irrigated soil (Ali and Ali, 2018).

In a summary, with respect to RSC virtually all the groundwater in the Bauchi-Alkaleri-Kirfi area are considered excellent for irrigation, with exception of locations 13 (Minza), 18 (Kenda), 69 (Yardin birshi), 70 (Siri) and 75 (Dargome), which revealed marginal RSC values suggesting slightly higher concentration of bicarbonates or low concentration of alkali earths in the groundwater as revealed by above locations which all fell within the basement setting. The RSC ratings further confirms the SAR values which also suggested that the groundwaters in Bauchi-Alkaleri-Kirfi areas are generally suitable for irrigation.

	Good (RSC ≤ 1.25)		Marginal (RSC 1.25-2.5)		Poor (RSC>2.5)
Rock type	Samples	%	samples	%	samples
Migmatite	25	92.6	2	7.4	0
Biotite hornblende	10	83.3	2	16.7	0
Bauchite	12	100.0	0	0.0	0
Sandstone	35	97.2	1	2.8	0
Total	82		5		0
Percentage	94.3		5.7		

Table 4.18. Classification of Residual Sodium Carbonate for the Aquifers in the Study Area (After Richards, 1954)

4.6.8.4 Soluble sodium percentage (SSP)

The soluble sodium percentage (SSP) also known as % Na is a measure of the dissolved sodium content of the water and an indication of Na hazard in water In base-exchange processes, calcium ions are substituted by sodium ions which reacts with the soil to reduce its permeability (Wilcox 1955). As revealed in Table 4.16, the values of SSP in this study ranged from 3.93 to 99.06 with an average value of 37.49. As presented in Table 4.19, the SSP values of the basement setting are generally better than those of the sedimentary setting. From the table, 100 % of biotite hornblende aquifers samples showed good SSP values (<50), migmatite and bauchite aquifers revealed 92.6 and 83.3% respectively while the sandstone samples have the lowest percentage of 55.6%. The implication is that close to 50% of the Kerri-Kerri aquifers are deemed to be of bad quality as far as SSP is concerned and this is expected because the dominant mechanism responsible for the dissolved species in the Kerri-Kerri aquifers as pointed out in the earlier sections is the cation exchange process which tends to increase the concentration of sodium in the groundwater. In conclusion, the basement bedrocks revealed good SSP values (<50) and hence suggests excellent irrigation water quality and this shows a good correlation However, the Kerri-Kerri aquifers have a greater percentage (>40%) of unsuitable irrigation waters and this can be ascribed to cation exchange process which is more prevalent in the sedimentary settings.

4.6.8.5 Permeability index (PI)

Doneen created the Permeability Index in 1964 to assess the impact on soil permeability of long-term use of irrigation water. PI is used to evaluate the likely impact of water quality on soil physical properties (Doneen, 1966). Factors such as total dissolved solids, sodium bicarbonate and soil type determine the permeability of soil. As revealed in Table 4.16, the values of PI in this study ranged from 8.62 to 473.95 with an average value of 75.01. For irrigation, values of PI > 75 suggests excellent quality whereas values ranging from 25 and 75, typifies good quality.

Table. 4.19. Classification of Soluble Sodium Percentage for Aquifers in the Bauchi-Alkaleri-Kirfi area (After USDA, 1954).

	Good(SSP<50)		**Poor (SSP>50)**	
Rock type	Samples	%	samples	%
Migmatite	25	92.6	2	7.4
Biotite hornblende	12	100.0	0	0.0
Bauchite	10	83.3	2	16.7
Sandstone	20	55.6	16	44.4
Total	67		20	
Percentage	77.0		23.0	

However, PI values less than 25, reflect unsuitable nature of water for irrigation. As presented in Table 4.20a, the groundwater from Bauchi-Alkaleri-Kirfi area can be considered as excellent to good because 73.4% of the groundwater samples fall within this range, while 26.6% of the samples are unsuitable for irrigation purposes. 66.7% of the migmatite samples (18 samples) rated as good to excellent, 50% of the biotite hornblende aquifers (6),83% of the bauchite aquifers (10 samples) and 83% of the sandstone aquifers (30 samples) displayed good to excellent quality. The migmatite and the biotite hornblende granites recorded the highest percentages of unsuitable samples, 33.3% and 50% respectively and this is attributable to the generally high levels of Ca^{2+} and Mg^{2+} (81mg/l Ca^{2+} and 26mg/l Mg^{2+}) in there groundwater samples which also corroborates the hardness in both bedrock settings (227-311 mg/l) and this also confirming the silicate weathering origin suggested in the earlier sections.

4.6.8.6 Kelly ratio (KR)

Kelley's ratio is the ratio of Na ions to Ca and Mg ions expressed in meq/l. As revealed in Table 4.20 (b), the values of KR in this study ranged from 0.04 to 104.96 with an average value of 75.01. According to Kelly, 1951 and Karanath, 1987, Kelly's ratio of ≤ 1 is considered to be good for irrigation whereas KR >1 is unfit for irrigation owing to alkali hazards (Kelly, 1951; Karanth, 1987). As shown in Table 4.20 (b), about 79.3% of the groundwater in Bauchi-Alkaleri-Kirfi area are good for agricultural purposes, while 20.7% are not. The migmatite and the biotite hornblende groundwater samples all fall within the suitable category, followed by the bauchite groundwater with 83.3% of the samples under the suitable category. The sedimentary groundwater samples however, revealed the lowest percentage of 55.6 % (20 out of 36 samples) as suitable with respect to Kelly ratio is concerned. This indicates that, nearly all the samples from the basement bedrocks of the area are good for irrigation based on Kelly ratio, while close to half of the Kerri-Kerri samples are of unsuitable quality on the basis of Kelly ratio.

Table 4.20 (a). Classification of Permeability Index for Aquifers in the Bauchi-Alkaleri-Kirfi area (After Doneen, 1966)

	Excellent (PI>75)		**Good** (PI 25-75)		**Unsuitable** (PI<25)	
Rock type	Samples	%	samples	%	samples	%

Table 4.20 (b). Classification of Kelly ratio for Aquifers in the Bauchi-Alkaleri-Kirfi area (After USDA, 1954),

	Good (KR< 1)		**Unsuitable** (KR>1)	
Rock type	samples	%	samples	%
Migmatite	27	100.0	0	0.0
Biotite hornblende	12	100.0	0	0.0
Bauchite	10	83.3	2	16.7
Sandstone	20	55.6	16	44.4
Total	69	79.3	18	20.7

Migmatite	2	7.4	16	59.3	9	33.3
Biotite hornblende	1	8.3	5	41.7	6	50.0
Bauchite	3	25.0	7	58.3	2	16.7
Sandstone	22	61.1	8	22.2	6	16.7
Total	28	32.2	36	41.4	23	26.4

This scenario is attributable to comparatively higher levels of Na^{+} relative to Ca^{2+} and Mg^{2+} in some of the groundwaters which corroborates well with the Kerri-Kerri (sandstone) setting where cation exchange reaction is the predominant hydrochemical process. The above conclusion is in tandem with the studies by Kelly, 1951 and Karanth, 1987. The results of the Kelley ratio corroborates those of SSP obtained from the Bauchi-Alkaleri-Kirfi area as the sedimentary terrain of this study revealed the highest percentage of unsuitable irrigation water which is 44.4 % (16 out of 36 samples) for both Kelly ratio and SSP.

4.6.8.7 Magnesium hazard (MH)

Soils with high level of exchangeable magnesium ion causes infiltration problem due to the fact that excessive magnesium is detrimental to the quality of soil and reduces crop productivity (Ayers and Westcot, 1985). As revealed in Table 4.14, the values of MH in this study ranged from 3.61 to 69.06 with an average value of 39.97. MH < 50 is appropriate for irrigation and MH values > 50 are inappropriate (Lloyd and Heathcoat, 1985). Also, as presented in Table 4.21, the groundwater from Bauchi-Alkaleri-Kirfi area can generally be regarded as suitable for agricultural purposes, as 79.3% (69 out of 87) of the samples are within the good range, while 20.7% (18 out of 87) of the samples are unsuitable for irrigation purposes.

MH also known as Magnesium adsorption ratio (MAR) (Raghunath, 1987), MH is known to have detrimental effect to soil when it value is greater than 50 (Gupta & Gupta 1987).

Table 4.21. Classification of Magnesium Hazard for Aquifers in the Bauchi-Alkaleri-Kirfi area (After Lloyd and Heathcoat, 1985)

	Good(MH≤50)		**Poor (MH>50)**	
Rock type	samples	%	samples	%
Migmatite	20	74.1	7	25.9
Biotite hornblende	11	91.7	1	8.3
Bauchite	12	100.0	0	0.0
Sandstone	26	72.2	10	27.8
Total	69		18	
Percentage	79.3		20.7	

Based on the aforementioned classification scheme, 74.17% of the migmatite samples (20 samples) rated as good, 91.7% of the biotite hornblende aquifers (11 samples), 100% of the bauchite aquifers (12 samples) and 72.2% of the sandstone aquifers (26 samples) are of good irrigation quality. By implication, over 20% of the migmatite and Kerri-Kerri aquifers are unsuitable for irrigation purpose as the have the tendency to enrich irrigated soils with magnesium overtime, as compared to 8.3% in the biotite hornblende rocks and 0% in the bauchite aquifers.

A general outlook and the spatial distribution of all the 6 irrigation indices evaluated in the Bauchi-Alkaleri-Kirfi area is shown in Fig. 4.34 and 4.35 revealed that the SAR for all the groundwater types are suitable for irrigation purposes. Meanwhile, the RSC and MH ratings are generally good for the groundwater in the Bauchi-Alkaleri-Kirfi area except for few regions of medium to poor RSC in the migmatite setting and some patches of poorly rated MH on the sandstone and migmatite settings. On the basis of KR and SSP, the basement aquifers are generally more suitable as compared to the sedimentary aquifers. However, the salinity ratings of the sedimentary aquifers are better that those of the basement rocks.

In conclusion and holistically speaking the basement setting would be best suited for irrigation or agricultural purposes. The Kerri-Kerri Formation however, are likely to be less suitable for irrigation use, owing to their high percentages of poor KR (<1) and SSP (>50) ratings owing to sodium enrichment during cation exchange reactions which is the dominant hydrochemical process in the Kerri-Kerri setting.

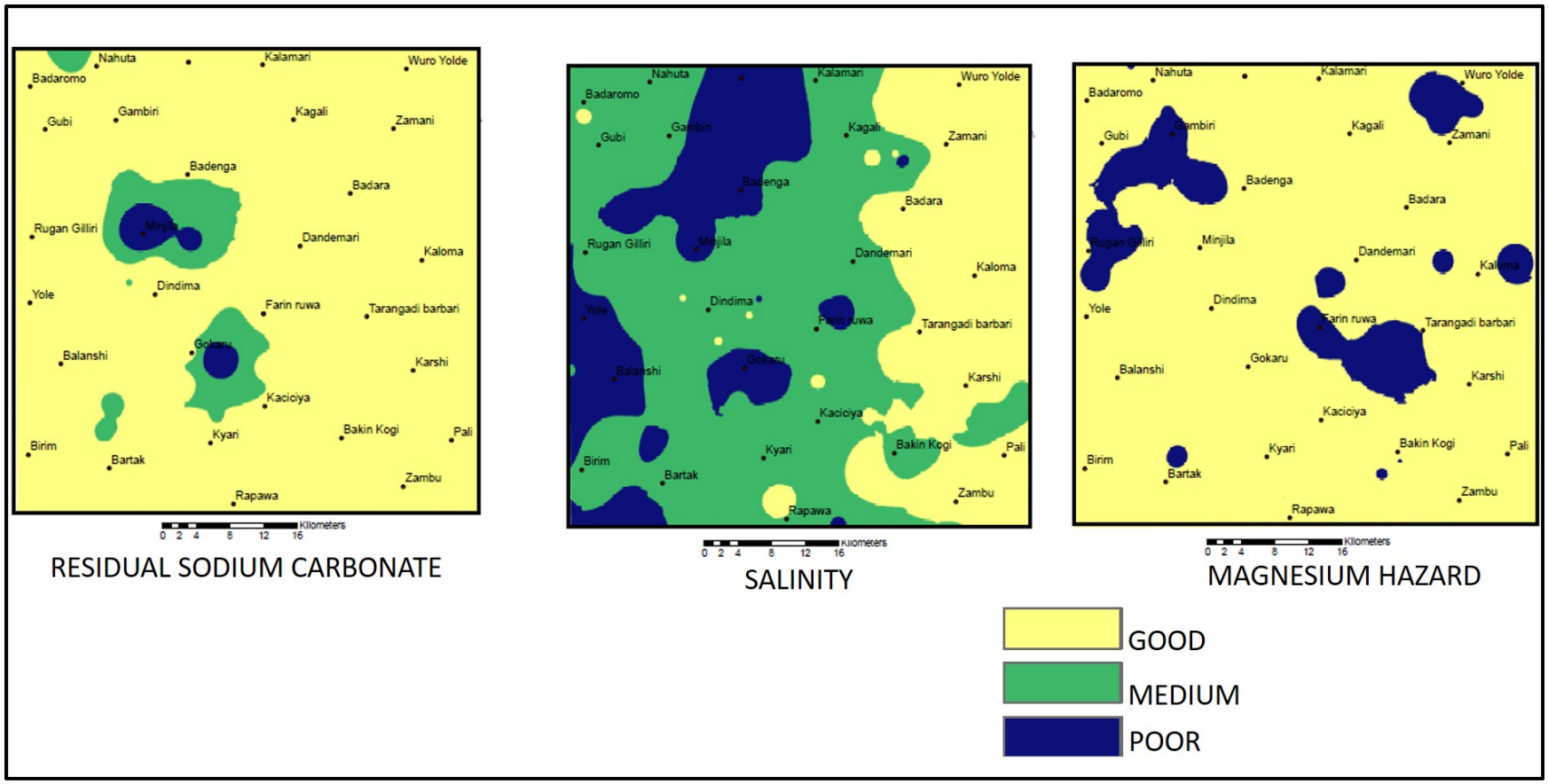

Fig. 4.34. Spatial distribution of RSC, Salinity and MH in Bauchi-Alkaleri-Kirfi area

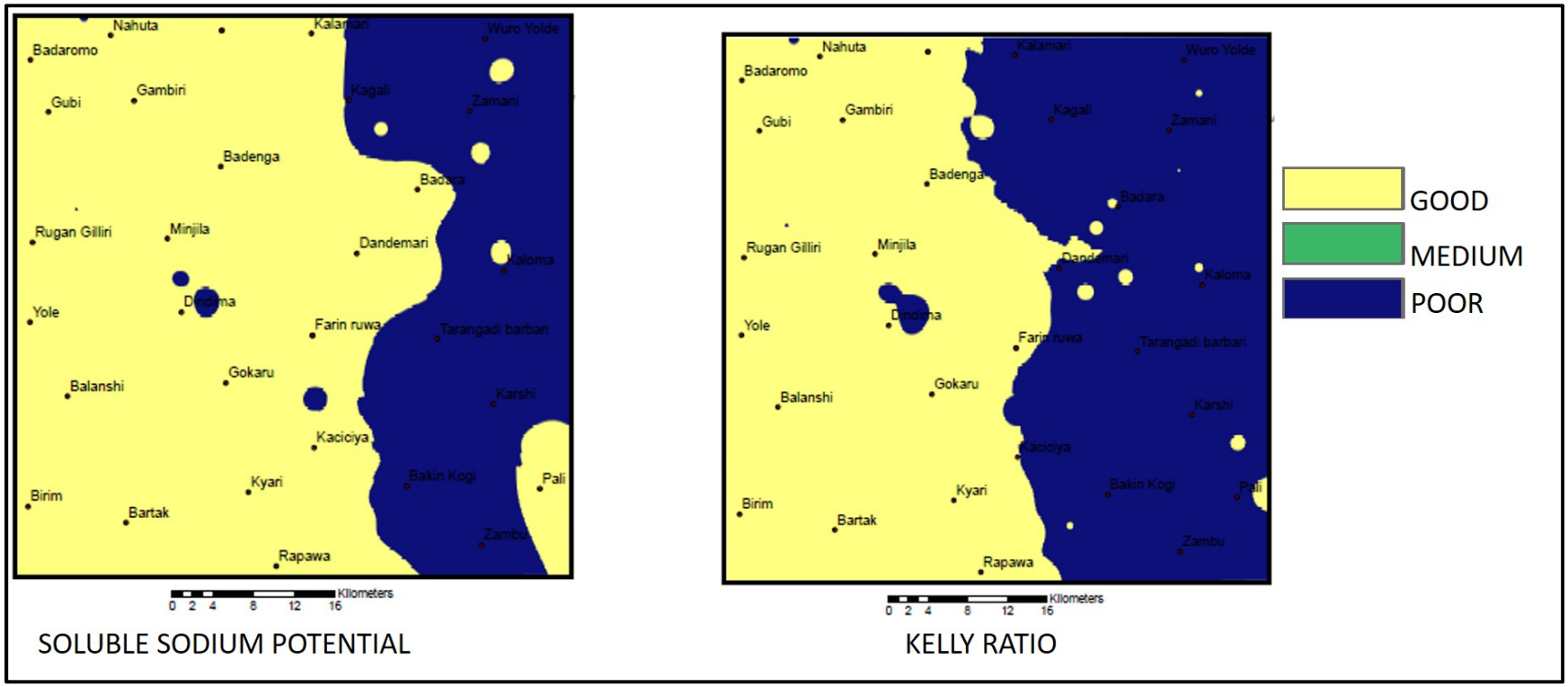

Fig. 4.35. Spatial distribution of Soluble Sodium Percent and Kelly Ratio in Bauchi-Alkaleri-Kirfi area

4.6.9 Hydrochemical Facies

The use of visualizations of the key ions in groundwater helps in describing the groundwater in aquiferous unitswhich vary in chemical composition, grouping and spatial distribution. The facies are determined by the flow patterns, aquifer's geology, and solution kinetics. In the present study, Schoeller diagrams, stiff diagrams and Piper trilinear diagram were employed to evaluate the different hydrochemical facies.

4.6.9.1 Schoeller diagrams

Schoeller diagrams are one of the numerous graphical ways of expressing the hydrochemistry of a multiple samples in a single plot (Figure 4.36 and 4.37). The Schoeller diagram for all the groundwater samples in this study revealed 3 major hydrochemical facies (the calcium bicarbonate, sodium bicarbonate and mixed water types) As can be seen from Fig. 4.36 and 4.37, the Ca^{2+}(Mg) HCO_3^- facie are the predominant in areas underlain by Basement Complex bedrocks. The migmatite bedrock (Fig. 4.36a) revealed 56% Ca-Mg-HCO_3 while the hornblende granites, the charnockites and the sandstones revealed 42%, 33% and 12% respectively. The Ca^{2+} (Mg) HCO_3^- facie is an indication of CO_2 charged meteoric water and silicate weathering and dissolution as suggested by Back, 1961.

The second hydrochemical facie in the studied groundwater Na (K)-HCO_3 facie which is predominant in the sedimentary aquifers (50%) suggesting that their hydrochemical evolution is by cation exchange processes. The sodium bicarbonates facie was also represented in the charnockite setting with about 8.3% which could be as a result of reactions with Na in clay minerals formed from weathering of the ferromagnesian minerals in the charnockites. The last group is the mixed Ca-Na-Mg HCO_3, Na-Mg-Ca HCO_3, and Na-Ca-Cl-HCO_3 which are product of groundwater mixing. This group cumulatively make up 43%, 58% and 66% of the migmatite, hornblende granites and charnockites respectively. In the sedimentary aquifers however, the mixed water type Ca-Na and Na-Ca-HCO_3 represents 22%.

a)

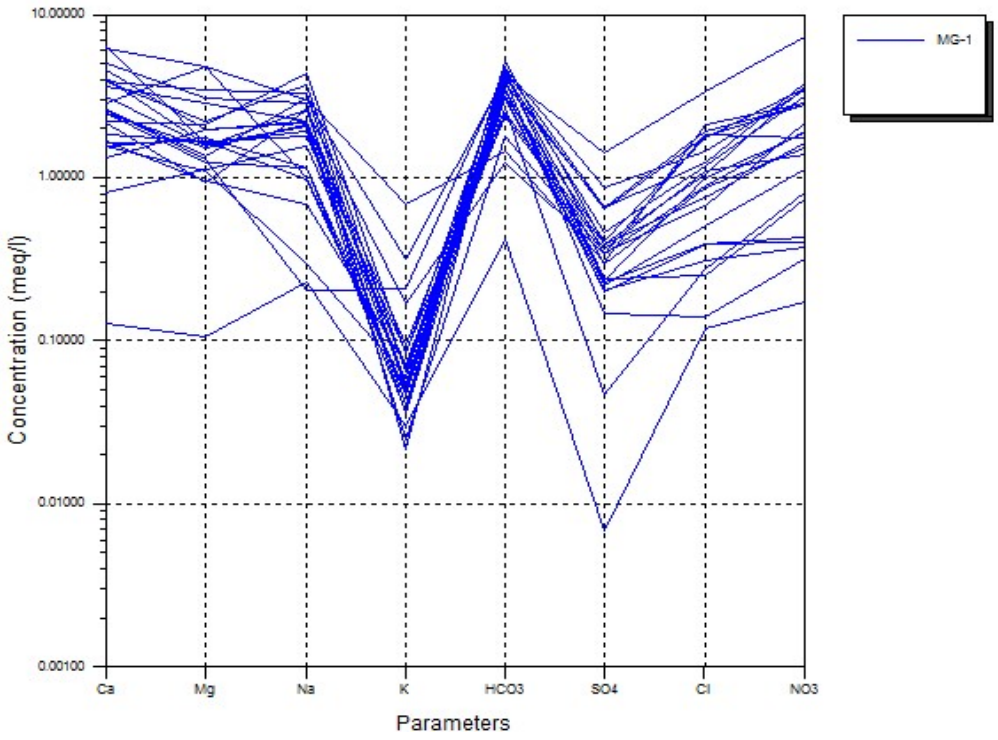

b)

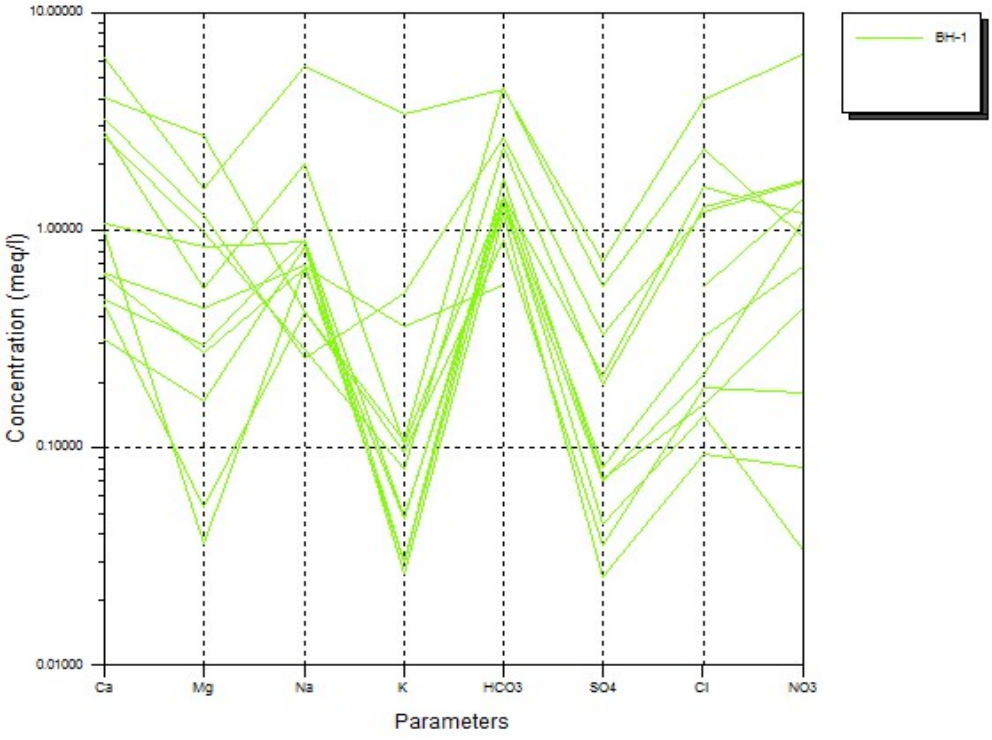

Fig. 4.36. Schoeller plots for (a) Migmatite aquifers and (b) Charnockite aquifers.

a)

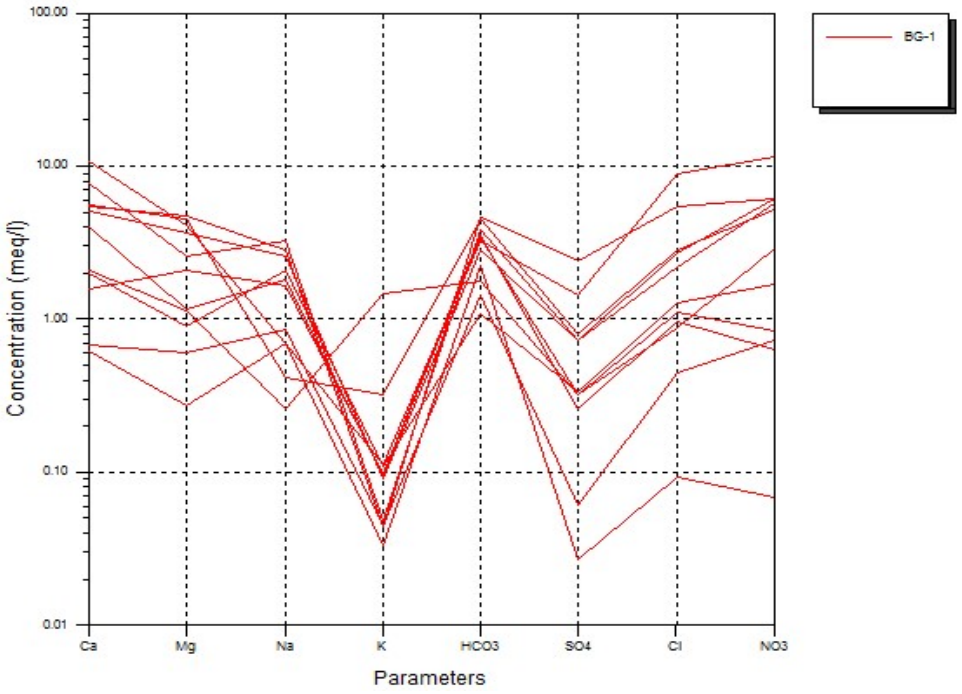

b)

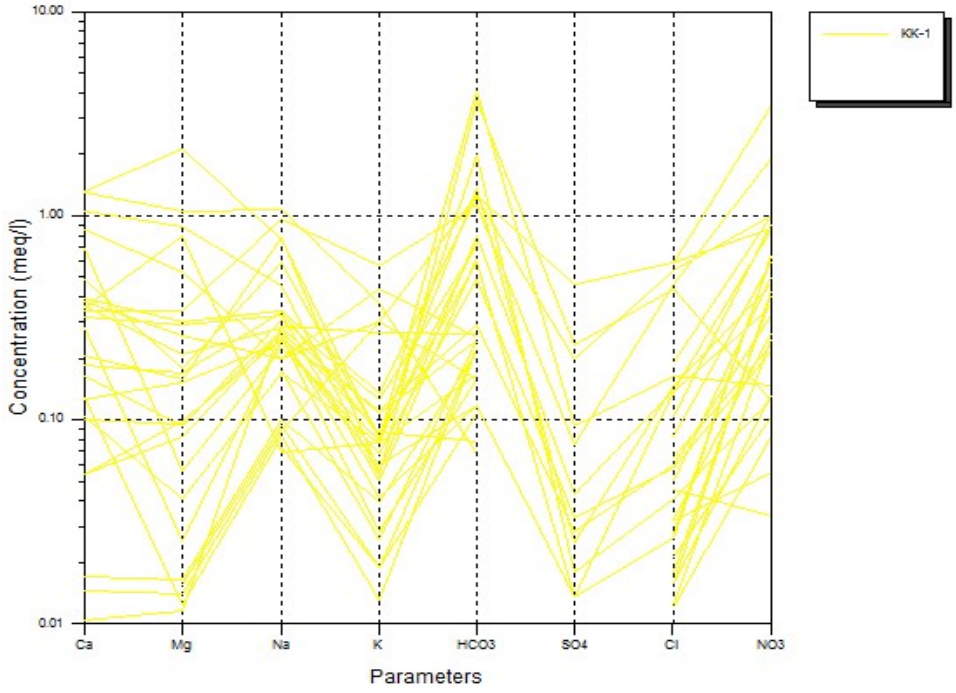

Fig. 4.37. Schoeller plots for (a) Biotite hornblende granite aquifers and (b) Kerri-Kerri aquifers.

4.6.9.2 Stiff plots

The major advantage of the Stiff plot is that it gives a visual picture of the water chemistry by displaying distinct polygons which are characteristic of the hydrochemical facie of groundwater (Uliana, 2012). Representative samples of the Stiff diagrams for the respective bedrock types were plotted and superimposed on the geology map of the area so as to get a spatial distribution of the hydrochemical facies of the aquifers on one hand and degree of mineralization of the groundwater on the other hand. (Fig. 4.38). The result of the Stiff diagram shows that the groundwater from the basement settings are more mineralized that those in the sedimentary as revealed by the sizes of the individual stiff plot which are generally larger in the basement setting. This is in agreement with the results of the total dissolved solids which are >500 mg/l in the basement and about 205 mg/l in the sedimentary setting. which is in tandem with those of the Schoeller plots suggest that Ca^{2+} has the highest concentration in the basement setting while Na^{+} constitute the dominant cations in the sedimentary aquifers with the HCO_3^{-} anion dominating both setting, which is an indication of CO_2 charged meteoric water as suggested by Back, 1961.

The Stiff diagram indicate 3 major water facies which also conforms to the result of the Schoeller plots. This groups are;

a) The (Ca (Mg)–HCO_3,

b) The Na (K)–HCO_3) and

c) The mixed cation water facie ((Ca-Na-HCO_3, Ca-Na-HCO_3-Cl and Ca-Mg-HCO_3Cl)

The Ca(Mg)–HCO_3 which is predominant in the mountainous areas occupied by basement aquifers and covering northwestern and southwestern parts of the Bauchi-Alkaleri-Kirfi area (Fig.4.38) and can be attributed to the recent recharging meteoric water and weathering of silicate minerals (Uliana and Sharp, 2001), the low TDS Na(K)–HCO_3 water type however, dominate the plains of the sandstone aquifers in the northeastern and southeastern parts of the Bauchi-Alkaleri-Kirfi area, suggesting cation exchange reactions, as evident by the higher Na/Cl ratios (4.6 average) in the sandstones as compared to the basement aquifers with (2.6).

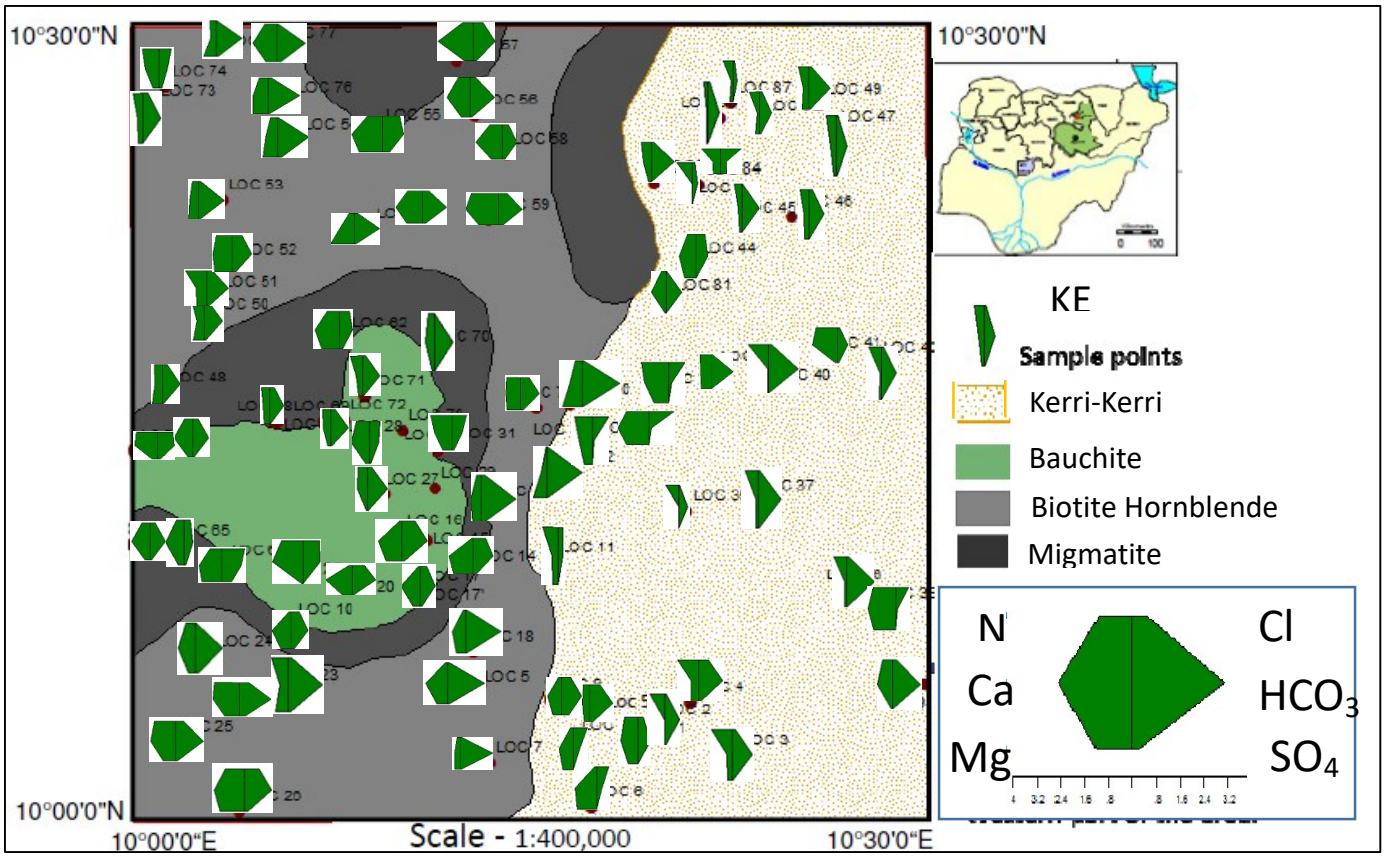

Fig. 4.38. Hydrochemical Facie Map of the Bauchi-Alkaleri-Kirfi area

Low TDS and high bicarbonate concentrations in aquifers suggest that these waters represent recent recharge (Back, 1961). In addition, the petrographic studies suggests that the weathering and dissolution of the rocks in the study are the source of major ions in the groundwater samples from the basement setting.

However, the mineralization of the water sample from Kerri-Kerri Formation is attributable to the dissolution of saline (connate water) and carbonate material (as cementing material) associated with the lacustrine depositional environment of the Kerri-Kerri Formation (Adegoke *et al*., 1989). The third group constitutes mixed facies (Ca-Na-HCO_3, Ca-Na-HCO_3-Cl and Ca-Mg-HCO_3Cl, etc.) arising from the combination of the Ca–HCO_3 type, Na–HCO_3 type and other cations and anions. These are consistent with evolution of groundwater in an unconfined regional system where water from two different areas meet as exemplified by some parts of the bauchite and biotite hornblende granite aquifers and parts of the basement/sedimentary contact zones in the Bauchi-Alkaleri-Kirfi (Fig.4.39).

In a summary, the analysis of the Stiff diagram revealed that the Bauchi-Alkaleri-Kirfi area is dominated by the bicarbonate facies represented recent CO_2-charged recharge modified by mineral dissolution to form Ca (Mg)–HCO_3 which predominate the basement setting. The cation exchanged Na (K)–HCO_3 water type however, dominates the sedimentary aquifers in the Bauchi-Alkaleri-Kirfi area and this are products of substitution reactions between the groundwater and sodium from saline connate water in lacustrine sediments of the Kerri-Kerri Formation. Other water types in the Bauchi-Alkaleri-Kirfi area constitutes the mixed water group which represents the mixture of groundwater from different aquifer settings (i.e. Ca (Mg)–HCO_3 combines with Na (K)–HCO_3 facie to produce CaNa–HCO_3 or NaCa–HCO_3.

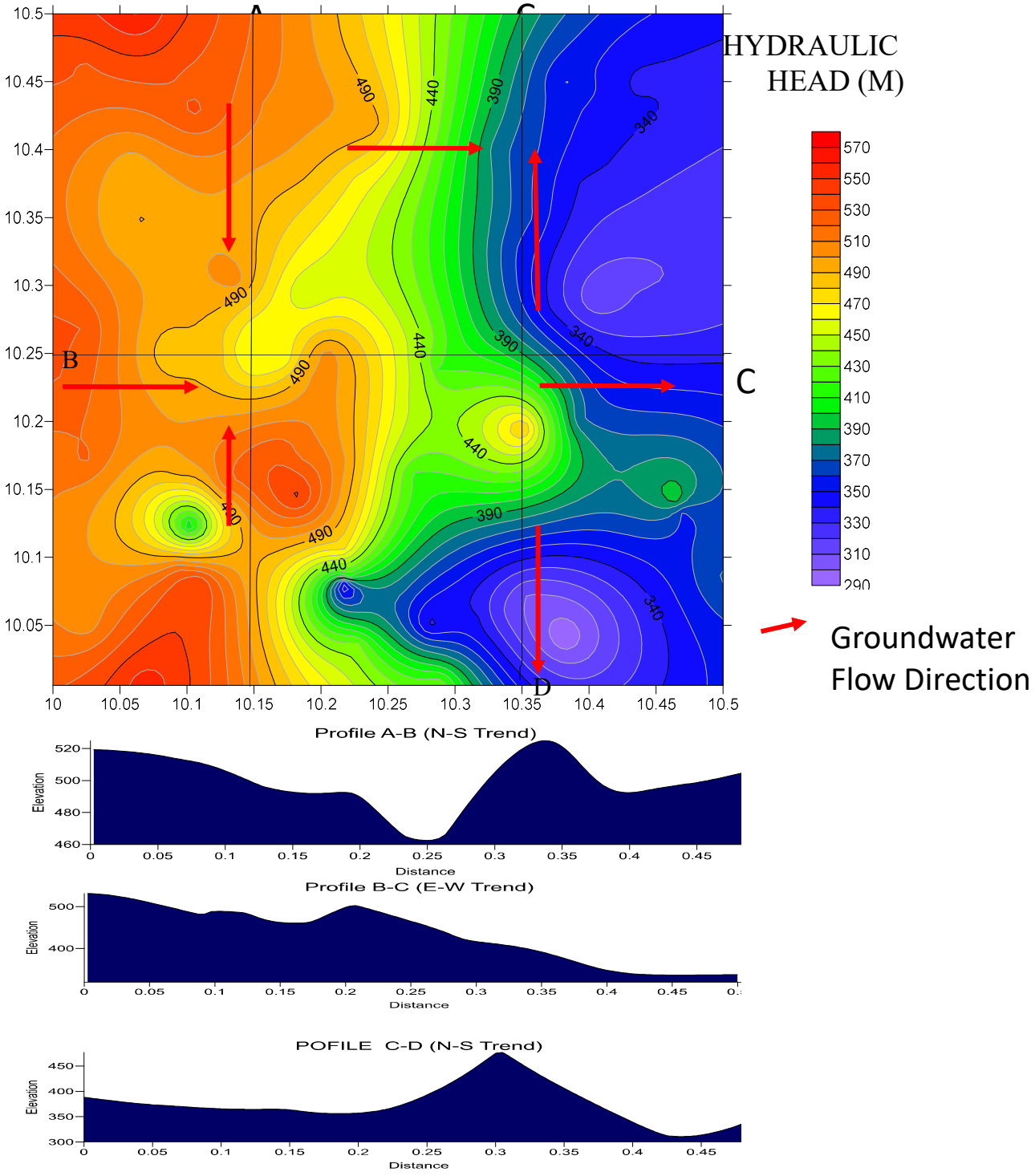

Fig. 4.39. Hydraulic Head Distribution and groundwater flow pattern of Bauchi-Alkaleri-Kirfi area (Contour Interval 10m).

4.6.9.3 Piper trilinear

Piper diagram is another efficient instrument for presenting hydrochemical information and characterizing hydrochemical facies. The piper plot of the hydrochemical result are presented in Fig. 4.40.

The overall characteristics of the water is represented in the diamond-shaped were characterised as:

I. Ca^{2+}-Mg^{2+}-Cl-SO_4^{2-},
II. Na^{+}-K^{+}–Cl^{-}-SO_4^{2-},
III. Na^{+}-K^{+}-HCO_3- and
IV. Ca^{2+}-Mg^{2+}-HCO_3^{-}

The four groups are further subdivided into 9 subcategories as follows:

1. (Ca +Mg) >(Na +K)
2. (Na +K) > (Ca+Mg)
3. (CO_3+ HCO_3)>(SO_4+Cl)
4. (SO_4-Cl)>(CO_3 +HCO_3)
5. HCO3- CO3& Ca –Mg (Temporary Hardness)
6. SO_4-Cl & Ca-Mg (Permanent Hardness)
7. SO_4-Cl & Na-K (Saline)
8. HCO_3- CO_3& Na-K (Alkali Carbonate)
9. Mixing Zone

The Piper trilinear diagram (Fig.4.40) of the samples from the Bauchi-Alkaleri-Kirfi area revealed that majority of samples (50.6%) belong to Ca^{2+}- Mg^{2+}-HCO_3^{-} while Na^{+}- K^{+}-HCO_3^{-} , Ca^{2+}-Mg^{2+}-$Cl^{-}SO_4^{2-}$, and Na^{+}-K^{+}- Cl^{-}-SO_4^{2-} types represented 14.1%, 3.5% and 3.5% respectively. This reflects a similar trend observed in the schoeller and stiff plot presented earlier. The remaining 28.2% fall under the mixing zone with no abundant ion.

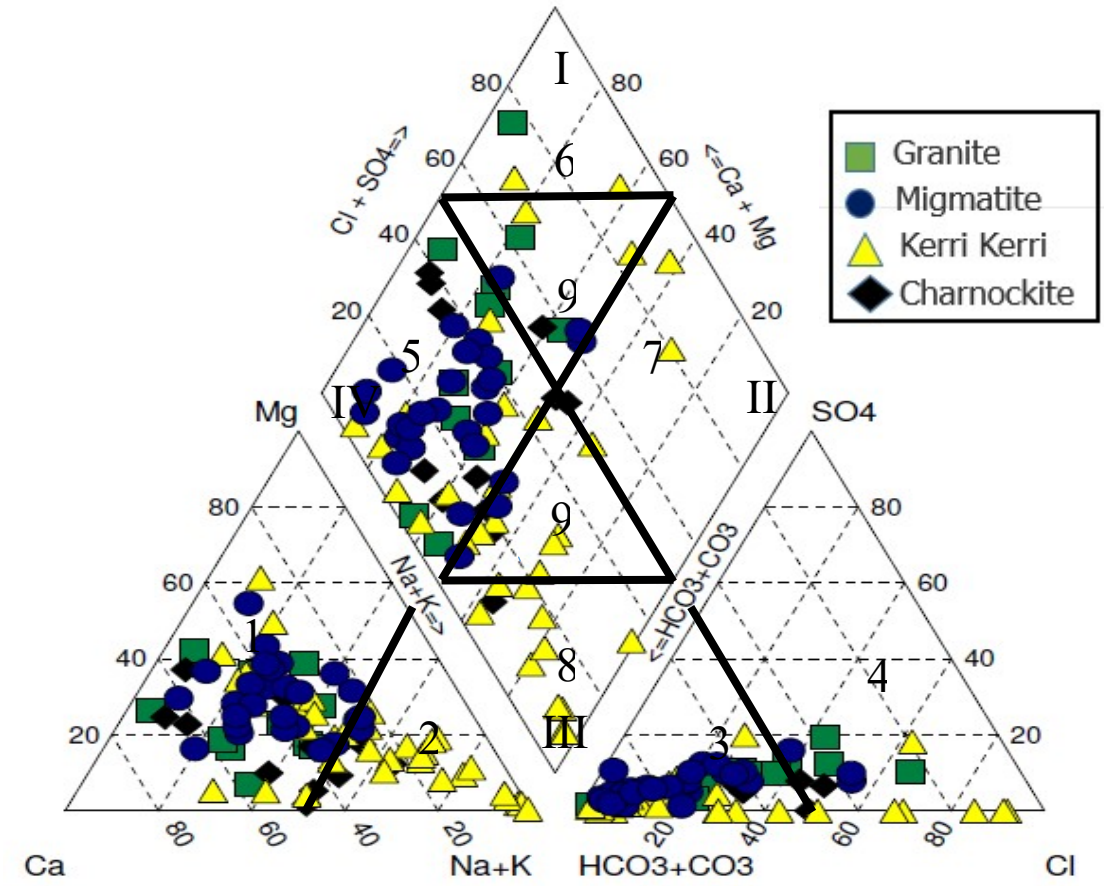

Fig. 4.40. Combined Piper Trilinear Plots of the Samples from the Bauchi-Alkaleri-Kirfi area

From the Piper trilinear plot (Fig. 4.40), it would be observed that Ca^{2+} and Mg^{2+} exceeds the Na^{+} and K^{+} in 65.9% of the samples and in 34.1% of the samples, the reverse was the case as (Na^{+} and K^{+}) exceeds (Ca^{2+} and Mg^{2+}). Furthermore, weak acids exceeds strong acids in 81.2% of the groundwater samples i.e. (CO_3+ HCO_3) > (SO_4+Cl) and the strong acids exceeds the weak acids in 18.8% of the samples. The Piper trilinear plot has illustrated that the predominant water type in the studied aquifers is the temporary hard water which covers 50.6%, followed by the mixed water with no abundant cation and anion (28.2%). The alkali carbonate water constitute 14.1% of the waters while the permanently hard and saline water make up 3.4% and 2.6% respectively. The groundwater facies summarized in Table 4.22 shows a general dominance of the Ca^{2+}-Mg^{2+}-HCO_3^{-} facie in the basement aquifers as compared to the sedimentary aquifers and this could be attributable to recharging meteoric water which dissolves mobile Ca and Mg from rock surfaces. It would be observed that 74% (20 samples) of the migmatite aquifers fall under the Ca^{2+}-Mg^{2+}-HCO_3^{-} water type, while the biotite hornblende granite, bauchite and the sandstone aquifers revealed 66.7%, 50% and 26.5% respectively. The plots also demonstrated the dominance of the alkali earths over the alkalis in the basement aquifers with the biotite hornblende granite aquifers having 100% dominance, migmatite (81.5%), bauchite (58.3%) and Kerri-Kerri (44.1%).

The piper plot showed a reverse trend in the distribution of the Na^{+}-K^{+}-HCO_3^{-} facie which is predominant in the Kerri-Kerri aquifers with 32.4% as compared to 8.3% in the bauchite confirming the earlier inference suggesting that mineralization of the Kerri-Kerri groundwater can be attributed to cation exchange reaction with the associated lacustrine clays of the sedimentary units (Adegoke *et al*., 1989). In conclusion, the 3 major hydrochemical facies were identified in this study. The calcium bicarbonate facies which dominates the basement settings (northwestern and southwestern zones) are a product of carbon dioxide charged meteoric recharge and silicate weathering and dissolution of rocks. However, the sodium bicarbonate water type dominated the sandstone aquifers and was formed through ion exchange reactions. The last water type are the mixed group which are the product of mixing of the aforementioned water types and this group mostly occur in contact zones between the different rocks.

Table 4.22. Hydrochemical facies of the different aquifer systems in the Bauchi-Alkaleri-Kirfi area.

Groundwater types/characteristics of subdivisions of diamond shaped fields	**Samples from the different aquifer types**									
	Biotite hornblende Samples		Migmatite Samples		Bauchite Samples		Kerri-Kerri Samples		Total Samples	
	No.	%	No.	%	No.	%	No.	%	No.	%
I. Ca^{2+}-Mg^{2+}-Cl-SO_4^{2-}	1	8.3	0.0	0.0	0.0	0.0	2.0	5.9	3.0	3.5
II. Na^{+}-K^{+}-$Cl^{-}SO_4^{2-}$	0	0.0	0.0	0.0	1.0	8.3	2.0	5.9	3.0	3.5
III. Na+-K+-HCO_3	0	0.0	0.0	0.0	1.0	8.3	11.0	32.4	12.0	14.1
IV. Ca^{2+}-Mg^{2+}-HCO_3	8	66.7	20.0	74.1	6.0	50.0	9.0	26.5	43.0	50.6
1. (Ca +Mg) >(Na +K)(Alkali earth >Alkali's)	12	100.0	22.0	81.5	7.0	58.3	15.0	44.1	56.0	65.9
2. (Na +K) > (Ca+Mg) (Alkali's >Alkali earth)	0	0.0	5.0	18.5	5.0	41.7	19.0	55.9	29.0	34.1
3. (CO_3+ HCO_3)>(SO_4+Cl)(weak acid > strong acid)	8	66.7	24.0	88.9	9.0	75.0	28.0	82.4	69.0	81.2
4. (SO4-Cl)>(CO_3 +HCO_3)(strong acid >weak acid)	4	33.3	3.0	11.1	3.0	25.0	6.0	17.6	16.0	18.8
5. HCO_3- CO_3& Ca -Mg (Temporary Hardness)	8	66.7	20.0	74.1	6.0	50.0	9.0	26.5	43.0	50.6
6. SO_4-Cl & Ca-Mg (Permanent Hardness)	1	8.3	0.0	0.0	0.0	0.0	2.0	5.9	3.0	3.5
7. SO_4-Cl & Na-K (Saline water);Sodium chloride type	0	0.0	0.0	0.0	0.0	0.0	2.0	5.9	2.0	2.4
8. HCO_3- CO_3& Na-K(Alkali carbonate waters)	0	0.0	0.0	0.0	1.0	8.3	11.0	32.4	12.0	14.1
9. Mixing Zone (no one cation or anion >50%)	3	25.0	7.0	25.9	4.0	33.3	10.0	29.4	24.0	28.2

To explore the source of the solutes and the geochemical mechanisms that lead to the different hydrochemical facies identified in Bauchi-Alkaleri-Kirfi area, stoichiometric ionic relations was employed in accordance with Fisher and Mullican, 1997 as presented in the subsequent section.

4.7 Mechanisms for Hydrochemical Evolution

Heterogeneities in the mineralogy of aquifer may occur within short distances and could have serious influence on the distribution of dissolved species in the groundwater (Mapoma *et al*., 2017). Also, noteworthy is the fact that, in addition to the host rock mineralogy, other mechanisms such as evaporation and evaporite dissolution amongst others can affect the distribution of dissolved ions in water. The distribution and compositional relationship of the major dissolved species in the groundwater from this study was employed to investigate the source of solutes and mechanisms responsible for groundwater hydrochemistry in the aquifers being studied.

As observed in the groundwater in the studied wells, the dominance of HCO_3 confirms CO_{2-} charged meteoric water and silicate weathering as some of the mechanisms responsible for the observed hydrochemical distribution as suggested in the earlier sections. Also, the elevated amounts of Na^+ in most parts of the sandstone aquifers also confirms cation exchange as the mechanism responsible for the hydrochemical evolution in the sedimentary settings and this is in agreement with the earlier conclusions. To further understand the mechanism of the hydrochemical evolution of the studied groundwater samples a Gibbs diagram was employed (Fig. 4.41). Gibbs (1970) observed that a great deal of the world's surface water falls within certain boundaries defined by the plot of the ratios of (1) (Na + K)/ (Na + K + Ca) and (2) (Cl/ Cl +HCO3) against TDS, and theorized the three major mechanisms controlling the hydrochemistry of water, which are presented in three fields: Evaporation, Rock or weathering and Rainfall dominance. The Gibbs plot (Fig. 4.38a and b) revealed that the groundwater system is primarily affected by rock dominance suggesting that the hydrochemistry of the various groundwater in this study were mainly influenced by the rock dominance (the

intermediate zone), which further confirms the silicate weathering/ dissolution origin made in earlier sections.

(a)

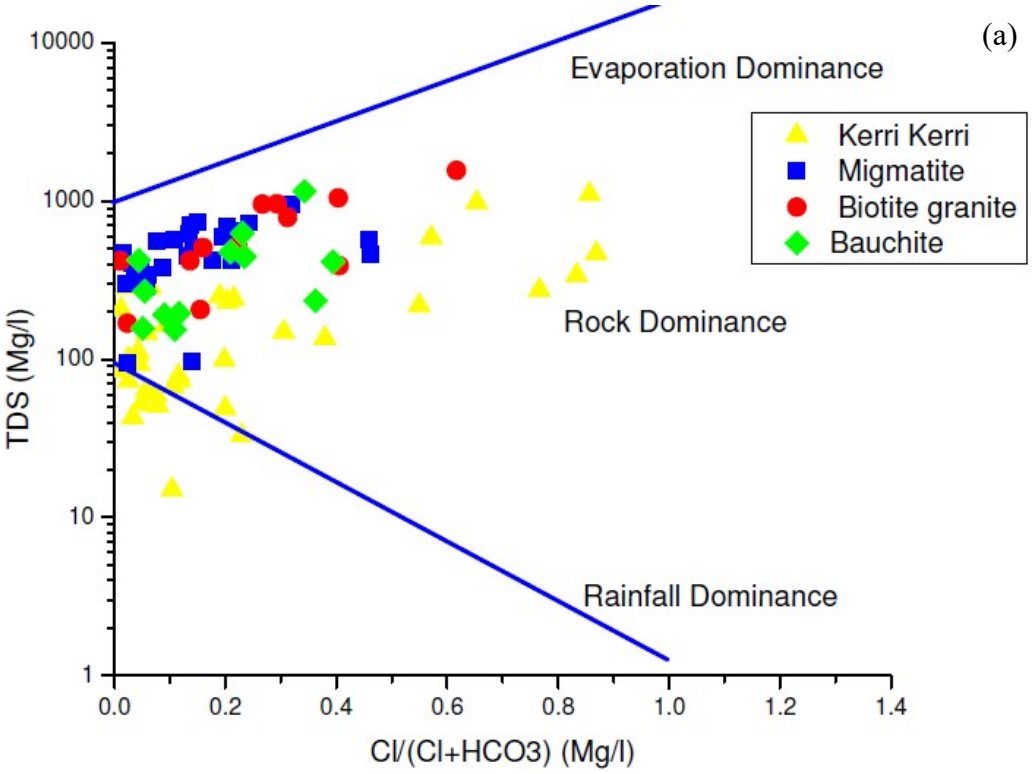

(b)

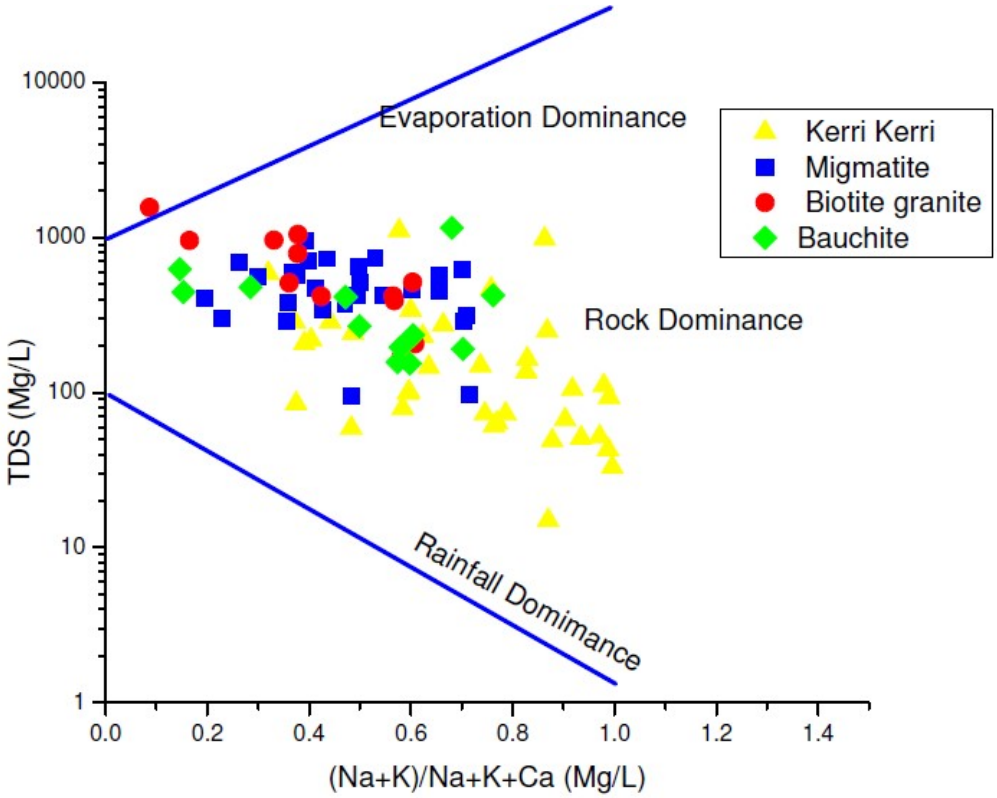

Fig. 4.41. Gibbs Plot Showing the development of groundwater hydrochemistry in Bauchi-Alkaleri-Kirfi area for (a) Anions and (b) Cations

Considering that an examination of the stoichiometric relations between the cations and anions could suggest the mechanism or combination of processes responsible for groundwater geochemical development in aquifers which is in tandem with the studies by Fisher and Mullican, 1997 and Mapoma et al., 2017. A hydrochemical diagram suggested by Chadha, 1999 (Fig. 4.42) was also employed to further investigate the mechanism responsible for the evolution of the hydrochemistry in the research region. The hydrochemical data was first converted to milli-equivalent percentages, and the difference between Ca + Mg and Na + K was plotted on the abscissa for cations, while the difference between weak acidic anions (HCO_3 + CO_3) and strong acidic anions (Cl + SO_4) was plotted on the ordinate. The hydrochemical processes proposed by Chadha, 1999, are shown in the four quadrants of the graph which are categorised as base ion exchange water (Na–HCO_3 type), reverse ion exchange-water (Ca–Mg–Cl type), recharging water (Ca–Mg–HCO3 type), and seawater/end-member waters (NaCl type). As can be seen from the Chadha plot, four (4) possible mechanisms were identified to be responsible for the hydrochemistry of the groundwater in the area.

i. Recharging waters through mineral dissolution and weathering

Chemical reactions also work on rocks and minerals exposed on the earth crust. These reactions which can be very complex take place between rocks / minerals and atmospheric substances like water, carbon dioxide and oxygen, giving rise to new minerals or dissolved minerals. Although some minerals, such as quartz, are virtually unaffected by chemical weathering, others are easily altered, e.g. feldspar.

As rain drops through the atmosphere it combines with carbon dioxide to form weak acid (carbonic acid) (equation 4.3).

$$H_2O + CO_2 \text{ —->} H_2CO_3 \quad \text{then} \quad H_2CO_3 \text{ —->} H^+ + HCO_3^- \qquad (4.3)$$

water + carbon dioxide —-> carbonic acid then carbonic acid —-> hydrogen ion + carbonate ion

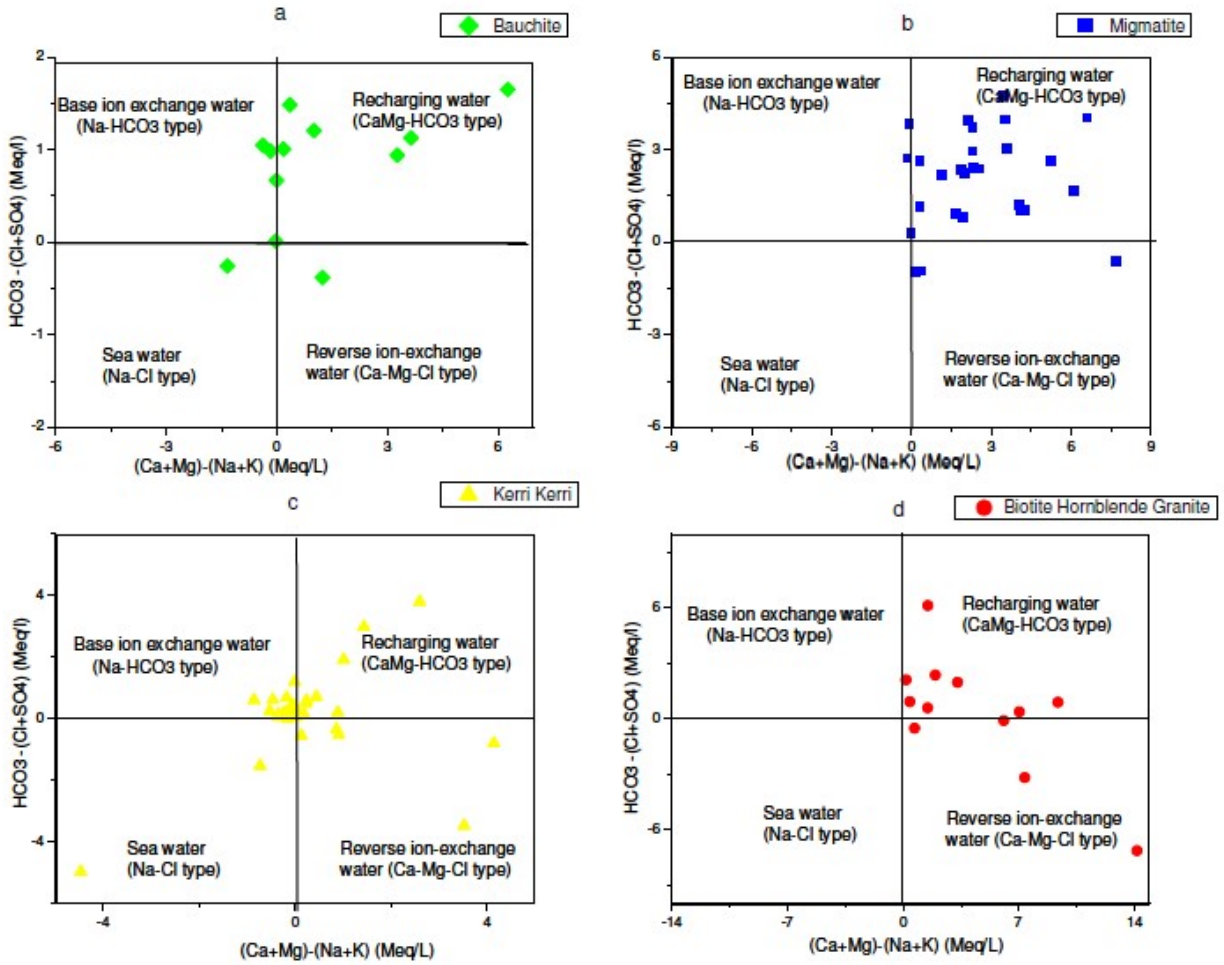

Fig. 4.42. Chadha plot showing the mechanism for hydrochemical evolution of groundwater in the different aquifers Bauchi-Alkaleri-Kirfi area; a. Bauchite, b. Migmatite, c. Kerri- Kerri , d. Biotite hornblende granite

Following the formation the weak carbonic acid, it dissociates into hydrogen and bicarbonate ions. The quantity of CO_2 in the atmosphere is sufficient to create only very weak carbonic acid, but typically there is much more CO_2 in the soil, such that water that infiltrates through the soil can become much more acidic. The carbonic acid then percolates into the underground from the surface, during which it attacks feldspars, carbonates and other minerals, dissolving them and yielding an aqueous solution of calcium and bicarbonate ions (equation 4.4 & 4.5).

$$CaAl_2Si_2O_8 + H_2CO_3 + ½O_2 \text{ —-> } Al_2Si_2O_5(OH)_4 + Ca^{2+} + CO_3^{2-} \quad (4.4)$$

Plagioclase + carbonic acid —-> kaolinite + dissolved calcium + carbonate ions

$$CaCO_3 + CO_2 + H_2O \text{ —-> } Ca^{2+} + 2HCO_3^- \quad (4.5)$$

Carbonates + carbon dioxide + water —->calcium ion + carbonic acid

From Fig 4.42 it would be observed that the recharging water type is the dominant mechanism responsible for the hydrochemical evolution of the aquifers under study revealed by the Chadha plot. The Chadha plots (Fig 4.42 and 4.43) indicates that the main mechanisms controlling ground water chemistry in the basement aquifers is the recharging water/mineral dissolution. It is evident from the combined Chadha plot, where 75%, 74% and 50% of the samples from the biotite hornblende granite, migmatite and

bauchite respectively revealed recharging water and rock weathering as the chief source of solute. Conversely, in the sedimentary aquifers (Kerri Kerri) only 22% of the samples revealed recharging water mechanism as the source of dissolved species in the aquifer units.

According to results of the petrographic analysis conducted on the various bedrocks in the Bauchi-Alkaleri-Kirfi area, the rocks are composed of the minerals quartz (SiO_2), muscovite (K Al (Si_3Al) O_{10} (OH, F)), albite ($NaAlSi_3O_8$), orthoclase $KAlSi_3O_8$), biotite ($K(Mg, Fe)_{2-3}Al_{1-2}Si_{2-3}O_{10}(OH,F)_2$), hornblende $(Ca, Na)_{2-3}(Mg, Fe, Al)_5(Si, Al)_8 O_{22}(OH,F)_2$) and fayalite ($Fe_2SiO_4$). According to Hem 1985, the extent with which mineral components interact with groundwater is determined by the availability of protons, surface area per unit volume of water and contact time.

ii. Base ion exchange

When levels of alkaline earth metals (Mg^{2+} , Ca^{2+}), and chloride ionsreduceswhile levels of alkali metals (K^+, Na^+),SO_4^{2-} and bicarbonates rise as indicated in Fig. 4.43 ; this may be correlated with processes of base ion exchange. Thisoccurs between aquifer grains and the groundwater (Jalali, 2005). Also, the coexistence of Na^+ and HCO_3^- in a sample of watercould indicate the likelihood of suchreactions (Morales et al. 2015). The necessary exchangers may be provided for by the presence of clay minerals such as kaolinite, as shown in Eq. 4.6, where X represents clay:

$$2Na^+ + Ca/Mg\text{-}X_2 \longleftrightarrow Ca^{2+} + 2Na\text{-}X \qquad (4.6)$$

In the reverse reaction of equation 4.7 it would be observed that the divalent cation is replaced with Na^+ from the clay mineral X to elevate Na^+ in the groundwater.

Similarly, monovalent K^+ may replace divalent cations from feldspars, as exemplified by the reaction of an orthoclase (Na, K) $AlSi_3O_8$) to produce anorthite ($CaAl_2Si_2O_8$) as shown in Eq. (4.5), releasing Na^+ and K^+.

$$2(Na, K)\,AlSi_3O_8(s) + Ca^{2+} \longrightarrow CaAl_2Si_2O_8(s) + (Na^+; K^+) + 4SiO_2 \qquad (4.7)$$

Orthoclase anorthite monovalent ions silica

Ion exchange reactions are more peculiar to the Kerri-Kerri aquifers of the Bauchi-Alkaleri-Kirfi area (Fig 4.43) as 58% of the samples from these sedimentary aquifers covering mostly the eastern half of the Bauchi-Alkaleri-Kirfi area revealed evolution from base ion reactions as compared to 33.3%, 11.1% and 0% in the bauchite, migmatite and the biotite hornblende granite aquifers respectively. The chloro-alkaline indices has been a vital tool used by hydrochemists to detect the mechanism base ion exchange reactions which controls groundwater chemistry (Zhu *et al*., 2007). It is also known to provide relevant information on base ion exchange reactions in aquifers (Equations 4.8 and 4.9). $\mathrm{CAI\ 1} = (\mathrm{Cl} - (\mathrm{Na} + \mathrm{K})/\mathrm{Cl}$

(4.8)

$\mathrm{CAI\ II} = (\mathrm{Cl} - (\mathrm{Na} + \mathrm{K})/ (\mathrm{Cl} + \mathrm{HCO_3} + \mathrm{SO_4} + \mathrm{NO_3})$ (4.9)

Negative values of chloro-alkaline indices signifies ion exchange reactions. The dominance of negative values (89%) of the chloro-alkaline indices further confirms the role of base ion exchange reactions as a major mechanism controlling the hydrochemical development in the sedimentary aquifers in the Bauchi-Alkaleri-Kirfi area.

iii. Reverse ion exchange

Reverse ion exchange waters are groundwaters where Ca + Mg exceeds Na + K as characterised by some of the research region samples. This process occurs where the calcium and magnesium ions in the matrix of aquifer are substituted by sodium ions at suitable exchange locations either owing to the preferential release of Ca and Mg from dissolution of minerals or potentially reverse base cation exchange responses of Ca + Mg into solution and later adsorption of Na on mineral surfaces (Ravikumar, and Somashekar, 2011). Positive values of chloro-alkaline indices signifies reverse ion exchange reactions. Thus, an exchange between alkalis in the liquid phase of the aquifer with alkali earth metals in the aquifer solid phase will result in a positive index attributable to reverse exchange reactions. This mechanism played a major role in the predominance of Ca and Mg ions over Na ion in 13 samples covering 5 locations in the Kerri-Kerri, 4 in the migmatite zone, 3 in the biotite hornblende bedrock and only 1 location in the bauchite setting.

iv. Sea water

The seawater category are mostly confined to coastal areas where the Na-Cl water type predominates, which was not the case in the Bauchi-Alkaleri-Kirfi area. However 3 samples (location 8, 66 and 84) showed the said mechanism and this can be regarded as secondary salinity because it is attributed to human activities e.g. large level of salt effluent from intensive agriculture or septic tanks. This is evident as all the affected samples were collected from residential or farming areas. The combined Chadha plot (Fig. 4.43) above shows that the dominant mechanism controlling the development of the hydrochemistry in the Bauchi-Alkaleri-Kirfi area is the recharging water which is predominant in the migmatite aquifers and covers 43% of the aquifers in the Bauchi-Alkaleri-Kirfi area, It is followed by the base ion exchange mechanism which represents 28% of the aquifers and more abundant in the Kerri-Kerri aquifers.

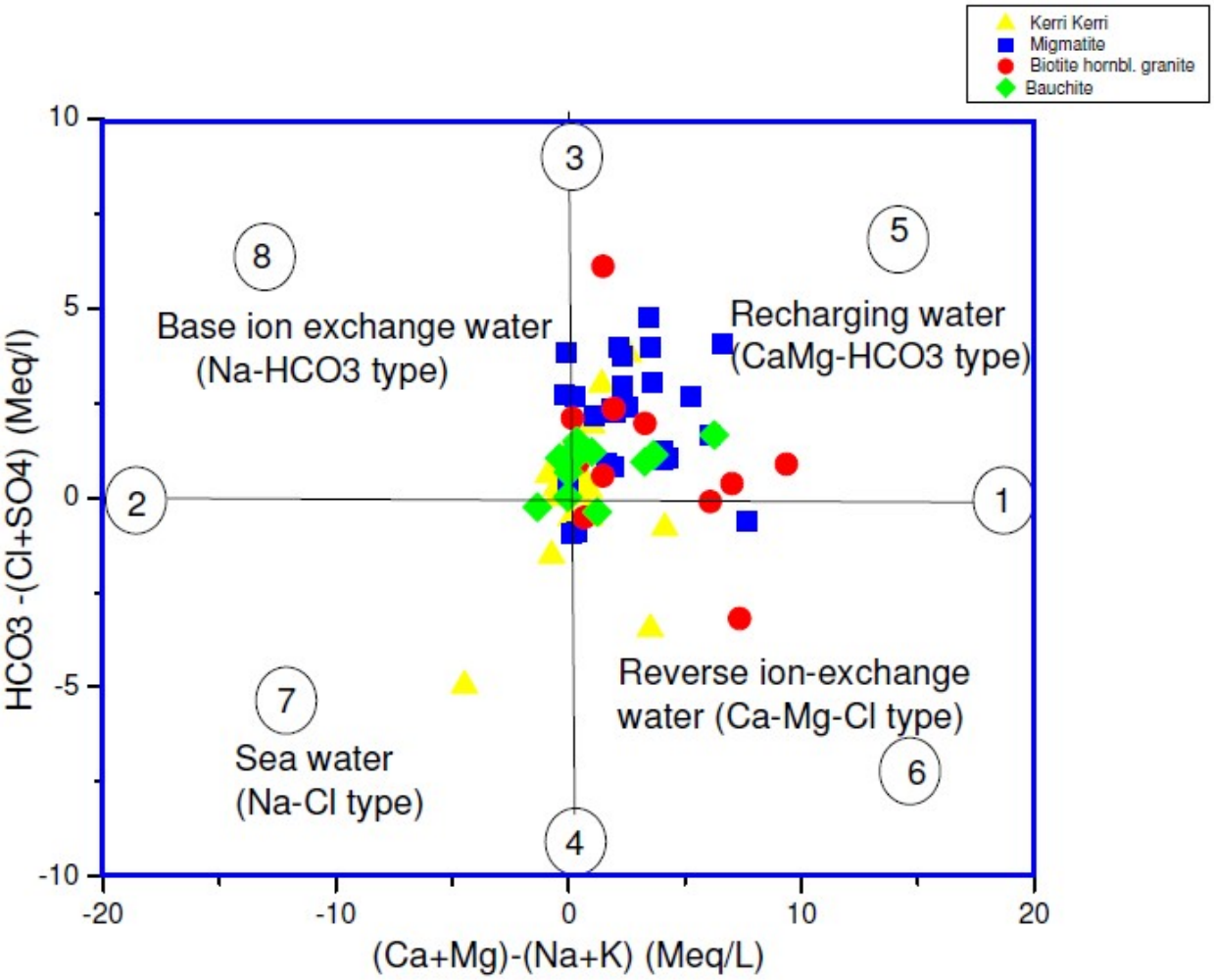

Fig. 4.43. Combined Chadha plot showing the mechanism for hydrochemical evolution of groundwater in the Bauchi-Alkaleri-Kirfi area

The reverse cation exchange accounts for 13% of the groundwater samples and is responsible for 25% of the biotite hornblende granite bedrocks. The sea water mechanism represent only 3% of the groundwaters under study.

While the Gibbs and Chadha plots have provided a lot of information on the mechanism for hydrochemical evolution of groundwater in the Bauchi-Alkaleri-Kirfi area, only little information has been provided on the nature and lithology of the rocks species involved in the hydrochemical reactions in the study area. In view of the above, bivariate plots of the major ions was employed to further understand the processes controlling the ground water chemistry with more emphasis on the reacting masses in line with Hallouche, 2017.

The plot (Fig. 4.44 a) of alkaline earth ions (Ca^{2+} + Mg^{2+}) versus HCO_3^- shows that the majority of samples does not scatter along 1:1 line, indicating that these solutes are not contributed by dissolution of carbonates but rather by other sources possibly silicate weathering/ weathering of amphiboles and pyroxene minerals from the basement rocks (Hallouche, 2017). Also, when the ratio of Ca^{2+} + Mg^{2+}/HCO_3 is lower than 1, it is suggestive of recent meteoric recharge and this scenario is in agreement with the study of Nazzal *et al*., 2014. Most of the studied samples with the exception of a few locations (6, 8, 32,33,34,38 under the Kerri-Kerri, 31, 55 and 58 from migmatite aquifers and 15, 62 and 65 within biotite hornblende granite aquifers) satisfied the above condition thus

showing great input of fresh groundwater recharge in the investigated area. The cross plot of Na against Cl (Fig. 4.44b) revealed that most of the samples are > 1 or fall away from 1:1 line suggesting input from silicate weathering as opined by Al amry, (2008). Halim *et al*. (2010) and Yidana *et al*. (2010) also surmised that halite dissolution is not the primary cause of high Na^+ in groundwater, when the samples disperse considerably away from the halite dissolution line (1:1) in Na^+ vs Cl^- plots (Fig. 4.44b). However, when the samples scatter significantly away from the halite dissolution line (1:1), the causative mechanism could be ascribed to base ion exchange reactions and to some extent weathering of silicates which is the case in parts of the charnorckite and the sedimentary areas of the study area.

Similarly, ratios of $Ca^{2+}/Mg^{2+}>2$ indicates silicate weathering and this corroborates the aforementioned ionic relationships (Ca^{2+} + Mg^{2+}/HCO_3 and Na^+ vs Cl^-) because the mean values of the Ca^{2+}/Mg^{2+} for all the rocks are greater than 2 except for the migmatite aquifers which is 1.52 but when the whole basement is considered the ratio is greater than 2 indicating a silicate weathering origin for the solutes in the aquifers under study and this is in tandem with study conducted by Ayadi *et al*. (2018).

Furthermore, the plot of Ca^{2+} + Mg^{2+} vs cation (total) (Fig.4.44c) revealed a growing contribution of Na and K as TDS increases as most of the samples falls below the 1:1 line. The dominance of Na^+ in sandstone aquifers is a weathering index which indicates that the ions result dissolution of salts (from connate water or cementing material) and this in agreement with the work of Rahman *et al*. (2011). The normalised Mg^{2+} versus Ca^{2+} (Fig. 4.45a) suggests silicate weathering as the primary source of hydrochemicals in the studied groundwater (Appelo and Postma, 1993), as most plots disperse in the silicate weathering region, with 13 samples (having representation in all the aquifer types) approaching carbonate dissolution. Similarly, a plot of normalized HCO_3 versus Ca^{2+} (Fig. 4.45b) show that elevated Ca^{2+} in the system is mostly from silicate weathering and possibly carbonate dissolution (Mukherjee and Fryar 2008; Halim *et al*. 2010). Most of groundwater samples fall in the proximity of the silicate dissolution end member with a few points plotting close to the carbonate and evaporite dissolution. (Fig. 4.45b)

The plot normalised Mg^{2+} versus Ca^{2+} (Fig. 4.45a) suggests silicate weathering as the primary source of hydrochemicals, as most plots disperse in the silicate weathering region, with 13 samples (having representation in all the aquifer types) approaching carbonate dissolution. Similarly, a plot of normalized HCO_3 versus Ca^{2+} (Fig. 4.45b) show that elevated Ca^{2+} in the system is mostly from silicate weathering and possibly carbonate dissolution (Mukherjee and Fryar 2008; Halim *et al*. 2010). Most of groundwater samples fall in the proximity of the silicate dissolution end member with a few points plotting close to the carbonate and evaporite dissolution. (Fig. 4.45b)

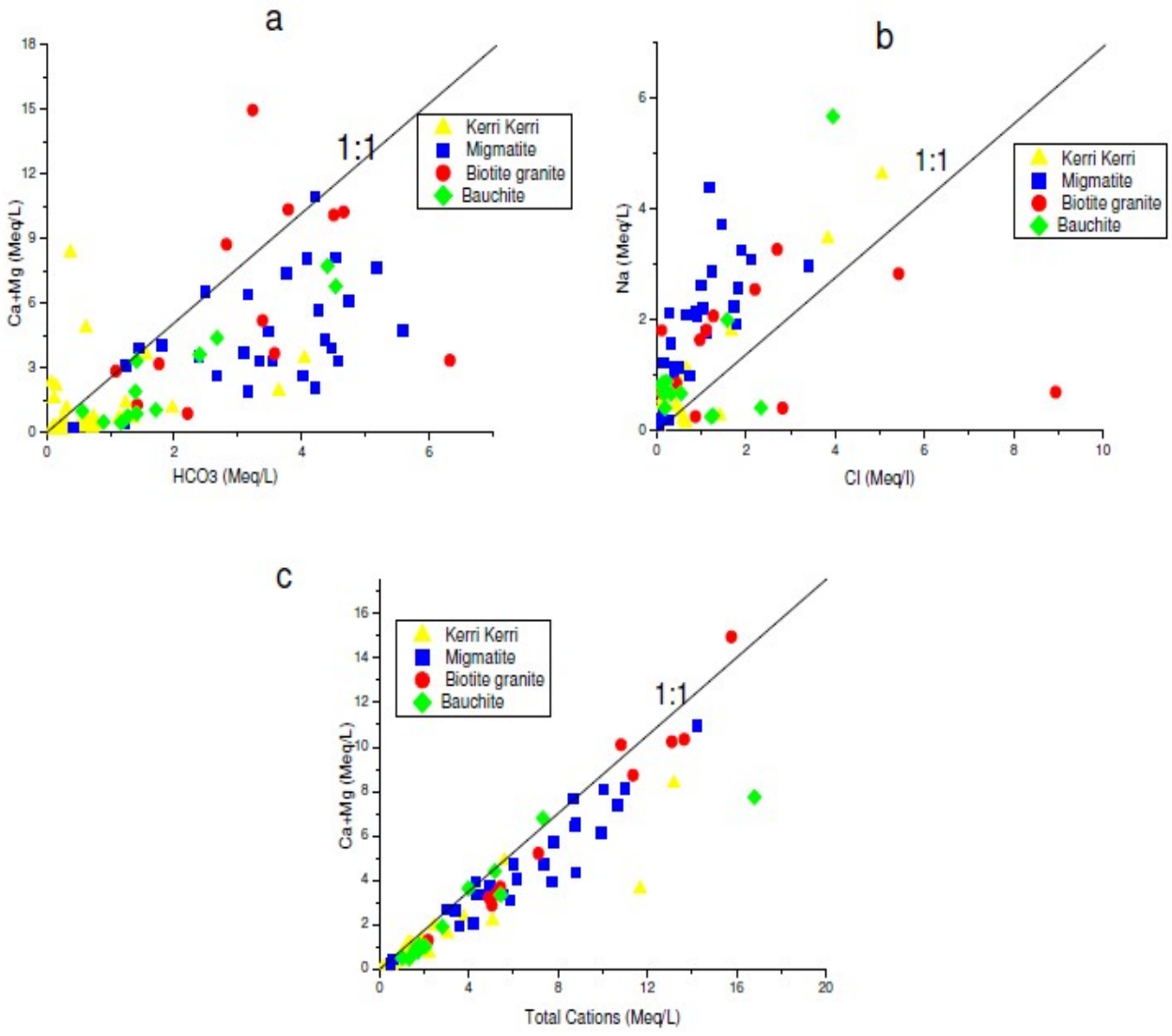

Fig. 4.44. Bivariate plots of (a) Ca^{2+} +Mg^{2+} vs. HCO_3, (b) Na^{+} vs Cl^{-}, (c) Ca^{2+} +Mg^{2+} vs. total cations

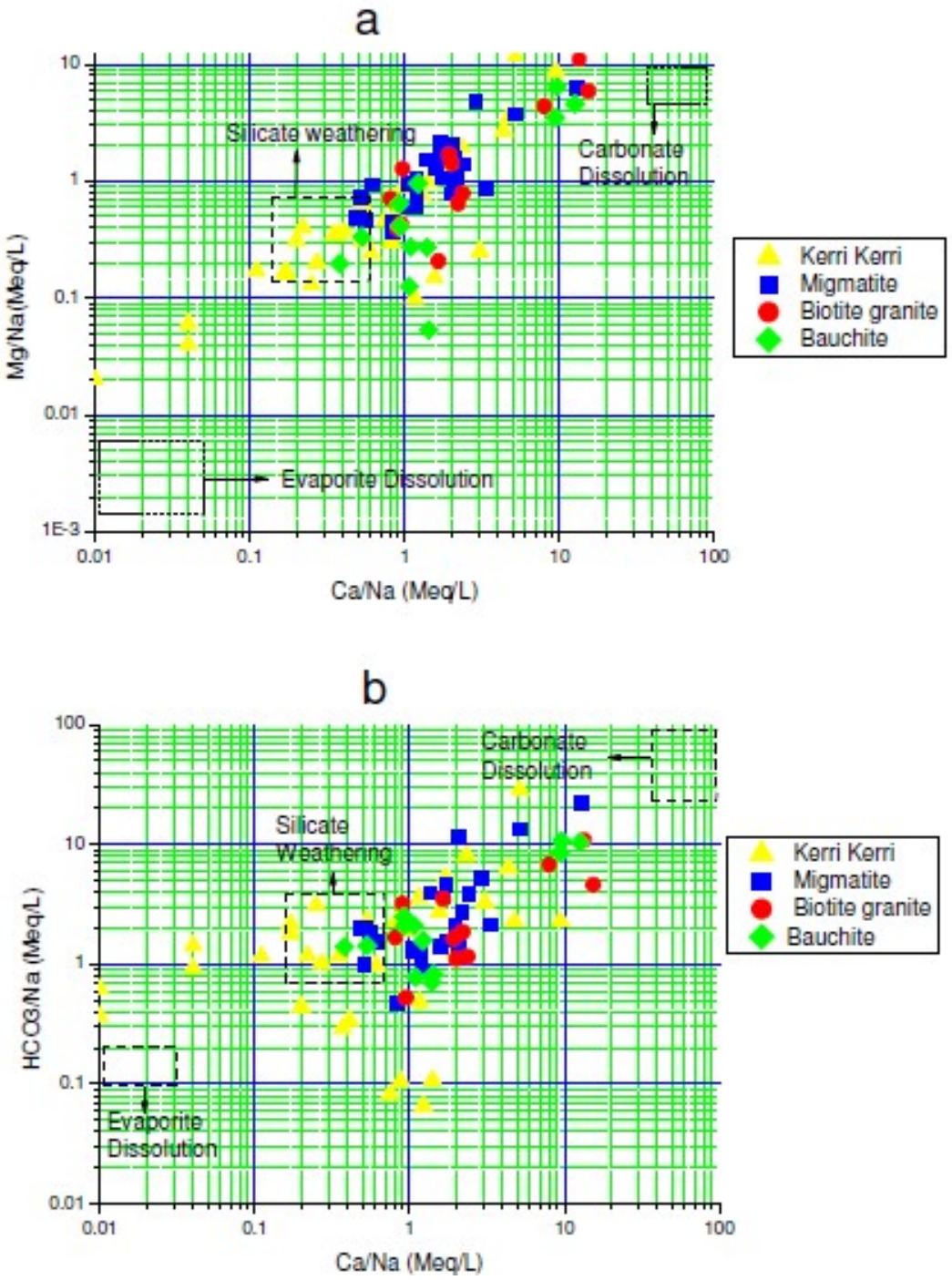

Fig. 4.45. Bivariate molar ratio plots of (a) Normalized Mg^{2+} versus Ca^{2+} and (b) HCO_3^- versus Ca^{2+} illustrating silicate weathering as the predominant control mechanism.

In a summary, the main mechanism responsible for the hydrochemical evolution of the aquifers is rock weathering as pointed out by the Gibbs plot and this was corroborated by Chadha plot which also revealed rock weathering as the dominant controlling mechanism in addition to cation exchange and reverse cation exchange. Ionic relationships of the dissolved chemical species (Fig.4.46) also pinpointed weathering of silicates as primary sources of ions in the studied aquifer. Low levels of Mg^{2+} and Ca^{2+} in some of the studied aquifers (Fig. 4.46a), could be ascribed to the formation of the secondary minerals. This is due to the fact that Mg^{2+} and Mg/Ca ratios are exceptionally small in low-salinity geothermal schemes because Mg^{2+} and Ca^{2+} are maintained in the solid phase during the formation of secondary minerals (micas, montmorillonite and kaolinite) and this in agreement with the studies conducted by Appelo and Postma 1993 and Morales *et al*., 2016.

4.8 Stable Isotope Analysis

In hydrology, stable isotope ratios are traditionally reported as per mil (‰) variance from those of a standard which use the notation δ (delta).

$$\delta \text{ (in ‰)} = (R_x / R_s - 1) \cdot 1000 \qquad (4.10)$$

Where R represents the heavy to light isotope proportions ($^{18}O/^{16}O$), and Rx and Rs are sample and standard ratios, respectively. Isotope ratios are often reported as permil deviations from SMOW (standard mean ocean water) as

$$\delta^{18}O = \left[\frac{(^{18}O / ^{16}O)_{sam} - (^{18}O / ^{16}O)_{SMOW}}{(^{18}O / ^{16}O)_{SMOW}} \right] \times 10^3$$

The use of SMOW should indicate that the measurements have been calibrated based on IAEA guidelines for expression of δ values, relative to the reference materials available on standardized permil scales (Coplen, 1994; 1996). A linear relationship has been created between δ^2H and $\delta^{18}O$ from samples of rainfall gathered from a global network of stations. This relationship represents the Global Meteoric Water Line (GMWL) given below;

$$\delta^2H = 8.\ \delta^{18}O + 10 \qquad (4.11)$$

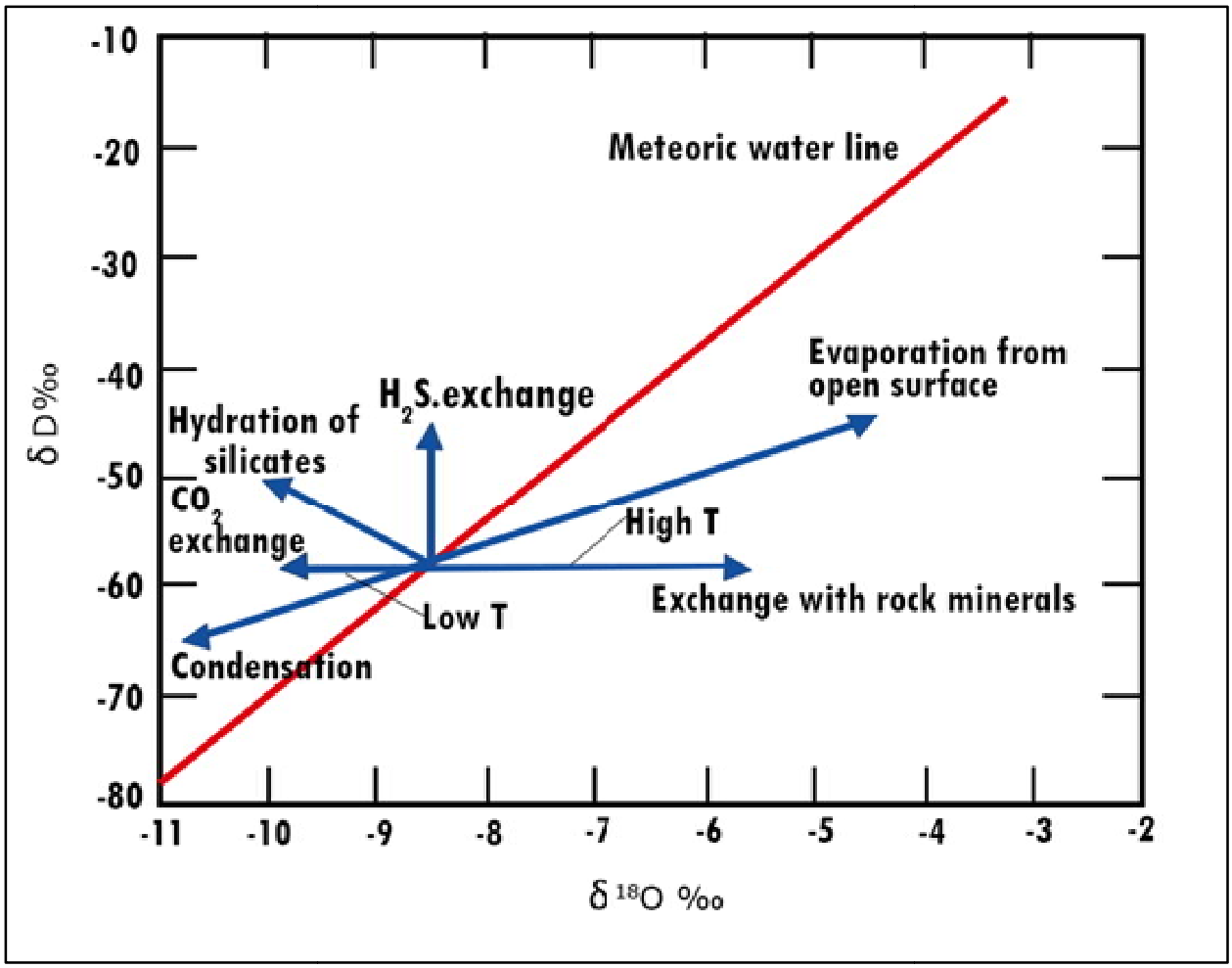

Fig. 4.46. Variations in stable isotope ratios of natural ware as controlled by chemical reactions and phase changes. (http://waterisotopes.org)

During isotope fractionation processes, the reacting phases (water and solutes) often develop unique isotopic fingerprints which is often indicative of the processes that formed them (Fig. 4.47). Isotopic fractionation is mainly influenced by the geology, origin of the water, climatic processes (condensation, evaporation, melting) and mixing (Faure, 1998). Two category of processes are responsible for isotopic fractionations: Equilibrium reactions and Kinetic processes (Aggarwal *et al*., 2009).

Stable isotope analyses of 45 groundwater samples in the Bauchi-Alkaleri-Kirfi area are shown in Table 4.23. The results revealed that the isotopic compositions of the studied groundwater samples in the area exhibit narrow range, from −5.36 to −2.79‰ and averages −3.7‰ for $\delta^{18}O$ and −29.2 to −17.4‰ with an average −23.1‰ of for $\delta^{2}H$, and suggest that majority of the samples are influenced by evaporation. This could have been occasioned by the semi-arid conditions in the area which are usually characterized by low rainfall and high sunshine which favours evaporation. The summary of the isotopic ratios of the different bedrock settings is presented in Table 4.21 while the detailed results are presented in Appendix XIV.

The compositions deuterium and oxygen18 isotopes in groundwater samples were plotted in alongside the global meteoric water line. (GMWL; $\delta^{2}H=8\ \delta^{18}O +10$; Craig 1961) as reference line. The stable isotope diagram (Fig. 4.47) shows that majority of the samples plotted to the right of the GMWL and the follow an evaporation line (linear regression line with a slope of 5.2) as defined by equation $\delta^{2}H = 5.2 * \delta^{18}O + 6.5$ (Clarke and Fritz, 1997; Nyende *et al*., 2013). This suggests that the recharge of aquifers is mainly via direct infiltration of rainfall with limited kinetic evaporation. Although, locations 6, 35, 46, 57 (in the Kerri-Kerri zone) and locations 56 and 61 (migmatite zone) and locations 66 and 78 in the charnockite aquifers, plotted on or to the left of the GMWL, suggesting depleted heavy isotopes arising from direct infiltration of recent precipitation.

S/n	Bedrock	δ18O (‰)			δ2H(‰)			D-excess(‰)		
		min	max	mean	min	max	Mean	min	max	mean
1	Migmatite/Gneiss(13)	-4.1	-2.1	-3.4	-25.8	-18.6	-25.8	6.24	12.94	8.79
2	Horbl-Granite(8)	-3.9	-3.2	-3.6	-22.0	-19.7	-24.7	2.00	9.68	6.36
3	Charnockite (7)	-4.0	-3.2	-3.6	-22.1	-17.4	-19.6	-016	14.25	5.40
4	Sandstones (17)	-5.4	-3.2	-4.1	-29.2	-20.2	-25.7	1.75	16.86	7.19

Table 4.23. Stable Isotope Results for Bauchi-Alkaleri-Kirfi area

.

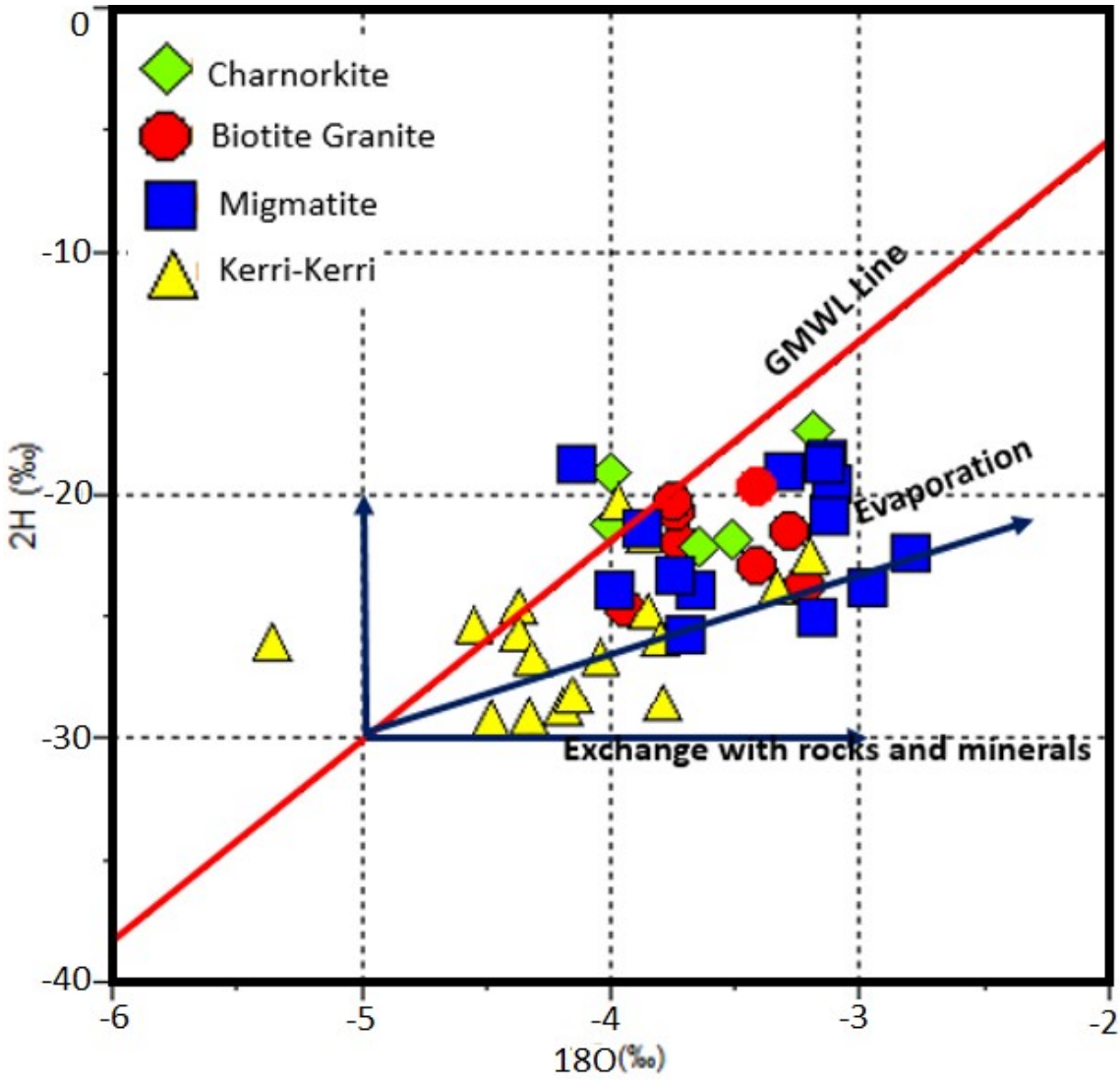

Fig. 4.47. Plot of Isotopic ratios of samples and Meteoritic Water Line for Groundwater of Bauchi-Alkaleri-Kirfi area.

A closer look at the groundwater from Kerri-Kerri revealed that they are more depleted than the groundwater from the basement setting suggestive of longer groundwater residence time in the sandstone aquifers.

As shown in Table 4.23, seventeen groundwater samples were analysed from the sedimentary aquifers (Kerri-Kerri) which revealed $\delta^{18}O$ range of −5.4‰ to −3.2‰ (ave. −4.1‰) and −29.2 to −20.2‰ with an average −25.7‰ for $\delta^{2}H$. 47% (8 out of 17) of the Kerri-Kerri samples, indicated kinetic evaporation prior to recharge as the fall along the evaporation regression line. However, groundwater samples from locations 6, 35, 46 and 87 constituting 24% plotted on or above the GWML indicating meteoric origin while sampling points 1,11,38,43 and 44 (29%) can be attributed to isotopic exchange with rocks minerals or rock water interaction (Fig. 4.47). In most aquiferous units, the isotopic composition of water remains unchanged, unless exchange with the oxygen in rock matrix. This process of exchange is called oxygen isotope-exchange with rock material and it is significant especially at elevated temperatures (about 31^{o}C).

The isotope composition of groundwater is essentially affected by ambient temperatures, thus, at increased temperatures, interaction with the rock matrix may perturb the isotope composition (Nyende *et al*., 2013). The water rock interaction process exhibited by samples 1, 11, 38, 43 and 44 of the Kerri-Kerri zone which all fall close to the exchange with rock mineral regression line (Fig.4.47) is attributable to the interaction of the rock matrix with the groundwater in deep sandstone aquifers, under ambient temperatures. It is important to note that these samples were collected in areas (Maianmaji) with reported cases of warm springs (Wikki warm springs).

As can be observed from the stable isotope plot (Fig. 4.47), most of groundwater samples from the basement setting (23 out of 28 samples) comprising of groundwater from the migmatite/gneiss, biotite hornblende granites and charnorckite settings which revealed isotopic composition of $\delta^{18}O$= -3.4‰ and $\delta^{2}H$=−19.6‰ (Table 4.23) plotted to the right of the GMWL and are consistent the linear regression along an evaporation line, which suggests meteoric water subjected to kinetic evaporation prior to recharge. However the remaining 5 groundwater samples (52, 53, 66, 71 and 78) from the basement setting

plotted on or to the right of the GWML suggesting direct recharge from meteoric water. On a general note, 79% of the groundwater from the Basement Complex settings are derived from evaporated rainfall water, while the remaining 18% revealed a direct meteoric recharge. The stable isotope plot showed that groundwater samples from the Kerri-Kerri aquifers occupy the lower parts of the GWML and the evaporation regression line while the groundwater from the basement setting plot in relatively upper zones of the GMWL and the evaporation slope. This scenario suggests that groundwaters in the sedimentary units are far more depleted owing to their generally deeper nature with average depth of 35m as compared to 16.1m in the basement settings which are less depleted suggesting that this shallow wells receives more seasonal meteoric recharge as compared with the deep sandstone aquifers of the Kerri-Kerri.

From the above discussion it can be concluded that the sandstone aquifers are relatively more depleted in heavy oxygen (δ18O= -4.1‰), and deuterium isotopes (δ2H=−25.7‰) as compared with the basement setting ($\delta^{18}O$= -3.4‰ and δ2H=−19.6‰) and this could be due to the fact that the groundwater in the sedimentary units have more residence time as compared to those of the basement terrain.

4.8.1 Deuterium excess (D-excess) of groundwater samples

To further unravel the impact of evaporation in changing the isotopic character of precipitation prior to groundwater recharge, a parameter known as the deuterium-excess (D-excess) was evaluated from the isotope ratios of the groundwater samples. D-excess' is described as the surplus deuterium that is unaccounted for by equilibrium fractionation between water and vapour. The deuterium excess (δ-excess) is given as δ (%) = δ^2H - 8 $\delta^{18}O$ (Dansgaard, 1964). The 'δ-excess' is mostly applied to kinetic fractionation exemplified by evaporation (Dansgaard, 1964; Clark and Fritz, 1997). It is important to note that relative humidity is a key ingredient of kinetic fractionation. Thus, in the Global Meteoric Water line 'd-excess' value of 10 represents evaporation at 85% relative humidity. Although, the'd-excess' value associated with regional rainfall can exceed 10 if the region's evaporation occurs under lower humidity (Gat and Carmi, 1970). It can be observed from Fig. 4.48 that the 'd-excess' values for most of the wells are less than ten

in most part of the Bauchi-Alkaleri-Kirfi area except in some parts of the basement settings to the northwest and some small pockets in Kerri setting in the northeastern and northwestern parts. 7 out of 45 of the wells (location 53,66 and 78 in the basement area and locations 6,35,46 and 87 in the sedimentary part) analysed, showed 'δ-excess' $\geq$ 10 and are thus presumed to represent principal precipitation in the Bauchi-Alkaleri-Kirfi area, the low 'δ-excess' values (< 10) observed in the majority of the analysed samples (75%) could be attributed to significant contribution of evaporation to the rainwater enriching the remnant groundwater with lower δ-excess values. This is in tandem with the regression line slope values for analysed groundwater samples being lower than GWML (precipitation). Furthermore, the bivariate plot of D-excess against $\delta^{18}O$ (Fig. 4.48) further corroborated that role of kinetic evaporation in the recharge process in the Bauchi-Alkaleri-Kirfi area as the depletion of $\delta^{18}O$ coincided with gradual decrease of d-excess of the studied groundwater hence, Indicative of groundwater evaporative influences (Allison and Hughes, 1983).

A closer look at the Fig 4.48, revealed two major trends (indicated by blue circles I &II) with respect to the depletion of δ18O. The first trend discernible from group I revealed that the aquifers in the sedimentary setting showed more levels of depletion in $\delta^{18}O$ ($\delta^{18}O$ values falling between -3.73 to -5.5 permil). This scenario is attributable relatively older groundwater system with longer residence time with limited influence from recent recharge by meteoric water.

Conversely, the second group (group II), comprising of mostly of groundwater from the Basement Complex setting revealed comparatively lesser amount of depletion of $\delta^{18}O$ ($\delta^{18}O$ values between -3.75 to -2.5 permil) which can be ascribed to the replenishment of the saprolitic units by recent meteoric recharge. In addition, the basement wells which are mostly shallow in depth receives more precipitation during rainy season, which as a result leads to the relatively lesser amounts of the depletion of stable isotopic composition of the groundwater system.

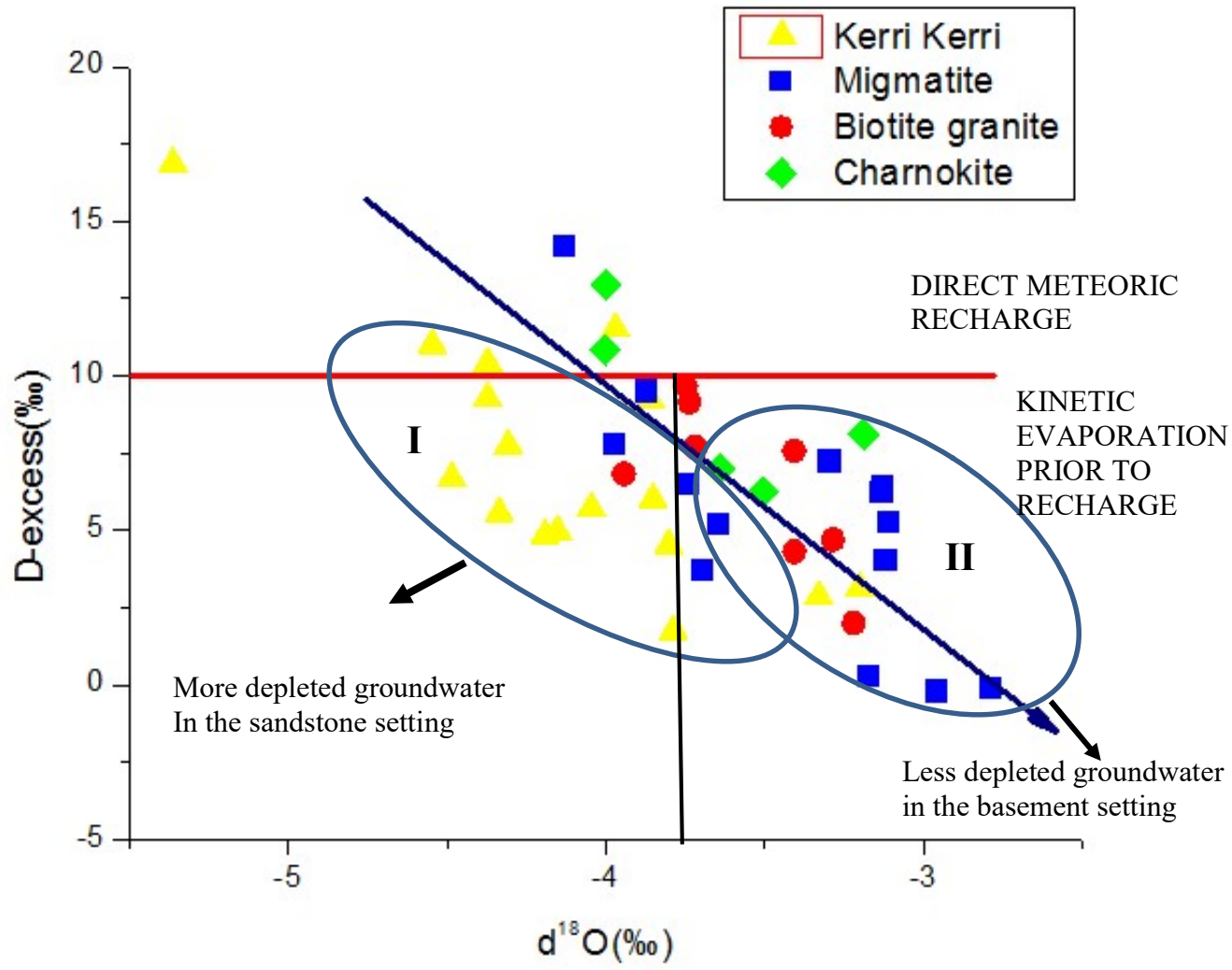

Fig. 4.48. Scatter diagram of D-excess vs. δ ^{18}O in Bauchi-Alkaleri-Kirfi area,

4.8.2 Origin of dissolve ions in the groundwater

Over the years stable isotopes have proven to be very instrumental in identifying the mechanism of salinization in various water sources (Gibrilla *et al*., 2010). The mechanism responsible for salinization and nitrate enrichment in the groundwater of Bauchi-Alkaleri-Kirfi areas are shown in the cross plot of Cl vs. $\delta\ ^{18}O$ in Fig. 4.49a and NO_3 vs. $\delta\ ^{18}O$ in Fig 4.49b. As can be observed in both figures, when the data are considered holistically, no distinct trend was observed but when the data was divided into separate clusters exhibiting similar behaviors, two main group of waters have been identified. As revealed in Fig 4.49a, in the first group the chloride levels in the groundwater appears to be lower (<75 mg/l) with the sandstone aquifers which are generally more depleted and occurring at deeper aquifer settings revealed even lower concentrations (< 25 mg/l) while the chloride levels gradually increased in the less depleted groundwater which characterised mostly by the basement bedrocks which are relatively shallower. This scenario suggests that the Cl are attributable to anthropogenic processes which predominantly affects the shallower wells in the basement setting. In the second group however, depletion influenced by kinetic evaporation can be observed from samples above with chloride levels above 75mg/l. As can be seen in Fig 4.49b, the nitrates also showed the same trend as the chlorides.

By and large, it can be concluded that in the deeper wells exemplified by the sedimentary setting (majorly) the chloride and nitrate levels are generally lower, attributable to limited influence of evaporation on one hand and the increased denitrification with depth on the other hand. However, in the shallow basement setting, there is a gradual increase in the concentration of Cl and NO_3 attributable to kinetic evaporation on one hand and increased influence of anthropogenic processes relating to dumpsites, sewage and agro pastoral activities in the research area.

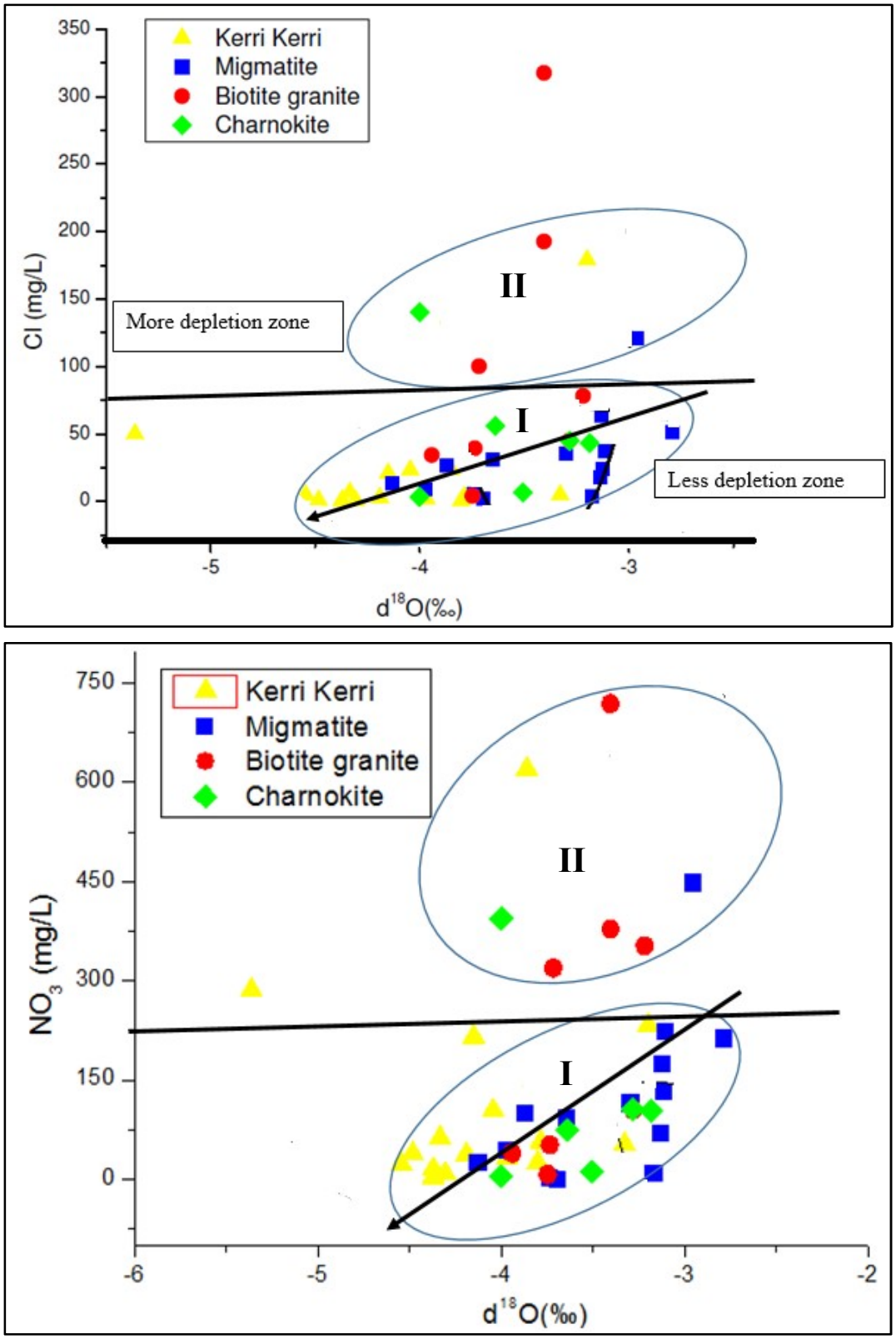

Fig. 4.49 (a) Scatter diagram of Cl vs. δ ^{18}O n Bauchi-Alkaleri-Kirfi area.

(b) Scatter diagram of NO_3 vs. δ ^{18}O in samples.

4.8.3 Latitude (Continental) Effects

When the isotopes data from the Bauchi-Alkaleri-Kirfi area is considered in a regional perspective and compared with similar works from other geographical locations in Nigeria, a trend that reflect continental effect was observed. As can be seen from the Fig. 4.50, the trend revealed decreasing $\delta^{18}O$ and $\delta^{2}H$ with declining annual precipitation which is in tandem with the conventional depletion of stable isotopes with decreasing rainfall and increasing latitude as it tracks northward from the south western coast of Nigeria inland as observed by Lapworth *et al*. (2013).

As shown in Fig. 4.50, the groundwater stable isotopes composition in the analysed samples displayed two discernible trends, the first group of the samples comprising more depleted samples plotted close to stable isotopes samples for north eastern Nigeria as outlined by Edmunds *et al*. 1999; Favreau, 2000 and Lapworth *et al*., 2013, who have differently conducted stable isotope studies of groundwater in north eastern parts of the country, although this studies were in the far northern sahelian zones exemplified by Maiduguri in Bornu area (Edmunds *et al*. 1999; Favreau, 2000) and in Gusau in Zamfara area (Lapworth *et al*., 2013).

The second group of samples which were however less isotopically depleted were located closer to stable isotopes data from Zaria (Kaduna area) and Minna (Niger area) in the north central parts of Nigeria (Adanu, 1991; Lapworth *et al*., 2013). This scenario is attributable to the difference in the rainfall distribution in the zones where the aforementioned group of samples were collected. The first group which are predominantly from the sedimentary zone (with average rainfall of 850mm) have deeper aquifers with more depleted groundwater as compared to the second group of samples which in most cases occupy the basement complex areas characterized by shallow wells and relatively higher rainfall distribution (1000 mm) associated with seasonal meteoric recharge, hence less depleted.

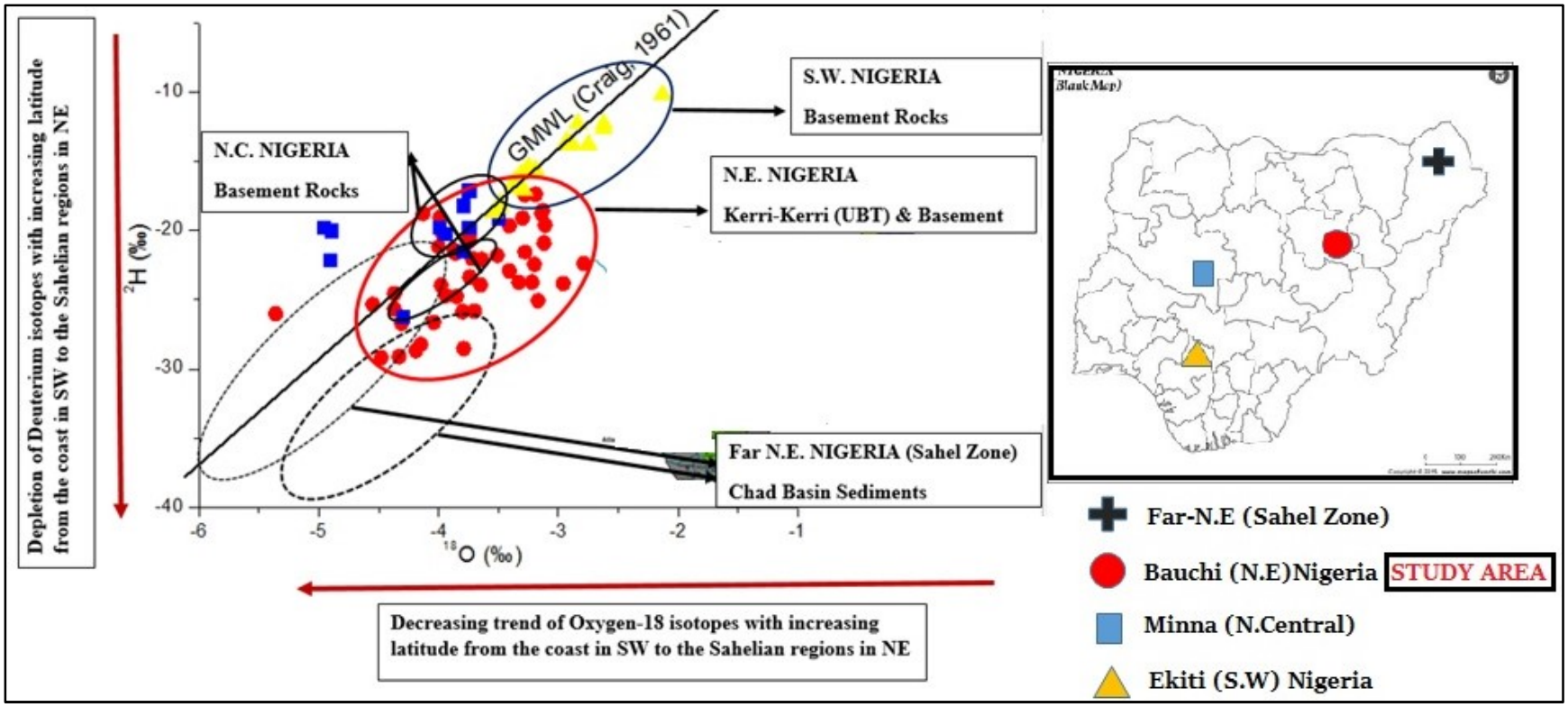

Fig. 4.50. Continental (latitude) Effects on Isotope Composition with Distance from the Coast Inland

When the samples from the Bauchi-Alkaleri-Kirfi transition zone were compared to isotope data from Ekiti area which is further southwest and closer to the coast (Talabi and Tijani 2013), the samples in the Ekiti area revealed less depletion in the isotopes and this is a reflection of increasing depletion in stable isotopes with increasing latitude and distance from the coastline (Gulf of Guinea) which signifies latitude effect (Lapworth *et al.,* 2013). Based on the above premise, the effects of decreasing precipitation and latitude on the stable isotopic composition of groundwater in the study area has been established and this has revealed that stable isotopes in groundwater are influenced by changes in latitude. By implication as one moves from the coast in the southwest of the country to the sahelian regions in the northern parts, an appreciable depletion is observed in the isotopic composition of groundwater owing to rain-out or latitude effect. This also implies that the isotopic composition of rainfall also decreases as you move inland from the shores of the country and this scenario has a direct impact on the groundwater as well.

4.9 Synthesis

This section describes the overall integration of the interpreted result from this research to produce a cross sectional model highlighting the processes involved in groundwater evolution in the Bauchi-Alkaleri-Kirfi transition zone. The cross sectional model is presented in Fig.4.51 and elucidated in the subsequent paragraphs. As can be seen from the cross sectional model presented in Fig. 4.51, the area is underlain by Basement Complex rocks in the eastern half and the Kerri-Kerri Formation to the western portions. The groundwater potential index derived from integration of surface/ hydrological and subsurface hydrogeological thematic maps indicated low to medium indices in the basement setting while the sedimentary setting revealed moderate to high indices. The pore-type aquifers characterises the sedimentary zones which are generally thicker and more prolific as suggested by the groundwater productivity map of the Bauchi-Alkaleri-Kirfi area. The basement terrain however, constitute saprolitic units of limited permeability and yield. This conclusion is in tandem with Eduvie, 2006.

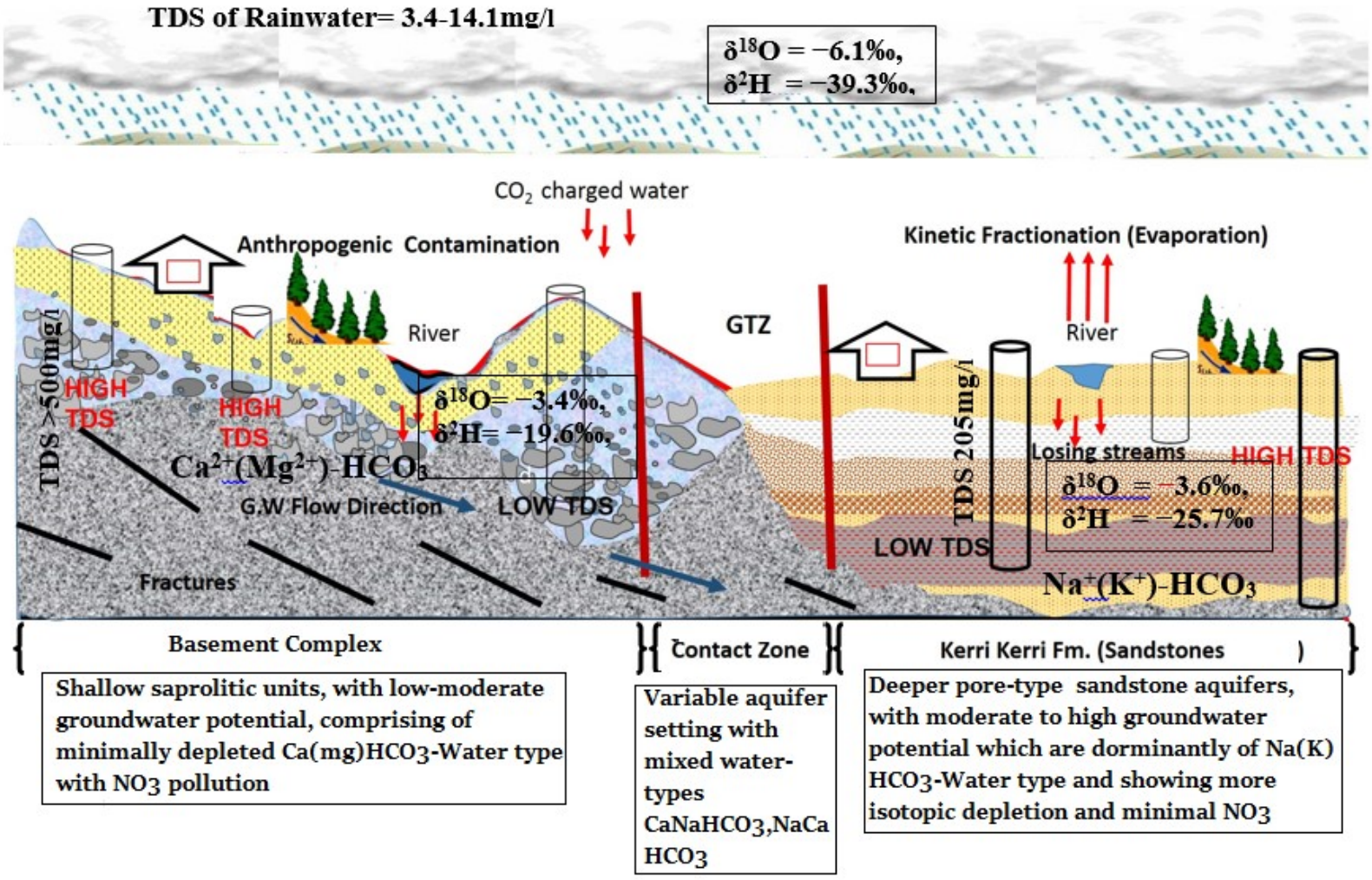

Fig. 4.51. Cross-sectional Model Highlighting the Processes involved in the Evolution of Groundwater in Bauchi-Alkaleri-Kirfi area.

The well inventory studies revealed that the wells in basement settings have shallower depth (average of 15m) rendering them more susceptible to pollution from anthropogenic sources as revealed by high concentration of nitrates (137.15 mg/l) in the basement setting as compared to wells tapping the sedimentary aquifers which generally have greater depth (average of 37m) and showed minimal contamination from anthropogenic factors. Furthermore, the total dissolve solids were generally higher in the groundwater from the basement setting (512 mg/l) as compared to the sedimentary terrain implying that the groundwater from the sandstone aquifers have limited migratory history (TDS of 205 mg/l). As presented in the flow chart in Fig. 4.52, the chemical analysis of groundwater from the basement setting revealed that the predominant hydrochemical facie in this setting is the $Ca^{2+}(Mg^{2+})$-HCO_3^-, arising from CO_2-charged meteoric recharge and silicate weathering which is in agreement with Malomo, 1983.

Conversely, the hydrochemical analysis of the groundwater from the sedimentary setting revealed lower amounts of dissolved ions as reflected by the low TDS values (205 mg/l) and the dominant water type in the sandstone aquifers is Na^+ (K^+)-HCO_3^-, which is a product of action exchange reaction leading to the replacement of Ca^{2+} ion in the groundwater with Na^+ from the lacustrine clays of the Kerri-Kerri depositional environment reported by Adegoke *et al*., 1989. As observed in the cross-sectional model (Fig. 4.51), the groundwater in the study has a narrow isotopic variation, which indicates the groundwater originated from the same source and area of recharge, which is predominantly from rainfall. The isotopic fingerprints for rainfall in the study region as reported is $\delta^{18}O = -6.1‰$, $\delta^2H = -39.3‰$, as compared to $\delta 18O = -3.4‰$, $\delta^2H = -19.6‰$ in the basement setting and $\delta^{18}O = -3.6‰$, $\delta^2H = -25.7‰$ in the sedimentary setting. This scenario revealed a gradually increasing depleting trend as you move from the rainfall to the shallow basement aquifers and even more depletion in the deeper groundwater from the Kerri-Kerri aquifers. Furthermore, the above inference connotes that the shallow basement wells receives more seasonal meteoric recharge, thus less depleted than the groundwater from the sedimentary setting which appears to have longer residence time owing to the greater depth of the wells and limited precipitation in such terrain.

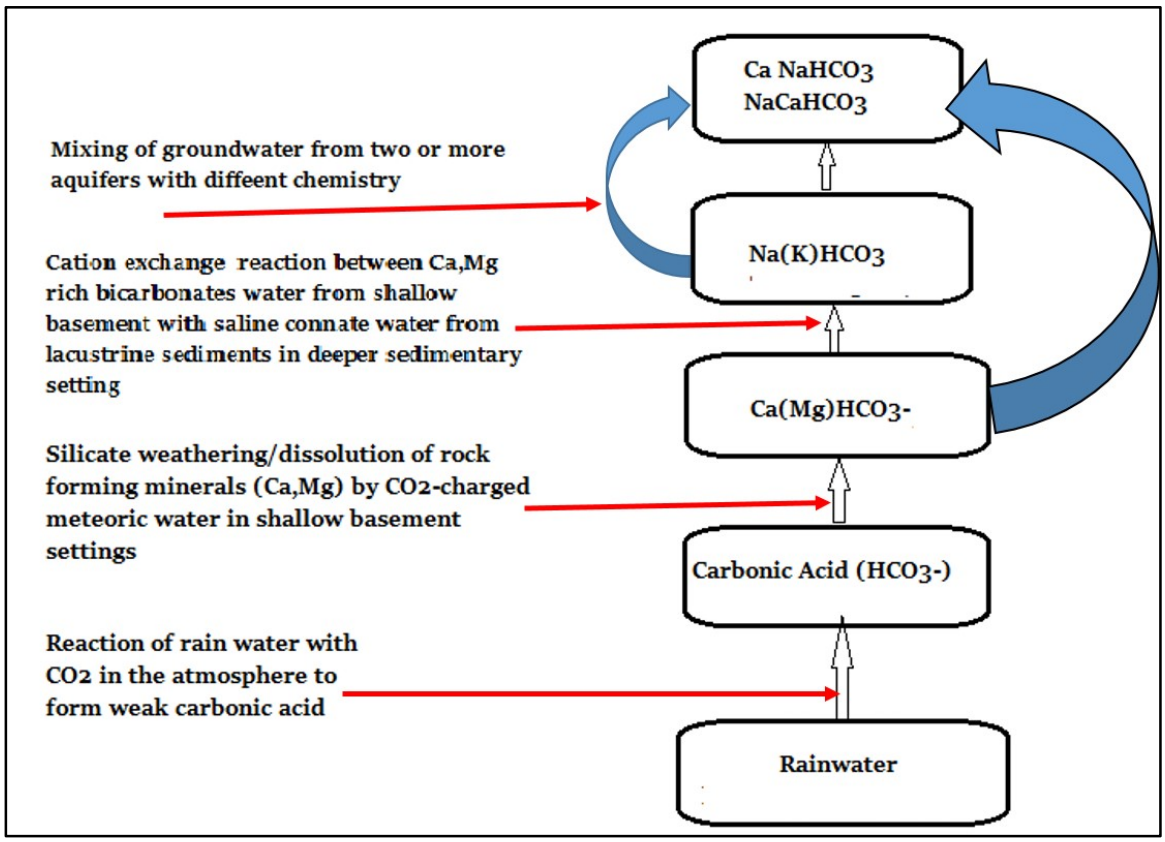

Fig. 4.52. A Flow Chart Highlighting the Processes involved in the Hydrochemical Evolution of Groundwater in the Bauchi-Alkaleri-Kirfi transition zone.

CHAPTER FIVE

SUMMARY, CONCLUSION AND RECCOMMENDATIONS

5.1 Summary

The ultimate goals of this research is to characterise the aquifers in the geological transition zones of southwestern Bauchi, to evaluate the hydrochemistry and to investigate the stable isotopic fingerprints of the groundwater in the Bauchi-Alkaleri-Kirfi area. Three distinct methods were used to accomplish the study goals set. The first method was focused on remote sensing/GIS, geophysical information and MCDA integration to evaluate aquifer characteristics and also delineate the prospective zones for groundwater exploitation in the geological transitional zones of Bauchi-Alkaleri-Kirfi areas, NE, Nigeria. The strategy to the research involved the integration of 10 thematic maps from remote sensed information (Aster data and Landsat 8), conventional maps and geophysical data (geo-electrical sounding and aeromagnetic data). The thematic maps consisting of 6 surface and hydrological parameters (elevation, slope, drainage density, soil, rainfall distribution land use/cover) and 4 subsurface themes (lineaments, geology, and aquifer resistivity and aquifer thickness) were generated using the ArcGIS 10.1 software. The thematic maps were assigned appropriate weights using the Saaty scale 1-9 based on the comparative control of the thematic layers on the occurrence of groundwater. Using the analytical hierarchical process (AHP) multi decision criteria analysis (MCDA). The thematic maps assigned weights were compared in pairs and normalized accordingly. Based on the hydrological parameters, the Kerri-Kerri Formation aquifers displayed sandy and alluvium top soils, characterised by dominantly bare land, scrub land and forest land use, low-medium elevations, gentle slopes, high percentage of low- medium drainage density values and dominantly low to moderate rainfall distribution. All the aforementioned characteristics are reflective of the good groundwater prospective areas. Conversely, in the basement areas, the aquifers formed

over the gneissic rocks have top soils that are partlysandy loam and mostly sandy clay loam, medium to high elevation, bare land is the dominant land use and slopes are generally moderate to high, moderate drainage density and medium rainfall distribution. Most of the saprolitic units in the migmatite /gneiss zone suggests medium groundwater potential ratings. Furthermore, the biotite hornblende granites which show great similarity with the migmatite/ gneiss zones have top soils that are partly mostly sandy clay loam, dominantly highly elevated, bare land is the dominant land use, slopes and drainage density are generally moderate to high, and low-medium rainfall distribution. The charnockite which are restricted to the southwestern flank of the Bauchi-Alkaleri-Kirfi area are characterised largely by sandy clay loam and partly sandy loam soils, dominantly highly elevated, varied land use which encompasses water body, built up, bare land and shrub land, slopes are generally high (relatively higher percentage of steep slope areas), high drainage density and medium rainfall distribution. The occurrence of built up areas, steep slope and high drainage density in the charnockite zones could hinder groundwater recharge.

From the hydrogeological perspective, the Kerri-Kerri Formation are dominantly sandstones ranging from fine to coarse grained and partly clays, characterised by depth to magnetic basement of 0-1045m, low lineament density, dominated by resistivity of 1000-3000Ωm and 300-1000Ωm, aquifer and overburden thickness of 35 to >50m. By contrast, in the Basement Complex areas, the migmatite/gneiss aquifers consisting of saprolites, are characterised by depth to magnetic basement of 0-45m, moderate to high lineament density, dominated by resistivity of 151-400Ωm and partly 400-.≥750 Ωm, aquifer and overburden thickness of 15 to >50m. Furthermore, the biotite hornblende granite aquifers are also typified by depth to magnetic basement of 0-45m, moderate lineament density, dominated by resistivity of 51-150Ωm and 400-.≥750 Ωm, aquifer and overburden thickness of <10 to 35 and 35- >50m. Lastly, the charnockite aquifers revealed depth to magnetic basement of 0-45m, low lineament density, dominated by resistivity of 51-150Ωm, others resistivity zones that characterise the charnockite zones are 0-50Ωm, and 400- ≥750 Ωm, aquifer and overburden thickness of <10 to 35m. Arising from the hydrogeological assessment, the aquifers in the Kerri-Kerri areas were found to be generally thicker but more argillaceous (especially in the central parts) than those of the

Basement Complex zones. Also, the bedrock of the latter are comparatively more deformed as pointed out by the aeromagnetic studies, hence will contribute more to their groundwater potential. The general evaluation of the characteristics of the aquifers in the Bauchi-Alkaleri-Kirfi area revealed that the hydrologically derived characteristics conforms with the hydrogeologically derived parameters and all indicated that the Kerri-Kerri sandstones are the most prolific, seconded by the aquifers of the migmatite/ gneiss region. The biotite hornblende granites are rated higher than the bauchite aquifers, which displayed poor aquifer properties and generally low groundwater potential zone. The final combination of the derived thematic maps using the weighted overlay method followed, which delineated the Bauchi-Alkaleri-Kirfi area into three distinctive regions, namely: poor zones, covering 645.1km^2 (21.12%), moderate zones, occupying 1134.1km^2 (34.12%) and good zones constituting 1275.8 km^2 (41.8%) of the area. The areas underlain by the Kerri-Kerri Formation correspond to the good groundwater potential zones as revealed by the high groundwater potential index of (3.2- 4.0), compared to the moderate potential of migmatite/ gneiss and part of the biotite hornblende granites with GWPI of (2.6 -3.2). Low groundwater potential index of (1.69-2.6) characterise the charnockite and parts of biotite hornblende granite areas, although the latter are rated higher than the charnockite because some percentage of moderate GWP zones exist within granitic aquifers. Furthermore, the characterisation of the aquifers in the Bauchi-Alkaleri-Kirfi area was carried out using the hydrological and hydrogeological parameters in line with objectives of the study. The groundwater prospect map was validated with pumping test data from 120 existing wells within and around the Bauchi-Alkaleri-Kirfi area. The wells with the highest values of productivity were found to be situated in the good GWP zones delineated by the groundwater prospect map of the study. The validation of the groundwater potential map showed good correlation with the well yield obtained from existing wells in the study, thereby justifying the efficacy of GIS techniques in identifying target zones for more detailed evaluation and well siting.

The second approach comprise a more qualitative aquifer characterisation and entailed the hydrochemical analysis of 87 groundwater samples spread across the different lithologies in the study. The samples were collected in accordance with AHP standards and tested for major anions and cations in the Water Science Laboratory at the University

of Nebraska in Lincoln, USA. The results of the hydrochemical analysis was utilized in determining the drinking and irrigation water quality of the different aquifer waters, the hydrochemical facies and the mechanism responsible for the evolution of the hydrochemistry of the aquifers. The percentages of groundwater of poor and unsuitable WQI in the study are more in the basement rocks as revealed by 66.7% in the biotite hornblende granite aquifers, 59.3% in the migmatite/gneiss aquifers and 41.7% in the bauchite aquifers as compared to 19.4% in the Kerri-Kerri aquifers. Similarly 75% of samples from the Kerri-Kerri aquifers fall under the good and very good WQI category, followed by the bauchite aquifers with 50% and the biotite hornblende granite and migmatite having 25% and 22.5% respectively. The general evaluation of the water quality of the Bauchi-Alkaleri-Kirfi area revealed that anthropogenic factors are largely responsible for evolution of the quality of groundwater in the area. By contrast, the basement aquifers especially the charnockite and the biotite hornblende granite aquifers would be best suited for irrigation or agricultural purposes, followed by the migmatite/gneiss aquifers. The sandstone aquifers however, are likely to be less suitable for irrigation use, owing to their high percentages of poor KR and SSP ratings, by implication the aquifers of the Kerri-Kerri formation have the tendency to enrich irrigated soils with magnesium overtime on one hand and on the other hand the aquifers are easily enriched with sodium during cation exchange process giving rise to high K.R and SSP values. Hydrochemical facie evaluation of the groundwater from the Bauchi-Alkaleri-Kirfi area revealed that most of samples (50.6%) correspond to Ca^{2+}-Mg^{2+}-HCO_3^- while Na^+-K^+-HCO_3^- , Ca^{2+}-Mg^{2+}-$Cl^-SO_4^{2-}$, and Na^+-K^+–Cl^--SO_4^{2-} types represented 14.1%, 3.5% and 3.5% respectively. The remaining 28.2% fall under the mixing zone with no abundant ion (Ca-Na-HCO_3, Ca-Na-HCO_3-Cl, Mg-Na-Ca-HCO_3, Na-Ca-HCO_3 and Na-Ca-K-Cl). A general dominance of the Ca^{2+}-Mg^{2+}-HCO_3^- facie was observed in the basement aquifers which is a product of CO_2-charged meteoric recharge and dissolution of silicate minerals in the basement complex aquifers. It was also observed that 74% (20 samples) of the migmatite/gneiss aquifers fall under the Ca^{2+}-Mg^{2+}-HCO_3^- water type, while the biotite hornblende granite, bauchite and the Kerri-Kerri aquifers revealed 66.7%, 50% and 26.5% respectively. The distribution of the Na^+-K^+-HCO_3^- facie which is predominant in the sandstone aquifers with 32.4% as compared to 8.3% in the bauchite

aquifers and totally absent in the migmatite and biotite hornblende granite aquifers respectively is a reflection of the dominance of the alkalis over the alkali earth in the sedimentary zones.

The coexistence of sodium ion (Na^+) and bicarbonates (HCO_3^-) in some of the studied groundwater also indicates the likelihood of ions exchange reactions that may be associated with the low-medium geothermal temperature scheme (Saemundsson, 2009).This is substantiated by the presence of clay rocks (e.g., kaolin) in the Kerri-Kerri formation which are known to provide the required exchangers for the base ion exchange process. In addition to the delineation of the various hydrochemical facies in the study, the mechanism/processes responsible for evolution of the dissolved species in the groundwater was found to be rock weathering as pointed out by the Gibbs plot and corroborated by Chadha plot which also revealed rock weathering as the dominant controlling mechanism in addition to cation exchange and reverse cation exchange. Ionic relationships of the dissolved chemical species also pinpointed weathering of silicate minerals as the main sources of ions in the studied area.

The third approach deployed was the stable isotope analysis for deuterium and oxygen in 45 groundwater samples in the Bauchi-Alkaleri-Kirfi area, which suggests that 79% of the Basement Complex waters are derived from evaporated surface water, while 18% of the waters, which are mostly restricted to the mountainous north-west zones of the study revealed a meteoric source. 47% of the Kerri-Kerri samples were derived from recent meteoric recharge with limited kinetic evaporation. The sandstones (24%) samples plotted on or above the GWML indicating meteoric origin while 29% of the samples can be attributed to isotopic exchange with rocks minerals or rock water interaction. From the stable isotope plot it can be concluded that the Kerri-Kerri aquifers are relatively more depleted in heavy oxygen ($\delta^{18}O$= -4.1‰), and deuterium isotopes ($\delta^{2}H$=−25.7‰) as compared with their basement counterparts (δ18O= -3.4‰ and δ2H=−19.6‰) and this could be attributed to latitude effect and longer residence time. It is noteworthy that the result of the stable isotope studies further corroborates the fact that, rock minerals dissolutions is the major controlling factor for the hydrochemistry in the Bauchi-Alkaleri-Kirfi area.

When the isotopes data from the Bauchi-Alkaleri-Kirfi area is considered in a regional perspective and compared with similar works from other geographic locations in the country, the stable isotopes results displayed two discernible trends, while a group of the samples) were consistent with stable isotopes results of north eastern Nigeria as outlined by Edmunds et al. 1999; Favreau, 2000 and Lapworth *et al*., 2011), the second group of samples however, show more similarity to the results of stable isotopes from central Nigeria (Adanu, 1991; Lapworth *et al*., 2011). When the samples were compared to results from Ekiti area which is further south and closer to the coast (Talabi and Tijani 2013), the samples from Ekiti showed less depletion in the isotopes and this is a reflection of increasing depletion in stable isotopes with increasing latitude and distance from the coastline which is attributable to the so-called latitude effect (Lapworth et al., 2011).

From the above discourse, it would be observed that the present study has not only contributed to knowledge of hydrogeology of geological transition zones (GTZ), especially in terms of groundwater quality, hydrochemistry and stable isotope assessments; which are consequential to sustainable management of the groundwater system of these zones, it has also shown the efficacy of the GIS tool in the aquifer characterisation. It is also worthy of note that the quality, hydrochemical and isotope characteristics of groundwater in GTZ, which have not received much attention has been adequately captured by this study, making the present work a good contribution to the existing body of knowledge.

5.2 Conclusion

This study shows that despite the subjective nature of RS/GIS in mapping groundwater potential zones using hydromorphogeological or surface parameters, the technique has proven to be an efficient approach in characterising groundwater potential. Integrating RS/GIS with other subsurface techniques such as hydrogeophysical and hydrochemical is an even better approach. An additional reason why the integrated approach is useful is that it reduces the bias nature of the single technique by accounting for other subsurface processes which are equally consequential in the distribution of groundwater in a region.

In line with the objective of this study, the quantitative and qualitative characterisation the aquifers and groundwater prospective areas in Bauchi-Alkaleri-Kirfi area has been undertaken using and integrated RS/GIS, hydrogeophysics, hydrochemical and stable isotope approach.

In this research, prospective groundwater areas were delineated by the integration of 10 thematic maps prepared from remotely sensed information (Aster data and Landsat 8), conventional maps and geophysical data (geo-electrical sounding and aeromagnetic data). The thematic maps consisting of 6 surface hydrological parameters (elevation, slope, drainage density soil, rainfall distribution and land use/cover) and 4 subsurface thematic layers (lineaments, geology, aquifer resistivity and aquifer thickness) were generated using the ArcGIS 10.1 software. Using the analytical hierarchical process (AHP) multi decision criteria analysis (MCDA), the weights assigned to the thematic maps compared in pairs. The final overlay analysis of the thematic layers created a groundwater potential model which delineated the study into good, moderate and poor groundwater potential zones. The validation of the resulting map with pumping test data showed good correlation. The aeromagnetic data revealed basement topography map gave a clearer picture of the lateral and basal contact between the rocks in the immediate fringes of the geological transition zones. In addition, the aeromagnetic data also revealed the preponderance of lineaments in the basement terrain as compared with sedimentary zones. The interpretation of VES data indicated generally 3-5 geo-electric layer system with aquifer thickness of 11-158m in the sandstones units. However, the Basement Complex areas revealed saprolite thicknesses of 2.4-83.8m (migmatite/gneiss), 1.3-67.3m (granite) and 1.2-44.6m (charnockite), suggesting favorable aquiferous medium in the migmatite/gneiss units. Saprolites and medium to coarse sandstones are the aquiferous units in the Bauchi-Alkaleri-Kirfi areas.

Assessment of hydrochemical information from the research region unraveled groundwater system's hydrochemistry, quality and stable isotope fingerprints in aquifers. The interpretation of the hydrochemical data in the Bauchi-Alkaleri-Kirfi areas revealed mostly fresh water ($15 \leq TDS \leq 1588$ milligram/L) which isminimallymineralized.

Further, the results showed that groundwater is slightly acidic to alkaline in nature ($5.0 \leq pH \leq 8.5$) and 55% of samples falls soft to moderate category ($TH \leq 150$ mg/L). The elevated nitrate (>50 mg/L) and conductivity values (> 1000 mg/L) of some of the wells suggests influence of anthropogenic contamination. The water quality index revealed generally poor to unsuitable drinking water quality in the basement areas and very good to moderate in the sedimentary parts. In terms of agricultural uses, all the calculated indices were within the prescribed limits for irrigation purposes in the basement areas. The sandstone aquifers however, are likely to be less suitable for irrigation use, owing to their poor Kelly ratio and soluble sodium percent ratings. The identification of about four to five hydrochemical facies in the Bauchi-Alkaleri-Kirfi area suggests a heterogeneous and complex hydrogeological system in the geological transitional zones. Reaction of groundwater in a low-temperature aquifer setting exemplified the Bauchi-Alkaleri-Kirfi area, changes acidic rocks like biotite hornblende granites and granite gneiss clay minerals and silica. The occurrence of kaolin beds and other clayey materials in the Kerri-Kerri Formation further supports this assertion. Furthermore, the result of the principal component analysis and hydrochemical plots like Gibbs and Chadha all revealed recharging water / weathering of silicates, cation exchange as the major mechanism for hydrochemical evolution in the Bauchi-Alkaleri-Kirfi area.

The fundamental relation between δ^{2}Hand δ^{18}O revealed the mechanisms and sources of groundwater recharge in the Bauchi-Alkaleri-Kirfi area. The stable isotope assessment of suggest that the isotopic compositions exhibit narrow range, from −5.36 to −2.79‰ and averages −3.7‰ for δ^{18}O and −29.2 to −17.4‰ with an average −23.1‰ of for δ^{2}H, and suggests that most of the samples are influenced by kinetic evaporation prior to recharging the aquifers in the area. Such a narrow isotopic variation suggests that all groundwater samples originated from the same area of recharge or the same water regime. Predominantly from the ground surface and rainfall (non-evaporated). Some samples within the Kerri-Kerri zone (1, 11, 38, 43 and 44) plotted close to the exchange with rock mineral regression line which is suggestive of oxygen isotope-exchange with rock material at elevated temperatures. Furthermore, the overall trend revealed by the stable isotope studies in the Bauchi area showed a general decrease δ^{18}O and δ^{2}H with

decreasing annual rainfall and this corroborates the conventional depletion of stable isotopes with decreasing rainfall and increasing latitude as it tracks northward from the south western coast of Nigeria (Gulf of Guinea) inland. The fallout of the isotope studies is that the groundwater system in the saprolitic aquifers are more influenced by precipitation as compared to the sandstone aquifer units.

5.3 Recommendations

Arising from the research findings the following recommendations were put forward;

1. Extensive electrical resistivity tomography of the Bauchi-Alkaleri-Kirfi area will give a clearer picture of the aquifer distribution especially in the transitional zones of the Bauchi-Alkaleri-Kirfi area.

2. Microbial studies for E Coli and Coliform bacteria in the study would aid in clarifying the actual sources of nitrates, which are generally high in the Bauchi-Alkaleri-Kirfi area and also the influence of agricultural activities on groundwater quality in the Bauchi-Alkaleri-Kirfi area.

3. Future hydrochemical research in Bauchi area should include refining the basin conceptual model in terms of groundwater age and residence time distributions and collecting weathered basement geochemical data to examine the influence of the mineral assemblages of the different rock types on the hydrochemistry of the Bauchi-Alkaleri-Kirfi area and the mixing dynamics.

5.4 Contributions to Knowlegde

The uniqueness of the present work lies in the integration of GIS, geophysical, hydrochemical and stable isotopes techniques to enhance the utility of groundwater potential zone and quality maps for groundwater management and making informed policy choices on the use and protection of groundwater.

REFERENCES

Abdullahi, I., Ndububa, O.I., Tsoho, U., Garba, H. Haladu, S., and Bayang F. 2014. Gubi Water Treatment Plant as a Source of Water Supply in Bauchi Township. American Journal of Engineering Research, Volume-03, Issue-06, pp-107-119

Abimbola, A.F., Tijani, M.N., Nurudeen, S.I. 1999. Some aspects of groundwater quality in Abeokuta and its environs southwestern Nigeria. NAH Water Res J 10:6–11

Abimbola, A.F., Odukoya, A.M. and Olatunji, A.S., 2002. Influence of the bedrock on the hydrogeochemistry characteristics of groundwater in northern parts of Ibadan metropolis, Southwestern Nigeria. Journal of Water Resources, Vol.13.pp.1-6.

Acworth, R. I. 1987. The development of crystalline basement aquifers in a tropical environment. *Quarterly Jour. of Engineering Geology 20*.pp265-272.

Adegoke, O. S., Jan Du chene, R. E., Agumanu, A. E., and Ajayi, P. O., 1978. Paleontology and age of the Kerri-Kerri Formation, Nigeria. Revista Espaňola. Micropalaeontología 2, 267-283.

Adelana, S.M.A., MacDonald, A.M., 2008. Groundwater research issues in Africa. In: Adelana SMA, MacDonald AM (eds) Applied research studies in Africa. IAH selected papers on hydrogeology, vol 13, CRC/Balkema, Amsterdam, pp 1–7

Adelana, S.M.A., Bale, R.B., and Wu, M., 2003. Quality of assessment of pollution vulnerability of groundwater in Lagos metropolis, SW Nigeria in: proceedings of the aquifer vulnerability Risk Conference AURO3 Salamenia Mexico, 2, pp.1-17.

Adeniji, A. E., Omonona, O.V., Obiora, D.N. and Chukudebelu, J.U., 2014. Evaluation of soil corrosivity and aquifer protective capacity using geoelectrical investigation in Bwari basement complex area, Abuja J. Earth Syst. Sci. 123, No. 3, pp. 491–502

Aggarwal, R., Kaur, S, Juyal, D., 2009. Micro level assessment of water resources in bist doab tract of Indian Punjab. J Agric Eng 46(2):33–39

Akanbi OA (2018) Hydrogeological characterisation and prospect ofbasement Aquifers of
Ibarapa region, southwestern Nigeria. ApplWater Sci 8(89):1–22. https ://doi.org/10.1007/s1320 1-018-0731-9

Ako, B. D. and Olorunfemi, M. O. 1989. Geoelectric Survey for Groundwater in the Newer
Basalts of Vom, Plateau State. Journal of Mining and Geology 25, pp.247- 250.

Ajakaiye, D.E. 1970. Gravity Measurements over the Nigerian Younger Granite Province.
Nature, 225, 50-52.

Ajakaiye, D. E., Hall, D. H., Miller, T. W., Verherjen, P. J. T., Awad, M. B. And Ojo, S. B. 1986. Aeromagnetic Anomalies and Tectonic Trends In and Around the Benue Trough, Nigeria. Nature, 319, pp. 582–584

Akaha, C.T and Promise A. A. 2009. Hydraulic properties from pumping tests data of aquifers in Azare area, North Eastern Nigeria.Journal of Applied Sciences and Environmental Management, Vol. 12, No. 4, 2009, pp. 67-78

Ako, B.D., and V.C. Osondu, 1986. Electrical resistivity of the Kerri-kerri Formation, Darazo, Nigeria: Journal of African Earth Sciences, v. 5/ 5, p. 527-534.

Alagbe, S. A. 2006. Preliminary evaluation of hydrochemistry of the Kalambaina Formation, Sokoto Basin, Nigeria. J. of Environmental geology, v. 51, pp. 39-45.

Al-Amry, A.S. 2008. Hydrochemistry and groundwater quality assessment in an arid region: a case study from Al Salameh Area, Shabwah, Yemen, The 3rd International Conference on Water Resources and Environments, The first Arab water forum

Al Faitouri, M. and Sanford W.E. 2015. Stable and radio-isotope analysis to determine recharge timing and paleoclimate of sandstone aquifers in central and southeast Libya. Hydrogeology Journal 23: 707–717

Ali, S., Shemang. E.N and Likkason, O.K. 1993. The Basement structure in Barkumbo valley, Bauchi, Nigeria; A revelation from seismic refraction and D.C Resistivity. Journal of Mining and geology, Vol.29 No.2:47-51

Ali, S.A., Ali U. 2018. Hydrochemical characteristics and spatial analysis of groundwater quality in parts of Bundelkhand Massif, India, Applied Water Science (2018) 8:39 https://doi.org/10.1007/s13201-018-0678-x

Allison, G.B., Stone W.J., Hughes M.W. 1985. Recharge in karst and dune elements of a

semi-arid landscape as indicated by natural isotopes and chloride. J Hydrol 76:1–26

Alhajjar B.J., Chesters G, Harkin JM 1990. Indicators of chemical pollution from septic systems. Ground Water 28(4):559–568

Al Saud, M., 2010. Mapping potential areas for groundwater storage in wadi Aurnah Basin,
western Arabia peninsula, using remote sensing and geographical system techniques. Hydrogeol J 18:1481–1495.

Arnous, M.O., Green D.R. 2015. Monitoring and assessing waterlogged and salt-affected areas in the Eastern Nile Delta region, Egypt, using remotely sensed multi-temporal data and GIS. J Coast Conserv 19(3):369–391.

Ariyo S.O and Adeyemi G.O, 2016. Hydrogeophysical Investigation for Groundwater Potential of Ishara/Ode-Remo geological transition zone, southwestern Nigeria. Arabian Journal of Geosciences, Vol.9: 631

Asadi, S, Vuppala P, Reddy M.A. 2007. Remote sensing and GIS techniques for evaluation
of groundwater quality in municipal corporation of Hyderabad (Zone-V), India. Int J Environ Res Public Health 4:45–52. doi:10.3390/ijerph2007010008

Asfahani, J. 2007a, Geoelectrical investigation for characterizing the hydrogeological conditions in semi-arid region in Khanasser valley, Syria, J. Arid Environ. Environ. 68, 1, 31-52,

Asfahani, J. and Abou Zakhem B. 2013. Geoelectrical and Hydrochemical Investigations for Characterizing the Salt Water Intrusion in the Khanasser Valley, Northern Syria.Acta Geophysica vol. 61, no. 2, Apr. 2013, pp. 422-444

Ayadi, Y., Mokadem, N., Besser, H., Khelifi, F., Harabi, S., Hamad, A., Boyce, A., Laouar, R., and Hamed, Y. 2018. Hydrochemistry and stable isotopes (18O and2H) tools applied to the study of karst aquifers in southern Mediterranean basin (Teboursouk area, NW Tunisia). Journal of African Earth Sciences, vol. 137. pp. 208–217.

Ayers, R.S and Westcot, D.W. 1985. Water quality for agriculture FAO Irrigation and Drain Paper No. 29 (1), 1-109.

Babu, H. V. R., Rao, N. K. and Kumar, V. V.1991. Bedrock topography from magnetic anomalies An aid for groundwater exploration in hard-rock terrains (short note): Geophysics, 56, no. 07, 1051-1054.

Balakrishnan, P., Saleem, A., and Mallikarjun N.D. 2011. Groundwater quality mapping

using Geographic Information System (GIS): A case study of Gulbarga City, Karnataka, India. Afr. J. Environ. Sci. Technol., 5: 1069-1084.

Barber, W., Jones, D.C. 1965. The geology and hydrogeology of the Maiduguri area, Borno
Province. Geol Surv Niger Bull 27:1–117

Barber, W. & Jones, D. G. 1960. The geology and hydrology of Maiduguri, Bornu Province. Record of the Geological Survey Nigeria.

Basavarajappa, H.T., Manjunatha, M.C., Jeevan, L. 2014. Application of Geoinformatics on Delineation of Groundwater potential zones of Chitradurga district, Karnataka, India. International Journal of Computer Engineering and Technology (IJCET), IAEME 5, pp.94-108.

Bauchi State Water Board, 2015. A technical report on the survey of boreholes in Bauchi State (Unpublished report)

Benkhelil, J. 1989. The origin and evolution of the Cretaceous Benue Trough (Nigeria). Journal African Earth Sciences 8, 251-282.

Blakely, R.J., 1995. Potential theory in gravity and magnetic applications. University Press,
NY,Cambridge, 441 pp.

Bonsor, H.C., MacDonald, A.M., Calow, R.C. 2011. Potential impact of climate change on
improved and unimproved water supplies in Africa. RSC Issues Environ Sci Technol 31:25–50

Bonsor, H. C., and Araguás-Araguás, L.J. 2013. Residence times of shallow groundwater in West Africa: implications for hydrogeology and resilience to future changes in c limate.Hydrogeology Journal 21: 673–686

Boswinkel, J. A., Information Note, 2000. International Groundwater Resources Assessment Centre (IGRAC), Netherlands Institute of Applied Geoscience, Netherlands.

British Geological Survey, 2003. Groundwater quality: Nigeria. NERC, pp. 1-9.

Buba, D., Anjorin, F.O., Jacob, A. 2015. The Analysis of Influence of Weather Conditions on Atmospheric Extinction Coefficient over Bauchi, North Eastern Nigeria, Journal of Atmospheric Pollution, Vol. 3, No. 1, 2015, pp 31-38. doi: 10.12691/jap-3-1-6

Burrough, P.A. 1986. Principals of geographical information systems for land resources

assessment. Clarendon Press, Oxford.

Calow, R.C., MacDonald's, A.M., Nicol, A.L and Robins, N.S. 2010. Groundwater security and drought in Africa: Linking availability. acesses and demand. Groundwater 48:246-56

Carter, J.D; Barber, W. M., Tait, E.A. 1963. The Geology of parts of Adamawa, Bauchi and Bornu provinces of North Eastern Nigeria. Geol. Surv. Nig. Bull. 30, 180p.

Chadha, D. K. 1999. A proposed new diagram for geochemical classification of natural waters and interpretation of chemical data. Hydrogeology Journal 7: 431-439

Chidambaram, S., Ramanathan, A.L., Srinivasamoorthy, K., Anandhan, P. 2003. WATCLAST—A computer program for hydrogeochem- ical studies, recent trends in hydrogeochemistry (case studies from surface and subsurface waters of selected countries). Capital Publishing Company, NewDelhi, pp 203–20

Chilton, J., Seiler, K.P., 2006. Groundwater occurrence and hydrogeological environments.
In: Schmoll, O., Howard, G., Chilton, J., Chorus, I. (eds.) Protecting Groundwater for Health: Managing the Quality of Drinking-water Sources. WHO, IWA Publishing, London.

Chilton, P.J. 1996. Groundwater. In Water Quality Assessments: A guide to the use of biota, sediments and water in environmental monitoring, 2nd edn, (ed. D. Chapman), pp. 413-510, E & FN Spon, London.

Chilton, P.J. and Foster, S.S.D. 1995. Hydrogeological characterization and water supply potential of basement aquifers in tropical Africa. Hydrogeology J., 3, 36-49.

Chowdhury, A, Jha MK, Chowdary VM, Mal BC (2009) Integrated remote sensing and GIS-based approach for assessing groundwater potential in West Medinipur district, West Bengal, India. Int J Remote Sens 30(1):231–250

Clark, I. and Fritz, P. 1997. Environmental Isotopes in Hydrogeology. 328 pp. New York, Boca Raton: Lewis Publishers. [A textbook on isotope hydrology]

Cooray P.G. 1975. The charnockitic rocks of Nigeria. Pitchamutu Volume, Banglore University, India, pp 50–73

Coplen, T.B., 1994. Reporting of stable hydrogen, carbon, and oxygen isotopic abundances. Pure & Appl. Chem. 66, 273–276.

Coplen, T.P., 1996. New guidelines for reporting stable hydrogen, carbon and oxygen isotope-ratio data. Geochim. Cosmochim. Acta 60, 3359–3360.

Cox, A. 1973. Plate tectonics and geomagnetic reversals. W. H. Freeman and Company

Goodchild. M.F. 1993. The state of GIS for environmental problem solving. In: Goodchild
MF, Parks BO, Steyaert LT (eds) Environmental modeling with GIS. Oxford University Press, New York, pp 8–15

CPCB. 2008. Guideline for water quality management. Central Pollution Control Board, Parivesh Bhawan, East Arjun Nagar, Delhi

Craig, H. 1961. Standard for reporting concentrations of deuterium and oxygen-18 in natural waters. Science 133, 1833–1834. [A historical benchmark paper defining the isotope reference standard and the meteoric water line.

Dada, S. S., 1989. Evolution de la croute continental au Nord Nigeria: apport de la geochimie, de la geochronologic U-Pb et des traceurs isotopiques Sr, Nd et Pb. (Doctorate Thesis.): Univ. Sci. Tech. Languedoc, Montpellier. 194

Dada S.S. 2006. Proterozoic evolution of Nigeria. In: Oshi O (ed) The basement complex of Nigeria and its mineral resources (A Tribute to Prof. M. A. O. Rahaman). Akin Jinad & Co. Ibadan, pp 29–44

Dansgaard, W. 1964. Stable isotopes in precipitation. Tellus 16, 436–468. [A historical benchmark paper describing distribution of isotopes of hydrogen and oxygen in precipitation around the world.]

Dalton, H.S., and Upchurch S.B. 1978. Interpretation of hydrochemical facies by factor analysis, Groundwater, Vol.16, No.4 pp-228-233

Dar, I.A., Sankar, K., Dar, M.A., 2010. Deciphering groundwater potential zones in hard rock terrain using geospatial technology. Environmental Monitoring and Assessment 173, 597e610.

Davies S.N., and De Wiest R.J.M. 1996. Hydrogeology, John Welly and Sons, Inc, New York.

Department of Public Information (DPI). 2006. Theme of world water day "water and culture," Secretary-General says in message for international day. *United Nations*. Retrieved June 2, 2008.

Dike, E.F.C, Aga, T and Bashayi, T.E.O. 2008. Geochemical investigation of groundwater
in shallow hand-dug wells in Railway area, Bauchi. Continental J. Applied Sciences 3:57 - 64, 2008

Dike, E.F.C. 1993.Stratigraphy and Structure of the Kerri-Keri Basin, NE Nigeria. Journal of Mining Geology 29(2):pp.77-93

Dike, E.F.C. and Egbuniwe, I. G. 1993. An unconformity between the Kerri-Kerri Formation and the Basement Complex at Mainamaji, Bauchi State. Journal Mining and Geology 29.

Diop, S. and Tijani, M. N. 2008. Assessing the basement aquifers of Easter Senegal. *Hydro-geology Journal,* Vol. 16: 1349 – 1369

Dobrin, M.B. and Savit, C. H. 1988. Introduction to Geophysical Prospecting, 4thEdition, McGraw-Hill, New York. 867pp.

Domenico, P.A. and Schwartz, F.W. 1998. Physical and Chemical Hydrogeology, 2nd edn, John Wiley, New York.

Doneen, L.D. 1964. Notes on water quality in agriculture, water science and engineering. 4001, University of California, Davis

Doell, R., Cox, A. 1967. Magnetization of rocks, In: Mining Geophysics Volume 2: Theory, Society of Exploration Geophysicists SEG Mining Geophysics Volume Editorial Committee (Eds.): 446-453, Tulsa

Du preez, J.W. and Barber W. 1965.The distribution and chemical quality of groundwater in Northern Nigeria, Geological Bulletin, pp.1-82

Eaton, F. M. 1950. Significance of carbonates in irrigation waters. Soil. Sci. V 69: 123-133. Indian Standards, 1967. Quality Tolerances for water for ice manucacture. Indian Standard Institution, New Delhi.

Edet, A.E. Okereke, C.S., Teme, S.C., Esu, E.O. 1998. Application of remote sensing data to groundwater exploration: a case study of the Cross River state, southeastern Nigeria. Hydrogeol J 6:21–30

Edet A.E. (1993) Hydrogeology of parts of Cross River State, Nigeria:evidence from aerogeological and surface resistivitystudies: PhD Dissertation, University of Calabar, Calabar, Nigeria,316 pp

Edok Eter Mandilas Ltd. 1976. Hydrology and Geophysical Investigation for Groundwater in Bauchi State. Unpublished Report.

Edmunds, W.M., Fellman, E., Goni, I.B., 1999 Lakes, groundwater and palaeohydrology of the Sahel of NE Nigeria: evidence from hydrochemistry. J Geol Soc 156:345–355

Eduvie, M.O. 2006. Borehole failures in Nigeria. Paper presented at a National Seminar held on the Occasion of Water Africa Exhibition (Nigeria 2006) at Eko Hotels & Suites, Victoria Island, Lagos, on 15th November, 2006.

Elimian, KO; Musah, A; Mezue, S; Oyebanji, O; Yennan, S; Jinadu, A; Williams, N; Ogunleye, A; Fall, IS; Yao, M; Eteng, WE; Abok, P; Popoola, M; Chukwuji, M; Omar, LH; Ekeng, E; Balde, T; Mamadu, I; Adeyemo, A; Namara, G; Okudo, I; Alemu, W; Peter, C; Ihekweazu, C (2019). Descriptive epidemiology of cholera Outbreak in Nigeria, January-November, 2018: implications for the global roadmap strategy. *BMC Public Health.* 19(1): 1264- 1274

Eludoyin, O. M. 2011. Air Temperature and Relative Humidity Areal Distribution over Nigeria, Ife research publications in geography (IRPG) Vol. 10, No. 1, pp. 134 - 145,

Falconer, J.D. 1911. The geology and geography of Northern Nigeria. Macmillan, London,
135pp

Fashae, O.A., Tijani, M.N., Talabi, A.O. and Adedeji, O.I. 2014. Delineation of groundwater potential zones in the crystalline basement terrain of SW-Nigeria: an integrated GIS and remote sensing approach. Applied Water Science 4: 19-38

Federal Ministry of Water Resources. 2011. Executive Summary of Nigeria Water sector Road map.

Federal Ministry of Water Resources. 2013. National Water Resources Master Plan.

Ferre, E.C., Caby, R. 2007. Granulite facies metamorphism and charnockite plutonism: Examples from the Neoproterozoic Belt of northern Nigeria, Proceedings of the Geologists Association 118(1):47-54

Fetter C.W. 2001. Applied Hydrogeology, 4th edition, prentice Hall. Inc

Fetter C.W. 2010. Homepage for Applied Hydrogeology from: http: //www .applied hydroge- ology .info

Fisher, R. S., & Mullican, W. F. 1997. Hydrochemical evolution of sodium-sulphate and sodium-chloride groundwater be- neath the Northern Chihuahuan desert, Trans-Pecos, Texas, USA. Hydrogeology Journal, 5, 4–16.

Folk, R. L., 1968. Petrology of sedimentary rocks. Hemphill's, Austin, Texas, 170 pp.

Foster, D., Lawrence, A.R., and Morris, B.M. 1998. Groundwater in Urban Development.

World Bank technical Paper no 390, Washington DC. 121.

Foster, S.S.D., and Chilton, P.J., 2003. Groundwater: The processes and global significance of aquifer degradation. Phil. Trans. R. Soc. B 258:1957-72

Frohlich, R.K., Fisher, J.J., Summerly, E., 1996. Electric–hydraulic conductivity correlation in fractured crystalline bedrock: Central landfill, Rhode Island, USA. Journal of Applied Geophysics 35, 249–259.

Freeze, R.A. and Cherry, J.A. 1979. Groundwater, Prentice Hall, Englewood Cliffs, New

Fritz, S J., 1994. A survey of charge-balance errors on published analyses of potable ground and surface waters. United States: N. p., Web. doi:10.1111/j.1745-6584.1994.tb00888.x.

Jersey, P. M. 1996. Introducing Groundwater, 2nd edn, Chapman and Hall, London.

Gat, JR, Carmi, I. 1970. Evolution of the isotopic composition of atmospheric waters in the mediterranean sea area. J Geophys Res 75:3039–3048

Geological Survey of Nigeria. 1978. Geological Map of Nigeria, on scale 1:2,000,000. Printed and published by Directorate of Federal Surveyors, Federal Ministry of Housing and Surveys, Nigeria.

Gibrilla, A., Osae, S., Akiti, T.T., Adomako, D., Ganyaglo, S.Y., Bam, E.P.K., Hadisu, A.
2010. Origin of dissolve ions in groundwaters in the northern Densu river basin of Ghana using stable isotopes of 18O and 2H. J. Water Resour Protection 2:1010–101

Gleeson, T. Wada, Y., Bierkens, M.F.P, Van Beek L.P.H. 2012. Water balance of global aquifers revealed by groundwater foot print. Nature 488:197–200

Glynn, P.D., and Plummer, N.L., 2005. Geochemistry and the understanding of ground-water systems,Hydrogeol J (2005) 13:263–287

Glynn, P.D, Voss, C.I. 1999. Geochemical characterization of Simpevarp ground waters near the Aspo Hard Rock Laboratory. Swedish Nuclear Power Inspectorate (SKI), SKI Rep 96:29, 210 pp

Gnanachandrasam, G., Ramkumar, T., Venkatramanan, S., Vasudevan, S., Chung, S.Y., Bagyaraj, M. 2014. Accessing groundwater quality in lower part of Nagapattinam district, Southern India: using hydrogeochemistry and GIS interpolation techniques, Appl Water Sci, DOI 10.1007/s13201-014-0172

Goni, I.B., Solomon, Y., Musami S.B., and Zarma. A.A. 2016. Determination of Thickness
of Sedimentary Cover in the Nigerian Sector of the Chad Basin Using High Resolution Aeromagnetic Data, Petroleum Technology Development Journal: 2016 - Vol. 6 No. 1,38-50pp

Grant, F. S. and West, G. F. 1965. Interpretation Theory in Applied Geophysics. New York: McGraw-Hill.

Groundwater Foundation, (G.F). 2008. Groundwater glossary: Freshwater. Groundwater Foundation. Retrieved June 3, 2008.

Guiraud, M. 1991. Mecanisme de formation da bassin Crétacé sur decrochements. Multiples de la Haute- Bénoué (Nigeria). Bulletin Centres Recherches Exploration – Production Elf-Aquitaine 15, 11-67.

Guiraud, R. and Maurin, J. C. 1992. Early Cretaceous rifts of westerns and central Africa an Overview. Tectonophysics 282, 39-82.

Gupta, S.K and Gupta, I.C 1987. Management of saline soils and water. Oxford and IBH Publication Coy, New Delhi, India.

Eduvie, M.O. 2006. "Borehole Failures and Groundwater Development in Nigeria". A Paper Presented at a National Seminar Held on the Occasion of Water Africa Exhibition Nigeria (2006) at Ikoyi Hotels and Suites, Victoria Island, Lagos, on 15th November, 2006.

Hadithi, M.A, Shukla, D.C., Israil, M. 2003. Evaluation of groundwater resources potential
in Ratmau-Pathri Rao watershed Haridwar district, Uttaranchal, India using geo-electrical, remote sensing and GIS techniques. Proceedings of the International Conference on Water and Environment (WE-2003), Bhopal, India, Ground Water Pollution pp. 123–125

Halim, M.A, Majumder, R.K., Nessa, S.A., Hiroshiro, Y., Sasaki, K., Saha, B.B., Saepuloh
A, Jinno, K. 2010. Evaluation of processes controlling the geochemical constituents in deep groundwater in Bangladesh: spatial variability on arsenic and boron enrichment. J Hazard Mater 180:50–62. doi:10.1016/j.jhazmat.2010.01.008

Healy, R.W., Winter, T. C., LaBaugh, J.W., and Frankie, O.L. 2007. Water Budgets: Foundation for effective water resources and environmental management: USGS Circular 1308:90p.

Heath, R.C. 1983. Basic groundwater hydrology.USGS Water Supply Paper 2220:64p.Denver, C.O.

Helena, B., Pardo, R., Vega, M., Barrado, E., Fernandez, J.M., Fernandez, L. 2000. Temporal evolution of groundwater composition in an alluvial aquifer (Pisuerga river, Spain) by principal component analysis. Wat Res 34:807–816

Hem, J.D. 1985. Study and interpretation of the chemical character- istics of natural water, third edition. US Geol Surv Water Supp Pap 2254, pp 80–105

Hazel, J.R. and John, B.W. 1985. The development of Groundwater Resources for farming communities in Bauchi state, Nigeria. Jour. of Hydrogeologists vol.2 Cambridge, United Kingdom pp154.

Herman, R. 2001. An introduction to electrical resistivity in geophysics. American Association of Physics Teachers.

Http://waterisotopes.org

Hussien, H. M., Kehew, A. E., Aggour, T., Korany, E., Abotalib, A. Z., Hassanein, A., & Morsy, S. 2017. An integrated approach for identification of potential aquifer zones in structurally controlled terrain: Wadi Qena basin, Egypt. *Catena*, *149*, 73-85.

Ishola, K., Ogunsanya, S., Adiat, K., and Abdulrahaman, A. 2013. Assessing Groundwater Potential Zones in Basement Complex Terrain Using Resistivity Depth Soundings: A case of Challenge and Oluyole in Ibadan, Southwestern Nigeria. Journal of Science; Vol.1: pp 11-32

Istifanus, Y.C., Elisha, K., Ishaku, Z., and Ephraim, D.A. 2013. Physicochemical Analysis of Groundwater of Selected Areas of Dass and Ganjuwa Local Government Areas, Bauchi State, Nigeria.World Journal Of Analytical Chemistry; vol1,Issue 4.

Iyiorioghe, S.E., Ako, B.D. 1983. The hydrogeology of Gombe subcatchment, Benue Valley, Nigeria, Journal of African Earth Sciences, Vol.5, issue 5, pages 509-518

Jackson M.L. 1970. Weathering of primary and secondaery minerals in soils, Trans. 9th int. conf. of soil science, vol4:281-292

JICA. 2014. The project for review and update of Nigeria national water resources master plan; Vol.2 Japan International Cooperation Agency: Yachiyo Engineering Co., Ltd.: CTI Engineering International Co., Ltd.: Sanyu Consultants Inc.

Jain, K. P. 1998. Hydrogeology and quality of ground water around Hirapur district Sagar (M.P.) (A case study of Proterozoic rocks). Pollution Research 17(1): 91-94.

JICA, Japan International Cooperation Agency.2009. Basic design study report on the project for water supply in Bauchi State and Katsina State in the Federal Republic of Nigeria, pp 1–82.

Jones, B.F, Hanor, J.S, Evans, W.R. 1994. Sources of dissolved salts in the central Murray Basin, Australia. Chem Geol 111:135–154

Karanth, K.R. 1987. Ground water Assessment, Development and Management, Tata Mc Graw Hills Publications Company Limited, New Delhi.

Kauffman, S.J, Herman J.S., Jones, B.F. 1998. Lithological and hydrological influences on groundwater composition in a heterogenous carbonate-clay aquifer system. Geol Soc Am Bull 110(9):1163–1173

Kearse, T.and Brooks, C. 1984. An Introduction to Geophysical Exploration. Blackwell Science Ltd. Oxford U.S.A pp. 256.

Keating, P., Zerbo, L. 1996. An improved technique for reduction to the pole at low latitudes. Geophysics 61:131–137

Kelley, W.P (1963): Use of saline irrigation water. Soil Science, 95 (4), 355-391.

Kellogg, O. D. 1953. Foundations of potential field theory. Dover New York;

Kessler, T., Hesse, A. 2000. Cross-over study of the influence of bicarbonate-rich mineral water on urinary composition in comparison with sodium potassium citrate in healthy male subjects. Br. J. Nutr. 84(6):865-887.

Khodapanah, L., Sulaiman, W. N. A., & Khodapanah, N. 2009. “Groundwater quality assessment for different purposes in Esh-tehard District, Tehran, Iran”, European Journal of Scientific Research, 36, 543 - 553.

Kogbe, C.A. 1989. Geology of Nigeria, 2nd Edition. Rockview Nige Ltd, Jos, 538pp

Krishna, K.S., Logeshkumaran, A., Magesh, N.S., Prince, S.G., Chandrasekar, N. 2015.

Hydro-geochemistry and application of water quality index (WQI) for groundwater quality assessment, Anna Nagar, part of Chennai City, Tamil Nadu, India. Appl Water Sci 5:335–343

Kumar, M., Kumari, K., Singh, U.K., Ramanathan, A. 2009. Hydrogeochemical processes in the groundwater environment of Muktsar, Punjab: conventional graphical and multivariate statistical approach. Environ Geol 57(4):873–884

Kumar, A., Tomar, S. and Prasad, L.B. 1999. Analysis of fractured inferred from DBTM and remotely sensed data for groundwater development in Godavari sub-watershed, Giridih, Bihar. J Indian Soc Remote Sens 26(2):105–114

Lachassagne, P., Wyns, R., Bérard, P., Bruel, T., Chéry, L., Coutand, T., Desprats, J.-F. and Le Strat, P. 2001. Exploitation of high-yields in hard-rock aquifers: downscaling methodology combining GIS and multicriteria analysis to delineate field prospecting zones. Ground Water, 39 (4), 568-581.

Lapworth, D. J., MacDonald, A. M., Tijani, M. N., Darling, W. G., Gooddy, D. C., Bonsor, H. C., Araguás-Araguás, L. J. 2013. Residence times of shallow groundwater in West Africa: implications for hydrogeology and resilience to future changes in climate, Hydrogeology Journal, 21: 673–686

Lawal A, Tijani M.N, D'Alessio M. 2020 Geoelectrical characterisation of aquifers in Bauchi-Alkaleri-Kirfi geological transition zones, Northeast Nigeria. Environ Earth Sci 79:224. https ://doi. org/10.1007/s1266 5-020-08978 -5

Lawal A, Tijani MN, D'Alessio M Maigari. A.S. 2021 Application of geographical informationsystem to geoelectrical data for evaluation of the vulnerability of aquifers in parts of Bauchi, Northeastern Nigeria", Environmental Earth Sciences, 80:16https://doi.org/10.1007/s12665-020-09308-5

Lindsey, B.D., Phillips, S.W., Donnelly, C.A., Speiran, G.K., Plummer, L.N., Bohlke, J.K., Focazio, M.J., Burton, W.C., Busenberg, E. 2003. Residence times and nitrate transport in ground water discharging to streams in the Chesapeake Bay watershed. US Geol Surv Water Resour Invest Rep 03-4035, 201 pp

Lillesand, T.M., Kiefer, R.W. 1994. Remote sensing and image interpretation, 3rd edn. Wiley, New York 750 pp

Llyod, J.W. and Heathcoat, J.A. 1985. Natural inorganic hydrochemistry in relation to groundwater: An introduction. Oxford Uni. Press, New York, 296p.

Lo, C.P., Yeung, A.K.W. 2003. Concepts and Techniques of Geographic Information

Systems. Prentice-Hall of India Pvt. Ltd., New Delhi pp. 492

MacDonald, A.M., Davies, J., Calow, R.C., Chilton, P.J. 2005. Developing groundwater: A guide for rural water. ITDG Publ. UK.38p

MacDonald, A., Bonsor H., Dochartaigh, B., Taylor, R. 2012. Quantitative maps of groundwater resources in Africa. Environ Res Lett 7.

Machiwal D, Jha M.K, Mal B.C. 2011. Assessment of groundwater potential in a semi-arid
Region of India using remote sensing, GIS and MCDM techniques. Water Resour Manage 25:1359–1386

Madrucci, V., Taioli F., deArau´jo C.C. 2008. Groundwater favorability map using GIS multi-criteria data analysis on crystalline terrain, Sa˜o Paulo State, Brazil. J Hydrol 357(3–4):153–173

Magesh, N.S., Chandrasekar N, and Soundranayagam, J.P. 2012. Delineation of groundwater potential zones in Theni district, Tamil Nadu, using remote sensing, GIS and MIF techniques. Geosci Front 3(2):189–196

Marghade, D., Malpe, D.B., Zade, A.B. 2012. Major ion chemistry of shallow groundwater
of a fast growing city of Central India. Environ. Monit. Assess. 184, 2405e2418.

Malomo, S. 1983. Weathering and Weathering Products of Nigerian Rocks– Engineering Implications, in Tropical soils of Nigeria in Engineering Practice, edited by S. A. Ola, A. A. Balkema- Rotterdam. pp. 39-60.

McCurry, P. 1973. Geology of degree sheet 21, Zaria, Nigeria. Overseas Geol Mineral Res
45:1–30

McCurry, P. 1976. The geology of the Precambrian to Lower Palaeozoic Rocks of Northern
Nigeria – A Review. In: Kogbe CA (ed) Geology of Nigeria. Elizabethan Publishers, Lagos, pp 15–39

McCurry, P. and Wright, J. B. 1971. On Place and Time in Orogenic Granite Plutonism. Geological Society America Bulletin 82:1713- 1776.

Metwaly, M, Elawadi, E, Moustafal, S.S.R., Al Fouzan F, Mogren S, Al Arifi N. 2012. Groundwater exploration using geoelectrical resistivity technique at Al-Quwy'yia area central Saudi Arabia. Int J Phys Sci 7(2):317–326

Merrill, R. T., McElhinny, M. W., McFadden, P. L. 1996. Magnetic field of the earth; paleomagnetism, the core and the deep mantle: Academic Press, San Diego;

Meybeck, M. 1987. Global chemical weathering of surficial rocks esti- mated from river dissolved loads. Am J Sci 287(5):401–428

Miller, C., Routh P., Brosten, T., and McNamara, J. 2007. Watershed characterization using seasonal time-lapse DC resistivity data, SEG. Expanded Abstr 26(1):1177–1181

Mogaji, K. A., Lim, H. S. & Abdullah, K. 2014. Regional prediction of groundwater potential mapping in a multifaceted geology terrain using GIS-based Dempster–Shafer model. Arab J Geosci DOI 10.1007/s12517-014-1391-1

Mohamed, L., Sultan, M., Ahmed, M., Zaki, A., Sauck, W., Soliman, F., Yan, E., Elkadiri,
R., Abouelmaged, A. 2015. Structural controls on groundwater flow in basement terrains: geophysical, remote sensing, and field investigations in Sinai. Surv Geophys. Doi: 10.1007/s10712- 015-9331-5

Mohammed M .Z, Olorunfemi M.O. & Idonigie A.I. (2012), Geoelectric Sounding for Evaluating Soil Corrosivity and the Vulnerability of Porous Media Aquifers in Parts of the Chad Basin Fadama Floodplain, Northeastern Nigeria, Journal of Sustainable Development; Vol. 5, No. 7; 2012

Mapoma, H.W.T., Xie, X.,Lui, Y., Zhul, Y., Kawaye, F.P., Kayira, T.M., 2017. Hydrochemistry and quality of groundwater in alluvial aquifer of Karonga, Malawi, Environ Earth Sci,76:335,pp1-18

Morales, I., Rodriguez, R., Armienta, M.A., Villanueva-Estrada, R.E. 2016. The origin of groundwater arsenic and fluorine in a volcanic sedimentary basin in central Mexico: a hydrochemistry hypothesis, Hydrogeoleoloy Journal 24:1029–1044.

Müller, K., Vanderborght, J., Englert, A., Kemna, A., Huisman, J.A., Rings, J., and Vereecken, H. 2010. Imaging and characterization of solute transport during two tracer tests in a shallow aquifer using electrical resistivity tomography and multilevel groundwater samplers. Water Recur Res 46:W03502

Mukherjee, A., Fryar, A.E., Thomas, W.A. 2009. Geologic, geomorphic and hydrologic framework and evolution of the Bengal basin, India and Bangladesh. J Asian Earth Sci 34:227–244. doi:10. 1016/j.jseaes.2008.05.011 Mumford

Mukherjee, P, Singh, C.K., Mukherjee, S. 2012. Delineation of groundwater potential

zones in arid region of India—a remote sensing and GIS Approach. Water Resour Manage 26(9):2643–2672

Nabighian, M.N. 1972. The analytical signal of two- dimensional magnetic bodies with polygonal cross-section: its properties and use for automated anomaly interpretation. Geophysics 37: 507-517.

Nabighian, M.N. 1984. Toward a three-dimensional automatic interpretation of potential field data via generalized Hilbert transforms-fundamental relations. Geophysics 49:780–786

Nace, R.L. (ed) (1971) Scientific Framework of World Water Balance, Technical Papers in Hydrology 7, UNESCO, Paris.

Nag, S.K., Ghosh P. 2013. Delineation of groundwater potential zone in Chhatna Block, Bankura District, West Bengal, India using remote sensing and GIS techniques. Environ Earth 70:2115–2127

Narendra, K., Rao, K.N., Latha P.S. 2013. Integrating Remote Sensing and GIS for Identification of Groundwater Prospective Zones in the Narava Basin, Visakhapatnam Region, Andhra Pradesh, Journal Geological Society of India 81:248-260.

National Water Supply and Sanitation Baseline Survey (NWSSBS), 2006. Reanalyzed by JICA Project Team

Nazzal, Y., Ahmed, I., Al-Arifi, N. S. N., Ghrefat, H., Zaidi, F. K., El-Waheidi, M. M., Batayneh, A., & Zumlot, T. 2014. A pragmatic approach to study the groundwater quality suit- ability for domestic and agricultural usage, Saq aquifer, northwest of Saudi Arabia. Environmental Monitoring and Assessment, 186, 4655–4667.

Nigerian Standard for Drinking Water Quality (NSDQW). 2007. Nigerian Industrial Standard NIS 554, Standard Organization of Nigeria: Lagos, Nigeria

Nur, A. Ishaku, J. M. and Yusuf, S. N. 2012. Groundwater Flow Patterns and Hydrochemical Facies Distribution Using Geographical Information System (GIS) in Damaturu, Northeast Nigeria. IJG, Vol.3 No.5

Nur, A. Obiefuna, G.I and Uche, M.U. 2005. Hydrogeophcial Investigation of Bauchi and environs, North Eastern Nigeria. *Global Journal of Geological Sciences, Vol. 3* (2), pp 143 – 151

Nyende, J., van Tonder, G., Vermeulen, D. 2013. Application of Isotopes and Recharge Analysis in Investigating Surface Water and Groundwater in Fractured Aquifer under Influence of Climate Variability, J Earth Sci Clim Change 2013, 4:4,pp.1-14

Offodile, M.E. 1972. Groundwater Level Fluctuation in the East Chad Basin of Nigeria.

Min. Geol. Vol. 7. No. 1&2: 19-34

Offodile, M. E. 2002. Groundwater study and development in Nigeria. Mecon, Jos, Nigeria, 451 pp

Okhue, E.T., Olorunfemi, M.O. 1991. Electrical resistivity investigation of a Typical Basement Complex area- the Obafemi Awolowo University Campus case study. J. Min. Geol. 27(2).66-70.

Oladapo, M.I., Akintorinwa, O.J. 2007. Hydrogeophysical Study of Ogbese Southwestern, Nigeria. Global J. Pure and Applied Sci. 13(1): 55-61.

Oladapo, M. I., Mohammed, M. Z., Adeoye, O. O., & Adetola, O. O. 2004. Geoelectric investigation of the Ondo-State Housing Corporation Estate, Ijapo, Akure, Southwestern Nigeria. Journal of Mining and Geology, 40(1), 40(1), 41-48.

Olasehinde, P.I., Amadi A.N., Idris-Nda, A., Katu, M.J., Unuevho C.I., Jimoh M.O. 2015. Aquifers Characterization in Agaie, North-Central Nigeria Using Electrical Resistivity Method and Borehole Lithologs. American Journal of Environmental Protection, 3(3): 60-66

Olatunji, A. S., Abimbola, A. F., Oloruntola, M. O., & Odewade, A. A. 2005. "Hydrogeo-chemical evaluation of groundwater resources in shallow coastal aquifers around Ikorodu area, Southwestern Nigeria", Water Resources, 16, 65 - 71.

Olayinka, A. and Barker, R. 1990. Borehole Siting in Crystalline Basement Areas of Nigeria with a Microprocessor Controlled Resistivity Traversing System. Groundwater, vol. 28, pp. 178-183.

Olayinka, A. I. and Olorunfemi, M. O. 1992. Determination of Geoelectrical Characteristics in Okene Area and Implication for Boreholes Siting. Journal of Mining and Geology (28): 403- 412.

Olayinka, A.I., Akpan, E.J., Magbagbeola, O.A., (1997) Geoelectric sounding for estimating aquifer potential in the crystalline basement area around Shaki, Southwest Nigeria. Water Resources, 8(1, 2): 71–81.

Olorunfemi, M.O., Ojo, J.S., Akintunde, O.M. 1999. Hydrogeophysical eval- uation of the groundwater potentials of the Akure metropolis, Southwestern Southwestern Nigeria. JMin Geol 35(2):201–228

Ophori, D.U., and Tòth, J. 1989. "Patterns of Ground-Water Chemistry, Ross Creek Basin,
Alberta, Canada," vol. 27, No. 1, pp 20-26.

Osinowo, O.O., and Olayinka, A.I. 2012. Very low frequency electromagnetic (VLF-EM) and electrical resistivity (ER) investigation for groundwater potential evaluation in a complex geological terrain around the Ijebu-Ode transition zone, southwestern Nigeria. Journal of Geophysics and Engineering, Vol.9 N0.4

Osinowo O.A., and Olayinka A.I. 2013. Aeromagnetic mapping of basement topography around the Ijebu-Ode geological transition zone, Southwestern Nigeria, Acta Geod Geophys (2013) 48:451–470

Omosuyi, G. O., Ojo J. S. and Olorunfem M. O. 2008. Geoelectric Sounding to Delineate Shallow Aquifer in the Coastal Plain Sands of Okitipupa Area, South Western Nigeria. Pacific J. Sci. Technol., 9(2): 562-577.

Omran, A.A. 2008. Integration of remote sensing, geophysics and GIS to evaluate groundwater potentiality – a case study in Sohag Region, Egypt. In: The 3rd international conference on water resources and arid environments and the 1st Arab Water Forum;

Omotoyinbo, O.S., and Okafor, F.C. 2008. Influence of rock mineralogy on subsurface water in Ado Ekiti, Nigeria. Afr Res Rev Index Afr J Online: www.AJOL.info.pp 175–186

Oyawoye, M.O. 1972. The basement complex of Nigeria. In: Dessauvagie TFJ, Whiteman
AJ (eds) African geology. Ibadan University Press, pp 66–102

People's Daily, 16th February, 2016 retrieved from
http://www.peoplesdailyng.com/bauchi-govt-Set-to-tackle-water-scarcity-sanitation-in-rural-communities/

Piper, A.M. 1944. A graphic procedure in the geochemical interpretation of water analysis.
Trans Am Geophy 25(6):914–92

Qu, W., and Kelderman, P. 2001. Heavy metal contents in the Delft canal sediments and suspended solids of the River Rhine: multivariate analysis for source tracing. Chemosphere 45(6–7):919–925

Rahman, A.T., Majumder, R.K., Rahman, S.H., Halim, M.A. 2011. Sources of deep groundwater salinity in the southwestern zone of Bangladesh. Environ Earth Sci 63:363–373. doi: 10.1007/s12665-010-0707-zCrossRefGoogle Scholar

Rao, N.S. 2006. Groundwater potential index in a crystalline terrain using remote sensing

data. Environ Geol 50:1067–1076

Ravat, D. 1996. Analysis of Euler Method and its Applicability in Environmental Magnetic
Investigations, Journal of environmental and engineering geophysics, Vol. 1 issue 3

Ravikumar, P. & Somashekar, R.K. (2017) Principal component analysis and hydrochemical facies characterization to evaluate groundwater quality in Varahi river basin, Karnataka state, india Appl Water Sci 7: 745. Volume 7, Issue 2, pp 745-755

Richards, L.A. 1954. Diagnosis and improvement of Agriculture Handbook, Saline and alkali soil, U.S. Department of Agriculture, pp. 60

Reuben, K. U. 1970. Geographical regions of Nigeria. University of California Press. p. 150.

Saaty, T.L. 1992. Decision making for leaders. RWS Publications, Pittsburgh

Saaty, T.L. 1980. The analytic hierarchy process: planning, priority setting, resource allocation. McGraw-Hill, New York

Saaty, T.L. 1986. Axiomatic foundation of the analytic hierarchy process. Manage Sci 32(7):841–855

Sadashivaiah, C., Ramakrishnaiah, C.R., Ranganna, G. 2008. Hydrochemical analysis and
evaluation of groundwater quality in Tumkur Taluk, Karnataka State, India, Int. J. Environ. Res. Public Health, 5 (2008), pp. 158–164

Saemundsson, K. 2009. Geothermal systems in global perspective: short course on exploration for geothermal resources. UNU GTP, Reykjavík, Iceland, 11 pp

Sahu, P. and Sikdar, P.K .2008, Hydrochemical framework of the aquifer in and around East Kolkata Wetlands, West Bengal. India Environ Geol, 55,823–835.

Sawyer, E.W. and Brown, M. 2008. Working with migmatites; Mineralogical Association of Canada, Short Course Volume 38, 158p.

Selvam, S., Manimaran, G., Sivasubramanian, P., 2012. Hydrochemical characteristics and
GIS-based assessment of groundwater quality in the coastal aquifers of Tuticorin corporation, Tamilnadu, India, Appl Water Sci DOI 10.1007/s13201-012-0068-8

Salama, R.B., Tapley, I., Ishii, T., Hawkes, G. 1994. Identification of areas of recharge and

discharge using Landsat-TM satellite imagery and aerial photography mapping techniques. Journal of Hydrology 162(1– 2):119–141

Salami, B.M., and Olorunfemi, M.O. 2014. Hydrogeophysical Evaluation of the Groundwater Potential of the Central Part of Ogun State, Nigeria. Ife Journal of Science vol. 16, no. 2 pp291-299

Sawyer, C.S. and Mc Carty. 1967. Chemistry for sanitary engineers. 2 edition, Mc Graw Hill Co. New York, 518p.

Schoeller, H. 1962. Les eaux. Soutenaines Masson et Cie, Paris.

Setianto, A., and Triandini, T. 2013. Comparison of kriging and inverse distance weighted
(IDW) Interpolation methods in lineament extraction and analysis. J. SE Asian Appl. Geol., Jan–Jun 2013, Vol. 5(1), pp. 21–29

Shahid, S., Nath, S.K. 2002. GIS integration of remote sensing and electrical sounding data
for hydrogeological exploration. Journal of Spatial Hydrology 2(1):1–10

Shemang, E.M., and Jiba. K.T. 2005. Assesment of the Hydrogeologic Properties Of The Basement Aquifers of Western Part of Bauchi, Nigeria, African Journals Online, Vol 3, No 1

Schroeder, H.A. 1960. Relationship between hardness of water and death rates from certain
chronic and degenerative disease in the United States. J Chronic Dis 12:586–91.

Schroeter, D.N. 1974. Hydrology of Bauchi Town. Geological Survey of Nig. Vol. 7, No. 1 pp 77-90.

Talabi, A.O. and Tijani, M.N. 2013. Hydrochemical and stable isotopic characterization of
shallow groundwater system in the crystalline basement terrain of Ekiti area, southwestern Nigeria Appl Water Sci 3: 229. doi: 10.1007/s1320101300763.

Talabi, A.O., Tijani, M.N. 2011. Integrated remote sensing and GIS approach to Ground-water potential assessment in the basement terrain of Ekiti area south-western Nigeria. RMZ—materials and geoenvironment, vol. 58, no 3, pp 303–328

Teeuw, R.M. 1995. Groundwater exploration using remote sensing and a low-cost geographical information system. Hydrogeology Journal 3(3):21–30

Telford, W.M., Geldart, L.P., and Sheriff, R.E. 1990. *Applied Geophysics*. UK: Cambridge

University Press.

Tijani, M.N. 1994. Hydrochemical assessment of groundwater in Moro area, Kwara State,
Nigeria. Environ Geol 24:194–202

Tijani, M.N., Abimbola, A.F. 2003. Groundwater chemistry and isotope studies of weathered basement aquifer: a case study of OkeOgun area, SW Nigeria. Afr Geosci Rev 10(4):373–387

Tijani, M.N., 2016. Groundwater: The buried vulnerable treasure. Inaugural Lecture, University of Ibadan, Ibadan University Press.

Tijani, M.N., Crane, E., Upton, K. and O Dochartaigh, B.E. 2016. Africa Groundwater: Atlas: Hydrogeology of Nigeria. British Geological Survey. Accessed, March, 2016: http:// earthwise.bgs.ac.uk/index.php/hydrogeology_of_Nigeria.

Truswell, J.F., Cope, R.N. 1963. The geology of parts of Niger and Zaria Provinces, Northern Nigeria. Geol Suvey Nigeria Bull 29:1–104

Todd, D.K. 1980. Groundwater hydrology, 2nd edition. John Wiley and sons, New York.

Todd, D.K., Mays, L.W. 2005. Groundwater hydrology. 3rd edition, John Wiley & Sonpp.636

Uliana, M.U., Sharp, J.M. 2001. Tracing regional flow paths to major springs in Trans-Pecos Texas using geochemical data and geochemical models, Chemical Geology 179 2001 53–72

UNESCO.1999. World Water Resources at the Beginning of the 21st Century, CD version,
UNESCO, Paris.

UNEP. 1992. Glaciers and the Environment, UNEP/GEMS Environment Library No. 9, p.8. UNEP, Nairobi, Kenya

Umaru, A., Schoeneick, F.M. 1992. Hydrogeological investigations of the aquifers of Bauchi Area. Jour. Min. Geol. Vol. 28, No.1 pp45-53.

UNICEF. 2009. Water, Sanitation and Hygiene. Available at t http://www.unicef.org/wash
(Assessed 28/1/2012).

Vasanthavigar, M., Srinivasamoorthy, K., Vijayaragavan, K., Rajiv Ganthi, R., Chidambaram, S., Anandhan, P., Manivannan, R., Vasudevan, S. 2010. Application of water quality index for groundwater quality assessment:

thirumanimuttar sub-basin, Tamilnadu, India. Envi- ron Monit Assess 171:595–609

Velpen, V. 1988. Resist program, Ver. 1.0. MSc Research project, ITC, Delft, The Netherlands

Wadrobe Engineering inc. 1989. Phase II Rural Borehole Project, Volume 2 hydrogeology and borehole data. A report submitted to Bauchi State Agricultural Development Programme (BSADP)

Ward, S.H. 1990. Resistivity and Induced Polarization Methods. In: S. H. Ward, Ed. Geotechnical and Environmental Geophysics, 2nd Edition, Society of Exploration Geophysicists, Tulsa, 147-190.

Water Surveys, 1978. A limited investigation for rural water supplies and land use in Bauchi State. Unpublished Report. Vol. 1, 108p

WGMS Monitoring Strategy, 1998. at www.geo.unizh.ch/wgms.

White, D.E., Hem J.D., Waring, G.A. 1963. Chemical composition of subsurface waters. In: Data of geochemistry, 6th edn. US Geol Surv Prof Pap 440-F: F1–F67

WRI, UNEP, UNDP, and World Bank, World Resources 1998-99. A Guide to the Global Environment, 1998. Oxford University Press, New York.

Wright, C.P. 1992. Hydrogeology of Crystalline Basement aquifer in Africa. Geological Society of London Special Publication No. 66 Pp. 1 – 27.

World Health Organisation, 2011. Guidelines for drinking water quality (4th edn), World Health Organisation.

WHO, & UNICEF, JMP–Nigeria, 2008. A Snapshot of drinking water and sanitation in Africa:A regional Perspective under WHO/UNICEF Joint Monitoring Programme.

WSMP, 2008. Water and sanitation summary sheet: Nigeria. Water and Sanitation Monitoring Platform.

www.iaea.org

Yammani, S. 2007. Groundwater quality suitable zones identification: application of GIS, Chittoor area, Andhra Pradesh India.Environ.Geol,.53(1) pp.201-210

Yidana, S.M., Banoeng-Yakubo, B., Akabzaa, T.M. 2010. Analysis of groundwater quality using multivariate and spatial analyses in the Keta basin, Ghana. J Afr Earth Sci 58(2):220–234

Zaborsky, P.M., Ugodunluwa, F., Idornigie, A., Nnabo, P., Ibe, K.1997. Stratigraphy and structure of the Cretaceous Gongola Basin (N.E Nigeria). Bulletin des centres de Researches Exploration Production ElfAquitaine 21 (1), 153-177.

Zohdy, A.A. 1989. Programs for the automatic processing and interpretation of Schlumberger sounding curves in Qbasic 4.0.US Geol Surv Open-File Rep 89–137 A and B

Zhang, X., F.W. Zwiers, G.C. Hegerl, F.H. Lambert, N.P. Gillett, S. Solomon, P.A. Stott, and T. Nozawa, 2007. Detection of human influence on twentieth-century precipitation trends. Nature, 448(7152), 461-465.

Zhu, G. F., Li, Z. Z., Su, Y. H., Ma, J. Z., & Zhang, Y. Y. 2007. Hydrogeochemical and isotope evidence of groundwater evolution and recharge in Minqin Basin, Northwest China. Journal of Hydrology, 333(2), 239–251

APPENDIX I: Field Procedure for Vertical Electrical Sounding

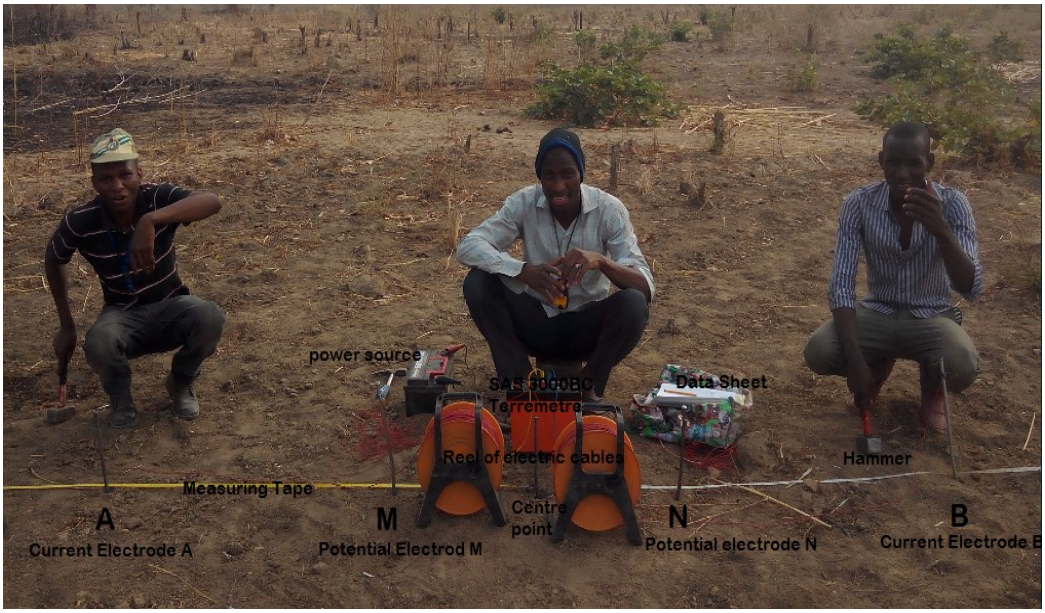

Plate 1.1. Field set up and instruments for Vertical Electric Sounding (VES)

APPENDIX II: Laboratory Procedures for Thin Sectioning and Granulometric Analysis

The technique adopted for the preparation of the thin section slides involved slicing of the rock sample using diamond saw and mounting the sliced rock on a glass plate using a resin (lakeside 70C cement). Followed by grinding the mounted rock slice to a standard thickness of 0.03mm by means of successive finer and finer abrasives. The 0.03mm

section was then covered with a cover glass using transparent balsam for examination under a petrological microscope

In doing the granulometric analysis, the friable sandstone samples were carefully disaggregated using a ceramic mortar and pestle and 200 grams of each of the crushed samples were placed in a standard set of sieves arranged such that the mesh sizes increased from bottom to top. The mesh sizes used from the top to the bottom respectively are: 3.35mm, 2.36mm, 1.18mm, 0.850mm, 0.425mm, 0.300mm, 0.212mm, 0.075mm, and 0.063mm. Each sample was placed on a mechanical shaker for a period of 5- 10 minutes, after which the individual weight retained on each of the sieves was measured using a sensitive weighing balance. The corresponding values of weight % and cumulative weight % were computed and tabulated. Using the data so obtained, cumulative frequency curves were plotted, from which, values for sorting and graphic mean (grain size) were duly computed

APPENDIX III: Laboratory Protocols for the Determination of Alkalinity of Water Samples

The alkalinity of water samples can be determined in the following steps:

Determination of the normality of the acid by titrating 5 mL of the ~**0.05 N Sodium Carbonate Solution with Standard 0/01 N Hydrochloric Acid** until pH=5. Rinse the pH probe into the same beaker, and boil gently for 3 to 5 minutes. Cool to room temperature and rinse cover glass into beaker. Finish titrating the sodium carbonate solution to pH=4.5. Record the volume of acid used. Calculate the normality of the acid.

See formula 3.1. Place a known amount of sample into an appropriately sized beaker. And add a magnetic stir bar. Add enough Distilled and Deionized Water (DDW) to ensure that the pH electrode has adequate contact with the solution. Place the beaker on the magnetic stirrer and position the pH electrode so that it does not interfere with the mechanical stirring. Titrate with standardized acid to the endpoint pH of 4.5. Record the volume of acid used. Calculate the alkalinity of the sample. See formula 3.2.

Determination of Acid Normality

$$Normality, N = A * \frac{B}{5300 * C} \quad 3.1$$

A = g Na_2CO_3 weighed into 1 L flask (from ~**0.05 N Sodium Carbonate Solution** preparation)

B = mL Na_2CO_3, solution taken for titration

C = mL acid used

Total Alkalinity (in mg $CaCO_3$/L)

$$Alkalinity\ \left(\frac{mgCaco3}{L}\right) = A * N * \frac{50000}{mLSample} \quad 3.2$$

A = mL standard acid used

N = normality of standard acid

Since most groundwater samples will have an initial pH < 8.3, the concentration of carbonate alkalinity will be zero. Thus, all of the alkalinity can be attributed to bicarbonate. Determine the bicarbonate concentration (as mg CaCO3/L) by divide the mg CaCO3/L by 0.8202 (from stoichiometry conversion). The reporting concentration of Bicarbonate is (mg HCO3/L)

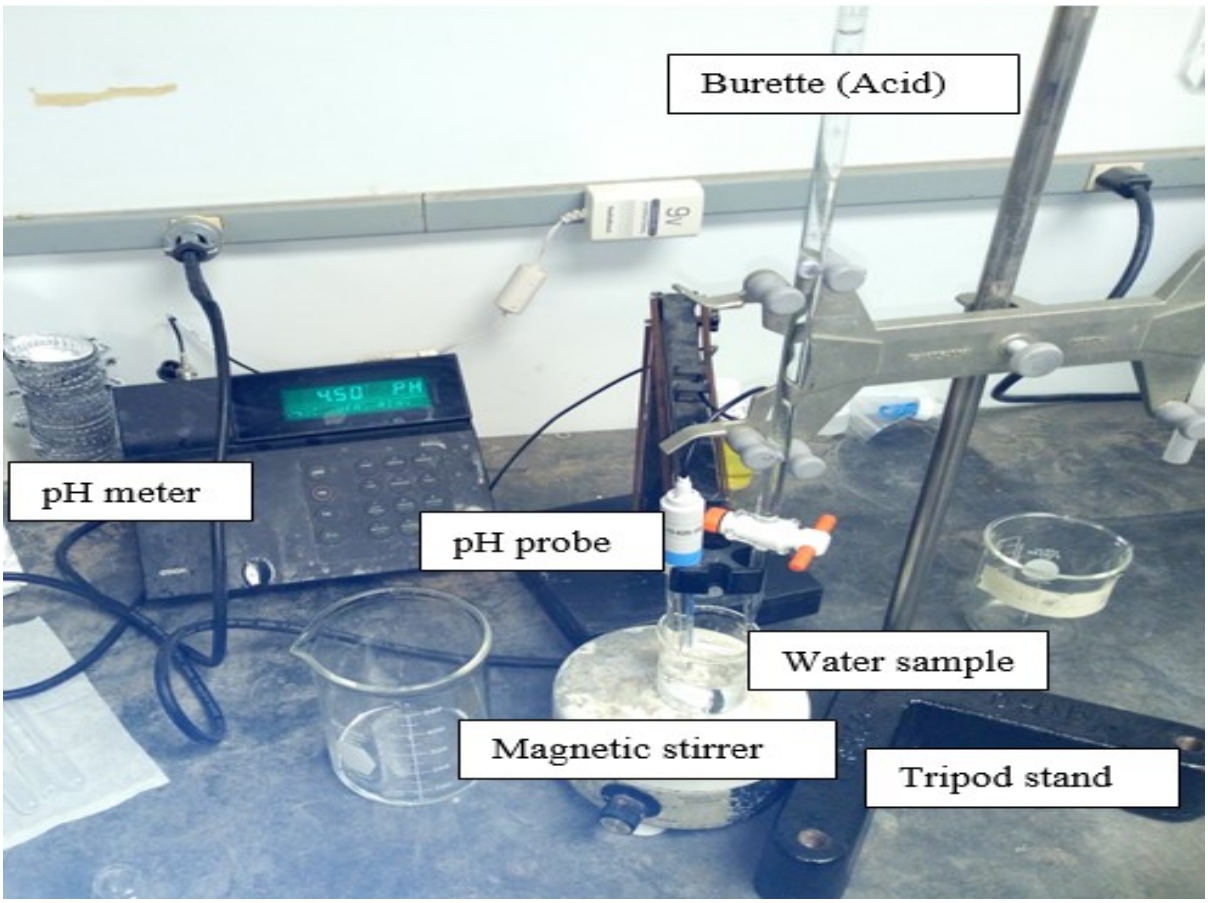

Plate 3.1 Set up for Alkalinity determination using Acid Titration

APPENDIX IV: Laboratory Protocols for the Determination of Concentration of Cations in Water Using Atomic Absorption Spectrometry.

The first step of the experimental procedure entails preparation of calibration standards which covers the blank solution (adding 1ml of nitric acid to 1000mL of DDW), the Mixed Stock Standard (pipetting 10 mL of each desired purchased element (Ca, Mg, Na, K – 1000mg/L) in a 100mL flask and diluting to the mark with 1% Nitric Acid or DD Water with 5 drops of concentrated HNO_3, and inverting and mixing properly) and the Working standard (prepared from the Mixed Stock standard (100 mg/L) as follows: pipetting 0.05, 0.25, 0.5, 1.5, 2.5 and 3.75ml of the mixed stock solution in 50mL flask and filling it to the mark with 1% nitric acid.

The second step of the analysis is sample preparation, preservation a dilution. Samples are filtered through 25mm, 0.45 micron, Polyethersulfone syringe filter and acidified to 0.1% HNO3.Followed by dilution in order to ensure the samples fall inside the calibration range. For most applications, a 10 times dilution is adequate for (Potassium and Magnesium) and 50xtimes for (sodium and calcium). Although in some instances, further or less dilution might be required.

The final step involves the generation of the calibration curve on the instrument and running the samples.

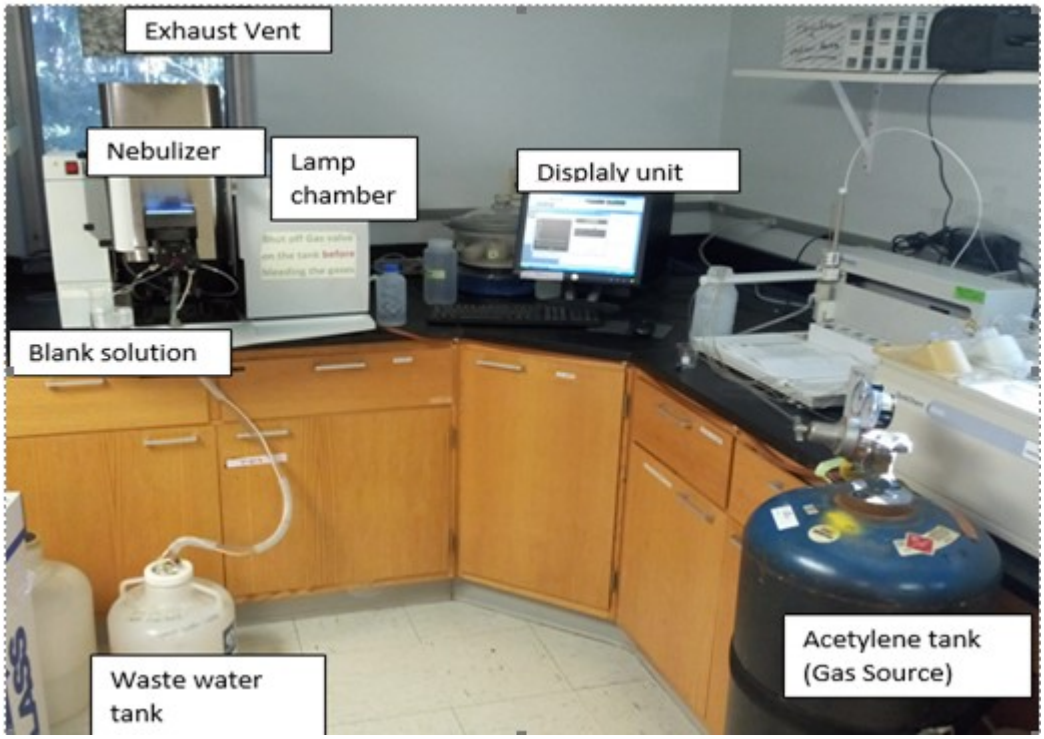

(a)

(b)

Plate 4.1. Perkin Elmer AA400 Atomic Absorption Spectrometer (AAS) 4.1.1

APPENDIX V: Laboratory Protocols for the Determination of Concentration of Anions in Water Using Ion Chromatogram.

This procedure starts with the preparation of I.C Eluents solution by diluting 14ml of Na_2CO_3 and 4ml of $NaHCO_3$ with degassed water to the 2 liter mark, followed by the preparation of I.C Reagent solution from dilution of 6ml of concentrated sulphuric acid with 94ml of deionized water. The diluted acid also known as the I.C reagent solution is transferred into the 2 liter reagent bottle and filled with degassed water. The I.C eluent and reagent solution are then transferred to their respective chambers on the Ion Chromatograph (Plate 3.6).Water samples were diluted 41times and filtered to remove particles larger than 0.20 μm. This was preceded by preparation of anions standard stock solution for all the anions in question from their respective anhydrous compounds (e.g. Fluoride from sodium fluoride, Chloride from sodium chloride and Bromide from sodium bromide and e.t.c). Subsequently, a Mixed Stock Solution and calibration standards was prepared respectively. The former was prepared by pipetting 10.0 mL of each stock standard into a 100 mL volumetric flask while the latter was prepared by pipetting 0.200, 0.500, 1.00, 3.00, 5.0, & 10.0 milliliters of the Mixed Stock Solution into six separate 100 milliliter volumetric flasks and diluting to volume with DDW. Anion concentrations will be 0.20, 0.50, 1.00, 3.00, 5.00, & 10.0 mg/L respectively. Prepare fresh calibration standards daily. All the samples and calibration standards were poured into special plastic tubes and fitted in the auto sampler in a sequential manner (Plate 5.1). The calibration standards were first run, followed by the diluted water samples and the full strain samples each group separated by blanks to avoid cross contamination. Ions are identified by their retention time and quantitated by measurement of peak area displayed by the chameleon software on the display unit of the instrument.

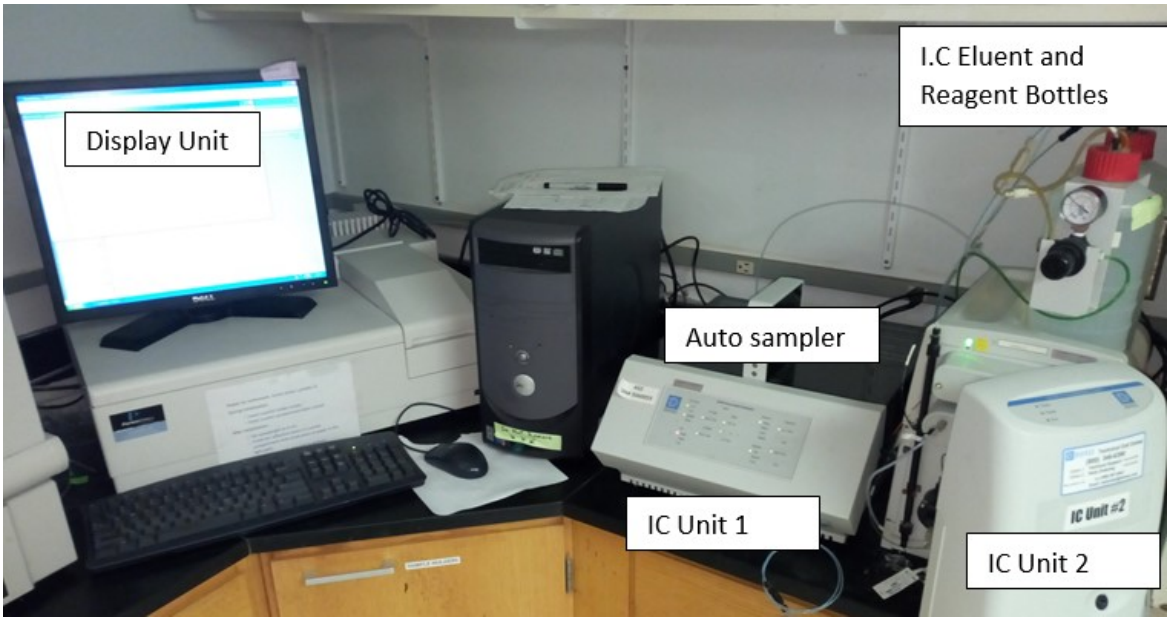

(a)

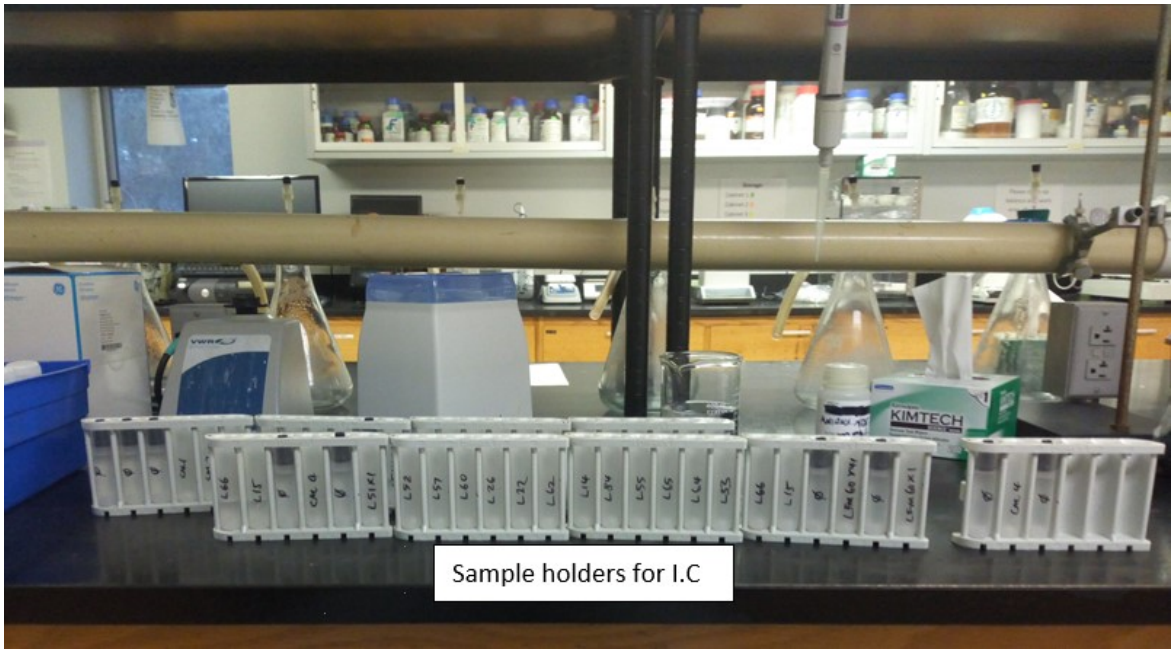

(b)

Plate 5.1. (a) Dionex Ion Chromatograph with a detection limit of 0.01 mg/L (Dionex ICS 1100) for Inorganic Anion Analysis in Water at the Water Science Laboratory, UNL, Lincoln, USA.

(b). Labelled sample holders for I.C prior to loading into the Auto sampler

APPENDIX VI: Laboratory Protocols for the Determination of Ratios of Stable Isotopes of Oxygen and Deuterium in Water.

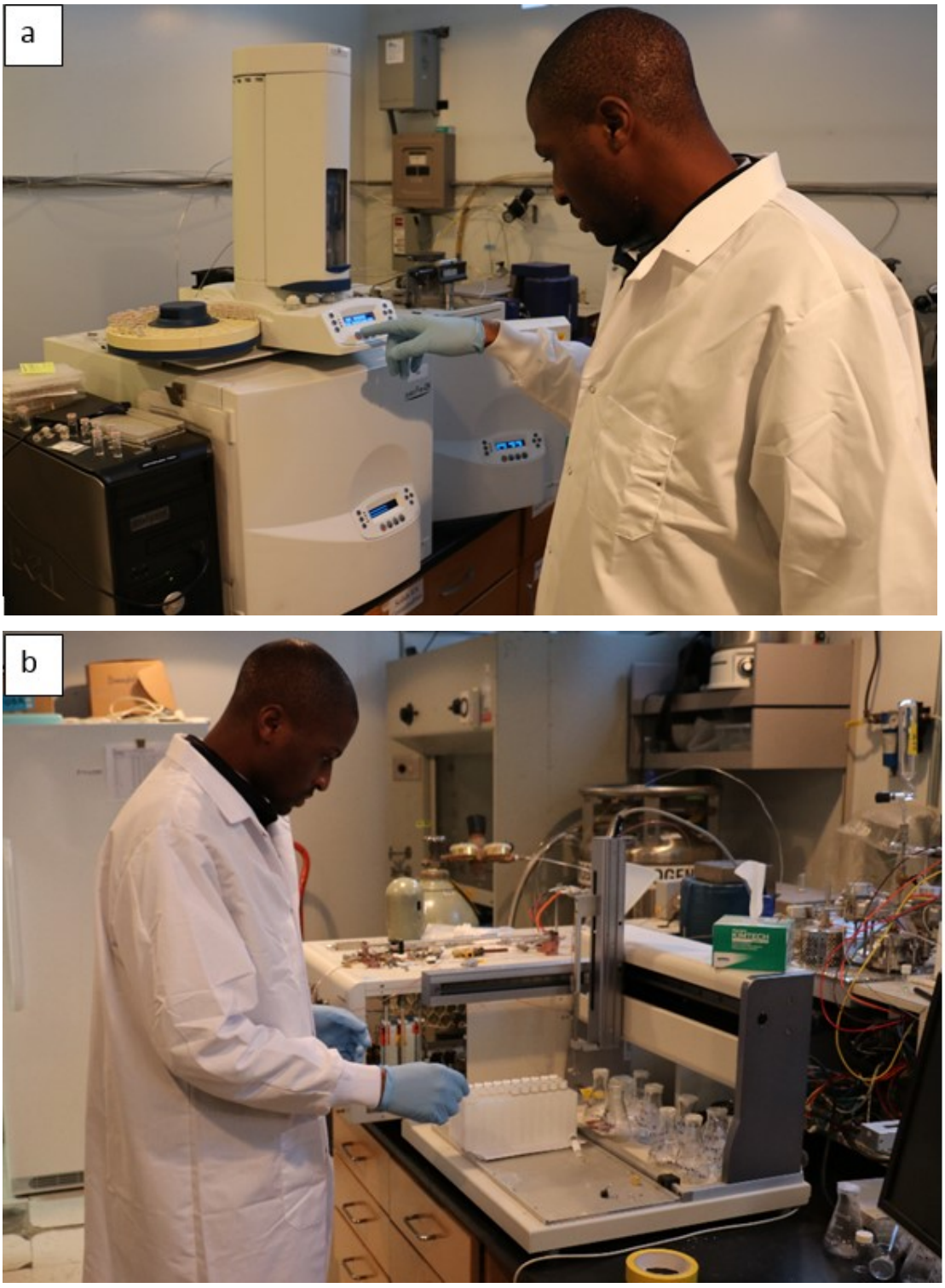

Plate 6.1 (a) Stable isotope ratio mass spectrometry (b). Isoprime continuous flow mass spectrometer

APPENDIX VII: Mathematical procedure for computation of Saaty's Consistency ratio (C.R)

Saaty (1980) suggests that a consistency ratio (C.R) be computed for themes and features should be computed as follows:

Step 1: Computation of principal eigen value denoted by λ through eigen vector technique.

Step 2: Calculating consistency Index (CI) using the following relationship (Saaty, 1980):

$$CI = \frac{\lambda max - n}{n-1} \qquad 3.4$$

n is the number of criteria under consideration.

Step 3: Calculation of consistency ratio as follows:

$$CR = \frac{CI}{RCI} \qquad 3.5$$

RCI = random consistency index.

The RCI value was derived from the Saaty's 3–9 scale. Consistency ratios >10 should indicates inconsistent weights and should be rechecked while ratios < 10 less than 10% (Saaty, 1980) are considered as consistent weights.

APPENDIX VIII: Mathematical formulation for evaluating Water Quality Index

First calculate the relative weight Wi for each parameter as follows

$$Wi = wi/\sum wi \quad (3.7)$$

Where

Wi represents the relative weight

wi represents the weight of each parameter

n stands for number of parameters

qi which represents the quality rating for individual parameter was evaluated by equation (3.8).

$$qi = (Ci / Si) \times 100 \quad (3.8)$$

A quality rating scale (qi) for each parameter was derived by dividing its concentration (Ci) in each water sample by its respective Nigerian Standard for Drinking Water Quality (Si) and the multiplying the result by 100.

The last step in the computation of WQI is the determination of the SI for each parameter using the equation (3.9).

$$SIi = Wi \times qi \quad (3.9)$$

Hence the WQI is given by equation (3.10)

$$WQI=\sum SIi \quad (3.10)$$

And overall WQI is evaluated as follows:

$$\text{Overall WQI} = \sum SIi / \sum wi \quad (3.11)$$

Where

SIi = the sub-index of the ith parameter

qi = the rating based on the concentration of the ith parameter.

wi = the weight of each parameter

APPENDIX IX: The General Principles of Stable Isotope Studies

Isotopes are atoms of the same element which have the same atomic number but different mass number, by implication isotopes have different numbers of neutrons, which is responsible for the differences in the masses of various isotopes of an element. Environmental isotopes can be divided into radioactive isotopes (e.g. 3H and 14C) and stable (2H and 18O). Radioactive Isotopes are nuclides with unstable nuclei with the tendency to decay into non-radioactive isotopes of other chemical elements, by emission of alpha, beta or gamma rays. Some of the useful radioactive isotopes as captured by Mazor, 1997, are Rb-SR, K-Ar, Sm, Nd, U-Th-Pb, 4H, 3H, 3He, and 40 Ar). Radioactive isotopes have variously been applied in the fields of Medicine, Biology, Agriculture and geology to trace natural processes and in dating geological rocks and orogenic episodes. Stable isotopes, as the name implies, are those that have stable nuclei and do not undergo radioactivity (non-radioactive ones).While stable isotopes may be products of radioactive decay of other isotopes, the isotopic composition of stable isotopes is dependent on natural variation as a result of dependent fractionation (Craig, 1961; Clark and Fritz, 1997).

Stable isotopes of many different elements are implemented in hydrological research (the most frequently utillised, however, are the Oxygen and Deuterium isotopes), as differences in stable isotope proportions of natural compounds are regulated by chemical interactions and phase changes, combined with the distinction in the energy of chemical bonds associated with different isotopes of an element. The disparity in the bond energy are due to the relative mass difference between isotopes (Aggarwal *et al*., 2009). Stable isotopes of light elements like hydrogen exhibit higher variability than those of heavier elements like oxygen because the relative mass differences of hydrogen are greater. The degree of varaiability in $^{2}H/^{1}H$ is higher $^{18}O/^{16}O$ owing to the difference in mass between ^{2}H and ^{1}H is 2:1, while ^{18}O and ^{16}O have a ratio 1.1:1. In hydrology, stable isotope ratios are taditionally reported as per mil (‰) variance from those of a standard which use thenotation δ (delta).

$$\delta \text{ (in ‰)} = (R_x / R_s - 1) \cdot 1000 \qquad (4.10)$$

Where R represents the heavy to light isotope proportions ($^{18}O/^{16}O$), and Rx and Rs are sample and standard ratios, respectively. Isotope ratios are often reported as permil deviations from SMOW (standard mean ocean water) as

$$\delta^{18}O = \left[\frac{(^{18}O / {}^{16}O)_{sam} - (^{18}O / {}^{16}O)_{SMOW}}{(^{18}O / {}^{16}O)_{SMOW}} \right] \times 10^3$$

The use of SMOW should indicate that the measurements have been calibrated based on IAEA guidelines for expression of δ values, relative to the reference materials available on standardized permile scales (Coplen, 1994; 1996). The use of deuterium and oxygen isotopes in hydrogeological studies in most cases apply the variations in isotopic ratios in rainfall. These variations are due to a number of physical processes (Fig. 4.58), the most cosequential of which are evaporation and condensation. The lighter water molecule, $H_2{}^{16}O$, escapes faster than heavier molecules during evaporation (that is, $^1H^2H^{16}O$ or $H_2{}^{18}O$). Thereby, concentrating the vapour phase with lighter isotopes and depleting it with the heavier isotopes. Studies have shown that the vapor evaporating from an ocean is depleted at a rate of 10 ‰ in ^{18}O and 80 to 120 ‰ in deuterium in relation to ocean water (Fig. 4.58).

Furthermore, during condensation, the formation of clouds and rainfall brings about the cooling of atmospheric water vapor, as a result, the heavier molecules of water preferentially condenses, causing the residual vapor phase to be more depleted in ^2H and ^{18}O. Consequently, subsequent rainfalls derived from the same original vapor will show more and more depletion in heavy isotopes (Aggarwal *et al*., 2009). Due to the fact that the extent of condensation of a vapor mass is controlled by temperature, there is a connection between the isotopic composition of the precipitation and its formation temperature. The formation temperature is directly proportional to the δ-values of precipitation, by implication as temperature of formation lowers or increases, the δ-values of rainfall also decrease or increase in a similar manner. A linear relationship has been created between δ^2H and $\delta^{18}O$ from samples of rainfall gathered from a global network of

stations near the so-called “Global Meteoric Water Line” (GMWL) represented by the relationship

$$\delta^2H = 8.\ \delta^{18}O + 10 \qquad (4.11)$$

Although the GMWL equation (Eq.4.11) does not support precipitation that has experienced substantial evaporation. Evaporated waters appear to be enriched in both heavy water isotopes, but not in the same comparative ratio shown in the above relationship (Eq.4.11).As rainfall trickles into the subsurface to replenish aquifers, mixing and selective infiltration of rainwater in the unsaturated zone creates seasonal isotopic fluctuations in rainfall. In most aquifers, there is no further change in isotopic water composition unless there is an exchange with oxygen from the rock. This exchange process is consequential for high-temperature geothermal systems only (Fig. 4.59).The goroundwater isotope composition is therfore connected to that of rainfall in the aquifer recharge at the moment of recharge. Ancient groundwater and climatic conditions of an area at the time of recharge may differ significantly from those of present day (Aggarwal *et al*., 2009). However, groundwater recharged from surface water bodies, tends to reflect the mean isotopic configuration of the river or the lake rather than that of local rainfall, which could be rather different. Also rivers which originates from precipitation in a in a mountainous region would show depletion in heavy isotope content when compared to rainfall in topographically plain areas, owing to altitude effect.

4.7.1.1 Stable isotope fractionation

Fractionation is reaction or process which selects for one of the stable isotopes of a particular element. If the process favours the heavier isotope, the reaction product is ‘heavy’, the reactant remaining is ‘light’. During fractionation processes, the reacting phases (water and solutes) often develop unique isotopic fingerprints which is often indicative of the processes that formed them (Fig. 4.58). Isotopic fractionation is mainly influenced by the geology, origin of the water, climatic processes (condensation, evaporation, melting) and mixing (Faure, 1998). Two category of processs are responsible for isotopic fractionations: Equilibrium reactions and Kinetic processes

(Aggarwal *et al*., 2009). In the equilibrium fractionation, the proportion of heavy isotopes to light isotopes in the molecules changes during the two phases. The heavier water isotopes (^{18}O and ^{2}H) become amplified in the liquid phase when the water vapor condenses in rain clouds (equilibrium process) while the lighter isotope (^{16}O and ^{1}H) remains in the vapor phase. However, bonds between the light isotopes are more easily broken in kinetic fractionation than similar bonds in the heavy isotopes. The light isotopes therefore react quicker and accumulate in the products, resulting in the enrichment of the remaining reactants in the heavy isotopes (Aggarwal *et al*., 2009). The extent of kinetic fractionation relies on the reaction path, the reaction rate, and the comparative energies of the bonds being broken or created by the reaction.

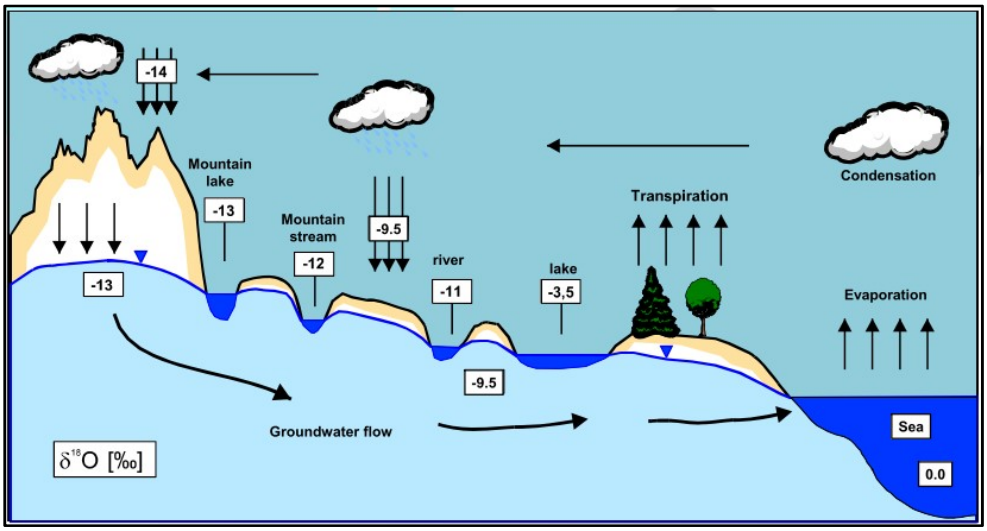

(a)

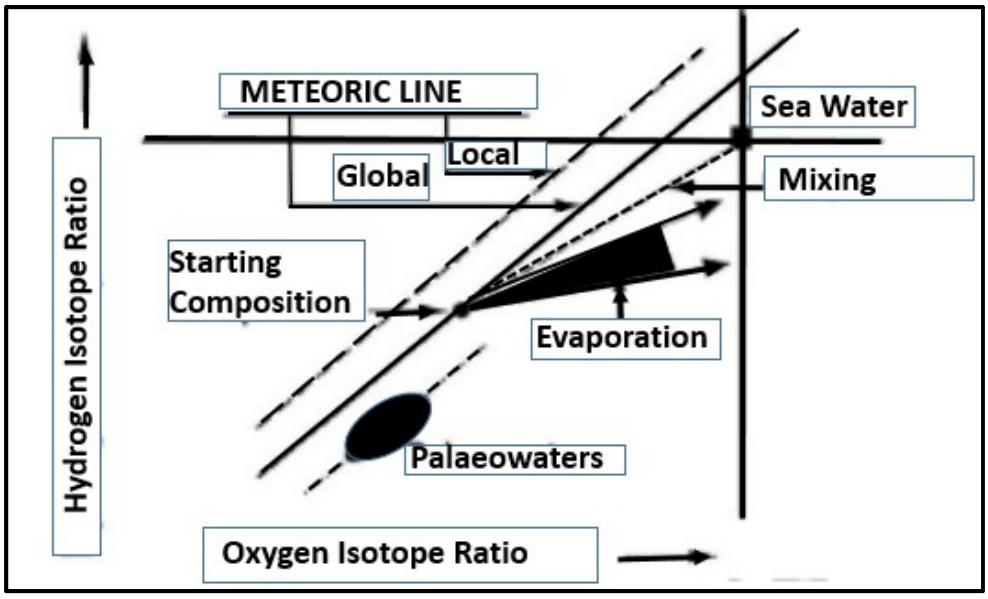

(b)

Fig. 4.58 (a) Mechanism of Isotope Hydrology (http://hydroisotop.de)

(b) Schematic representation of δ^2H–$\delta^{18}O$ in natural waters. (Modified after Aggarwal *et al.,* 2009*)*

APPENDIX X: Details of the Aeromagnetic Data Processing

Aeromagnetic Survey Data Processing

Arising from the pre-processing of the aeromagnetic data, detailed analysis of the resulting residual magnetic intensity data followed. The enhancement techniques employed include: reduction to equator (RTE), upward continuation approach, and horizontal component of tilt derivative was obtained and used as a starting grid for lineaments extraction because of its independence to inclination and declination similar to analytic signal. In order not to digress from the objective of this research which entailed production of subsurface thematic maps, only the result of magnetic lineaments extraction which generated the lineament thematic map was presented in Fig. 4.7.

Residual magnetic intensity and analytical signal map

The residual magnetic intensity map (Fig. 4.4a) was obtained by the separating the regional magnetic effect from the raw magnetic data and subsequent enhancement of the resulting magnetic data. Reduction to equator which is aimed at centering the peaks of

magnetic anomalies over their causative bodies was also applied to the residual magnetic data. The residual magnetic data ranged between−13.2 to +192.2 nT. Regions of magnetic lows (low amplitude magnetic anomaly) and highs (high amplitude anomaly) are apparent on the magnetic map. Residual magnetic lows ranged from 0.0 to −13.2nT and magnetic highs ranged from 1.0 to +192.2 nT. Conspicuously high amplitude magnetic intensities are observable on the southern part with some pockets in the eastern, western and the central parts of the residual magnetic anomaly map (Fig. 4.5a), a general trend of NE-SW was observed. Low amplitude magnetic anomalies characterise parts of the southeastern, northeastern and northwestern parts of the study. Most of these places correspond to areas with relatively thick sedimentary cover, where the effect of the thick weakly susceptible clastic materials tend to subdue the high magnetic susceptibility originating from relatively deeper basement rocks.

(a)

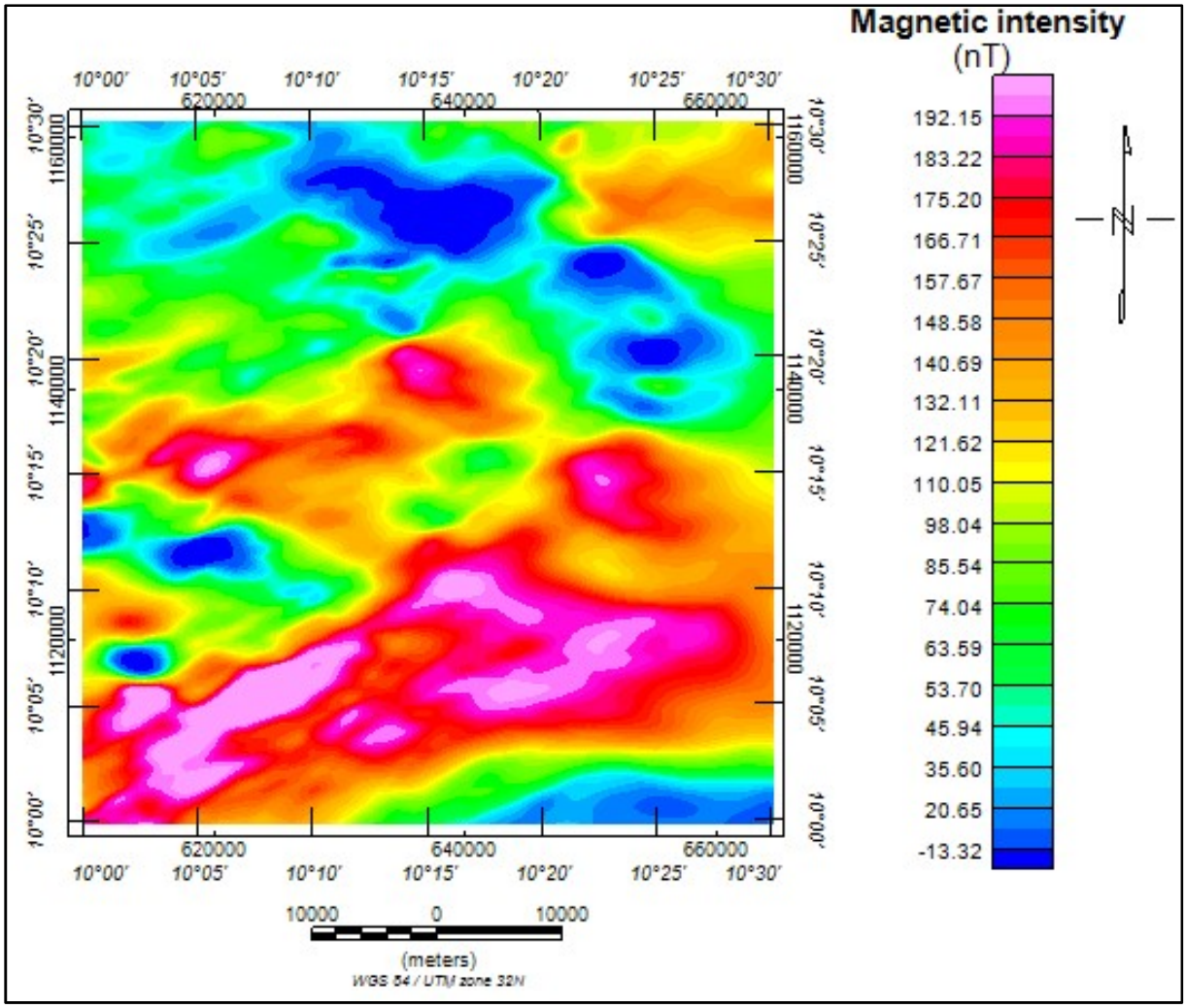

Fig 4.4 (a) Magnetic Intensity Map of the Bauchi-Alkaleri-Kirfi area (Reduced to Equator)

The analytic signal amplitude over the Bauchi-Alkaleri-Kirfi area (Fig. 4.4b), which was derived from analytic signal grid computed from 1st order vertical derivatives values of two horizontal gradients and one vertical gradient of the magnetic intensity of the area under study ranges from 0.0007 nT/m to 0.088 nT/m and averages 0.036 nT/m. The analytical signal is divided into different colour bands with each having different magnetic signatures. The bands ranges from blue (0.007-0.018 nT/m) through green (0.018-0.032 nT/m), yellow (0.032-0.038 nT/m), brown (0.0378-0.051 nT/m), red (0.051-0.063 nT/m) to purple (0.063- 0.088 nT/m) in ascending order. Prominent amplitude anomalies (Red-Purple bands) predominates the basement complex zones of the area as observable around Rugan Gilliri, Minjila, Badenga, Nahuta and Kagali in the north- west and northern part of the map. High signals also characterised Yole, Kyari, Gokaru and Balanshi in the south-western part of the analytical signal map. High amplitude analytic signal anomaly reflects high magnetic intensity contrast between crystalline basement rocks (positive magnetic intensity). Conversely, the areas with relatively thick sedimentary piles correspond to low magnetic intensity (blue bands) within the sedimentary units of the Tertiary Kerri- Kerri basin. The green colored bands occupy most of the geological transitional zones and parts of the basement complex with considerably thick overburden as exemplified by Badoromo and Gubi areas in the extreme north-western parts of the area and the central parts of the study (around Dindima area). The yellow and the brown bands represents basement zones with relatively thin overburden sediments. Generally speaking, the Basement Complex zones display higher analytical signals as compared to the sedimentary zones. However some parts of the basement parts underlain mostly by migmatite and partly biotite hornblende granite and charnockite revealed comparatively thick sedimentary pile (overburden) in the basement terrain which could be of hydrogeological advantage.

Depth to basement map (Euler Deconvolution)

Three dimensional (3D) Located Euler Deconvolution was employed in this study to determine depth to basement due to its advantage of giving reasonable solutions without prior information about the source magnetization direction, and its results are not affected by the remanent magnetization (Ravat, 1996).

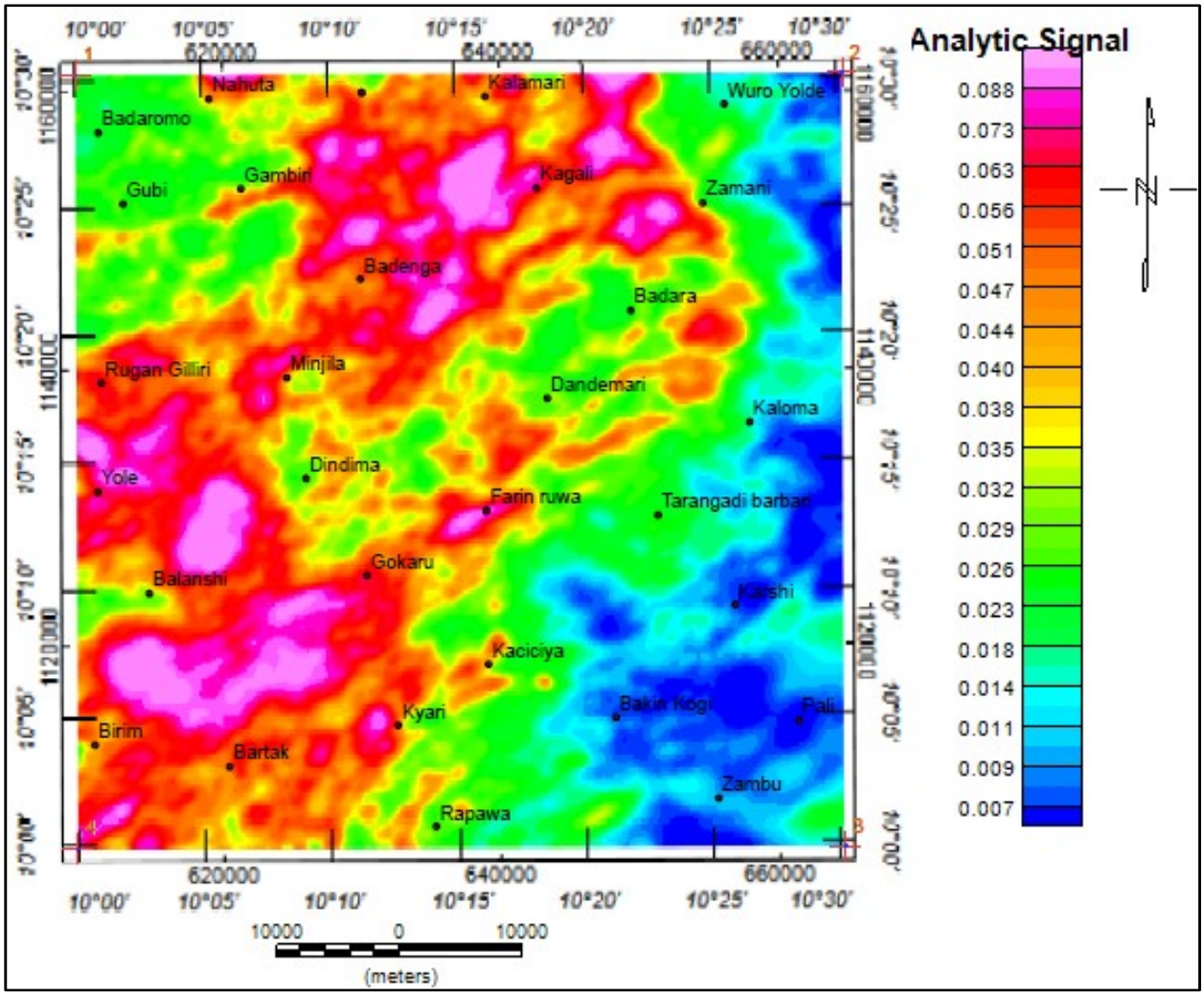

Fig 4.4 (b) Analytical Signal Plot of Bauchi-Alkaleri-Kirfi area

The qualitative interpretation of the residual magnetic data (Fig 4.4a) using the Euler Deconvolution technique indicated that the depth to the basement surface in the Bauchi-Alkaleri-Kirfi area ranges from 0 to ≥ 800 m (Fig.4.5a). The Euler deconvolution solution points corresponds to regions of high analytic signal amplitude and by implication would represent regions with meaningful anomalies whose Euler depth shall provide information of geomorphological and geological significance. The Euler depth solutions are presented as colour coded circles, with the circle's colours indicating depth range and the circle size reflecting depth variation within the range. It is evident from the circle sizes that the depths in the basement complex areas are highly variable as compared to those of the sedimentary areas. Euler depth solutions were referenced to Minna datum in Nigeria and all negative solutions corresponds magnetic sources below the mean sea level while positive solutions represent depths values above mean sea level. Euler depths result range of 1 to 200 m coincides with region where basement rocks outcrop on the surface while depth range between 0 and −800 m correspond to sedimentary terrain (Kerri Kerri Fm.) or part of the Bauchi-Alkaleri-Kirfi area where the basement rocks are overlain by thick overburden sediments. However, some pockets of comparatively deep areas were recorded in the extreme northwestern portions, some isolated parts of the Basement Complex and these are believed to coincide with deeply faulted and downthrown zones as most of the so called areas tend to have high lineament densities. Solutions around the basement complex areas indicate basement source, greater than 45 m in depth which progressively gets deeper in some parts (northern and southwestern parts) and shallower in some pockets of places with rock outcrops. The deeper most part of the Bauchi-Alkaleri-Kirfi area (1045 meters) lies in the southeastern zones, underlain by the Kerri Kerri Formation as revealed by the 2 dimensional depth to basement map derived from the Euler deconvolutin data (Fig.4.5b).

According to Dike, 1993, the sediment fill thickness in the Kerri-Kerri basin is estimated at over 320m for the west (where the present Bauchi-Alkaleri-Kirfi area lies) and the central and becomes thinner eastwards to about 262m. The present study revealed maximum sediment thickness of over 1045 meters (Fig. 4.5b) for the western margin of the Kerri-Kerri basin which is far higher as earlier workers made estimates on the basis of

boreholes and stratigraphic data, the present work however, employed a quantitatively analyzed modern aeromagnetic data.

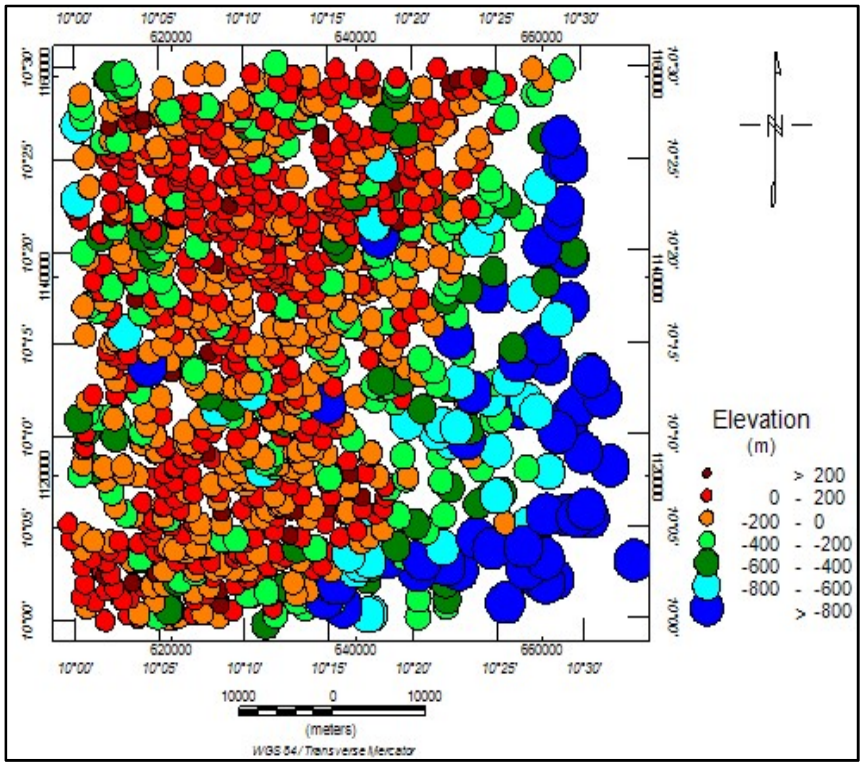

Fig 4.5. (a) Euler Deconvolution Classified Plot of Bauchi-Alkaleri-Kirfi area.

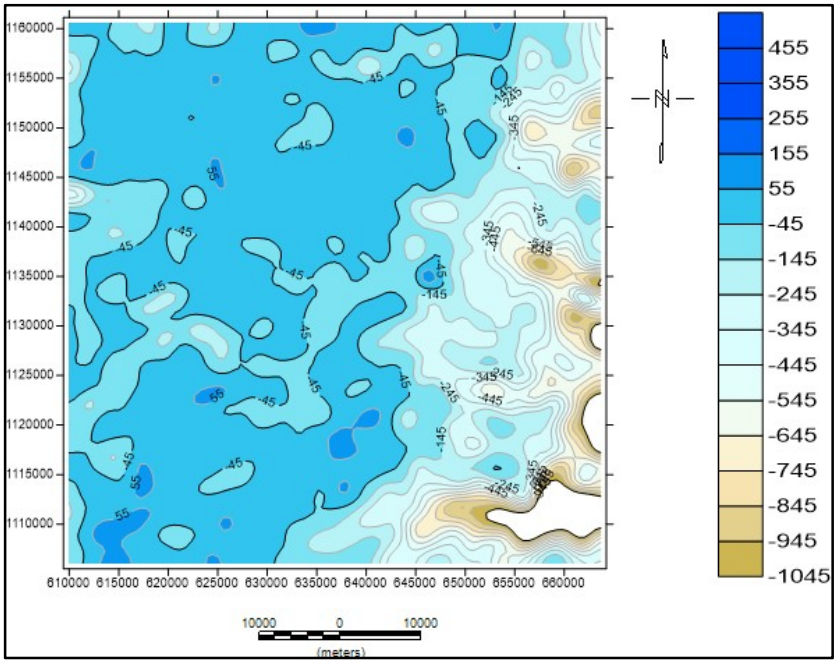

Fig 4.5. (b) 2D Basement Map Topography Map of the Bauchi-Alkaleri-Kirfi area

Appendix XI. Geophysical type curves

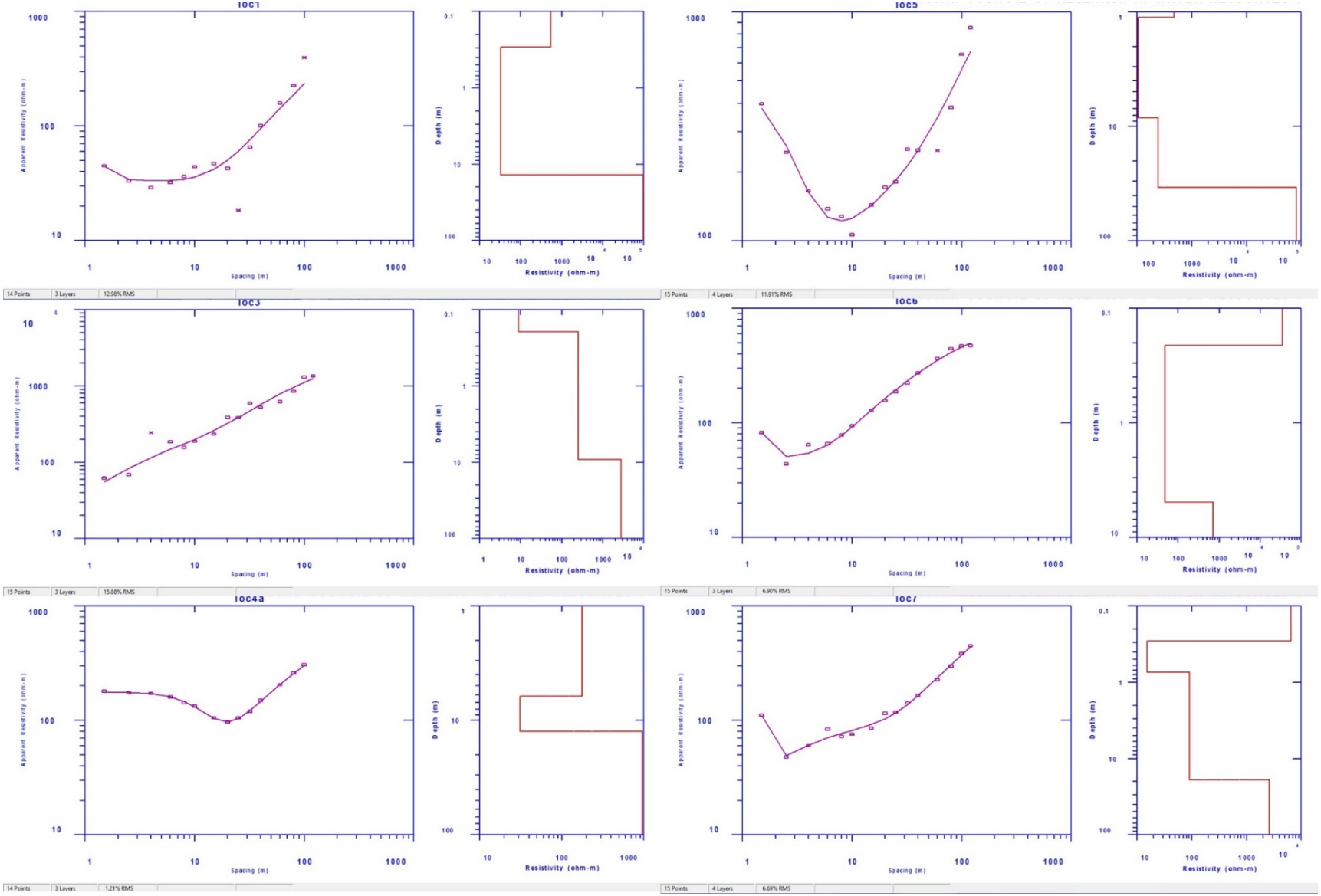

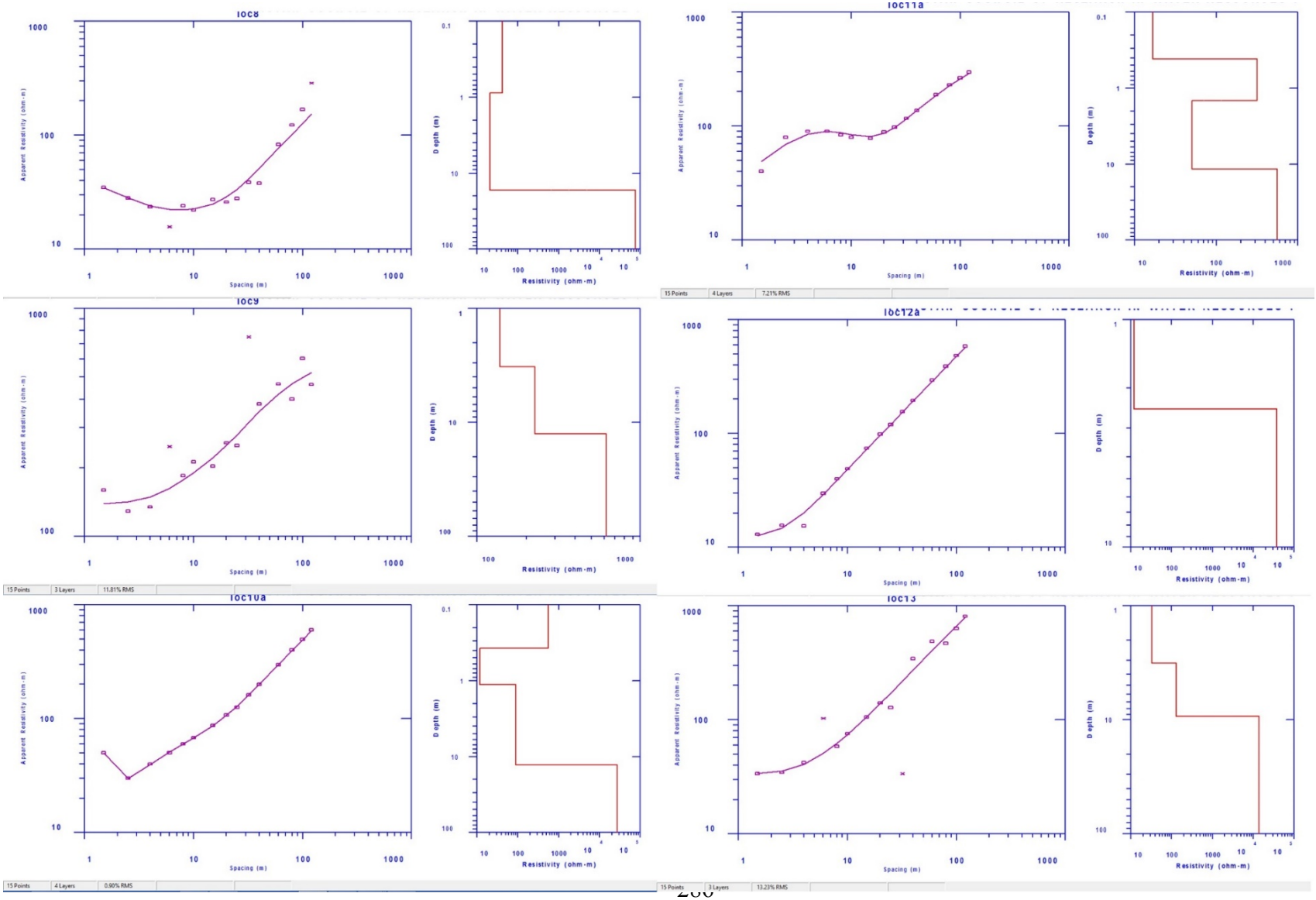
Apparent Resistivity (ohm-m)
Spacing (m)
Depth (m)
Resistivity (ohm-m)
15 Points
4 Layers
7.21% RMS
15 Points
3 Layers
11.81% RMS
15 Points
4 Layers
0.90% RMS
15 Points
3 Layers
13.23% RMS

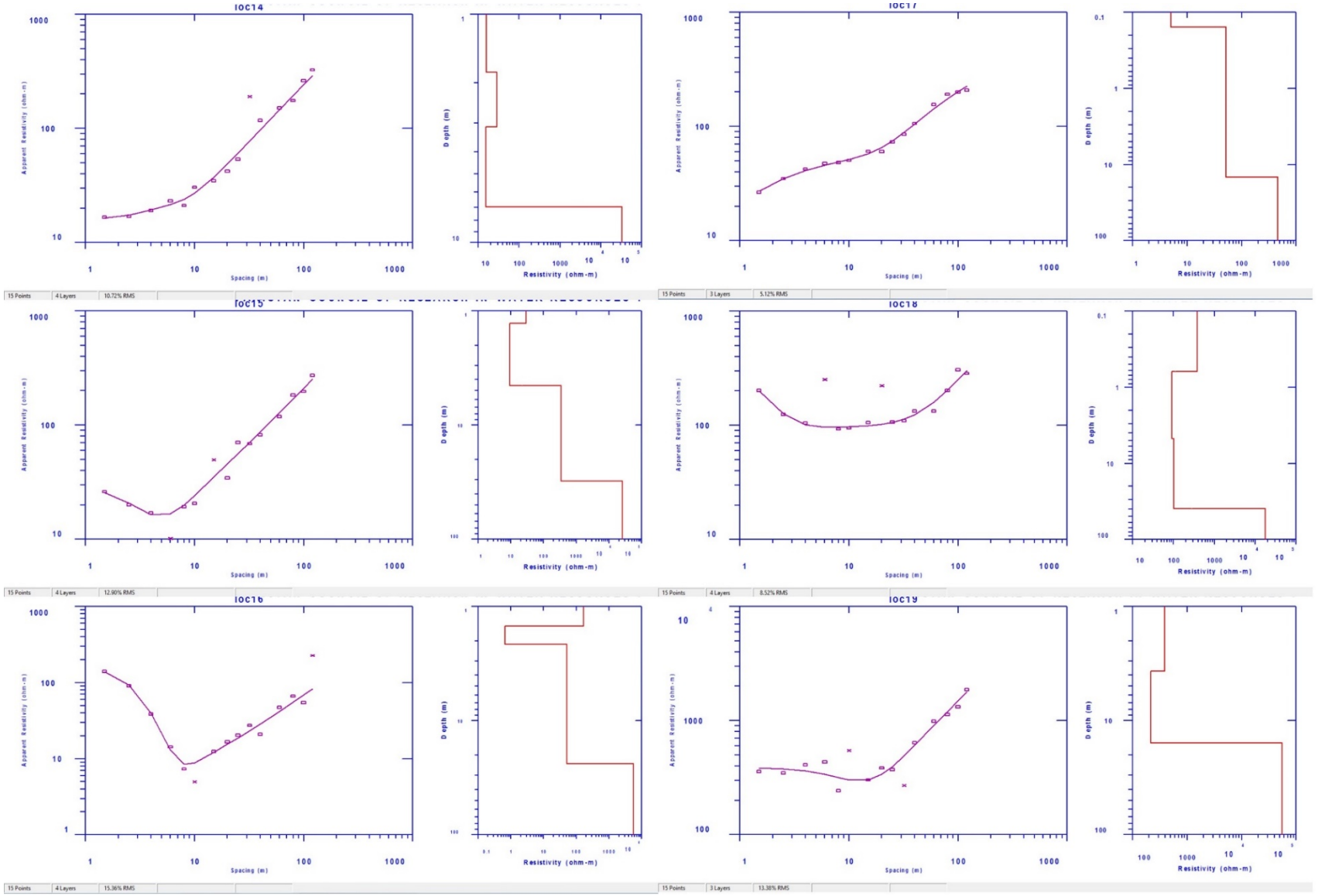
Apparent Resistivity (ohm-m)
Spacing (m)
Depth (m)
Resistivity (ohm-m)
15 Points
4 Layers
10.72% RMS
15 Points
3 Layers
5.12% RMS
15 Points
4 Layers
12.90% RMS
15 Points
4 Layers
8.52% RMS
15 Points
4 Layers
15.36% RMS
15 Points
3 Layers
13.38% RMS

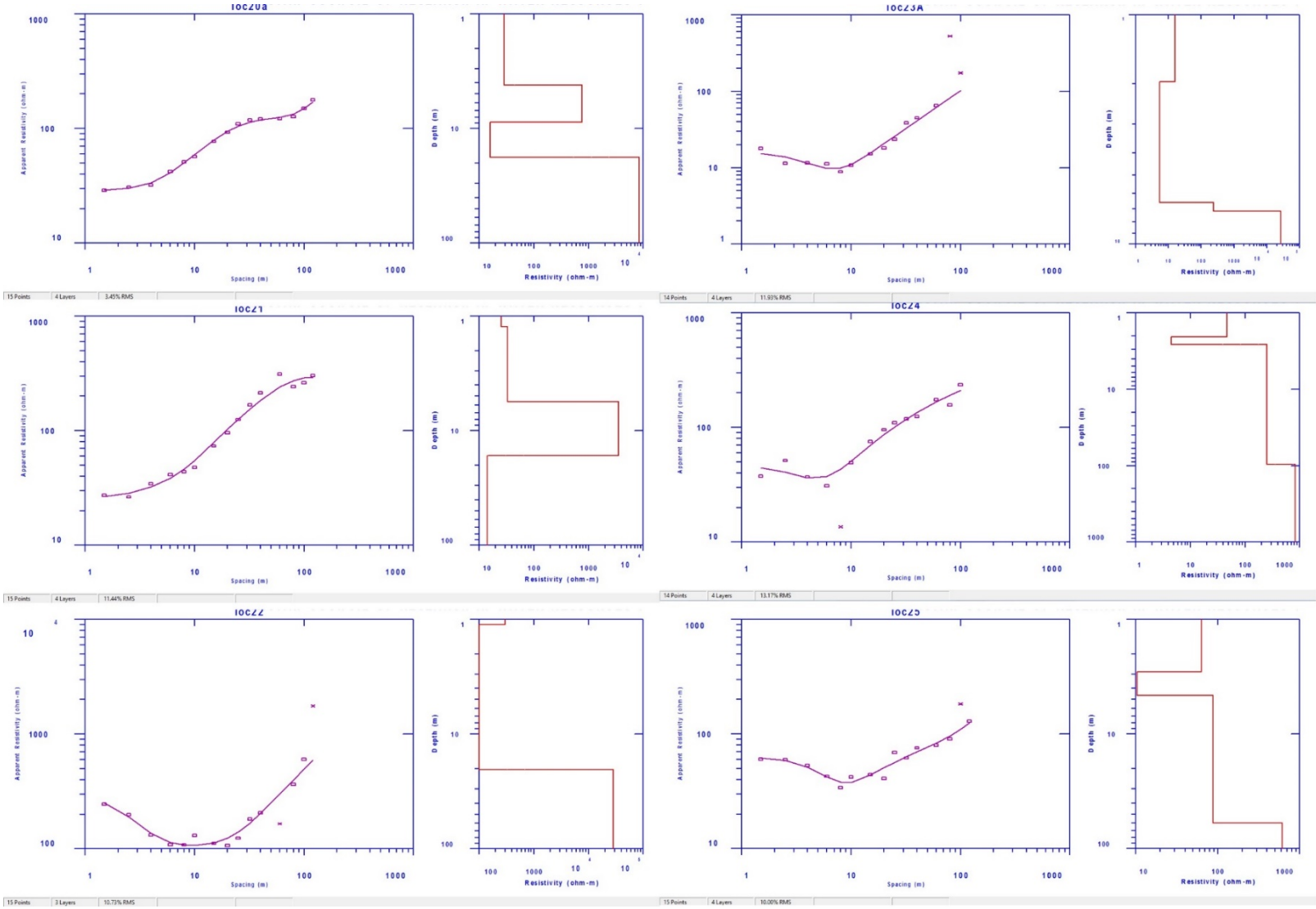
Apparent Resistivity (ohm-m)
Spacing (m)
Depth (m)
Resistivity (ohm-m)
15 Points
4 Layers
3.45% RMS
14 Points
4 Layers
11.93% RMS
15 Points
4 Layers
11.44% RMS
14 Points
4 Layers
13.17% RMS
15 Points
3 Layers
10.73% RMS
15 Points
4 Layers
10.00% RMS

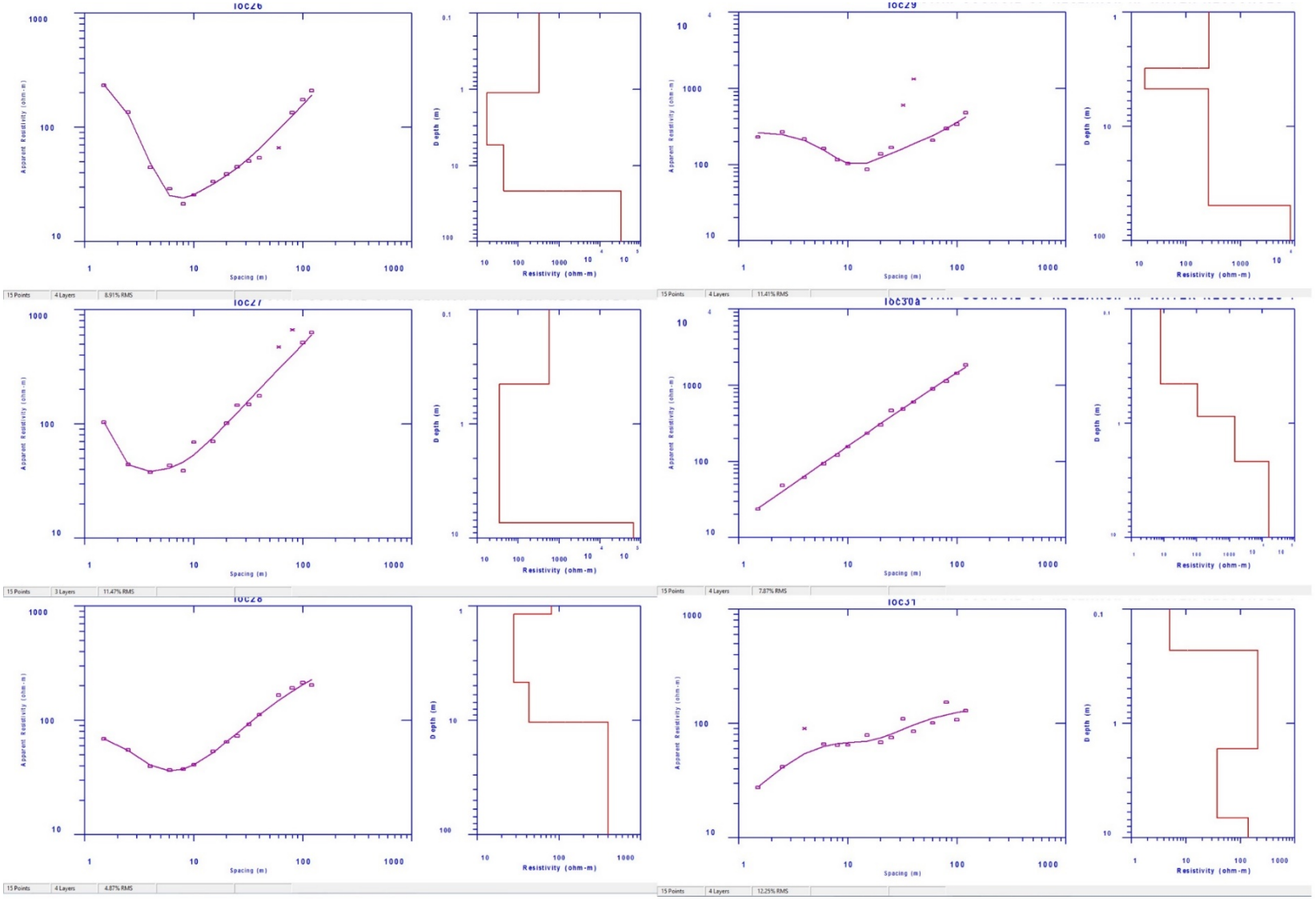
Apparent Resistivity (ohm-m)
Spacing (m)
Depth (m)
Resistivity (ohm-m)
15 Points
4 Layers
8.91% RMS
11.41% RMS
3 Layers
11.47% RMS
7.87% RMS
4.87% RMS
12.25% RMS

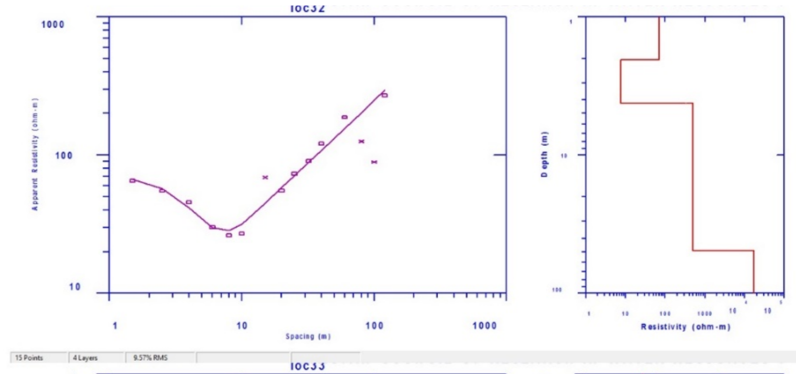
loc32
Apparent Resistivity (ohm-m)
Spacing (m)
Depth (m)
Resistivity (ohm-m)
15 Points
4 Layers
9.57% RMS

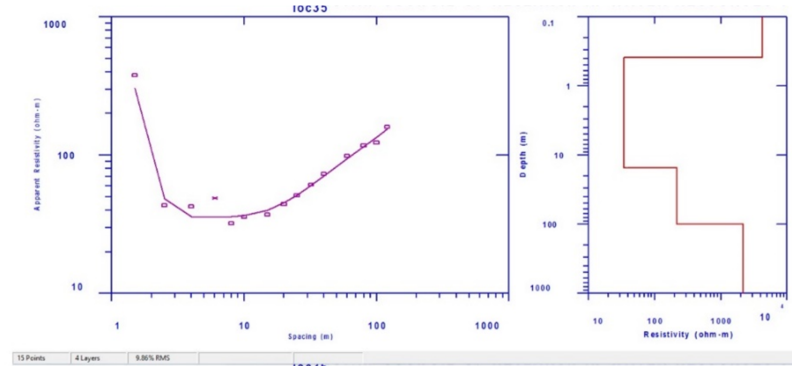
loc35
Apparent Resistivity (ohm-m)
Spacing (m)
Depth (m)
Resistivity (ohm-m)
15 Points
4 Layers
9.86% RMS

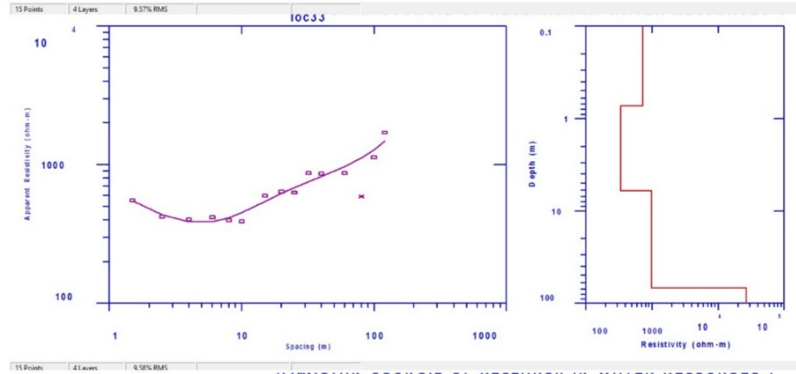
loc33
Apparent Resistivity (ohm-m)
Spacing (m)
Depth (m)
Resistivity (ohm-m)

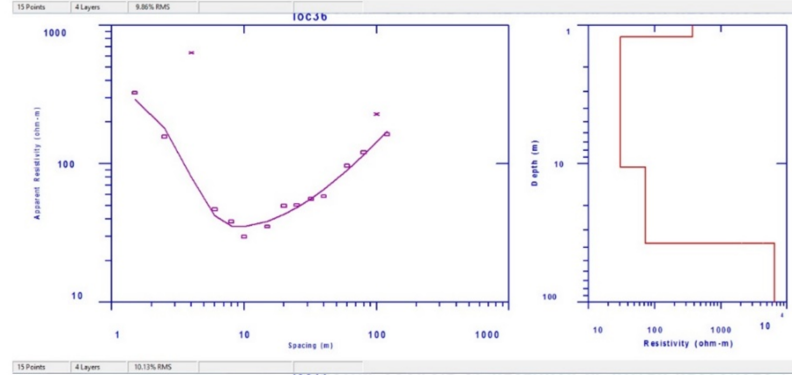
loc36
Apparent Resistivity (ohm-m)
Spacing (m)
Depth (m)
Resistivity (ohm-m)
15 Points
4 Layers
10.13% RMS

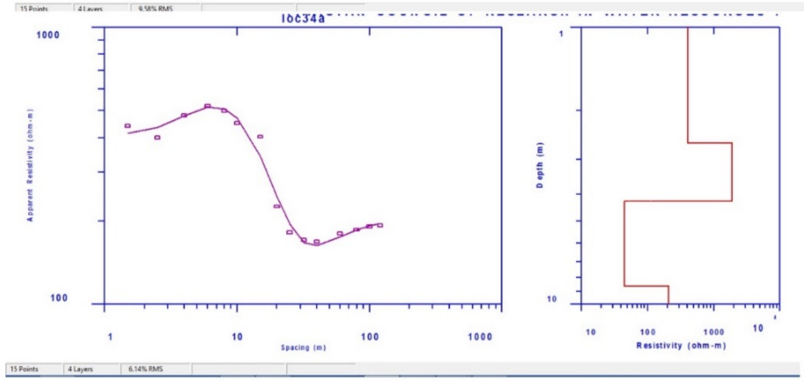
loc34a
Apparent Resistivity (ohm-m)
Spacing (m)
Depth (m)
Resistivity (ohm-m)
15 Points
4 Layers
6.14% RMS

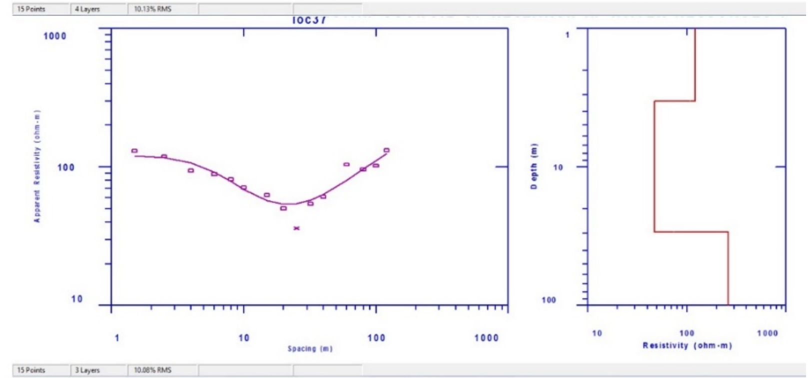
loc37
Apparent Resistivity (ohm-m)
Spacing (m)
Depth (m)
Resistivity (ohm-m)
15 Points
3 Layers
10.08% RMS

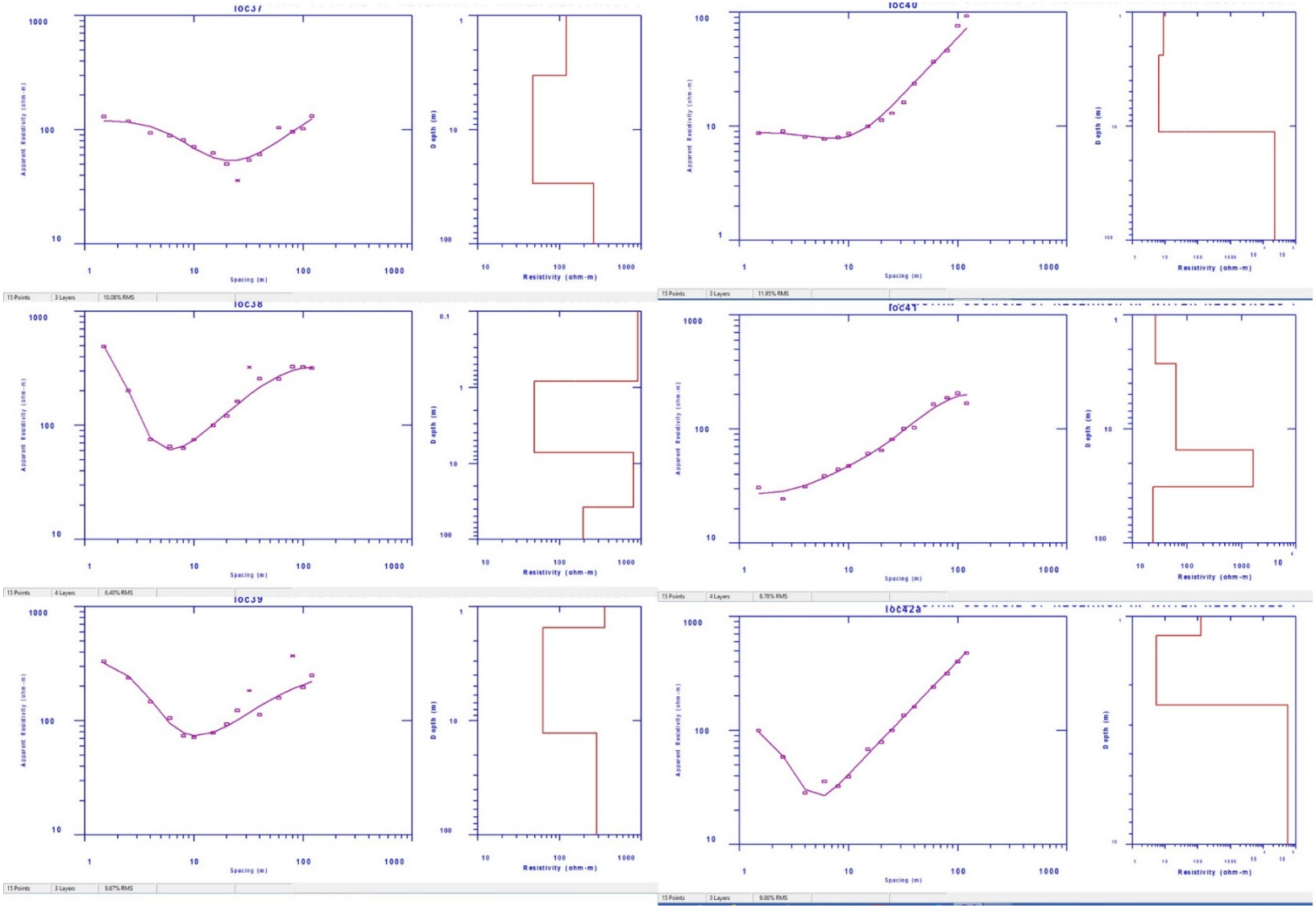
Apparent Resistivity (ohm-m)
Spacing (m)
Depth (m)
Resistivity (ohm-m)
15 Points
3 Layers
10.08% RMS
15 Points
3 Layers
11.95% RMS
15 Points
4 Layers
6.40% RMS
15 Points
4 Layers
8.78% RMS
15 Points
3 Layers
9.67% RMS
15 Points
3 Layers
9.00% RMS

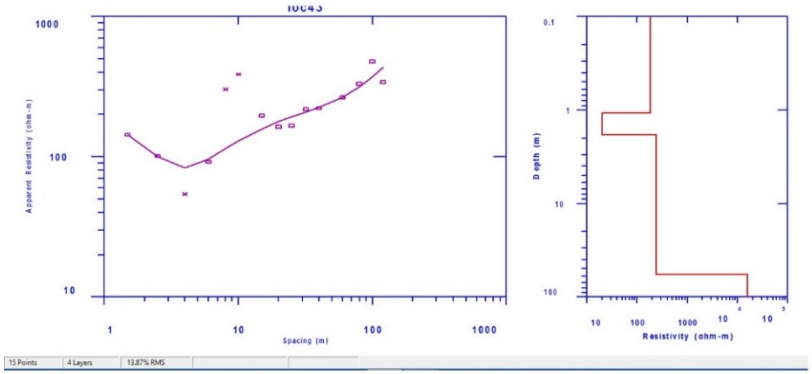
Apparent Resistivity (ohm-m)
Spacing (m)
Depth (m)
Resistivity (ohm-m)
15 Points
4 Layers
13.87% RMS

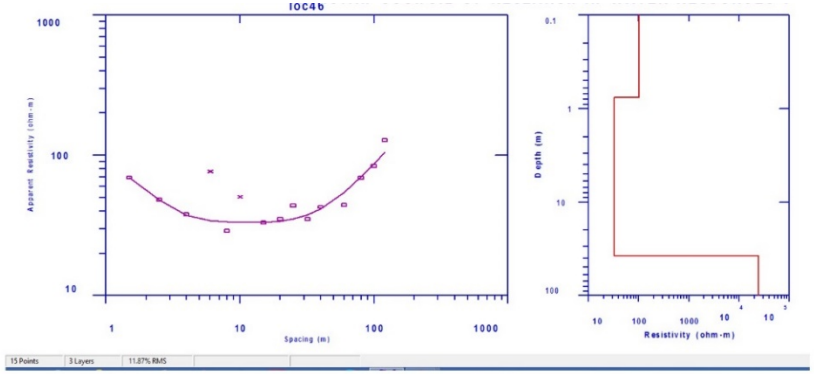
Apparent Resistivity (ohm-m)
Spacing (m)
Depth (m)
Resistivity (ohm-m)
15 Points
3 Layers
11.87% RMS

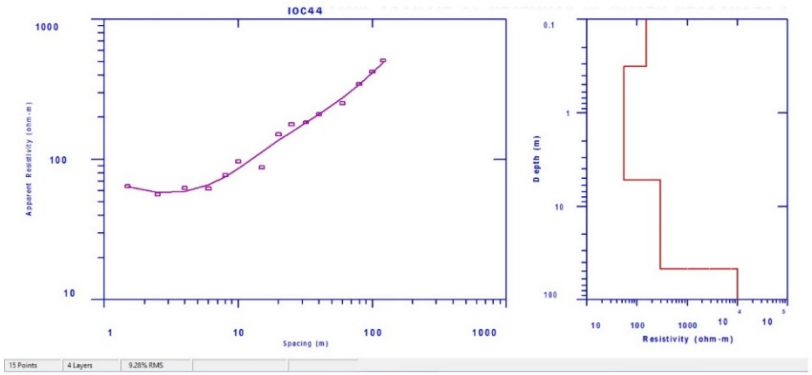
Apparent Resistivity (ohm-m)
Spacing (m)
Depth (m)
Resistivity (ohm-m)
15 Points
4 Layers
9.28% RMS

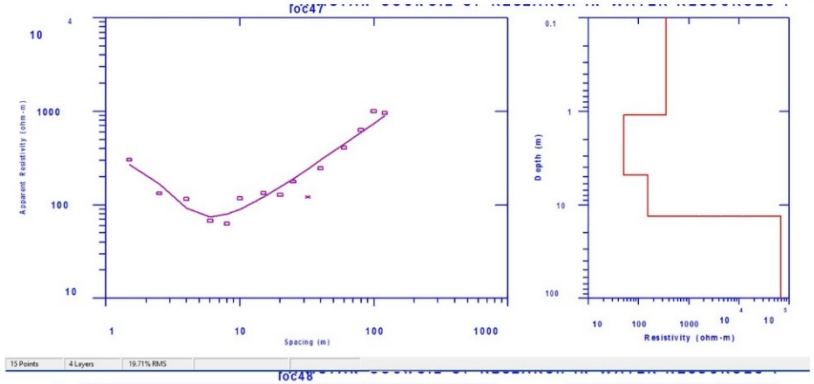
Apparent Resistivity (ohm-m)
Spacing (m)
Depth (m)
Resistivity (ohm-m)
15 Points
4 Layers
19.71% RMS

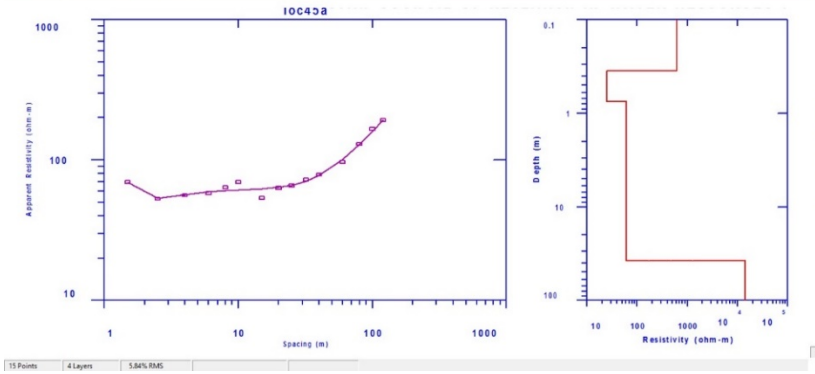
Apparent Resistivity (ohm-m)
Spacing (m)
Depth (m)
Resistivity (ohm-m)
15 Points
4 Layers
5.84% RMS

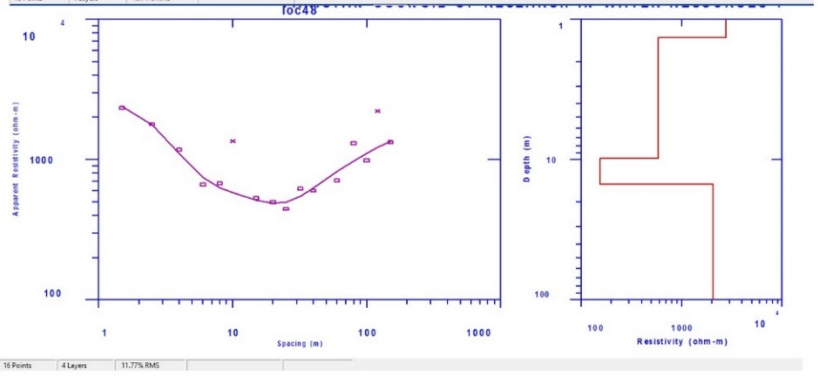
Apparent Resistivity (ohm-m)
Spacing (m)
Depth (m)
Resistivity (ohm-m)
16 Points
4 Layers
11.77% RMS

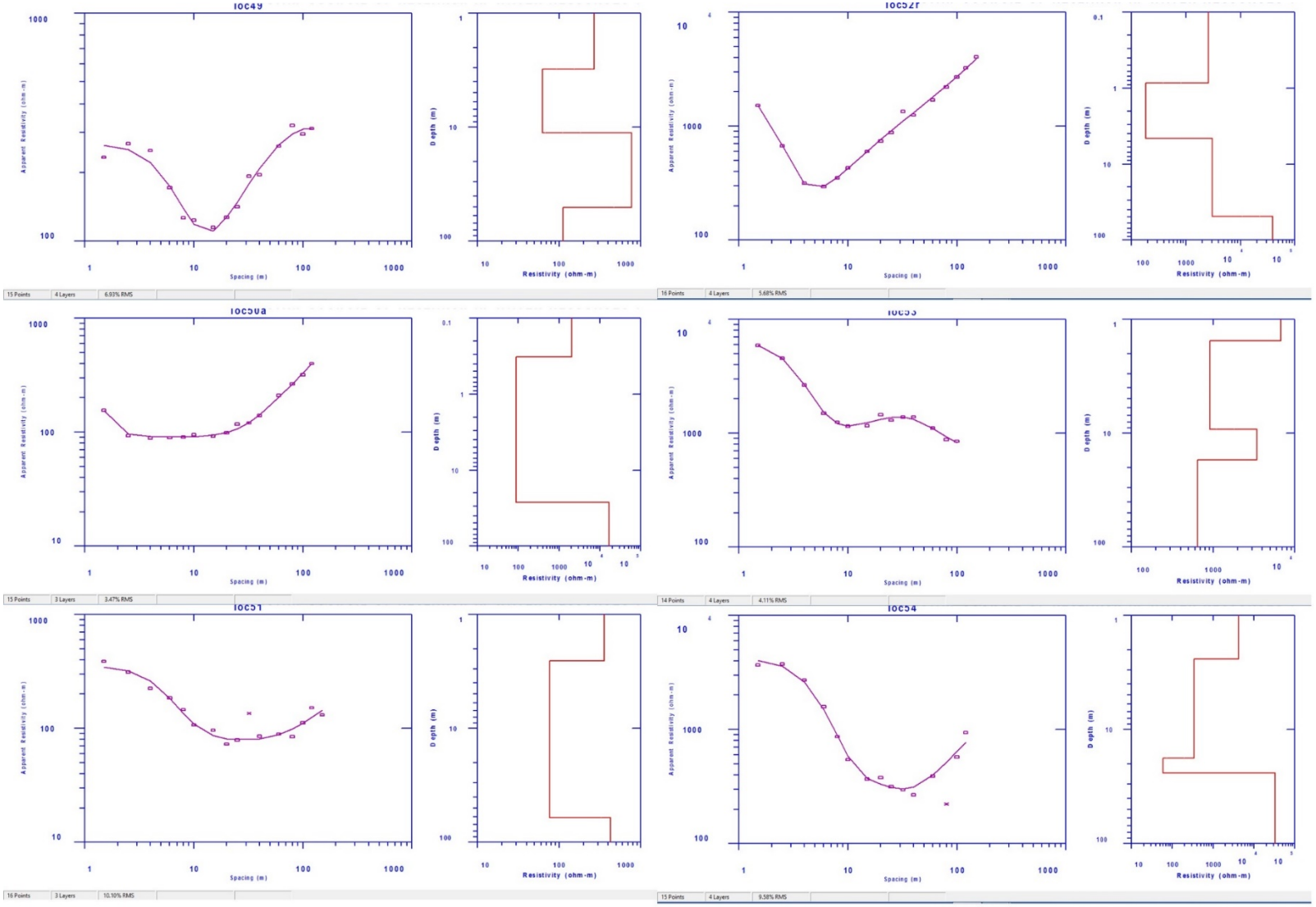
Apparent Resistivity (ohm-m)
Spacing (m)
Depth (m)
Resistivity (ohm-m)
15 Points 4 Layers 6.93% RMS
16 Points 4 Layers 5.68% RMS
15 Points 3 Layers 3.47% RMS
14 Points 4 Layers 4.11% RMS
16 Points 3 Layers 10.10% RMS
15 Points 4 Layers 9.58% RMS

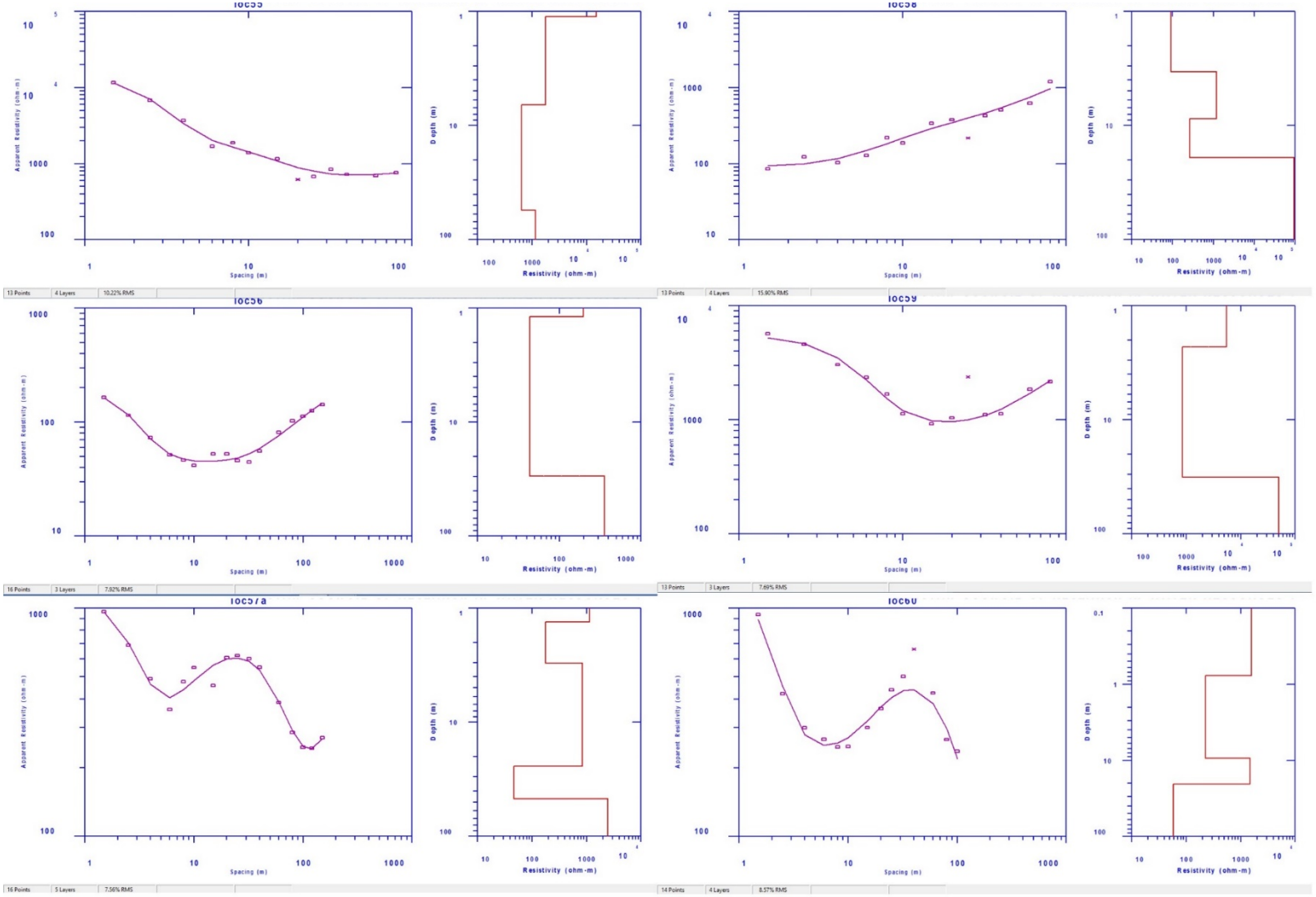
Apparent Resistivity (ohm-m)
Spacing (m)
Depth (m)
Resistivity (ohm-m)
13 Points 4 Layers 10.22% RMS
13 Points 4 Layers 15.90% RMS
16 Points 3 Layers 7.92% RMS
13 Points 3 Layers 7.69% RMS
16 Points 5 Layers 7.56% RMS
14 Points 4 Layers 8.57% RMS

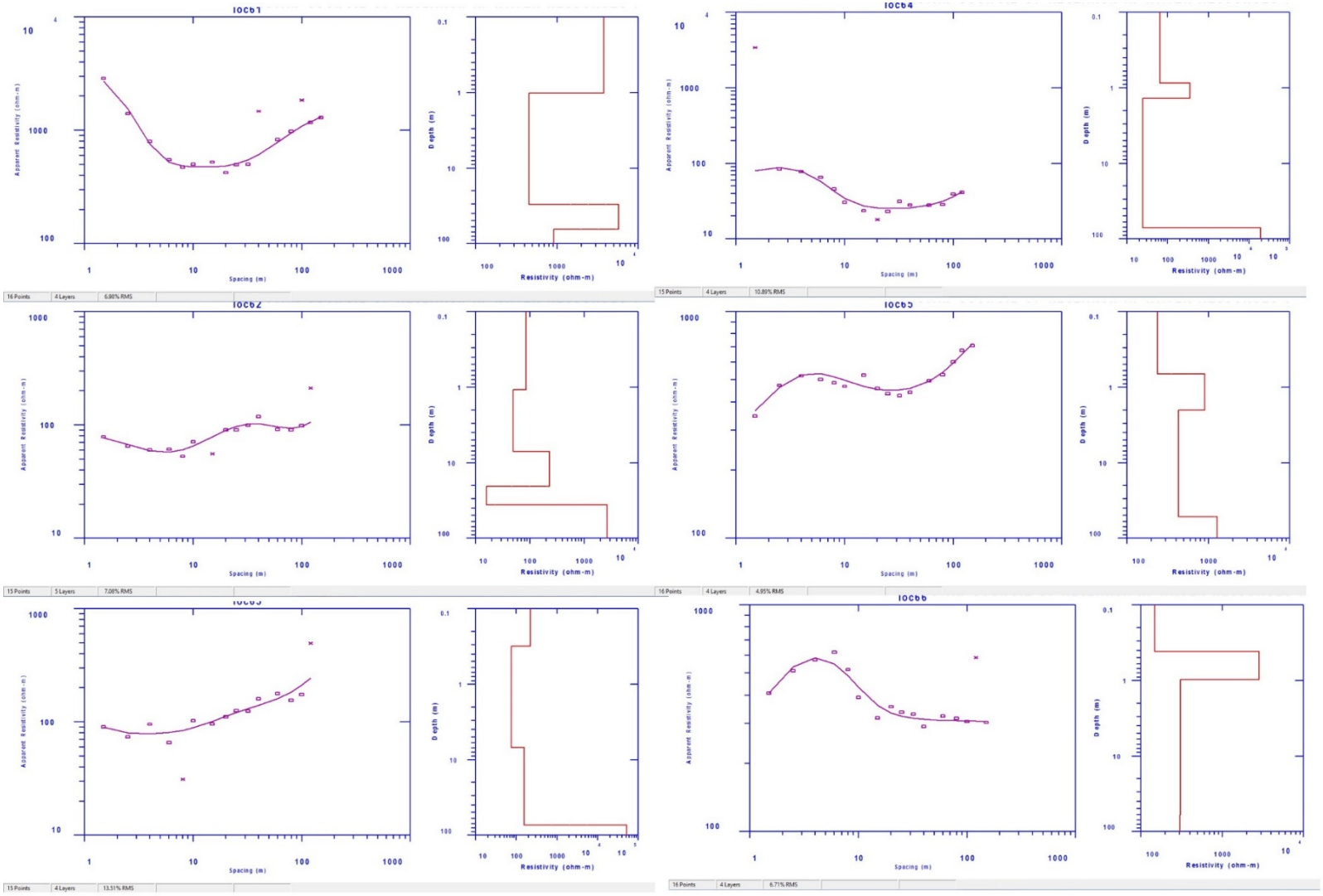
Apparent Resistivity (ohm-m)
Spacing (m)
Depth (m)
Resistivity (ohm-m)
16 Points 4 Layers 6.98% RMS
15 Points 4 Layers 10.89% RMS
15 Points 5 Layers 7.08% RMS
16 Points 4 Layers 4.95% RMS
15 Points 4 Layers 13.51% RMS
16 Points 4 Layers 6.71% RMS

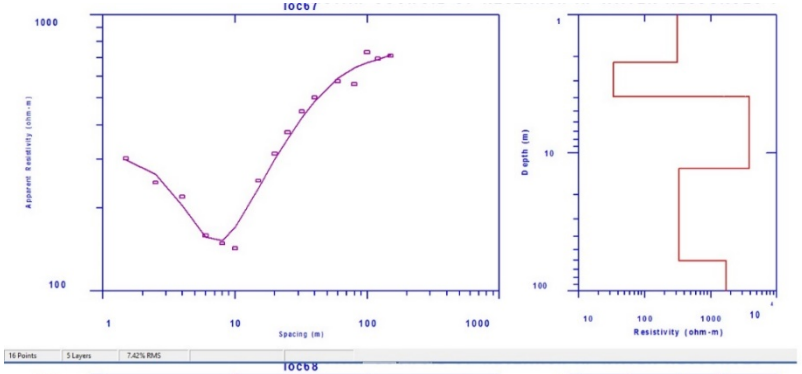
Apparent Resistivity (ohm-m)
Spacing (m)
Depth (m)
Resistivity (ohm-m)
16 Points
5 Layers
7.42% RMS

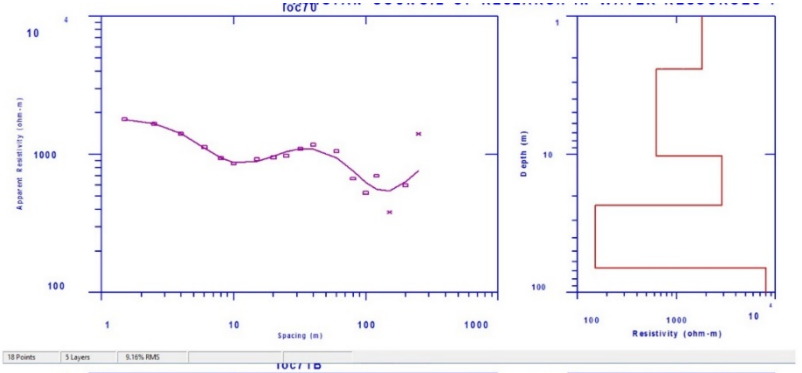
Apparent Resistivity (ohm-m)
Spacing (m)
Depth (m)
Resistivity (ohm-m)
18 Points
5 Layers
9.16% RMS

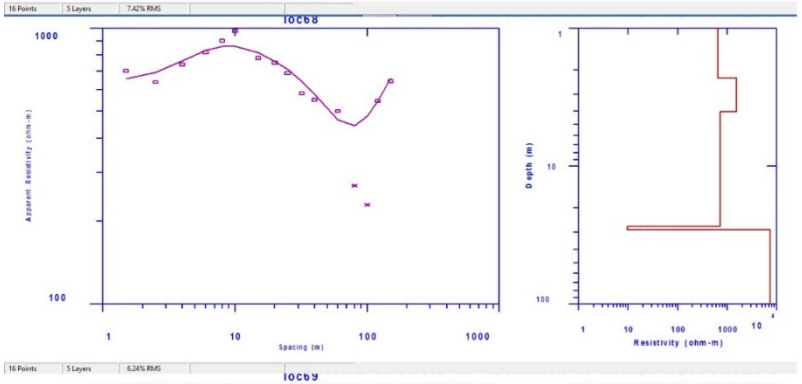
Apparent Resistivity (ohm-m)
Spacing (m)
Depth (m)
Resistivity (ohm-m)
16 Points
5 Layers
6.24% RMS

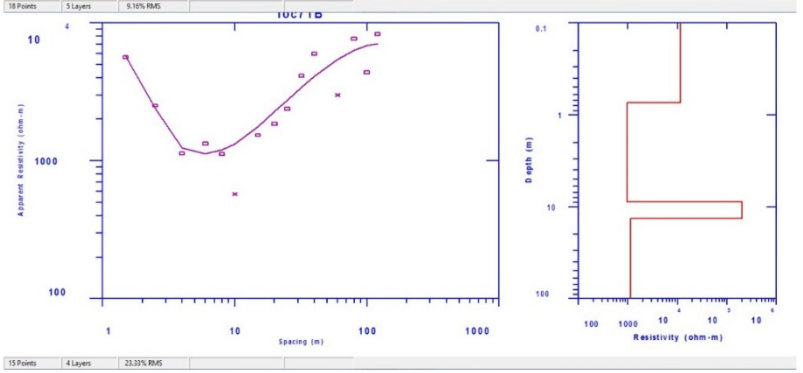
Apparent Resistivity (ohm-m)
Spacing (m)
Depth (m)
Resistivity (ohm-m)
15 Points
4 Layers
23.33% RMS

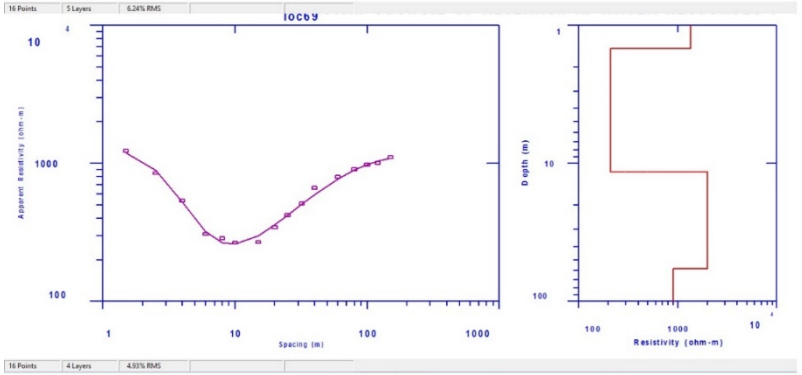
Apparent Resistivity (ohm-m)
Spacing (m)
Depth (m)
Resistivity (ohm-m)
16 Points
4 Layers
4.93% RMS

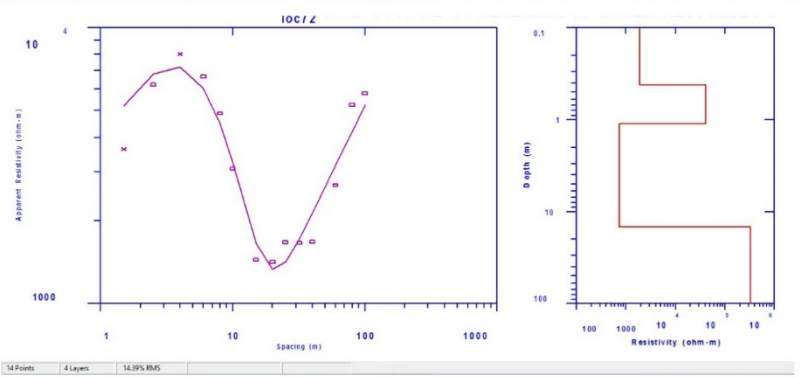
Apparent Resistivity (ohm-m)
Spacing (m)
Depth (m)
Resistivity (ohm-m)
14 Points
4 Layers
14.39% RMS

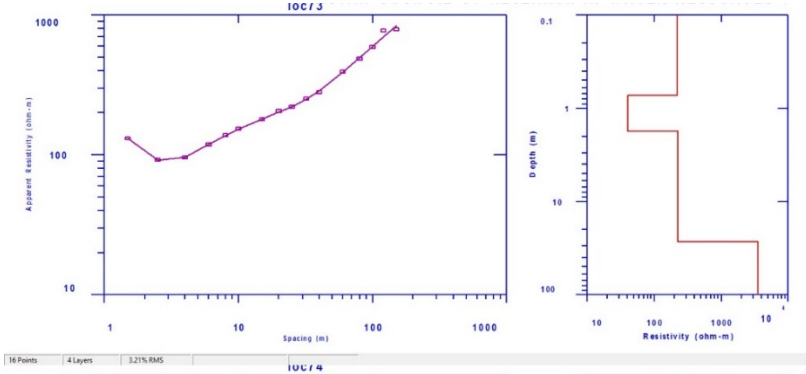
Apparent Resistivity (ohm-m)
Spacing (m)
Depth (m)
Resistivity (ohm-m)
16 Points
4 Layers
3.21% RMS

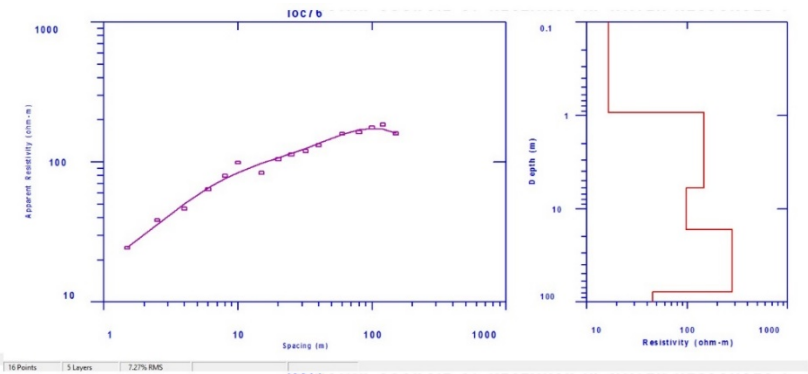
Apparent Resistivity (ohm-m)
Spacing (m)
Depth (m)
Resistivity (ohm-m)
16 Points
5 Layers
7.27% RMS

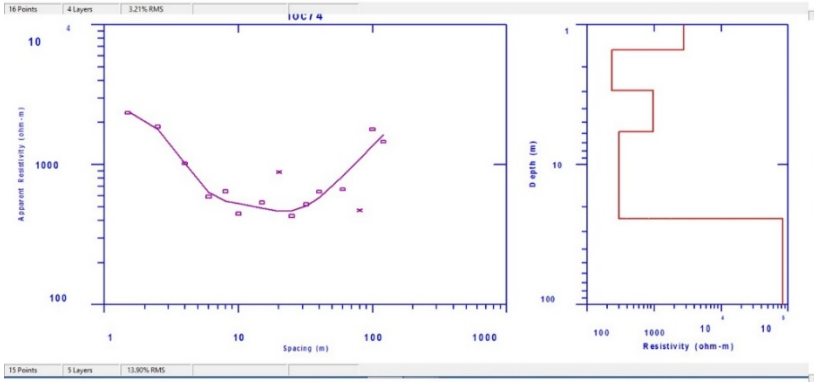
Apparent Resistivity (ohm-m)
Spacing (m)
Depth (m)
Resistivity (ohm-m)
15 Points
5 Layers
13.90% RMS

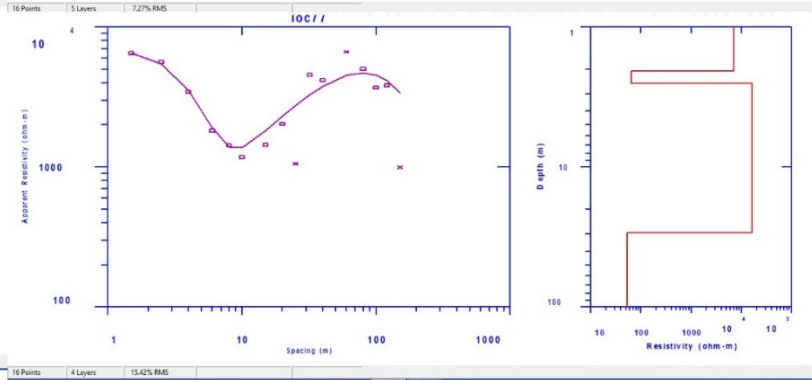
Apparent Resistivity (ohm-m)
Spacing (m)
Depth (m)
Resistivity (ohm-m)
16 Points
4 Layers
15.42% RMS

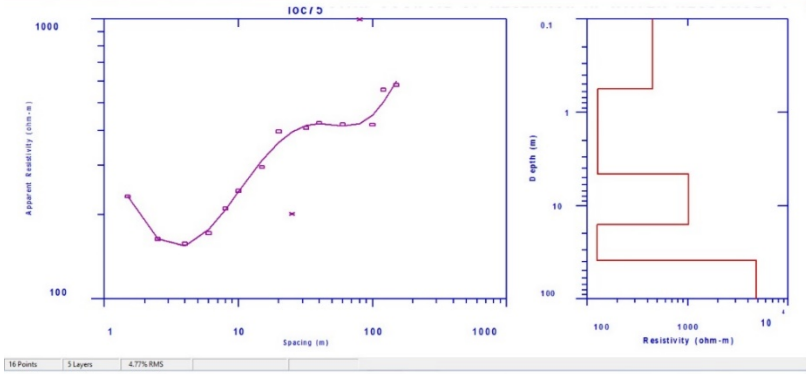
Apparent Resistivity (ohm-m)
Spacing (m)
Depth (m)
Resistivity (ohm-m)
16 Points
5 Layers
4.77% RMS

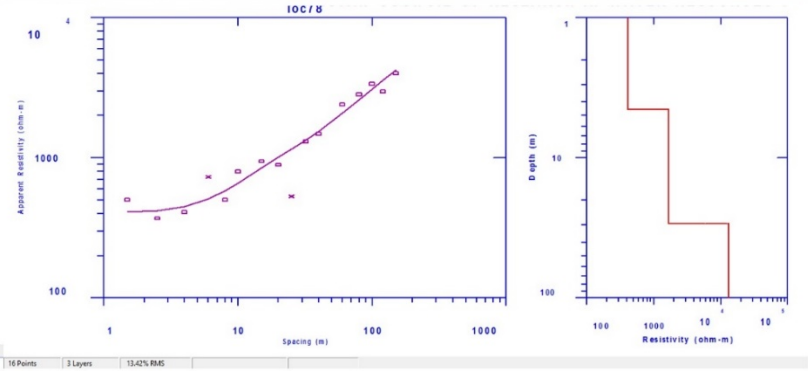
Apparent Resistivity (ohm-m)
Spacing (m)
Depth (m)
Resistivity (ohm-m)
16 Points
3 Layers
13.42% RMS

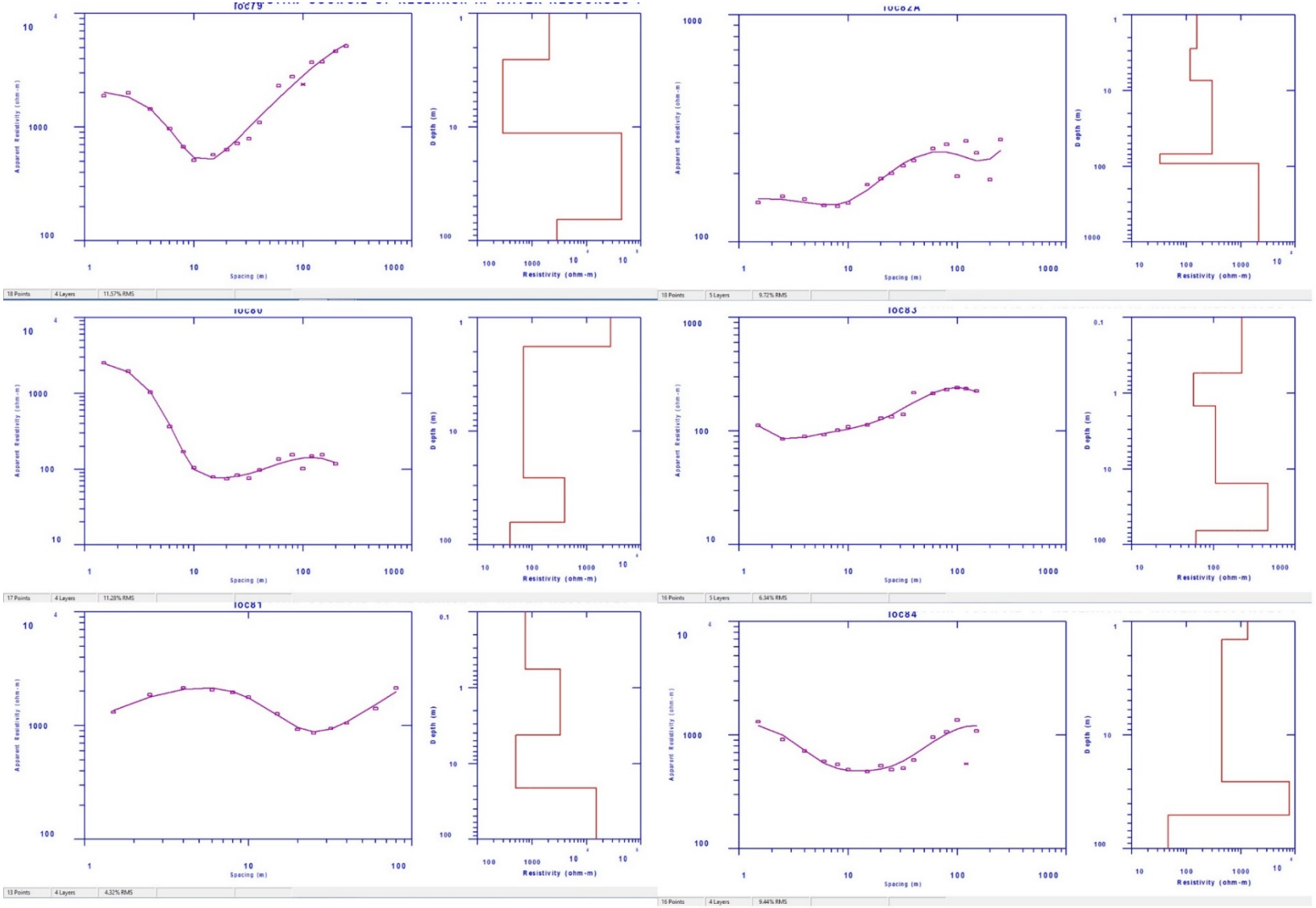
Apparent Resistivity (ohm-m)
Spacing (m)
Depth (m)
Resistivity (ohm-m)
18 Points 4 Layers 11.57% RMS
18 Points 5 Layers 9.72% RMS
17 Points 4 Layers 11.28% RMS
16 Points 5 Layers 6.34% RMS
13 Points 4 Layers 4.32% RMS
16 Points 4 Layers 9.44% RMS

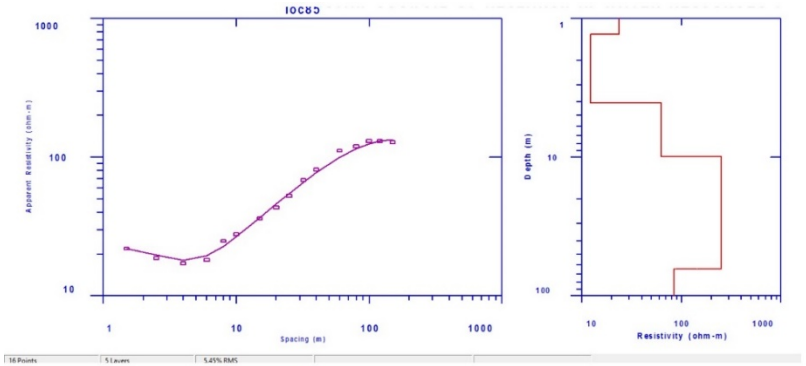
Apparent Resistivity (ohm-m)
Spacing (m)
Depth (m)
Resistivity (ohm-m)
16 Points
5 Layers
5.45% RMS

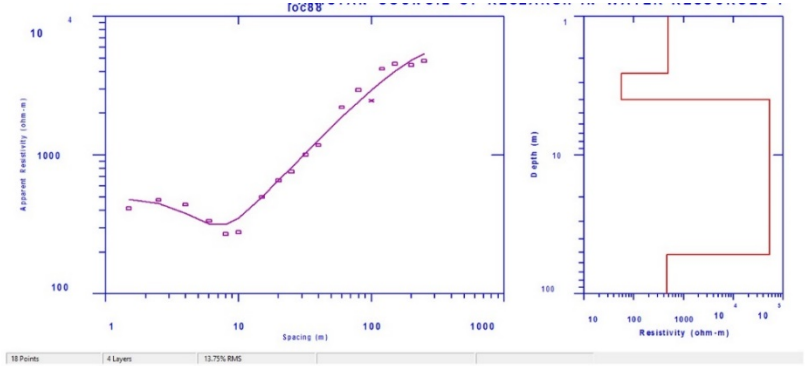
Apparent Resistivity (ohm-m)
Spacing (m)
Depth (m)
Resistivity (ohm-m)
18 Points
4 Layers
13.75% RMS

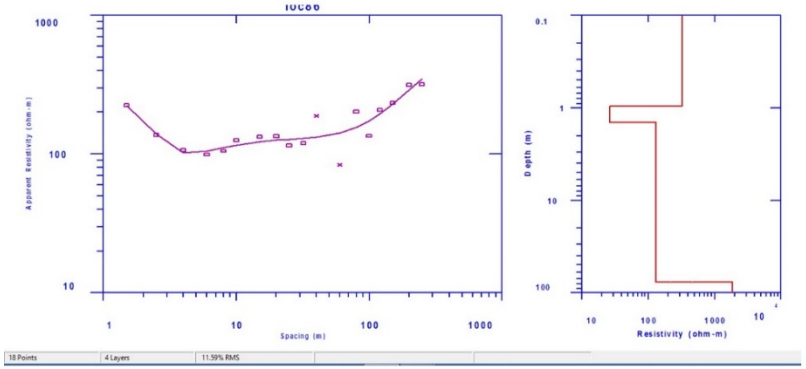
Apparent Resistivity (ohm-m)
Spacing (m)
Depth (m)
Resistivity (ohm-m)
18 Points
4 Layers
11.59% RMS

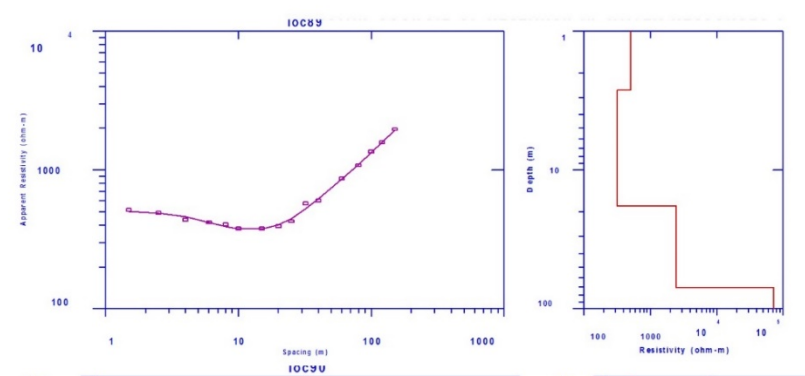
Apparent Resistivity (ohm-m)
Spacing (m)
Depth (m)
Resistivity (ohm-m)

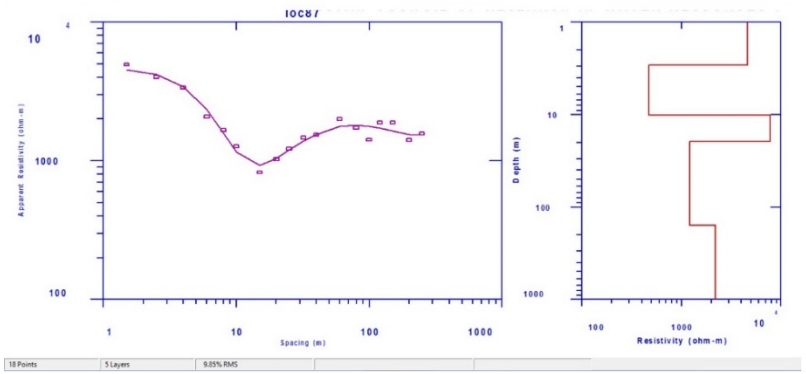
Apparent Resistivity (ohm-m)
Spacing (m)
Depth (m)
Resistivity (ohm-m)
18 Points
5 Layers
9.85% RMS

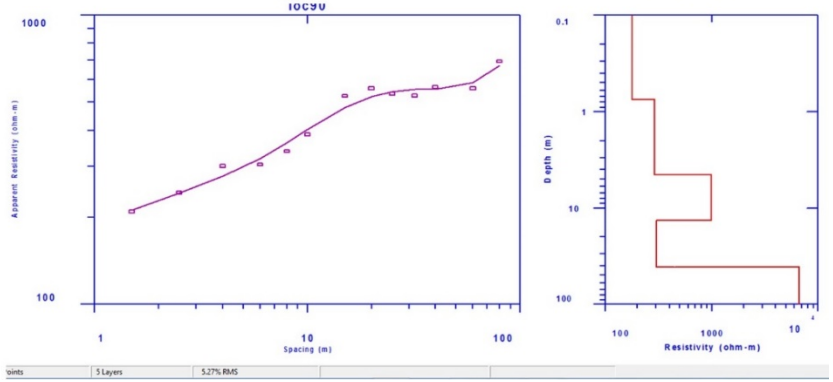
Apparent Resistivity (ohm-m)
Spacing (m)
Depth (m)
Resistivity (ohm-m)
5 Layers
5.27% RMS

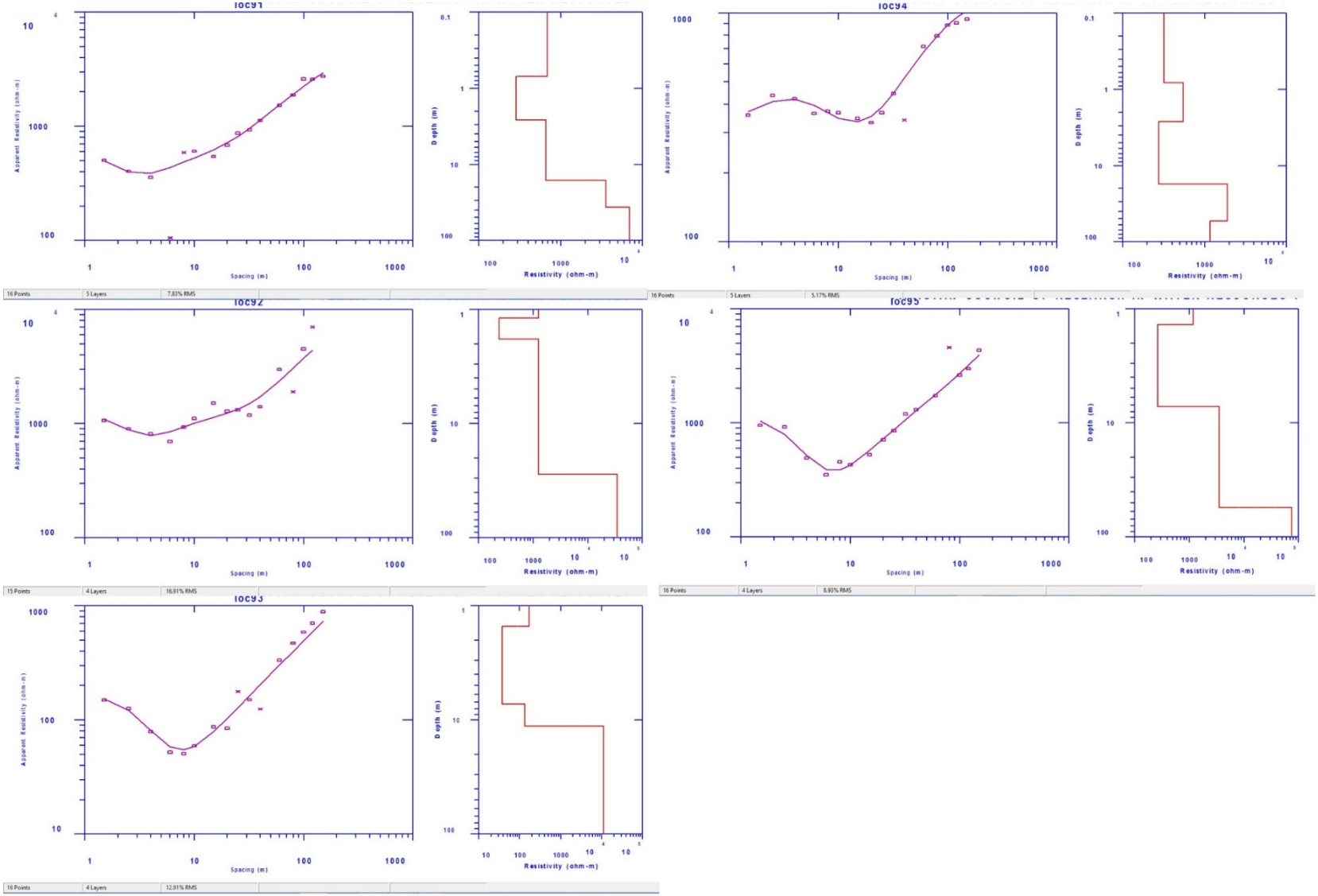
Apparent Resistivity (ohm-m)
Spacing (m)
Depth (m)
Resistivity (ohm-m)
16 Points
5 Layers
7.83% RMS
16 Points
5 Layers
5.17% RMS
15 Points
4 Layers
16.91% RMS
16 Points
4 Layers
8.93% RMS
16 Points
4 Layers
12.91% RMS

Appendix XII. Details of Primary Geoelectrical Parameters for Kerri Kerri Formation

VES NO	LAYERS	CURVE TYPE	ϱ TOP SOIL	H	ϱ	H	aquifer thickness	ϱ	H	ϱ INFINITE LAYER	H	
48	4	HA	2763.9	1.1	89.3	8.45	14.85	155	5.3	2061	INF	1>2<3<4
51	3	H	354	2.6			60.6	79.1	58	431.2	INF	1>2<3
52	4	HA	2607.7	0.8	183.9	3.8	48.8	3051.5	44.2	39558	INF	1>2<3<4
53	4	HK	6688.9	1.6	917.4	7.7	17.1	3435	7.8	645.72	INF	1>2<3>4
54	4	QH	4199	2.4	336.7	15.4	24.1	60	6.3	32727	INF	1>2>3<4
55	4	KH	1567.2	1.1	2017	4.4	53.2	43.9	47.7	1221	INF	1<2>3<4
56	3	H	198.6	1.2	43.4	28.6	29.8			359.5	INF	1>2<3
57	4	HKH	1133.4	1.3	175.8	1.7	46.8	863.3	21.3	2476.2	INF	1>2<3>4<5
58	4	KH	91.9	3.4	1199	5.3	19.1	259.5	10.4	93923	INF	1<2>3<4
59	3	H	5456.1	3.4	864.5	30	33.4			50335	INF	1>2<3
60	4	HK	1570.2	0.8	225.6	8.5	20.4	1493.8	11.1	57.7	INF	1>2<3>4
61	4	HK	3836	1	458	28.2	60.4	5251.7	31.2	947	INF	1>2<3>4
62	5	HKH	85.2	1.1	49.5	5.8	36.1	288.9	13.7	2686	INF	1>2<3>4<5
65	4	KH	236.7	0.6	906.9	1.3	52	432.8	50.1	1280.9	INF	1<2>3<4
66	4	KQ	147.2	0.4	2856	0.5	60.29	307.7	59.39	303.9	INF	1<2>3>4
67	5	HKH	312	2.2	34	1.7	60.3	3824.2	9.1	1695.9	INF	1>2<3>4<5
68	5	KQH	640.6	2.4	1558	1.7	29.2	745.3	23.1	7367.9	INF	1<2>3>4<5
69	4	HK	1361.1	1.4	209.9	10.1	58.2	2011.4	46.7	896.8	INF	1>2<3>4
70	5	HA	1829.6	2.4	629.4	7.8	66.1	2866.1	12.9	8003.7	INF	1>2<3<4
71	4	QH	6492.6	0.7	320.7	1.4	21.6	116.64	19.5	99662	INF	1>2>3<4
72	4	KH	2777.5	0.7	4389	0.6	13.9	689.2	12.6	81814	INF	1<2>3<4
73	4	HA	219.6	0.7	40.3	1	27	244.9	25.3	3539.5	INF	1>2<3<4
74	5	HKH	2763.7	1.5	235.2	1.4	24.4	958	2.9	82552	INF	1>2<3>4<5
75	5	HKH	446.4	0.6	128.4	4	39.3	1022.4	11.8	4793.3	INF	1>2<3>4<5
76	5	KHK	16.5	0.9	145.8	5	77.9	97.6	10.8	45.4	INF	1<2>3<4>5
78	3	A	409.7	4.5	1663	24.9	29.4			13226	INF	1<2<3
79	4	HK	2088	2.5	292.2	8.7	67.9	4127.3	56.7	3028.1	INF	1>2<3>4

80	4	HA	2750.4	1.8	69.6	24	63.1	395.1	37.3	39.8	INF	1>2<3<4
81	4	KH	761.5	4.6	3306	3.6	25.2	503.3	17	15182	INF	1<2>3<4
82	3	H	34.6	4.6	13.9	35.5	40.1			514	INF	1>2<3
82B	5	AKH	156.1	2.8	117.2	4.6	92.3	298.01	61.9	21370	INF	1<2<3>4<5
83	5	HAK	222.3	0.5	57.4	0.9	65.1	106.8	14	61.2	INF	1>2<3<4>5
84	4	HK	1336.8	1.4	458.7	24.2	50.5	7726.7	24.9	46.5	INF	1>2<3>4
85	5	HAK	23.6	1.3	12.2	2.7	66.7	62.5	5.4	83.9	INF	1>2<3<4>5
86	4	HA	328.3	1.3	26.9	0.45	79.15	128.7	77.4	2052	INF	1>2<3<4
87	5	HKH	4616.3	2.9	475.4	7.3	158	7842.2	9.3	22303	INF	1>2<3>4<5
88	4	HK	492.9	2.5	56.9	1.4	51.8	5360.2	47.9	459	INF	1>2<3>4
89	4	HA	508.13	2.7	319.7	15.5	70.2	2428	52	72188	INF	1>2<3<4
90	5	AKH	179.5	2.7	289.2	3.8	43.08	986.1	9	71367	INF	1<2<3>4<5
91	5	HAA	690.8	0.8	288.5	1.8	36.6	653	13.6	4784.9	INF	1>2<3<4<5
92	4	HA	1269.8	1.9	241.3	0.6	28.4	1260.3	25.9	34738	INF	1>2<3<4
93	4	HA	171.2	1.2	37.5	5.7	11	133.2	4.1	11007	INF	1>2<3<4
94	5	KHA	319.7	0.8	550.6	1.8	53.3	274.19	14.8	11595	INF	1<2>3<4<5
95	4	HA	1194.1	0.8	266.3	5.8	54.7	3555.5	48.1	74925	INF	1>2<3<4

Details of Primary Geoelectrical Parameters for Basement Complex Rocks

of Primary and Secondary Geoelectrical Parameters for the Basement Complex Bedrocks

(14 ves)

VES NO	LAYERS	CURVE TYPE	ϱ TOP SOIL	H	ϱ	H		P SAPROLITE	H	ϱ INFINITE LAYER	H	S.D
3	3	A	8.9	0.3			10.6	276.9	10.3	2892.7	INF	1<2<3
11	4	KH	44.8	0.8	223.1	1.1	13.5	56.5	11.6	566.8	INF	1<2>3<4
14	4	KH	15.8	3	23.5	1.2	9.1	18.9	4.9	12533	INF	1<2>3<4
14B	4	HA	377.9	0.69	75.3	6.4	35.69	638.5	28.6	88295	INF	1>2<3<4
15	4	HA	29.1	1.2	9.3	3.2	30.9	347.8	26.5	25681	INF	1>2<3<4
27	3	H	388.9	0.5			6	31	5.5	17783	INF	1>2<3
28	4	HA	80.6	1.2	27.9	3.4	10.3	43.3	5.7	398.03	INF	1>2<3<4
29	4	HA	266.1	3.1	17.6	1.6	49.3	261.1	44.6	8251.8	INF	1>2<3<4
30	3	A	7.9	0.5			1.7	1487.8	1.2	16690	INF	1<2<3
31	4	KH	6.2	0.2	185.5	12	20.2	44.9	8	143.24	INF	1<2>3<4
36	4	HA	373.2	1.2	30.5	9.38	37.38	72.9	26.8	6537.6	INF	1>2<3<4
37	4	A	121.7	3.07			34.47	48.1	31.4	425.8	INF	1<2<3
38	4	HA	906.6	0.8	49	6.4	37.8	799.3	30.6	195.4	INF	1>2<3<4
39	3	H	348.9	1.6			10.6	58.1	9	248.2	INF	1>2<3

Migmatite/Gneiss N=21

VES NO	LAYERS	CURVE	ϱ TOP SOIL	H	P	H		P SAPROLITE	H	ϱ INFINITE LAYER	H	
5	4	QH	475.8	1.8	105.3	7.2	34.6	245.2	25.6	80724	INF	1>2>3<4
6	3	H	3501.7	0.21			4.91	47.9	4.7	715	INF	1>2<3
7	4	HA	6508.3	0.2	15.3	0.4	18.9	90.5	18.3	2588.8	INF	1>2<3<4
8	3	H	41.7	0.9			16.6	20.8	15.7	75940	INF	1>2<3
9	3	A	138.4	3.2			12.6	226.4	9.4	618.1	INF	1<2<3
18	4	HA	380	0.6	91	4.1	39.3	100.7	34.6	17763	INF	1>2<3<4
19	3	H	385.2	3.6			15.8	218.3	12.2	68666	INF	1>2<3
20	4	KH	23.1	3.7	1887	1.6	10.6	11.1	5.3	4166.9	INF	1<2>3<4
23	4	HA	16.6	0.8	5.05	3.7	6.9	274.7	2.4	21424	INF	1>2<3<4
24	4	HA	45.5	2.9	11.1	1.1	84.4	244.9	80.4	716	INF	1>2<3<4
25	4	HK	63	2.9	10.4	1.7	59.6	87.4	55	610.36	INF	1>2<3<4
33	4	HA	723.16	0.7	341	5.3	68.3	980.1	62.3	26786	INF	1>2<3<4
34	4	KH	310.6	1.7	1912	1.6	7.2	52.2	3.9	199.5	INF	1<2>3<4
35	4	HA	4267.5	0.5	34.7	14.9	99.2	215.5	83.8	2239	INF	1>2<3<4
41	4	AK	26.6	2.7	63.8	12.5	33.05	1528.3	17.85	30.5	INF	1<2<3>4
44	4	HA	140.8	0.3	55.8	4.9	46.8	320.8	41.6	9232.6	INF	1>2<3<4
45	4	HA	533.3	0.4	28.9	0.5	37.8	61	36.9	1437.1	INF	1>2<3<4
46	3	H	113.1	0.7			40.6	35.66	39.9	20162	INF	1>2<3
47	4	HA	365.6	0.6	50.2	3.7	12.8	153.71	8.5	6737	INF	1>2<3<4
49	4	HK	268.7	3.1	65.1	8.1	51	775.6	39.8	111.65	INF	1>2<3>4
50	4	HA	2271.4	0.5	7.1	0.6	26.1	104.9	25	58168	INF	1>2<3<4

Biotite Hornblende Granite (16 VES)

VES NO	LAYERS	CURVE TYPE	ϱ TOP SOIL	H	P	H		ϱ SAPROLITE		ϱ INFINITE LAYER	H	
1	3	H	312.56	0.3			15	31.1	14.7	27850	INF	1>2<3
2	3	K	581.3	0.8			2.1	2371.4	1.3	1532.9	INF	1<2>3
4	3	H	177.8	6.1			12.4	31.3	6.3	951.9	INF	1>2<3
10	3	H	6623.7	0.2	2.79	0.3	13.4	135.7	12.9	50228	INF	1>2<3
13	3	A	32.9	3			10.6	155.5	7.6	13703	INF	1<2<3
16	4	HA	163.65	1.5	1	0.7	21.2	50.6	19	5635.5	INF	1>2<3<4
17	3	A	5.1	0.2			14.7	51.7	14.5	459.6	INF	1<2<3
22	3	H	298.24	1.1			24.17	100.8	23.07	69087	INF	1>2<3
26	3	H	329.3	1.1	17.1	4.2	21.6	44.5	16.3	32804	INF	1>2<3
32	4	HA	76.4	1.7	10.6	2.9	60.3	496.8	55.7	17355	INF	1>2<3<4
40	3	H	8.9	2.3			11.1	6.43	8.8	22732	INF	1>2<3
42	3	H	134.9	1.1			2.4	5.2	1.3	55867	INF	1>2<3
43	4	HA	181.01	1	27.2	0.7	57.1	277.1	55.4	25587	INF	1>2<3<4
63	4	HA	226.3	0.3	76.4	6.6	73.1	156.9	66.2	51401		P1>P2<P3<P4
64	4	KH	67.8	1	338.2	10.5	78.8	23.6	67.3	19257	INF	1<2>3<4

Appendix XIII: Detailed Results of Hydrochemical Analyses:Result of Physico-Chemical Parameters

Sample No	Rock Type	Location	Latitude	Longitude	Tem (oC)	Mili S	EC (uS/cm)	TDS	pH

Sample No	Rock Type	Location	Latitude	Longitude	Tem (oC)	Mili S	EC (uS/cm)	TDS	pH
LOC 1	KK	Maccido	10.05580556	10.31708333	22.6	0.13	130	99	5
LOC 2	KK	Sangar	10.05947222	10.33227778	29.3	0.05	50	43	5.6
LOC 3	KK	Shafan Banu	10.04022222	10.38205556	26	0.23	230	165	6.1
LOC 4	KK	Bakin Kogi	10.07361111	10.35369444	25.1	0.34	340	250	6.1
LOC 6	KK	Rapawa	10.00816667	10.29016667	28.6	0.83	830	588	5.8
LOC 11	KK	Unguwar wake	10.16152778	10.26777778	28.4	0.18	180	136	5.4
LOC 12	KK	Farin Ruwa	10.21969444	10.26633333	22.4	0.28	280	207	6.5
LOC 13	KK	Minza	10.19788889	10.22555556	27.1	0.4	400	286	7
LOC 34	KK	Alkaleri Town	10.26797222	10.33202778	26.4	0.38	380	274	5.1
LOC 35	KK	Kufa	10.19455556	10.35108333	23	0.11	110	93	5.7
LOC 36	KK	Tumuru	10.1435	10.46477778	27	0.14	140	105	5.6
LOC 37	KK	Tarangadi Fulani	10.20075	10.39319444	27.5	0.17	170	111	5.6
LOC 38	KK	Sabon gari	10.13252778	10.47044444	27.9	0.48	480	340	5.1
LOC 39	KK	Mararaban Pali	10.08472222	10.5	23.7	0.07	70	59	6.1
LOC 40	KK	Arawa (Mainari)	10.28913889	10.40380556	25.5	0.06	60	52	6.7
LOC 41	KK	Kaloma	10.29036111	10.43608333	27.4	0.1	100	79	5.8
LOC 42	KK	Jagalwa	10.28744444	10.47191667	26.2	0.08	80	51	6.1
LOC 43	KK	Badawere	10.28213889	10.36963889	23	0.13	130	101	6.3
LOC 44	KK	Badara	10.34969444	10.35663889	30.4	0.18	180	149	6
LOC 45	KK	Bedoji	10.3755	10.39216667	24	0.09	90	73	6.5
LOC 46	KK	Zamani	10.37908333	10.41827778	24.6	0.09	90	73	6.5
LOC 47	KK	Taure	10.43211111	10.44516667	31.7	0.08	80	64	6.4
LOC 49	KK	Wanka	10.44930556	10.43708333	29.6	0.08	80	61	5.4
LOC 81	KK	Kafin Maigari	10.32736111	10.34188889	26.1	0.11	110	85	7

Result of Physico-Chemical Parameters contd…..

LOC 83	KK	Woso	10.40083333	10.33113889	28.1	0.2	200	146	6.9
LOC 84	KK	Guyaba (Downstream)	10.4	10.35969444	28.8	1.25	1250	908	6.4
LOC 85	KK	Kucha	10.44511111	10.39811111	3.1	0.08	80	67	5.9
LOC 86	KK	Tumburwo	10.44058333	10.37302778	29.2	0.01	10	15	5.3
LOC 87	KK	Gumnalwo	10.45083333	10.37997222	21.4	0.06	60	49	5.1
LOC 9	KK	Gar	10.07572222	10.26458333	28.7	0.33	330	242	8.5
LOC 32	KK	Gwaram Mosq	10.23675	10.28327778	26.2	0.65	650	466	5.8
LOC 33	KK	Gwaram Town	10.23775	10.28547222	26.4	1.52	1520	1105	5.5
LOC 80	KK	Sabuwar Gwaram	10.26166667	10.27752778	25	0.4	400	285	7
LOC 7	MG	Kyawun Gani	10.03619444	10.22677778	27.5	0.12	120	95	6.8
LOC 18	MG	Kenda	10.10602778	10.21644444	28.3	0.41	410	300	7.4
LOC 19	MG	Kyabi	10.08447222	10.21988889	26	0.57	570	406	7.3
LOC 22	MG	Lariyel	10.09286111	10.09361111	28.3	1	1000	730	6.9
LOC 23	MG	Jama (Bartak Pali)	10.08225	10.10902778	22.5	0.39	390	285	7
LOC 24	MG	Yola Doka	10.10369444	10.05125	26.6	0.45	450	285	7.1
LOC 25	MG	Yuguda	10.05025	10.02575	26	0.7	700	510	7.2
LOC 26	MG	Zan Filani	10.00591667	10.06855556	26.1	0.98	980	728	7.3
LOC 31	MG	Shafan Fulani	10.25002778	10.20455556	27.7	0.78	780	572	7.3
LOC 50	MG	Gilliri	10.31547222	10.05	26.9	0.62	620	446	7.4
LOC 51	MG	Alkama	10.33019444	10.0555	25.3	0.87	870	624	7.4
LOC 52	MG	Beru	10.35030556	10.06744444	24.6	0.89	890	648	7.4

Result of Physico-Chemical Parameters contd…

Sample No	Rock Type	Location	Latitude	Longitude	Tem (oC)	Mili S	EC (uS/cm)	TDS	pH
LOC 53	MG	Jinkiri	10.39119444	10.05894444	28.6	0.52	520	372	6.9
LOC 54	MG	Gamhiri	10.42891667	10.10608333	27.5	0.66	660	475	7.7
LOC 55	MG	Habli	10.43430556	10.15855556	25.2	1.29	1290	945	7.1

Sample No	Rock Type	Location	Latitude	Longitude	Tem (oC)	Mili S	EC (uS/cm)	TDS	pH
LOC 56	MG	Takalafiya	10.44311111	10.21886111	29.1	0.8	800	574	6.9
LOC 57	MG	Garwali	10.47783333	10.20761111	27.8	0.96	960	694	7.1
LOC 58	MG	Mangawa	10.4185	10.23858333	28.5	0.85	850	599	7.4
LOC 59	MG	Jalia	10.37808333	10.22658333	29.5	0.59	590	424	6.9
LOC 60	MG	Rugan Badembo	10.38288889	10.18327778	27.9	0.98	980	707	7.2
LOC 61	MG	Gulawa	10.37269444	10.15208333	29	0.78	780	557	7.5
LOC 70	BG	Siri	10.29541667	10.18830556	27.6	0.58	580	418	7.5
LOC 73	MG	Katallen Badaromo	10.44988889	10.01638889	26.8	0.13	130	98	6.8
LOC 16	BH	Rugan Kela	10.17905556	10.17116667	25.5	0.86	860	624	7.7
LOC 74	MG	Badaromo Town	10.46255556	10.02341667	26	0.64	640	456	6.4
LOC 17	BH	Guma	10.14416667	10.18269444	26.7	0.66	660	477	7.7
LOC 75	MG	Dargome	10.5	10.06319444	27.8	0.43	430	312	7.2
LOC 20	BH	Shafa	10.15494444	10.12844444	22.6	0.62	620	445	6.9
LOC 76	MG	Kanawa	10.45141667	10.10258333	26.6	0.47	470	341	7.4
LOC 77	MG	Nahuta	10.48641667	10.09308333	25.7	0.53	530	382	7.6
LOC 79	MG	Shafan Dambo	10.25925	10.25633333	23.1	0.59	590	424	6.8
LOC 10	BG	Kaciciya	10.12338889	10.10233333	23.8	0.71	710	515	7.4
LOC 14	BG	Buda	10.17080556	10.21708333	24.2	1.23	1230	955	7.2
LOC 15	BG	Gokaru	10.17669444	10.18705556	26.4	2.04	2040	1558	7.1
LOC 48	BG	Bagali	10.26961111	10.02252778	22.5	0.59	590	419	7.2
LOC 62	BG	Minjila	10.30405556	10.13688889	28.4	1.09	1090	787	6.9
LOC 63	BG	Bidolo	10.17430556	10	21.5	0.7	700	508	6.8
LOC 64	BG	Balanshi	10.16077778	10.05986111	28.2	1.45	1450	1045	7
LOC 65	BG	Minjin	10.17294444	10.02394444	26.5	1.33	1330	961	6.9
LOC 67	BG	Birshi Central Mosque	10.25144444	10.09325	23.4	0.54	540	390	6.9
LOC 68	BG	Birshi Village	10.25116667	10.09125	29.1	0.28	280	206	6.8
LOC 69	BG	Yardin Birshi	10.25172222	10.12208333	27.7	0.23	230	169	7.4

Result of Physico-Chemical Parameters contd….

LOC 21	BH	Pau	10.16147222	10.09422222	27	0.32	320	234	6.4
LOC 27	BH	Dadin Kowa	10.20505556	10.16066667	25	0.19	190	154	7.5
LOC 28	BH	Dindima	10.23938889	10.14825	26.1	0.58	580	413	7
LOC 29	BH	Kwaga Pri School	10.20933333	10.19241667	28.3	0.38	380	268	6.8
LOC 30	BH	Kujamba	10.23311111	10.19413889	28.9	0.2	200	157	7.2
LOC 66	BH	Yole	10.23358333	10.00269444	26.6	1.58	1580	1154	7.5
LOC 71	BH	Barnawa	[illegible]	10.14808333	24.2		260	191	7.4
LOC 72	BH	Kwanan Dutse	10.25280556	10.13513889	28.2	0.27	270	196	7.2
LOC 78	BH	Turiya	10.24538889	10.17216667	22.4	0.59	590	423	6.9

Result of Chemical Parameters

LAB NO.	SAMPLE I.D	HCO3 (mg/l)	Fl (mg/l)	CL (mg/l)	NO3(N) (mg/l)	SO4 (mg/l)	Ca (mg/l)	K (mg/l)	Mg (mg/l)	Na (mg/l)
17-6873	L1B	14.935	0.000	3.694	12.796	0.000	7.250	4.180	2.560	6.450
17-6874	L2B	16.13	0.000	0.557	0.000	0.275	0.213	10.450	0.141	6.600
17-6875	L3B	48.39	0.121	4.924	11.917	2.045	4.150	2.160	1.930	17.900
17-6876	L4B	69.5	0.000	16.284	26.806	3.642	6.810	22.400	4.150	22.300

Result of Chemical Parameters contd…

LAB NO.	SAMPLE I.D	HCO3 (mg/l)	Fl (mg/l)	CL (mg/l)	NO3(N) (mg/l)	SO4 (mg/l)	Ca (mg/l)	K (mg/l)	Mg (mg/l)	Na (mg/l)
17-6877	L5B	74.676	0.000	19.252	13.975	9.469	7.880	5.270	3.640	7.790
17-6878	L6B	37.637	0.000	50.191	64.608	0.000	51.150	17.840	28.100	6.210
17-6879	L7B	73.274	0.193	1.928	0.000	1.731	4.440	1.680	2.700	2.470
17-6880	L8B	104.817	0.000	23.346	23.468	0.000	13.040	5.700	5.980	3.150
17-6881	L9B	75.871	0.000	20.861	12.142	21.966	17.140	11.720	6.450	4.520
17-6882	L10B	107.53[illegible]	[illegible]	30.823	40.964	15	1.310	57.000	13.750	5.960
17-6883	L11B	4.779	0.000	2.925	8.454	0.000	2.010	3.420	1.150	6.200
17-6884	L12B	120.08	0.267	1.462	1.766	0.862	7.140	2.990	9.680	1.590
17-6885	L13B	222.238	0.674	15.414	1.731	11.139	21.110	2.070	10.750	10.420
17-6886	L14B	274.811	0.000	100.151	72.028	38.514	110.850	12.440	55.350	9.510
17-6887	L15B	197.147	0.000	317.543	162.387	68.170	216.200	4.420	50.400	16.130
17-6888	L16B	276.603	0.000	83.054	13.094	26.109	81.500	4.200	33.050	9.750
17-6889	L17B	163.094	0.000	43.208	23.358	15.913	64.550	19.870	14.300	5.900
17-6890	L18B	244.94	0.879	4.939	4.490	7.047	31.050	2.340	13.450	6.870
17-6891	L19B	272.421	0.548	8.991	10.363	11.506	52.750	8.150	15.550	4.670
17-6893	L20B	146.366	4.891	44.925	23.818	9.341	52.950	3.110	11.950	6.470
17-6897	L21B	34.052	0.000	19.381	19.429	0.000	19.500	14.100	0.444	15.700
17-6899	L22B	289.149	1.280	51.442	48.297	41.928	78.300	2.530	26.830	85.850
17-6900	L23B	192.965	0.495	11.048	5.207	9.763	16.200	2.760	13.700	36.050
17-6901	L24B	163.094	0.228	9.893	11.426	2.256	33.550	2.800	11.650	15.850
17-6902	L25B	212.082	0.510	35.429	26.209	11.153	62.350	2.150	19.150	60.500
17-6903	L26B	192.368	0.356	61.512	49.247	19.495	71.750	3.670	34.450	51.500
17-6904	L27B	54.364	0.063	6.631	2.502	1.711	9.000	2.700	0.645	9.700
17-6905	L28B	86.027	0.000	56.017	16.761	10.181	55.950	4.030	6.560	40.900
17-6906	L29B	84.833	0.402	4.950	0.469	2.150	21.450	1.170	10.210	20.200
17-6907	L30B	104.548	1.730	5.637	6.125	3.418	12.550	1.169	3.340	15.750

LAB NO.	SAMPLE ID	HCO3 (mg/l)	Fl (mg/l)	CL (mg/l)	NO3(N) (mg/l)	SO4 (mg/l)	Ca (mg/l)	K (mg/l)	Mg (mg/l)	Na (mg/l)
17-6908	L31B	186.037	0.000	74.956	40.118	14.491	51.750	26.950	16.466	71.150
17-6909	L32B	186.061	0.060	59.467	41.961	0.000	26.960	42.860	9.980	41.400
17-6910	L33B	[illegible]	[illegible]	[illegible]	[illegible]	[illegible]	[illegible]	[illegible]	[illegible]	[illegible]
17-6911	L34B	[illegible]	[illegible]	[illegible]	[illegible]	[illegible]	[illegible]	[illegible]	[illegible]	[illegible]
17-6912	L35B	[illegible]		[illegible]	[illegible]	[illegible]		[illegible]	[illegible]	[illegible]
17-6913	L36B	13.143	0.027	0.552	0.000	0.296	0.344	1.543	0.200	2.280
17-6914	L37B	9.559	0.022	0.433	1.162	0.248	0.294	11.750	0.168	2.020
17-6915	L38B	4.182	0.000	20.965	48.569		26.030	14.600	12.660	24.400
17-6916	L39B	13.741		1.125	0.773	0.246		0.511	0.152	1.890
17-6917	L40B	14.935	0.037	0.762	1.440	0.186	0.147	1.010	0.122	3.930
17-6921	L41B	7.169	0.000	0.944	8.971	0.650	5.650	2.335	0.310	5.600
17-6923	L42B	6.572	0.000	0.560	1.851	0.100	0.199	0.735	0.186	2.130
17-6924	L43B	37.637	0.046	0.988	8.784	0.000	6.370	1.980	3.530	7.450
17-6925	L44B	15.533	0.000	6.836	14.030	0.000	7.670	16.980	3.128	4.530
17-6926	L45B	43.611	0.066	1.151	3.753	0.266	3.250	4.890	1.140	7.060
17-6927	L46B	35.845	0.094	4.817	5.074	0.645	3.730	3.280	2.070	7.660
17-6928	L47B	10.156	0.000	0.628	5.709	0.323	2.070	3.010	0.504	3.920
17-6929	L48B	218.057	0.000	34.446	8.924	12.533	31.850	3.800	25.430	37.700
17-6930	L49B	29.871	0.000	2.059	3.029	1.581	2.520	2.640	1.860	5.500
17-6931	L50B	203.719	0.269	30.823	21.404	14.358	26.730	1.400	24.200	49.650
17-6932	L51B	266.447	0.412	41.776	43.601	22.359	44.430	3.250	25.600	100.850
17-6933	L52B	230.005	0.742	67.652	39.000	31.506	77.750	1.940	42.300	74.950

LAB NO.	SAMPLE ID	HCO3 (mg/l)	Fl (mg/l)	CL (mg/l)	NO3(N) (mg/l)	SO4 (mg/l)	Ca (mg/l)	K (mg/l)	Mg (mg/l)	Na (mg/l)
17-6934	L53B	[illegible]	[illegible]	[illegible]	[illegible]	[illegible]	[illegible]	[illegible]	[illegible]	[illegible]
17-6935	L54B	[illegible]	[illegible]	[illegible]	[illegible]	[illegible]	[illegible]	[illegible]	[illegible]	[illegible]
17-6936	L55B	[illegible]	0.807	[illegible]	[illegible]	[illegible]	124.250	[illegible]	[illegible]	[illegible]
17-6937	L56B	259.876	0.604	31.896	26.843	16.465	81.950	1.600	19.450	47.550
17-6938	L57B	249.122	0.471	63.648	39.496	30.495	128.550	2.080	19.900	44.050
17-6939	L58B	151.743	0.000	36.934	50.856	18.971	91.700	2.600	25.850	50.550
17-6940	L59B	110.522	0.000	23.719	30.235	16.569	50.300	0.964	18.600	48.350
17-6941	L60B	276.603	0.434	43.621	53.475	31.426	101.250	0.837	37.100	66.000
17-6945	L61B	316.033	0.178	26.632	22.762	18.834	58.100	1.900	57.700	23.050
17-6947	L62B	172.056	0.000	78.191	79.698	34.761	102.250	3.520	43.950	58.600
17-6948	L63B	206.706	0.418	39.428	11.711	15.415	80.750	3.700	14.200	41.950
17-6949	L64B	284.37	0.000	192.631	85.436	116.486	109.850	1.730	57.600	65.150
17-6950	L65B	231.199	0.000	95.920	85.221	34.655	155.600	1.880	31.200	75.200
17-6951	L66B	268.836	0.000	140.273	88.947	34.194	123.550	132.550	18.900	130.500
17-6952	L67B	66.313	0.000	45.235	23.767	16.018	39.450	4.280	10.800	47.550
17-6953	L68B	86.625	0.200	15.917	10.116	2.930	13.700	1.740	7.300	19.500
17-6954	L69B	135.016	0.268	3.271	0.962	1.303	12.400	1.300	3.320	15.900
17-6955	L70B	385.93	0.307	4.127	1.593	5.147	59.650	2.230	4.560	41.700
17-6956	L71B	77.664	0.157	7.741	15.594	3.357	9.500	1.880	3.620	20.550
17-6957	L72B	86.0278	0.236	11.402	9.436	3.884	12.450	1.830	3.310	15.350
17-6958	L73B	25.689	0.050	4.172	2.444	0.333	2.570	1.160	1.290	5.300
17-6959	L74B	75.872	0.000	64.766	24.746	16.222	43.450	6.680	11.340	59.350
17-6960	L75B	256.889	0.550	10.113	2.508	4.023	20.450	1.230	12.640	48.800
17-6961	L76B	216.264	0.235	14.044	5.668	9.599	32.900	1.820	20.500	22.700
17-6962	L77B	188.783	0.430	17.805	15.921	10.472	50.100	1.880	14.940	26.300
17-6963	L78B	71.092	0.209	3.294	1.127	1.234	6.300	1.030	1.990	19.100

Result of Chemical Parameters contd…

LAB NO.	SAMPLE I.D	HCO3 (mg/l)	Fl (mg/l)	CL (mg/l)	Br (mg/l)	NO3 (mg/l)	SO4 (mg/l)	Ca (mg/l)	K (mg/l)	Mg (mg/l)	Na (mg/l)
17-6964	L79B	145.769	0.234	39.253	0.000	19.457	17.732	36.950	3.370	20.420	41.050
17-6965	L80B	246.732	0.333	5.785	0.000	2.073	4.489	26.300	3.180	25.910	17.650
17-6965	L81B	44.806	0.000	0.557	0.000	6.040	0.471	13.750	3.090	0.681	5.150
17-6966	L82B	7.766	0.000	2.313	0.000	3.281	0.000	0.035	0.191	0.019	8.000
17-6967	L83B	83.041	0.395	5.184	0.000	6.423	1.207	9.700	3.250	2.170	13.650
17-6968	L84B	94.989	0.000	179.140	0.000	52.492	70.373	38.350	134.900	20.550	106.300
17-6969	L85B	17.922	0.000	2.143	0.000	4.535	1.345	1.080	4.330	1.200	5.750
17-6970	L86B	13.741	0.009	1.600	0.000	0.473	0.193	0.360	0.737	0.116	1.670
17-6971	L87B	7.169	0.054	1.792	0.000	7.099	0.000	1.080	1.620	1.000	6.150

APPENDIX XIV: **Result of Stable Isotope Analysis of Water Samples in Bauchi-Alkaleri-Kirfi area**

S/NO.	Sample ID	Rock Type	$\delta^{18}O$ (‰)	$\delta^{2}H$ (‰)	D-excess (‰)
1	LOC 1	KK	-3.79	-28.54	1.75
2	LOC 3	KK	-3.33	-23.76	2.86
3	LOC 6	KK	-5.36	-26.04	16.86
4	LOC 34	KK	-3.85	-24.78	6.02
5	LOC 35	KK	-4.37	-24.56	10.41
6	LOC 38	KK	-4.15	-28.24	4.97
7	LOC 39	KK	-4.37	-25.69	9.28
8	LOC 42	KK	-4.31	-26.70	7.75
9	LOC 43	KK	-4.48	-29.19	6.69
10	LOC 44	KK	-4.33	-29.12	5.56
11	LOC 46	KK	-4.55	-25.36	11.01
12	LOC 47	KK	-3.80	-25.88	4.53
13	LOC 8	KK	-4.04	-26.64	5.72
14	LOC 11	KK	-4.19	-28.68	4.85
15	LOC 84	KK	-3.20	-22.46	3.14
16	LOC 87	KK	-3.97	-20.23	11.52
17	LOC 33	KK	-3.86	-21.63	9.25
18	LOC 7	MG	-3.70	-25.84	3.74
19	LOC 19	MG	-3.98	-23.96	7.84
20	LOC 22	MG	-2.79	-22.41	-0.06
21	LOC 25	MG	-3.30	-19.12	7.28
22	LOC 50	MG	-3.65	-23.95	5.25
23	LOC 53	MG	-4.13	-18.80	14.25
24	LOC 54	MG	-3.74	-23.38	6.55
25	LOC 55	MG	-2.96	-23.84	-0.16
26	LOC 57	BHG	-3.13	-18.57	6.48
27	LOC 58	MG	-3.11	-19.63	5.28
28	LOC 59	MG	-3.12	-20.91	4.07
29	LOC 61	MG	-3.87	-21.44	9.55
30	LOC 73	MG	-3.17	-25.08	0.31
31	LOC 77	MG	-3.14	-18.80	6.28
32	LOC 14	BHG	-3.72	-22.04	7.70
33	LOC 15	BCH	-3.41	-19.67	7.57
34	LOC 48	BHG	-3.94	-24.71	6.83
35	LOC 62	BHG	-3.22	-23.74	2.00
36	LOC 63	BHG	-3.74	-20.73	9.16
37	LOC 64	BHG	-3.41	-22.93	4.31
38	LOC 67	BHG	-3.28	-21.57	4.70
39	LOC 70	BHG	-3.75	-20.31	9.68
40	LOC 17	BCH	-3.19	-17.39	8.11
41	LOC 20	BCH	-3.28	-17.43	-8.83
42	LOC 27	BCH	-3.51	-21.81	6.24
43	LOC 28	BCH	-3.64	-22.11	7.01
44	LOC 66	BCH	-4.00	-19.06	12.94
45	LOC 78	BCH	-4.00	-21.20	10.81